~~$[Ca^{2+}]i$ oscillations at mammalian egg activation and during preimplantation development~~

THE ROLE OF CALCIUM OSCILLATIONS DURING PREIMPLANTATION EMBRYO DEVELOPMENT

Nina Trivedy Rogers

Department of Anatomy and Developmental Biology

University College London

A thesis submitted for the degree of Doctor of Philosophy

April 2006

ProQuest LLC
789 East Eisenhower Parkway
P.O. Box 1346
Ann Arbor, MI 48106-1346

Abstract

During fertilisation the sperm causes a series of $[Ca^{2+}]i$ oscillations in the egg that lead to events such as cortical granule exocytosis, pronuclei formation, exit from meiosis and entry into mitosis. These events are collectively termed "egg activation" and are essential for initiating development in the egg. Injection of PLCζ into mouse eggs has previously been shown to cause $[Ca^{2+}]i$ oscillations, egg activation and development to the blastocyst stage. In this Thesis I show that injection of PLCζ cRNA also causes $[Ca^{2+}]i$ oscillations in pig eggs and in human eggs which had failed to fertilise after assisted reproduction technologies (ART). The human eggs were shown to undergo further development up to the blastocyst stage.

The $[Ca^{2+}]i$ oscillations during egg activation are known to lead the immediate events of egg activation but the role of these $[Ca^{2+}]i$ oscillations on later preimplantation development in the mouse has not been established. The work presented in this Thesis addresses this issue by comparing differences in mouse embryo development after parthenogenetic activation using stimuli that induce a $[Ca^{2+}]i$ increase (e.g. Sr^{2+} and ethanol) with those that do not cause any $[Ca^{2+}]i$ change (e.g. cycloheximide). The data shows that parthenogenetic activation in the absence of a Ca^{2+} increase leads to embryo loss around the 8-cell stage, and that any blastocysts that form in absence of a $[Ca^{2+}]i$ increase have a reduced inner cell mass and an increased incidence of apoptosis. $[Ca^{2+}]i$ oscillations during activation do not appear to have an effect on the timing or amount of overall global gene expression during embryonic genome activation (EGA). However, when I used microarray analysis I found that a significant number of genes were differentially expressed in 8-cell stage embryos that were activated with a $[Ca^{2+}]i$ increases compared to those that activated in the absence of a $[Ca^{2+}]i$ change. These results provide evidence that $[Ca^{2+}]i$ increases at egg activation have an important role in regulating events during the later stages of preimplantation development.

Publications containing work from this thesis

Rogers NT, Hobson E, Pickering S, Lai FA, Braude P and Swann K.
Phospholipase Cζ causes $[Ca^{2+}]i$ oscillations and parthenogenetic activation of human oocytes.
Reproduction, 2004 Dec; 128: 697-702

Rogers NT, Larman M and Swann K.
The onset of zygotic genome activation measured in single mouse embryos using luciferase reporters and an imaging photon detector.
Reproduction, 2004 Abstract No 9; series No 31. Oral presentation

Contents

Chapter 1; General Introduction

1.1 Preimplantation embryo development

1.2 Ca^{2+} signalling and fertilisation

1.3 Embryonic Genome Activation

1.4 Gene Expression in the preimplantation embryo

Chapter 2
Materials and methods

2.1 Mouse egg experiments

2.2 Pig egg experiments

Chapter 4
$[Ca^{2+}]i$ oscillations during egg activation and their affects on preimplantation embryo development

Chapter 5
The affect of $[Ca^{2+}]i$ oscillations on Embryonic Genome Activation

Chapter 6
A comparison of gene expression in the 8-cell embryo after Ca^{2+}-dependent and independent parthenogenetic egg activation

6.3 Discussion

Chapter 7; General Conclusions

List of figures

List of tables

Abbreviations

Abbreviation	Name
$[Ca^{2+}]i$	Intracellular Ca^{2+} ions
µl	Micro litre
6-DMAP	6-Dimethylaminopurine
ANOVA	Analysis of Variance
ART	Assisted Reproductive Technologies
BSA	Bovine Serum Albumin
Ca^{2+}	Calcium ions
CAM	Calmodulin
CAMKII	Calmodulin-dependent kinase II
CD	Cytochalasin D
COC's	Cumulus Oocyte Complexes
CSF	Cytostatic Factor
CX	Cycloheximide
DAG	Diacylglycerol
dbCAMP	Dibutryl Cyclic AMP
DTT	Dithiothreitol
eCG	Equine Chorionic Gonadotrophin
EGA	Embryonic genome activation
EGF	Epidermal Growth Factor
ER	Endoplasmic reticulum
EST	Expressed Sequence Tag
FITC	Fluorescein Isothiocyanate
FSH	Follicle Stimulating Hormone
GFP	Green Fluorescent protein
GO	Gene Ontology
GV	Germinal vesicle
H1	Histone 1
hCG	human Chorionic Gonadotrophin
HPVA	Hepes Polyvinyl alcohol
ICM	Inner Cell Mass
ICSI	Intracytoplasmic Sperm Injection
$InsP_3$	Inositol-1,4,5-trisphosphate
$InsP_3R$	Inositol-1,4,5-trisphosphate receptor
IPD	Imaging Photon Detector
IVF	*In vitro* fertilisation
IVM	*In vitro* Maturation
KSOM	Potassium simplex-optimised media
L	Litre
M	1 molar concentration
Mg^{2+}	Magnesium ions
MI	Metaphase 1
MII	Metaphase 2
MPF	Maturation Promoting Factor
NCSU-23	North Carolina State University – 23
NEBD	Nuclear envelope breakdown
NIA	National Institute on Aging

NIH	National Institute of Health
NLS	Nuclear localisation Signal
NPS	Newcastle Photometric System
NT	Nuclear transfer
PBS	Phosphate Buffered Saline
PC 1 / 2	Principle Component 1 / 2
PCA	Principle Component Analysis
Pff	porcine follicular fluid
PI	Propidium Iodide
PIP_2	Phophatidylinositol 4,5-bisphosphate
PKC	Protein kinase C
PLC	Phospholipase C
PLCζ	The official designation of this gene is PLCZ1, (phospholipase C, zeta 1). Throughout this thesis it is referred to as PLCζ as it has been referred to in previously published literature
PMSG	Pregnant Mare Serum Gonadotrophin
PVA-TL-HEPES	Hepes-buffered Tyrode albumin lactate pyruvate medium
PVP	Polyvinylpyrrolidone
ROS	Roscovitine
RYR	Ryanodine receptor
SFP	Sulfinpyrazone
Sr^{2+}	Strontium ions
SSH	Suppression Subtractive Hybridization
TE	Trophectoderm
TRC	Transcription-requiring complex
TUNEL	Terminal deoxynucleotidyl Transferase Biotin-dUTP Nick End Labeling
UMRR	Universal Mouse Reference RNA
WGA	Wheat Germ Lectin
ZGA	Zygotic Genome Activation

Chapter 1

General Introduction

During mammalian fertilisation, a series of intracellular Ca^{2+} oscillations ($[Ca^{2+}]i$) in the egg trigger the transition from egg to embryo. It was recently discovered that a proteinaceous "sperm factor" called Phospholipase C zeta (PLCζ) is able to trigger these $[Ca^{2+}]i$ oscillations that are critical for development to proceed. The experiments represented in this thesis were designed to examine the influence these $[Ca^{2+}]i$ oscillations have upon specific aspects of mammalian preimplantation embryo development such as embryonic genome activation (EGA), gene expression and blastocyst quality. This general introduction will act as a review of topics that are particularly relevant to these areas of study. I will begin with an overview of mammalian preimplantation development after which I will discuss the mechanisms of $[Ca^{2+}]i$ signalling at egg activation. This will be followed by a discussion of EGA and how it is thought to impacts on embryo development. Finally I will discuss what is known about gene expression patterns in the preimplantation embryo.

1.1 Preimplantation embryo development

1.1.1 Oogenesis

Primordial germ cells develop in the foetus prior to birth. The mouse ovaries at birth contain only primordial follicles. The follicle is an essential functional unit of the ovary and the term folliculogenesis refers to the development of follicles from the primordial stage through a series of morphologically defined stages that culminate in the formation of large pre-ovulatory follicles. Over half of the primordial follicles present in the ovaries of newborn mice degenerate during the first few days after birth. Follicle formation in the mouse begins

shortly after birth and by approximately 5 days after birth these cells, which are known as primary oocytes, are arrested in prophase 1 of meiosis 1. During meiotic arrest the size of the oocyte increases from a diameter of 15 to 85 μm and growth is complete within 10-18 days. The growth phase is accompanied by the gradual appearance of the zona pellucida (ZP), a 7μm layer of extracellular material synthesized by the oocyte (Wassarman, 1988; Greve and Wassarman, 1985). A major component of the ZP is the glycoprotein Zona Pellucida 3 (ZP3), which functions as a sperm receptor preventing cross-species fertilisation and a trigger for the acrosome reaction, which is essential if fertilisation is to take place (Bleil and Wassarman, 1980). Oocyte growth is also characterised by the appearance of a large nucleus called the germinal vesicle (GV) and the accumulation of molecules important for embryogenesis. Each oocyte is initially contained within a follicle composed of a single layer of granulosa cells. The granulosa cells that immediately surround the egg form gap junctions with each other and the oocyte that allow the transfer of metabolites and other low mass molecules, between the oocyte and the somatic cells of the developing follicle. Oocyte growth is dependent on the communication between oocyte and granulosa cells, the growth rate depending on the number of granulosa cells in contact with the oocyte (Brower and Schultz, 1982). As the oocyte grows in size it acquires the competence to enter the last stages of meiosis in response to either the correct hormonal signal *in vivo* or release from the follicle *in vitro*.

In female mice, sexual maturity occurs at 6 weeks of age and by this time each ovary contains approximately 10^4 oocytes that are at different stages of maturity (Hogan et al., 1994). In a natural mouse estrous cycle, 6-15 follicles respond to an increase in Follicle Stimulating Hormone (FSH) by accumulating fluid secreted by the follicular cells (Gates, 1971). The follicle, now called a Graafian, or Antral follicle moves to the periphery of the ovary. A surge in Luteinising hormone (LH) initiates ovulation by causing the rupture of several follicles (6-12 in the mouse) from the ovary (Gates, 1971). Large numbers of oocytes

that are synchronous in their development can be stimulated to ovulate artificially (superovulation) by administration of gonadotrophins. For experiments on mouse eggs I used Pregnant Mare's Serum Gonadotrophin (PMSG) to mimic FSH and human Chorionic Gonadotrophin (hCG) to mimic LH (Hogan et al., 1994). Typically 30-40 eggs were ovulated per mouse after this treatment (See materials and methods-Chapter 2). After LH stimulation the GV loses its membrane through a process known as germinal vesicle breakdown. At this stage, the chromosomes that have assembled on the spindle move towards the periphery of the cell ready for the first meiotic division and although there is an equal division of chromosomes into each daughter cell, the size of one daughter cell is about 30 times larger in volume than the other due to unequal division of the cytoplasm. The smaller cell, termed the 1st polar body degenerates shortly after formation. The larger cell termed the secondary oocyte contains a full complement of chromosomes and the cell arrests at metaphase II (MII) of the 2nd meiotic division.

Whilst remaining in meiotic arrest, the oocyte may eventually be released from its follicle by a process called ovulation. Each ovulated MII-arrested oocyte is surrounded by a mass of follicle cells called the cumulus mass and can be referred to as an egg. The ovulated egg is swept into the infundibulum of the oviduct by the action of numerous cilia present on the oviduct epithelium. During ovulation, a section of the oviduct enlarges to form an ampulla where fertilisation will take place. In mice, around 6-12 eggs are ovulated over a 2-3 hour period rather than in synchrony as may occur in other species (Hogan et al., 1994).

1.1.2 Fertilisation

The stage of the cell cycle in which fertilisation takes place varies in different species. In the majority of mammals the egg arrests during MII and awaits fertilisation, there are however some notable exceptions. Canine oocytes arrest at prophase of the 1st meiosis (Holst and

Phemister, 1971), Ascidian and mollusc eggs arrest at MI while sea urchins complete meiosis before arresting. Starfish eggs complete MII without arresting and can be fertilised at any time (Whitaker, 1996).

In the mouse approximately 58 x 10^6 sperm are released into the female reproductive tract upon ejaculation (Hogan et al., 1994). Before the sperm can fertilise the egg it must undergo a specialised process of maturation known as capacitation. Sperm capacitation takes about 1 hour, although its molecular nature is unclear (Tulsiani et al., 1997). The sperm has to penetrate through the cumulus cells and ZP before its head can bind to the glycoprotein ZP3. Once bound to ZP3, the sperm triggers the acrosome reaction (Bleil and Wassarman, 1980). During the acrosome reaction, hydrolytic enzymes are released from the sperm head allowing it to penetrate the ZP. After penetration, the posterior part of the sperm head fuses with the egg membrane, triggering fertilisation. In normal circumstances one sperm enters the egg and contributes it haploid nucleus, after which the centriole from the sperm divides and forms part of the spindle. The introduction of multiple sperm into the egg is known as polyspermy, this often causes multiple spindles in the egg and leads to abnormal cleavage and death in the embryo (Austin and Braden, 1953). Different mechanisms exist to prevent polyspermy. In mammals, cortical granules that lie directly beneath the plasma membrane are released in a Ca^{2+} dependent manner. This process, termed cortical granule exocytosis (CGE), initiates the zona reaction, which involves modifications of the zona so that sperm can no longer bind and trigger the acrosome reaction. In some species such as the sea urchin there is an initial fast block to polyspermy that is caused by a change in the electrical potential of the egg plasma membrane. This block lasts for approximately 1 minute before being replaced by CGE. Some species undergo physiological polyspermy but have unusual mechanisms to prevent more than one male pronucleus becoming involved in further development. The etenophore *Beroe Ovata* egg for example can be fertilised by up to 10

sperm, the pronuclei of the sperm remain however at the sperm entry site beneath the egg surface while the egg pronuclei migrates directly to a single chosen male pronucleus (Carre and Sardet, 1984).

In mammals, fertilisation initiates a second asymmetrical meiotic division, resulting in extrusion of the 2nd polar body. Nuclear proteins form around the maternal and paternal chromosomes resulting in separate haploid female and male pronuclei that both start to migrate towards the centre of the egg. During migration, DNA replication occurs in both pronuclei. The nuclear membranes then break down and chromosomes align on the spindle shortly before the first mitotic cell division occurs.

1.1.3 Preimplantation embryo development

Embryonic cell cleavages in mammals are the slowest in the animal kingdom, typically occurring 12 to 24 hours apart (Hogan et al., 1994). Mammalian embryonic cells divide by rotational cleavage whereby during the second cleavage one of the two blastomeres divides meridonally and the other divides equatorially (Gulyas, 1975). Mammalian blastomeres do not divide at the same time, they are diachronous and thus embryos often have odd numbers of cells.

In mice the first embryonic cell division begins 17-20 hours post-fertilisation and produces an embryo with two identical Blastomeres (Hogan et al, 1994). *In vivo*, the 2nd cleavage (3-4 cells) begins 46- 54 hours post fertilisation and the embryo typically reaches the 8-cell stage by 60 hours. Formation of compacted morula occurs by 60-75 hours and blastocyst formation 84 – 96 hours (3.5-4 days) post fertilisation (Hogan et al., 1994). During these early cell cleavages, cilia and smooth muscle contractions of the oviduct wall help to push the embryo towards the uterus. Following the third cleavage the blastomeres of the 8-cell embryo maximise their contact with one another, forming a compact ball of cells. This

process marks the start of compaction. During compaction the blastomeres adhere together more tightly and this arrangement is stabilised by the formation of tight junctions that form between the outermost cells, sealing the inner cells off from the external environment (Pratt et al., 1982). This arrangement allows the cells to be exposed to two different microenvironments depending on their position within the embryo. The larger group of cells on the outside of the embryo are exposed to the media surrounding the embryo while the smaller group of inner cells do not have contact with the outside. Gap junctions form between the inner cells allowing small molecules to pass between them. The Ca^{2+}-dependent cell adhesion molecule E-cadherin (Uvomorulin) appears at the time of compaction and causes the cells to adhere more closely. Antibodies to E-cadherin have been shown to reverse the process of compaction (Peyrieras et al., 1983) revealing the importance of cadherins at this stage.

The first cell differentiation event in mammalian development is the distinction between the trophectoderm (TE) and inner cell mass (ICM). This event allows the embryo to adhere to the uterus. The descendents of the external cells of the embryo become the Trophectoderm (TE) cells, which form the extra-embryonic structures such as the placenta (chorion). The fate of the inner cells of the embryo is to form the inner cell mass (ICM). The ICM gives rise to the embryo and its associated allantois. At the 16-32 cell stage the ICM cells maintain a degree of plasticity which enables them to differentiate into TE cells (Fleming, 1986). This is thought to enable the regulation of the ratio of TE to ICM cell number (Fleming, 1986). At the 64 cell stage, the ICM consists of approximately 13 cells and is completely separate from the TE, thus neither group of internal or external cells contributes to the survival of the other. The embryo is now referred to as a morula.

Initially the morula does not contain a cavity after compaction however the TE cells begin to secrete fluid into the morula. The resulting cavity is known as a blastocoel, this defines the formation of the blastocyst. The cells positioned next to the presumptive

blastocoel have sodium (Na^+) and potassium (K^+) ion pumps that move sodium ions into the blastocoel, enlarging it by letting water flow in by osmosis (Watson and Barcroft, 2001). As the blastocyst continues to accumulate blastocoelic fluid, it increases in size to form an expanded blastocyst. By the blastocyst stage the ICM cells have lost the capacity to form extra-embryonic membranes but can contribute to any later embryonic tissue because they are still totipotent with respect to embryonic development. At this point the blastocyst cannot adhere to the oviduct wall due to the presence of the zona pellucida. Occasionally adherence does occur in the oviduct and this can result in ectopic pregnancy, a potentially life threatening condition that can lead to haemorrhage. Ectopic implantation however is a common occurrence in humans, but occurs only rarely in other species (Bronson and Cunnane, 1975). Once the blastocyst reaches the uterus, Strypsin, a trypsin like protease, which is present on the cell membranes of the outer trophoblast cells helps to lyse the fibrillase matrix of the zona. This causes an opening in the zona pellucida from which the blastocyst can be easily released. The blastocyst adheres to the uterine wall and starts to penetrate the uterine epithelium in a process mediated by TE cells. The uterus responds to implantation with the "decidual reaction," a process that allows the uterus to bring blood to the developing embryo by increasing the permeability of blood vessels in the uterus and allowing new blood vessels to be made (Psychoyos et al., 1995).

1.1.4 Embryo developmental capacity

Embryos are routinely cultured until the blastocyst stage *in vitro* since most embryos cannot develop in the uterus before the morula or blastocyst stage. Primate embryos are an exception to this rule and can be transferred into the uterus as early as the 4-8 cell stage resulting in pregnancy in 20% of cases (Hunter, 1998). This is a considerable advantage to human IVF since detrimental effects associated with in vitro culture can be kept to a minimum. The

culturing of embryos to the blastocyst stage before implantation has however been shown to improve successful implantation by 30% to a 50% overall success rate (Gardner et al., 1998). The ability to transfer only two blastocysts and still maintain high pregnancy rates will also facilitate the elimination of high order multiple gestations. The *in vitro* culture of embryos cannot succeed past the blastocyst stage since embryos at this stage need to implant in the uterus which is facilitated by *in vivo* conditions.

The quality of the blastocyst is imperative to high implantation rates and development to full term. Specific parameters are used to determine the viability of preimplantation embryos (Bavister, 1995; Van Soom et al., 1997). The timing of cell cleavages during early development has been reported to be a valuable parameter for intrinsic embryo quality (Bavister, 1995; Van Soom et al., 1997). Cinematographic analysis of cow embryos found that the faster the embryos cleaved into early stage embryos, the higher the probability that they would reach the morula or blastocyst stage (Grisart et al., 1994). Approximately 70% of embryos reaching the 2-cell stage by 30-31 hours post insemination developed to these stages (Grisart et al., 1994).

Assays based on nutrient uptake and subsequent utilisations as well as oxygen uptake and enzyme leakage have also been used to evaluate embryo viability (Gardner, 1999). Assays for production of growth factors such as trophoblast interferon have been used to assess cow blastocyst quality (Hernandez-Ledezma et al., 1993).

Scoring the percentages and rates of blastocysts hatching from the ZP can be a useful procedure to determine blastocyst quality since escape from the ZP is essential if the blastocyst is to implant. Differences in the timing, morphology and dynamics of ZP escape appear however to exist between *in vivo* and *in vitro* cultured blastocysts (Gonzales and Bavister, 1995) . *In vivo* blastocysts escape the zona by global zona dissolution whereby the zona 'dissolves' evenly around the blastocyst. In contrast *in vitro* blastocysts escape through

'focal lysis' by penetration of the zona by trophectodermal projections producing a small hole in the zona.

Invasive techniques to study the internal organelles, DNA quality, microtubule assembly and cell number have been used to investigate embryo potential. Information on the distribution of ICM and TE cells in the blastocyst is valuable since a minimal number of ICM cells are required for a successful pregnancy. During normal development, optimal numbers of TE and ICM cells are present to ensure embryonic and fetal survival (Hardy et al., 1989). The ratio of ICM and TE cell numbers is particularly important since a disproportionately large ICM has been associated with large-offspring syndrome (Leese et al., 1998). The determination of TE and ICM allocation has proved to be an important measure of embryo viability and has thus attracted the development of a large number of procedures in order to distinguish the two cell types (Handyside and Hunter, 1984; Hardy et al., 1989; De La Fuente and King, 1997; Thouas et al., 2001).

Apoptosis or cytoplasmic fragmentation has been commonly observed in mammalian blastocysts of excellent morphology. It has thus been suggested to play a role in the removal of defective cells as well as in the control of cell number and cell growth (Hardy et al., 2003). Extensive fragmentation is however associated with reduced blastocyst formation (Alikani et al., 2000; Hardy et al., 2003), reduced implantation potential (Alikani et al., 1999) and lower blastocyst cell number, especially in the TE (Hardy et al., 2003). Apoptosis has also been implicated in embryonic arrest (Jurisicova et al., 1996). The detrimental effects of fragmentation may be due to the release of toxins that damage neighbouring cells or the reduction in cytoplasm volume resulting in the loss of critical cellular components (Alikani et al., 1999). It has been demonstrated that extensive fragmentation results in the loss of whole blastomeres, which severely reduces blastocyst formation rate (Hardy et al., 2003). It has recently been proposed using a mathematical modelling approach that an embryos

developmental competency is established before or at the zygotic 1-cell stage (Hardy et al., 2001). The majority of arrested embryos exhibit high levels of chromosomal abnormalities which might arise because of a lack of cell-cycle checkpoints before embryonic genome activation (EGA) (Handyside and Delhanty, 1997) . A lack of functioning cell-cycle checkpoints would allow apoptosis to last till the eight-cell stage when embryonic arrest is first observed at high levels (Hardy et al., 2001). It has been suggested that chromosomal abnormalities that arise after fertilisation could be due to lack of maternal transcripts during oocyte maturation (Hardy et al., 2001).

Apoptosis has been detected in parthenogenetically activated preimplantation embryos, which shows that the initiation of apoptosis at this early stage does not require the paternal genome(Liu et al., 2002). The initiation of apoptosis in human embryos coincides with the timing of compaction which occurs at the same time as gap junction formation. The presence of gap junctions on somatic cells has been reported to propagate apoptotic signals to their neighbouring cells suggesting that establishment of cell-cell communication may play an important role in mediating apoptosis (Lin et al., 1998). It is unclear what process or signal initiates apoptosis in preimplantation embryos. Fragmented DNA is typically detected by terminal deoxynucleotidyl transferase (TdT) nick-end labelling (TUNEL) and been widely used to detect fragmentation in blastocysts from a number of species such as human (Jurisicova et al., 1996; Spanos et al., 2000), cow (Fahrudin et al., 2002) (Neuber et al., 2002) and rat (Pampfer et al., 1997).

It is apparent that a plethora of strategies are in use to quantify and qualify embryo quality and viability, a process that is essential in order to increase successful pregnancies and reduce the risk of abnormalities. These techniques are applicable in clinics participating in assisted reproductive technologies (ART) and biotechnology set ups carrying out nuclear transfer (NT) technology.

1.2 $[Ca^{2+}]i$ signalling and fertilisation

1.2.1 $[Ca^{2+}]i$ signalling: a universal egg activation stimulus

An intracellular Ca^{2+} increase ($[Ca^{2+}]i$) is an essential component of the fertilisation response in all plants and animals studied to date (Digonnet et al., 1997). In many eggs an increase in $[Ca^{2+}]i$ is triggered at the point of sperm entry before being propagated as a global wave across the whole egg (Stricker, 1999). Some eggs such as those of the marine worm do not exhibit $[Ca^{2+}]i$ waves but $[Ca^{2+}]i$ rises simultaneously around the egg cortex and peaks slightly later in the nucleoplasm (Stephano and Gould, 1997). This $[Ca^{2+}]i$ signal is responsible for triggering events such as cortical granule exocytosis (CGE), completion of meiosis (in mammals) and pronuclei formation. Collectively these processes are referred to as egg activation. In most mammals this $[Ca^{2+}]i$ signal takes on a distinct pattern in the form of repetitive $[Ca^{2+}]i$ transients or oscillations. In the mouse egg, the first $[Ca^{2+}]i$ transient is longer in duration compared to subsequent transients and has smaller sinusoidal $[Ca^{2+}]i$ rises at the peak. The following transients are of lower amplitude, shorter duration and occur at a frequency of several minutes from one another (Swann and Ozil, 1994). The $[Ca^{2+}]i$ transients continue for several hours and stop around the time of pronucleus formation (Kline and Kline, 1992; Jones et al., 1995a). The repetitive nature of the sperm-induced $[Ca^{2+}]i$ oscillations are essential for mammalian egg activation to be completed. Inhibition of these $[Ca^{2+}]i$ transients using the Ca^{2+} chelator BAPTA-AM completely blocks oocyte activation (Kline and Kline, 1992) and premature cessation of $[Ca^{2+}]i$ oscillations has been found to severely retard pronucleus formation (Taylor et al., 1993).

In most non-mammalians eggs such as frogs and sea urchins, the $[Ca^{2+}]i$ signal at fertilisation is in the form of a monotonic $[Ca^{2+}]i$ rise. During fertilisation in some species it is not the sperm that induces a $[Ca^{2+}]i$ increase in the egg, for example in the marine shrimp or

zebrafish the $[Ca^{2+}]i$ increase is induced by ovulation or contact with sea or pond water (Lee et al., 1999; Lindsay et al., 1992). These cases are unusual however they are noteworthy exceptions since it relays the importance of the $[Ca^{2+}]i$ signal at fertilisation which appears to have evolved from an early period in animal natural history to become a universal phenomenon.

1.2.2 Ca^{2+} release channels and intracellular stores

Ca^{2+} is responsible for stimulating a multitude of cellular processes from fertilisation to cell growth and adhesion (Berridge, 1993). The level of Ca^{2+} in the cytosol of a resting cell is very low (~100nM). Much higher concentrations of Ca^{2+} are found in the extracellular media (1-2mM) and specialised Ca^{2+}-sequestering compartments (~600uM) such as the endoplasmic reticulum (ER), mitochondria and nuclear envelope (Rizzuto et al., 1994; Subramanian and Meyer, 1997). The primary storage organelle for Ca^{2+} in most (non-muscle) cells is the ER (Berridge and Irvine, 1989).

Ca^{2+} channels on the plasma membrane or membrane of the Ca^{2+} sequestering compartments can be stimulated to open by extracellular signal transduction. Ca^{2+} can rapidly move down its concentration gradient into the cell's cytosol resulting in a dramatic increase in $[Ca^{2+}]i$. A sudden rise in $[Ca^{2+}]i$ can stimulate a cascade of celluar events mediated by Ca^{2+}-binding proteins and protein kinases. In order for $[Ca^{2+}]i$ to serve as an intracellular messenger it must be present at very low concentrations in the cell's cytosol. Many cells have ATP-dependent Ca^{2+}-ATPases in the plasma membranes and membranes of intracellular stores which act to pump Ca^{2+} from the cytosol to extraceullar media or intracellular stores, against its concentration gradient (Fig 1.1). The uptake of Ca^{2+} into the ER takes place via specialised Ca^{2+}-ATPase pumps referred to as Sarcoplasmic/Endoplasmic Reticulum Calcium

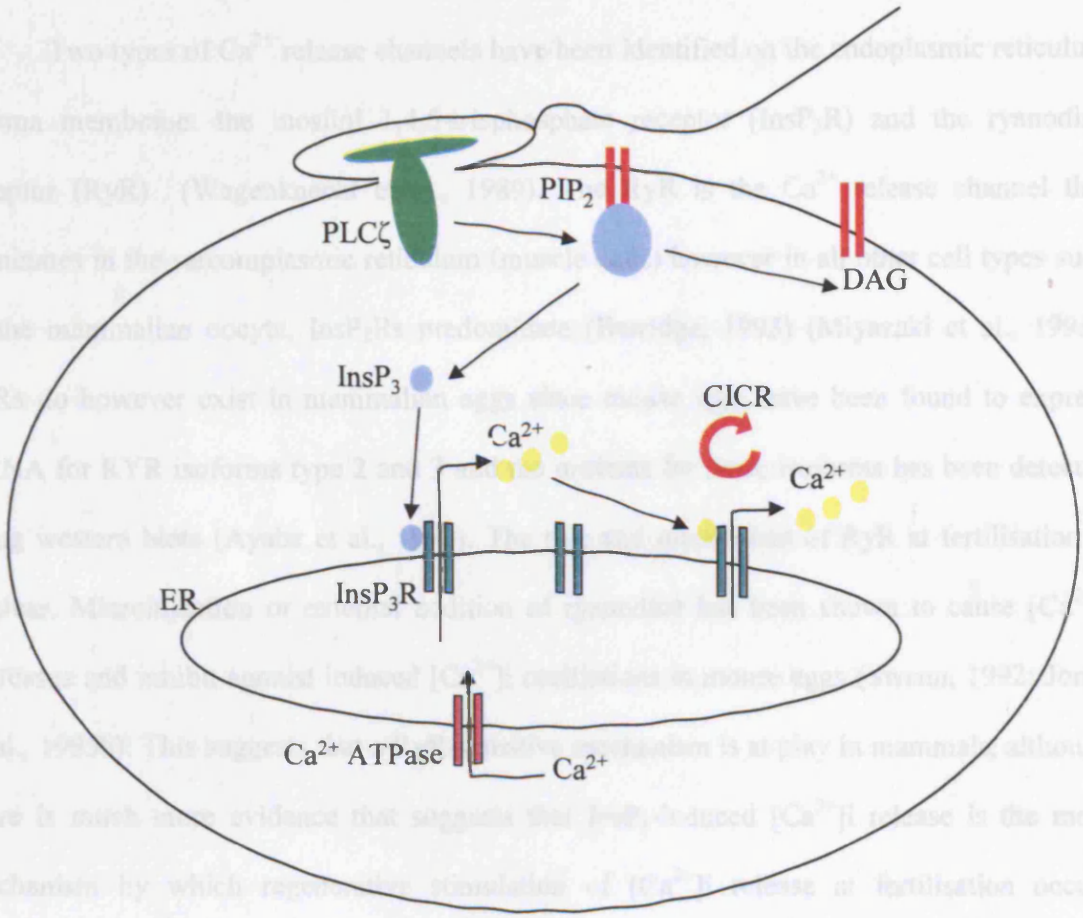

Figure 1.1 $[Ca^{2+}]i$ release via the Inositol 1,4,5-Trisphosphate ($InsP_3$) pathway during fertilisation. An active PLC hydrolyzes phosphatidylinositol bisphosphate (PIP2) into the two secondary messengers inositol 1,4,5-trisphosphate (InsP3) and diacyl glycerol (DAG). InsP_3 then diffuses into the cytosol and activates the InsP_3R on the membrane of the endoplasmic reticulum (ER), which subsequently releases Ca^{2+} from the ER. Further Ca^{2+} release via the $InsP_3R$ is thought to occur when the $InsP_3R$ is stimulated by Ca^{2+} binding during a process called calcium-induced calcium-release (CICR). ATP-dependent Ca^{2+}-ATPases in the membrane of the ER allow Ca^{2+} to be pumped back into the ER against a Ca^{2+} concentration gradient.

ATPase (SERCA) pumps because they are also found in the sarcoplasmic reticulum (Lytton et al., 1992).

Two types of Ca^{2+} release channels have been identified on the endoplasmic reticulum plasma membrane: the inositol 1,4,5-trisphosphate receptor ($InsP_3R$) and the ryanodine receptor (RyR) (Wagenknecht et al., 1989). The RyR is the Ca^{2+} release channel that dominates in the sarcomplasmic reticulum (muscle cells) however in all other cell types such as the mammalian oocyte, $InsP_3Rs$ predominate (Berridge, 1993) (Miyazaki et al., 1993). RyRs do however exist in mammalian eggs since mouse eggs have been found to express mRNA for RYR isoforms type 2 and 3 and the proteins for these isoforms has been detected using western blots (Ayabe et al., 1995). The role and mechanism of RyR at fertilisation is unclear. Microinjection or external addition of ryanodine has been shown to cause $[Ca^{2+}]i$ increases and inhibit agonist induced $[Ca^{2+}]i$ oscillations in mouse eggs (Swann, 1992; Jones et al., 1995b). This suggests that a RyR-sensitive mechanism is at play in mammals, although there is much more evidence that suggests that $InsP_3$-induced $[Ca^{2+}]i$ release is the main mechanism by which regenerative stimulation of $[Ca^{2+}]i$ release at fertilisation occurs (Miyazaki et al., 1993).

During fertilisation the hydrolysis of phosphatidylinositol 4,5 bisphosphate (PIP_2) is catalysed by a phospholipase C which results in the generation of two products, Inositol 1,4,5-trisphosphate ($InsP_3$) and diacyl glycerol (Fig 1.1). The binding of $InsP_3$ to the $InsP_3$ receptor ($InsP_3R$) situated on the ER causes $InsP_3$-induced $[Ca^{2+}]i$ release **(Miyazaki et al., 1993)**. Monoclonal antibodies against the type 1 $InsP_3R$ revealed that $InsP_3Rs$ are present in the cytoplasm near the egg surface to initiate the $InsP_3$-mediated signal and also in the deeper cytoplasm to propagate the waves of $[Ca^{2+}]i$ (Miyazaki et al., 1992). This work also showed that type 1 but not the type 11 or 111 $InsP_3R$ were essential for mediating the $InsP_3$-induced $[Ca^{2+}]i$ release **(Miyazaki et al., 1993)**. In addition, the microinjection of $InsP_3$ into

unfertilised mouse eggs has been found to trigger $[Ca^{2+}]i$ oscillations **(Swann, 1994)**. Inhibition of the $InsP_3R$ using a functionally inhibitory monoclonal antibody (18A10) inhibited sperm-induced $[Ca^{2+}]i$ oscillations and subsequent egg activation in hamster eggs (Miyazaki et al., 1992). $[Ca^{2+}]i$ oscillations that are induced during fertilisation or microinjection of adenophostin A are inhibited after the downregulation of $InsP_3R$ **(Brind et al., 2000)**. Opening of the IP_3R, in the presence of IP_3 is also thought to be stimulated by calcium binding to the Ip3R causing a process known as calcium-induced calcium-release (CICR) (Jaffe, 1991).

In sea urchin eggs, which have both RyR and $InsP_3R$, inhibition or either channel individually fails to prevent a $[Ca^{2+}]i$ rise at fertilisation, inhibition of both channels however completely inhibits Ca^{2+} release, indicating that $InsP_{3R}$ and RyR have redundant mechanisms during fertilisation in the sea urchin (Galione et al., 1993). It is unclear if RyR are able to fully substitute for $InsP_3R$'s since Ca^{2+} fluxes mediated by $InsP_3$ were shown to be needed for normal cleavage in sea urchins (Ciapa et al., 1994). $InsP_3$ induced $[Ca^{2+}]i$ release mechanisms appear to also be necessary for normal starfish development (Stricker, 1995). Further studies on different species will need to be carried out to elucidate whether the RyR plays a vital function in fertilisation, the evidence so far suggests however that $InsP_3R$ is the main $[Ca^{2+}]i$ release channel mechanism.

1.2.3 Meiotic arrest is maintained by high MPF activity

Early work carried out on frog eggs demonstrated that cytoplasm transferred from progesterone-treated (maturing) eggs caused recipient immature eggs to undergo premature maturation (Masui and Markert, 1971). The cytoplasmic substance responsible for this effect on maturation was referred to as Maturation-Promoting Factor (MPF). MPF was found to appear 6 hours after progesterone treatment and persist at high levels until fertilisation, after

which it declines to low level during cell cleavage (Masui and Markert, 1971). It was also suggested that MPF played a role in cell cycle progression since it was also shown to appear in frog eggs shortly before mitosis (Wasserman and Smith, 1978). MPF is now known to comprise of a regulatory cyclin B subunit (Evans et al., 1983) and a cyclin dependent kinase 1 (Cdk1) (Doree and Hunt, 2002). During early egg development the levels of MPF change dramatically. In frogs Meiosis I is activated by high levels of MPF that are stimulated by progesterone secretion. MPF is at its highest at metaphase of meiosis I (MI) but falls briefly to cause the transition from MI to anaphase I and first polar body extrusion (Ledan et al., 2001). MPF activity rises again as the MII spindle is reformed. Maintainance of high levels of MPF ensures the egg stays arrested at MII. A constant turnover of cyclin B occurs during MII arrest and maintains a continuous equilibrium between cyclin B synthesis and degradation (Kubiak et al., 1993). MPF activity is stabilised by a cytostatic factor (CSF) which acts to achieve cell cycle arrest prior to fertilisation. CSF was first discovered when cytoplasm from eggs at late stages of maturation were found to trigger metaphase arrest in the blastomeres of zygotes (Masui and Markert, 1971). It is unclear what mechanism CSF employs to keep MPF levels high, it is widely believed however that the Mos protein, mitogen-activated protein kinase (MAPK), early mitotic inhibitor 1 (Emi1) and a recently discovered early mitotic inhibitor 2 (Emi2) are involved. The injection of synthetic *mos* RNA into Xenopus blastomeres induces metaphase arrest. In contrast, immunodepletion of endogenous Mos from egg cytosol extracts prevented meiotic arrest in embryos (Sagata et al., 1989), it is thus clear that Mos is a component of CSF. Mos is not the sole component of CSF however since it is insufficient to maintain MII arrest when acting alone and cyclin B is degraded before activation of the Mos pathway.

The 44-kDa protein Emi1 was recently proposed to be necessary and sufficient for causing meiotic arrest (Reimann and Jackson, 2000). The addition of extra Emi1 to CSF-

containing extracts prevented the destruction of cyclin B and mitotic exit whilst in contrast, CSF-extracts immunodepleted with Emi1 exit from mitosis prematurely in the absence of $[Ca^{2+}]i$ increases (Reimann and Jackson, 2000). Another study which raised an antibody against Emi1 and failed to detect a 44-kDa band by immunoblot in the *Xenopus* egg or embryo until gastrulation concluded that Emi1 is unstable and cannot exist in the embryo until gastrulation and therefore is not required for CSF activity (Ohsumi et al., 2004) however no evidence exists to show that the 44kDa band observed at gastrulation was that of Emi1. Most recently an Emi1 homologue identified as Emi2 has been put forward as a CSF maintenance protein (Tung et al., 2005). Emi2 cross-reacts with antibodies raised against Emi1 which suggests that previous Emi1 immunoprecipitation experiments may have also resulted in inactivation of Emi2, a possible CSF candidate. Evidence in support of Emi2 as a CSF candidate includes evidence it is an APC inhibitor and that Emi2 is targeted for destruction by Polo-like kinase 1 (Plx1) in response to $[Ca^{2+}]i$ signalling (Tung et al., 2005).

Mitogen-activated protein kinase (MAPK) has been shown to be involved in meiotic arrest although its role is unclear. Components of the MAPK pathway such as p90rsk were reported to cause metaphase arrest when injected into Xenopus blastomeres (Bhatt and Ferrell, 1999). MAPK is capable of maintaining meiotic arrest and is believed to act downstream of the Mos-pathway since MAPK fails to activate eggs in *mos-/-* mice (Verlhac et al., 1996). It is clear that a number of important components seem to be present in CSF the exact mechanisms by which they maintain high levels of MPF are not however known at present.

1.2.4 $[Ca^{2+}]i$ signals release the egg from meiotic arrest

As discussed above, MII arrest is characterised by biologically active levels of MPF and thus cyclin B must be continuously synthesized and destroyed to ensure the activity of MPF. Exit

from meiotic arrest is caused by destruction of the cyclin B component which in turn greatly reduces the activity of MPF (Murray et al., 1989; Kubiak et al., 1993). Cyclin B is targeted for proteolytic destruction by the anaphase promoting complex/cyclosome (APC/C). APC is an E3 ligase complex that degrades its substrates (e.g. - cyclin B) by ligating them with ubiquitin which serves to target them for proteolysis by the 26S proteosome. Cyclin B contains a RXXL destruction-box motif, which is critical for ubiquitin ligation and thus proteolysis (Murray et al., 1989; King et al., 1995).

$[Ca^{2+}]i$ increases during fertilisation or parthenogenetic activation have been reported to induce cyclin B destruction and hence resumption of the cell cycle in frog and mice (Lorca et al., 1993; Winston et al., 1995). Cyclin B destruction in the mouse requires the presence of an intact spindle since exposure to nocodazole, a microtubule-depolymerising drug greatly reduced the rate of cyclin B degradation (Kubiak et al., 1993). Consistent with this, egg activation with the parthenogenetic agent, thimerosal destroys the spindle and also prevents exit from MII (Cheek et al., 1993).

One study monitored cyclin B activity during fertilisation using a cyclin B-GFP plasmid, revealing that repetitive $[Ca^{2+}]i$ transients are necessary for the continuous destruction of cyclin B (Nixon et al., 2002). Incremental drops in cyclin B were associated with each $[Ca^{2+}]i$ transient when they were high in magnitude such as that of the first $[Ca^{2+}]i$ transient at fertilisation, (Nixon et al., 2002).

In *Xenopus*, cyclin proteolysis is mediated by a Ca^{2+}-calmodulin dependent process (Lorca et al., 1991; Lorca et al., 1993). Calmodulin binds Ca^{2+} and functions as a multipurpose intracellular Ca^{2+} receptor and mediates most Ca^{2+} regulated processes. Ca^{2+}-calmodulin does not have enzymic activity itself but becomes active when bound to other proteins. Ca^{2+}-Calmodulin dependent protein kinase II (CAMKII) has been revealed as being essential for meiotic resumption and cell cycle progression in amphibian and mammalian eggs

(Lorca et al., 1993; Dupont, 1998). It was reported in frog eggs that inhibitors of CAMKII prevent Ca^{2+}-induced cyclin degradation and constitutively active CAMKII activates unfertilised eggs in the absence of any $[Ca^{2+}]i$ increase (Lorca et al., 1993).

CAMKII is likely to have a similar role in the mouse since ethanol-induced parthenogenetic activation which causes a single $[Ca^{2+}]i$ rise induces a similar rise in CAMKII (Winston and Maro, 1995; Tatone et al., 1999; Tatone et al., 2002). Monotonic rises in $[Ca^{2+}]i$ appear however to cause a transient activation of CAMKII rather then a sustained activation (Winston and Maro, 1995; Tatone et al., 2002). Complete egg activation can be hindered if the nature of the $[Ca^{2+}]i$ transient is insufficient to degrade cyclin B, for example, stopping Ca^{2+} oscillations prematurely has been shown to severely retard pronucleus formation (Lawrence et al., 1998). This suggests that the repetitive nature of sperm-induced $[Ca^{2+}]i$ oscillations in mammalian eggs act to activate CAMKII for a sustained time period to ensure progression through the cell cycle. While it is accepted that the immediate target of Ca^{2+}-calmodulin is CAMKII the exact mechanism of how CAMKII activates the cyclin B destruction pathway is unclear (Nixon et al., 2002).

Cyclin degradation is initiated by fertilisation-induced $[Ca^{2+}]i$ oscillations and is mediated via the Anaphase Promoting Complex (APC) pathway. Consistent with this, $[Ca^{2+}]i$ has been shown to induce assembly of the 26S proteosome from the 20S proteosome in *Xenopus* and ascidian eggs (Kawahara and Yokosawa, 1994; Aizawa et al., 1996). The switching-on of Ca^{2+}-dependent APC pathway which leads to meiotic resumption is likely to be triggered by CAMKII however the exact mechanisms of action are presently unknown. Recently a constitutively active cRNA construct of CAMKIIα was reported to trigger meiotic resumption, pronucleus formation and 2^{nd} polar body extrusion when microinjected into mouse eggs (Madgwick et al., 2005). The spindle poison nocodazole but not the Ca^{2+} chelator BAPTA blocked CAMKII-induced meiotic resumption showing that CAMKII mediates cell-

cycle resumption downstream of sperm-induced Ca^{2+} release but upstream of the APC (Madgwick et al., 2005).

1.2.5 Post-activation affects of $[Ca^{2+}]i$ signalling on preimplantation development

There is mounting evidence that $[Ca^{2+}]i$ oscillations at activation affect the development of the embryo after the first cell cycle. $[Ca^{2+}]i$ transients can be induced and manipulated by means of electrical field pulse which allows complete control over the amplitude, frequency and duration of each spike (Ozil, 1990; Ozil and Swann, 1995). The pattern of $[Ca^{2+}]i$ oscillations during egg activation has been shown to have a profound effect on the percentage of compacted embryos and blastocysts in rabbit (Ozil, 1990) and cow embryos (Collas et al., 1993). The pattern of $[Ca^{2+}]i$ oscillations has also been shown to affect composition of blastocysts in mouse embryos (Bos-Mikich et al., 1997). The same study showed that increasing the duration of St^{2+}-induced $[Ca^{2+}]i$ oscillations from two to four to six hours caused an incremental increase in the number of cells in the ICM (Bos-Mikich et al., 1997).

Improved development has been reported when stimuli which cause an elevation in Ca^{2+} are added to the culture media of developing embryos. The exposure of morula to ethanol or Ca^{2+} ionophore increases the rates of blastocyst cavitations and expansion (Stacheki et al., 1994a). Blastocyst exposure to the same Ca^{2+}-inducing stimuli improves implantation and blastocyst outgrowth in mouse embryos (Stacheki et al., 1994b). In post-implantation development, manipulating the pattern of $[Ca^{2+}]i$ transients has been shown to optimise somite and heart development in rabbit embryos (Ozil and Huneau, 2001), moreover $[Ca^{2+}]i$ elevations have been reported to be necessary for normal long-term developmental changes in somatic cells such as cellular differentiation in embryonic neuronal cells (Spitzer et al., 1994). The mechanism by which these $[Ca^{2+}]i$ signals can have an impact on preimplantation development are unknown yet there is evidence to suggest the nature of the

Ca^{2+} flux patterns can influence gene expression patterns. One report revealed that there was an optimal frequency of $[Ca^{2+}]i$ transients that was most efficient at driving gene expression (Li et al., 1998). This is consistent with other reports that also show repetitive $[Ca^{2+}]i$ oscillations are more efficient at inducing gene expression and were able to trigger expression of a higher number of transcription factors compared to a monotonic rise in $[Ca^{2+}]i$ (Dolmetsch et al., 1998). Mobilisation of Ca^{2+} has also been shown to be a major component in the activation of the transcription factors *fos* and *jun* in rat fibroblasts (Pribnow et al., 1992). Thus, $[Ca^{2+}]i$ oscillations clearly play a part in maintaining normal cellular development and at least in part by mediating changes in transcription factors.

1.2.6 Initiation of Ca^{2+} release by the sperm

Until recently the mechanism by which the sperm triggers Ca^{2+} release in mammalian eggs has been a highly contentious issue. Three models were proposed to explain the Ca^{2+} release mechanism and were termed the conduit, contact and content models (Jaffe, 1991) (Fig 1.1). The content (sperm factor) theory is now a widely accepted phenomenon in mammals and ascidians however it is appropriate to describe the 3 main theories to provide some background and understanding of what is known about $[Ca^{2+}]i$ increases at egg activation. I will discuss the conduit and contact (receptor-ligand) theory briefly in turn before describing the "sperm factor" mechanism in more detail.

In the Ca^{2+} conduit hypothesis, the sperm was proposed to act like a channel or pipe, allowing a continuous influx of extracellular Ca^{2+} into the egg through pores in the sperm membrane (Fig 1.1A). The massive rise of $[Ca^{2+}]i$ was proposed to overload intracellular stores, triggering calcium-induced calcium-release (CICR) (Jaffe, 1991). Support for this model came from reports which showed that sperm-egg fusion was a prelude to $[Ca^{2+}]i$ increase at fertilisation (McCulloh and Chambers, 1992; Lawrence et al., 1997; Jones et al.,

1998a) and Ca^{2+} injection into fish and frog eggs generated a single $[Ca^{2+}]i$ transient (Nuccitelli, 1991). Subsequent findings did not provide support for this model since Ca^{2+} influx into mammalian oocytes was only found to cause a single $[Ca^{2+}]i$ wave and did not produce the hallmark $[Ca^{2+}]i$ oscillations found at fertilisation (Swann and Ozil, 1994). It was also demonstrated that a very low concentration of extracellular Ca^{2+} of 13nM in culture media compared to 1.71mM did not prevent the initiation of $[Ca^{2+}]i$ transients at fertilisation (Jones et al., 1998a).

The contact or receptor-ligand theory states that $[Ca^{2+}]i$ oscillations are initiated through a signal transduction pathway involving the interaction of a sperm ligand to an oocyte plasma membrane receptor (Fig 1.1B) (Foltz and Shilling, 1993) (Schultz and Kopf, 1995). The receptor theory was proposed after studies on sea urchin eggs revealed an increase in $InsP_3$ turnover during fertilisation (Ciapa and Whitaker, 1986). The receptor was proposed to activate an egg derived PLC that in turn causes the hydrolysis of PIP_2, which generates the Ca^{2+}-releasing messenger $InsP_3$. The oocyte receptor was proposed to be coupled to a tyrosine kinase or G protein signalling pathway which triggers the $[Ca^{2+}]i$ increase. However, antibodies to the Gq family of G-proteins were unable to prevent sperm-induced $[Ca^{2+}]i$ increase in mouse eggs (Williams et al., 1998). Although there has been contention about the mechanism of activation at fertilisation it is now widely accepted that $InsP_3$ plays a role in regulating $[Ca^{2+}]i$ oscillations at this time. Many studies have demonstrated that injection of $InsP_3$ generates Ca^{2+} release in rabbit (Fissore and Robl, 1993), bovine (Fissore et al., 1995) and hamster (Miyazaki et al., 1992) eggs. Furthermore, sustained injection of $InsP_3$ has been shown to cause repetitive $[Ca^{2+}]i$ oscillations in mammalian oocytes (Swann and Ozil, 1994). Much of this evidence has been used to validate the receptor-ligand theory rather than supporting the role of $InsP_3$ in sperm-induced Ca^{2+} release. Furthermore, the isolation of many surface molecules involved in sperm-egg binding has not produced any evidence of a

membrane receptor that when activated by fertilisation can cause a $[Ca^{2+}]i$ increase. The most convincing piece of evidence against the receptor-ligand theory came from direct injection of the sperm (ICSI) which bypasses any interaction between the two gametes but results in egg activation and development to term (Kimura and Yanagimachi, 1995).

The sperm factor theory proposes that after sperm-oocyte fusion, a cytosolic sperm factor is introduced into the ooplasm and initiates $[Ca^{2+}]i$ release (Swann, 1990) (Fig 1.1C). This hypothesis justifies many of the observations that could not be explained from the "Ca^{2+} conduit" or "receptor" models. The first substantiation of this model came from studies showing that injection of sea urchin sperm extracts into unfertilised sea urchin eggs caused elevation of the fertilisation envelope; a sign that a $[Ca^{2+}]i$ increase had occurred (Dale et al., 1985). Consistent with the sperm factor hypothesis, in mouse eggs fluorescent dextrans (Lawrence et al., 1997) and large molecular weight proteins (Jones et al., 1998a) have been shown to diffuse between gametes prior to any observed $[Ca^{2+}]i$ changes. Sperm-egg fusion has also been shown to precede the initial $[Ca^{2+}]i$ transient in sea urchin eggs (McCulloh and Chambers, 1992).

During fertilisation in ascidian eggs the sperm triggers two phases of $[Ca^{2+}]i$ oscillations that are separated by duration of approximately five mins. The first few $[Ca^{2+}]i$ waves triggered by fertilisation stimulate cortical contractions, which form a contraction pole. An endoplasmic reticulum-rich domain at the contraction pole becomes a pacemaker from which the 2^{nd} phase of $[Ca^{2+}]i$ waves originates from (McDougall and Sardet, 1995). Injection of ascidian sperm extract roughly equivalent to a single spermatozoon mimics the temporal (Kyozuka et al., 1998) and spatial (McDougall et al., 2000) pattern of $[Ca^{2+}]i$ oscillations triggered by the sperm. These data strongly supports the sperm factor model.

The sperm factor has been reported to act universally across species. Injected porcine sperm extracts have been shown for example, to cause $[Ca^{2+}]i$ oscillations in cow,

mouse (Wu et al., 1997) and hamster (Swann, 1990) eggs. This Ca^{2+} releasing ability is not limited to mammalian sperm factors since microinjection of sperm extracts from frogs, chickens (Dong et al., 2000) and fish (Coward et al., 2003) cause $[Ca^{2+}]i$ oscillations that are similar in pattern to fertilisation-induced $[Ca^{2+}]i$ oscillations in mouse eggs (Dong et al., 2000). Similarly non-mammalian species eggs respond to mammalian sperm factor for example, pig sperm extracts induce $[Ca^{2+}]i$ oscillations when microinjected into the nemertean worm egg (Stricker et al., 2000). Cytosolic soluble extracts derived from flowering plant pollen in *Brassica campestris* have also been shown to stimulate $[Ca^{2+}]i$ oscillations when microinjected into mouse eggs (Li et al., 2001). Cumulatively these findings suggest that the function of the sperm-factor is universally conserved not only across mammalian and non-mammalian species in the animal kingdom but also in the plant kingdom.

Mounting evidence implied that the sperm factor is proteinaceous since it was sensitive to both trypsin and heat and had a high molecular weight (30kDa) (Swann, 1990). Another characteristic of the sperm factor was that it was tissue-specific. When mRNA was isolated from different tissues only mRNA from spermatogenic cells appeared to trigger $[Ca^{2+}]i$ oscillations after microinjection into mouse eggs, which suggested that mRNA encoding the sperm factor can be translated into an active protein in the egg cytoplasm (Parrington et al., 2000).

Further evidence for the sperm factor model comes from ISCI, which bypasses the normal barrier of sperm-egg binding but has been shown to induce $[Ca^{2+}]i$ oscillations in human and mouse eggs, which are similar to those seen at fertilisation (Tesarik et al., 1994; Palermo et al., 1997; Nakano et al., 1997). The biological issues of ICSI have been controversial (Ola et al., 2001), however the high rates of activation and resulting births indicate it is a successful Assisted Reproduction Technology (ART) for couples suffering from infertility problems (Palermo et al., 1992; Palermo et al., 1995).

One of the main criticisms of the sperm factor theory has been that large amounts of sperm extract, predicted to be more than a single sperm equivalent, are needed to cause egg activation (Swann, 1990; Stricker, 1997). However this prediction is likely to be due to the difficulty in extracting the protein from a single sperm without a significant loss of activity during purification. One report indicated that between 1 and 8 sperm is sufficient to trigger $[Ca^{2+}]i$ oscillations in a single egg (Nixon et al., 2000). The adequacy of a single sperm's factor is however obvious since ICSI is sufficient to cause $[Ca^{2+}]i$ oscillations, egg activation and development to term (Palermo et al., 1992; Tesarik et al., 1994; Sato et al., 1999).

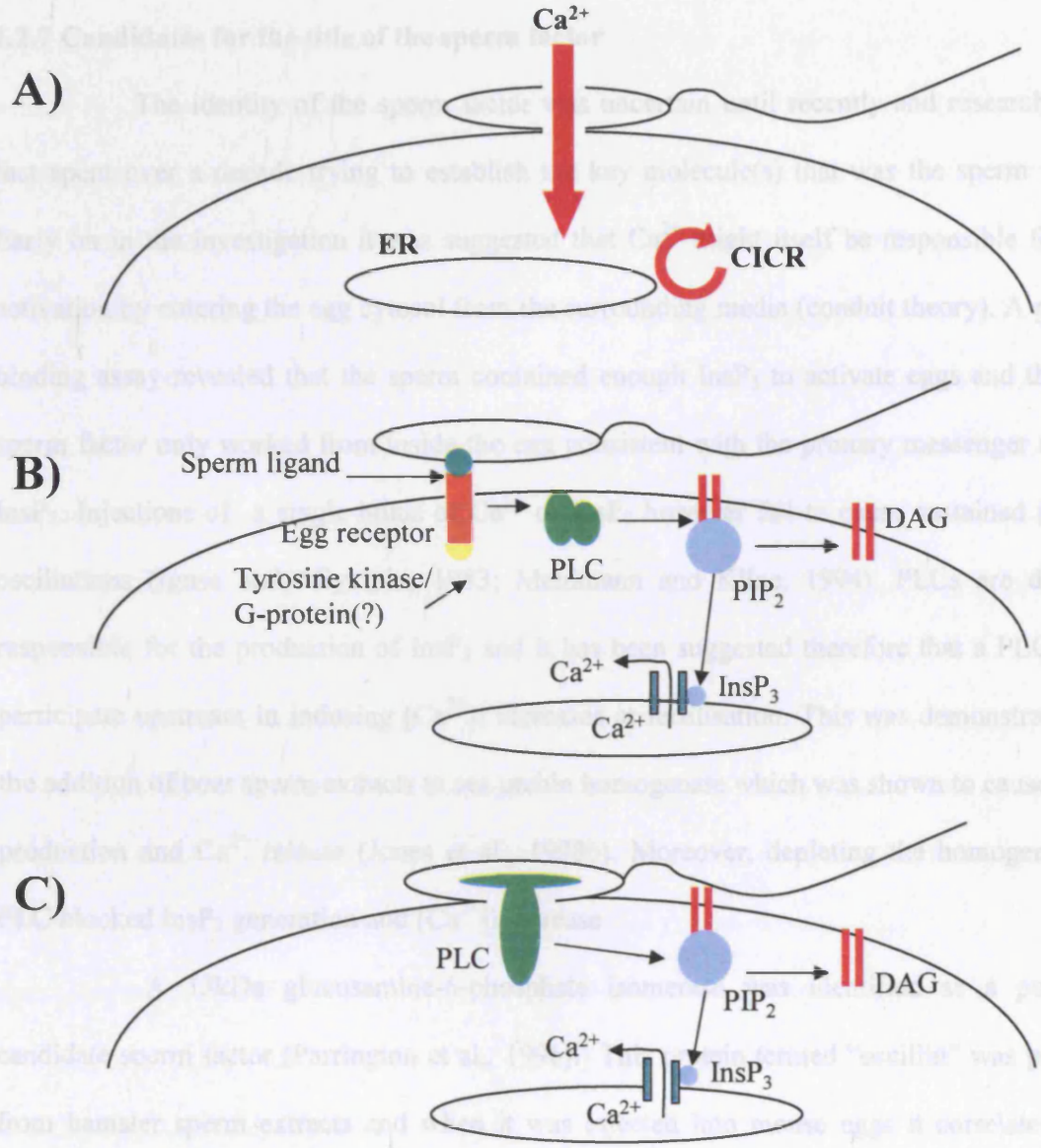

Figure 1.2 Three proposed models of sperm-induced Ca^{2+} release at fertilisation. A) The conduit model describes the sperm as a channel that allows the flow of extracellular Ca^{2+} into the egg which in turn overloads the ER. Subsequent transients were hypothesised to some from Calcium induced-calcium release mechanisms. **B)** The contact model proposes that Ca^{2+} increases are initiated through a signal transduction pathways which is activated through contact between a sperm ligand and egg receptor. The egg receptor may be coupled to a G-protein or Tyrosine kinase which in turn activates a phospholipase C (PLC) which splits phosphatidylinositol 4,5-bisphosphate (PIP_2) into inositol 1,4,5-trisphosphate ($InsP_3$) and diacylglycerol (DAG). $InsP_3$ binds to $InsP_3R$'s stimulating $InsP_3$-induced Ca^{2+} release. **C)** The content model proposes that a cytosolic sperm factor enters the egg from the sperm after sperm-egg fusion and induces Ca^{2+} release by the $InsP_3$ pathway. Recent evidence has put this model in favour and shown the sperm factor is in fact a PLC termed PLCζ (Saunders et al, 2002).

1.2.7 Candidates for the title of the sperm factor

The identity of the sperm factor was uncertain until recently and researchers in fact spent over a decade trying to establish the key molecule(s) that was the sperm factor. Early on in the investigation it was suggested that Ca^{2+} might itself be responsible for egg activation by entering the egg cytosol from the surrounding media (conduit theory). A protein binding assay revealed that the sperm contained enough $InsP_3$ to activate eggs and that the sperm factor only worked from inside the egg consistent with the primary messenger role of $InsP_3$. Injections of a single bolus of Ca^{2+} or $InsP_3$ however fail to cause sustained $[Ca^{2+}]i$ oscillations (Igusa and Miyazaki, 1983; Mehlmann and Kline, 1994). PLCs are directly responsible for the production of $InsP_3$ and it has been suggested therefore that a PLC must participate upstream in inducing $[Ca^{2+}]i$ increases at fertilisation. This was demonstrated by the addition of boar sperm extracts to sea urchin homogenate which was shown to cause $InsP_3$ production and Ca^{2+} release (Jones et al., 1998b). Moreover, depleting the homogenate of PLC blocked $InsP_3$ generation and $[Ca^{2+}]i$ increase

A 33kDa glucosamine-6-phosphate isomerase was identified as a potential candidate sperm factor (Parrington et al., 1996). This protein termed "oscillin" was purified from hamster sperm extracts and when it was injected into mouse eggs it correlated with $[Ca^{2+}]i$ release. Injection of recombinant oscillin into eggs did not however cause any $[Ca^{2+}]i$ oscillations (Wolosker et al., 1998). Parrington's group used SDS gels to reveal that oscillin was present in sperm extracts. The gel displayed a major band at 35kDa along with several other lower weight bands. It has been suggested that since they used a Coomasie brilliant blue R-250 dye which is less sensitive than silver stains the Ca^{2+} releasing ability of the oscillin extract was not directly attributable to oscillin but other proteins present in the extract (Wolosker et al., 1998).

Another possible candidate for the sperm factor is a truncated form of the c-kit receptor named tr-kit. Injection of recombinent tr-kit protein or its complementary RNA into mouse eggs was reported to be sufficient to cause egg activation and 30% of embryos reached past the 2-cell stage (Sette et al., 1997). There were however a number of different observations about tr-kit that did not fit into the sperm-factor theory, for example tr-kit was predominantly located in the sperm midpiece and not the sperm head, which is known to activate eggs after ICSI is performed. There was also no evidence that injection of tr-kit could induce $[Ca^{2+}]i$ oscillations in unfertilised eggs. A SH3 domain containing construct, inhibited activation in tr-kit injected eggs but did not block activation in fertilisation-induced activation suggesting that tr-kit activates eggs by a different mechanism than that which occurs at fertilisation.

One group have reported that nitric oxide (NO) triggers $[Ca^{2+}]i$ oscillations and all the events associated with egg activation in sea urchin eggs (Kuo et al., 2000). The same group also showed that the NO-scavenger oxyhaemoglobin prevented egg activation (Kuo et al., 2000). This finding is not however supported by studies on mouse and ascidian eggs that show sperm-induced $[Ca^{2+}]i$ increases were not associated with any global or local change in NO (Hyslop et al., 2001). Furthermore, an NO synthase inhibitor failed to block sperm-induced Ca^{2+} rises (Hyslop et al., 2001).

One of the definitive tests that all candidates for the title of the sperm factor should be tested on is their ability to reproduce the distinct $[Ca^{2+}]i$ oscillations that are observed at fertilisation. Until recently all candidates put forward for the title of the sperm factor had failed to induce these hallmark repetitive $[Ca^{2+}]i$ oscillations.

A novel phospholipase C termed PLCζ (zeta) was recently identified as the sperm factor following a mouse testis Expressed Sequence Tag (EST) database searches (Saunders et al., 2002). Injection of cRNA encoding PLCζ was found to trigger long lasting $[Ca^{2+}]i$

oscillations that were indistinguishable from those observed at fertilisation. Consistent with this, a recombinant PLCζ has also been shown to produce $[Ca^{2+}]i$ oscillations in mouse eggs that are indistinguishable from those observed at fertilisation (Kouchi et al., 2004). The amount of PLCζ required to induce $[Ca^{2+}]i$ oscillations similar to those at fertilisation were assayed and found to be equivalent to approximately one sperm's worth (Saunders et al., 2002). Removal of PLCζ from sperm extracts using antibodies specific to PLCζ inhibited $[Ca^{2+}]i$ oscillations when microinjected into mouse eggs and this confirmed that PLCζ is the single responsible factor which induces egg activation (Saunders et al., 2002). Microinjection of PLCζ cRNA has also been shown to cause activation and development up till the blastocyst stage with success rates similar to those seen after IVF (Saunders et al., 2002).

PLCζ complements previous clues about the nature of the sperm factor. The sperm factor was proposed to be a universal factor which acted across species. This proposition is supported by reports that show that human and monkey PLCζ can stimulate activation and development to the blastocyst stage in mouse eggs (Cox et al., 2002). Recent studies have also demonstrated that a PLCζ orthologue is present in a non-mammalian vertebrate, the domestic chicken. Recombinant chicken PLCζ cRNA can stimulate $[Ca^{2+}]i$ oscillations when microinjected into mouse eggs suggesting that PLCζ could be functionally conserved in other non-mammalian vertebrates (Coward et al., 2005).

1.2.8 $[Ca^{2+}]i$ releasing ability of PLCζ

Five isoforms of the PLC family (β, γ, δ, ε and ζ) have been classified on the basis of their sequence homology. PLCζ is a unique PLC on the basis that it can induce Ca^{2+} oscillations in eggs at concentrations as low as 10 femtograms per egg (Saunders et al, 2002). PLC isoforms β, γ, δ have been shown to be ineffective at inducing $[Ca^{2+}]i$ increases when tested in sea urchin homogenate and mouse eggs (Jones et al., 2000). A much higher concentration (~20-

fold) of recombinant PLCδ protein was shown to be required to induce $[Ca^{2+}]i$ oscillations compared to PLCζ, which had at least 100-fold higher Ca^{2+} sensitivity than PLC δ (Kouchi et al., 2004).

Structural analysis reveals that PLCs comprise of a number of core domains such as X and Y catalytic core domains which forms the active site where enzymic cleavage of PIP_2 takes place. All PLCs also contain a lipid-binding C2 domain and Ca^{2+} binding EF-hand domains. PLCζ is distinct from other PLCs because it lacks a PH domain which targets the PLC to phosphoinositides. Since all other PLC's contain a PH domain and are incapable of causing $[Ca^{2+}]i$ oscillations in mouse eggs, the lack of a PH domain may be an important characteristic of Ca^{2+} releasing ability in PLCζ (Saunders et al., 2002). Studies on human, monkey, chicken and mouse PLCζ are consistent with this since they have all been found to lack the PH domain found on other PLC isoforms (Cox et al., 2002; Coward et al., 2005).

Two recent studies examining the role of the EF-hand domains used PLCζ domain-deletion constructs to determine which domains were critical for PIP_2 hydrolysis and inducing $[Ca^{2+}]i$ oscillations in mouse eggs (Kouchi et al., 2005; Nomikos et al., 2005). One study showed that removal of either EF-hand domain did not affect PIP2 hydrolysis however Ca^{2+} sensitivity was greatly reduced (Nomikos et al., 2005). In contrast the other study revealed that deletions of EF1 and EF2 of the N-terminal four EF-hand domains caused a great reduction in PIP2 hydrolysis and complete loss of Ca^{2+} releasing ability (Kouchi et al., 2005). Deletion of all four EF-hand domains caused complete inactivity of PLCζ (Kouchi et al., 2005) indicating that both domains are crucial for the activity of PLCζ (Kouchi et al., 2005; Nomikos et al., 2005).

Comparisons of the cellular and molecular aspects of PLCζ from human (hPLCζ), cynomolgus monkey (cPLCζ) and mouse (mPLCζ) in their ability to cause $[Ca^{2+}]i$ oscillations in mouse eggs have recently been investigated (Cox et al., 2002). Microinjection of hPLCζ

cRNA was found to be most effective at causing $[Ca^{2+}]i$ oscillations in mouse eggs compared to microinjection of cPLCζ or mPLCζ (Cox et al., 2002).The reasons for this finding are unclear, although a number of reasons have been proposed. Firstly, the domain structures of all three PLC's were investigated and it was discovered that the X-Y linker segment (the region between the X and Y catalytic domains) was shortest in the hPLC and this may be related to the effectiveness of this PLCζ. Differences in the efficiency of PLCζ at causing $[Ca^{2+}]i$ oscillations may also reflect the variation in size of different species' eggs. The human egg for example, is several times larger than that of a mouse egg and may thus require a more potent Ca^{2+}-releasing PLCζ. Some species may alternatively have eggs which happen to be more sensitive to PLCζ than others, the hamster egg for example was found to be much less sensitive to sperm extracts compared to the mouse egg (Parrington et al., 1996). PLCζ injection could in the future become a possible treatment for eggs that fail to fertilise after ART since it provides a natural Ca^{2+} signal to the egg which appears to be absent in the case of male factor infertility. PLCζ may also be used as an alternative activation protocol in nuclear transfer or for the parthenogenetic generation of embryonic stem cells.

1.2.9 Sperm-induced Ca^{2+} release is cell-cycle dependent.

The generation of $[Ca^{2+}]i$ transients is regulated in a cell-cycle dependent manner. The sperm triggers a series of $[Ca^{2+}]i$ oscillations that last for several hours and cease at the time of the formation of pronuclei and the entry into interphase (Jones et al., 1995a). Interphase is marked by a time when no $[Ca^{2+}]i$ increases occur. Nuclear envelope breakdown (NEBD) at the first mitosis is associated with a single (Tombes et al., 1992) or multiple $[Ca^{2+}]i$ transients (Kono et al., 1996; Marangos et al., 2003; Larman et al., 2004). Some studies have reported that $InsP_3R$ down-regulation occurs after fertilisation or sperm extract injection (Brind et al.,

2000; Jellerette et al., 2000), which may explain the reduction in egg sensitivity to $InsP_3$-induced Ca^{2+} release during interphase.

These findings support the observations that $[Ca^{2+}]i$ oscillations cease after duration of several hours of fertilisation-induced $[Ca^{2+}]i$ oscillations, however it does not explain why this correlates with pronuclei formation and why $[Ca^{2+}]i$ increases occur at NEBD. Accumulating evidence indicates that during pronuclei formation a Ca^{2+} releasing factor (PLCζ) is sequestered into the pronuclei resulting in the cessation of $[Ca^{2+}]i$ oscillations (Marangos et al., 2003; Larman et al., 2004; Yoda et al., 2004). Nuclear sequestration has been supported using a number of different experimental approaches.

One study reported that inhibiting pronucleus formation with wheat germ agglutinin or preventing nuclear import prolonged $[Ca^{2+}]i$ oscillations for up to 12 hours compared to 4 hours in controls (Marangos et al., 2003). A recent key study has not only added support to the nuclear sequestration hypothesis but also provided confirmation that PLCζ is the Ca^{2+} releasing factor. PLCζ-induced $[Ca^{2+}]i$ oscillations were revealed to have the same cell-cycle dependency during the first cell-cycle as fertilised eggs. A nuclear localisation factor (NLS) present on the PLCζ X-Y linker region led to nuclear sequestration and mutating the NLS to be non-functional greatly prolonged the $[Ca^{2+}]i$ oscillations, which continued into interphase (Larman et al., 2004). Preventing pronuclei formation also prolonged PLC-induced $[Ca^{2+}]i$ oscillations (Larman et al., 2004). Mitotic $[Ca^{2+}]i$ transients have only been observed in fertilised but not parthenogenetic embryos which was interpreted as indicating that a paternally derived factor from the sperm was responsible for stimulating the $[Ca^{2+}]i$ oscillations observed at fertilisation (Kono et al., 1996).

1.2.10 Ca^{2+}-dependent parthenogenetic egg activation

As described above, the sperm provides a natural stimulus to the MII arrested egg, which is responsible for 'kick-starting' egg activation and embryo development. Parthenogenetic activation is defined as the process by which egg activation occurs in a female gamete to which there has been no contribution from the male genome (Kaufman, 1979). Induced parthenogenetic activation can be used as a model for studying the events of activation and early embryo development. Artificial activation can also be successfully applied clinically to facilitate ART and in a biotechnology setting to improve nuclear transfer rates to generate stem cells. Parthenogenetic activation is also particularly relevant to this thesis because I use this method as a main tool to activate eggs. I will therefore describe and explain the advantages and disadvantages of various stimuli used to activate eggs.

Egg activation can be induced parthenogenetically by treating eggs with various chemical or physical stimuli that trigger single or multiple $[Ca^{2+}]i$ increases (Fig 1.3A). Physical disruption by pricking the plasma membrane with a fine needle causes Ca^{2+} influx and has been reported to efficiently activate *Xenopus* (Uehara and Yanagimachi, 1977) and hamster eggs (Kline and Nuccitelli, 1985; Kline and Nuccitelli, 1985). A simple injection of Ca^{2+} into the eggs of a number of species such as the sea urchin (Hamaguchi and Hiramoto, 1981), mouse (Fulton and Whittingham, 1978) and pig (Machaty et al., 1996) has also been shown to induce all the events associated with egg activation (Fulton and Whittingham, 1978; Machaty et al., 1996).

Egg activation using chemical stimuli has commonly involved the use of treatments such as ethanol, ionomycin and Ca^{2+} ionophore A23187, which are sufficient to trigger egg activation by means of inducing a single $[Ca^{2+}]i$ transient in the egg (Swann and Ozil, 1994; Xu et al., 1997). Ethanol treatment causes the temporary opening of membrane calcium channels causing influx of extracellular Ca^{2+} as well as the formation of $InsP_3$, which

leads to release of Ca^{2+} from intracellular stores (Presicce and Yang, 1994). Ca^{2+} ionophore A23187 similarly promotes the release of Ca^{2+} from intracellular stores and the influx of extracellular Ca^{2+} (Kline and Kline, 1992). With increasing time after ovulation mammalian eggs become more sensitive to artificial stimuli that trigger egg activation. The rate of activation is low in freshly ovulated eggs that are treated with agents that induce single transients compared to stimuli that induce multiple $[Ca^{2+}]i$ transients (Ozil, 1990; Xu et al., 1997). Although agents that cause a monotonic rise in $[Ca^{2+}]i$ are sufficient to cause activation, an initial rise in $[Ca^{2+}]i$ during mammalian fertilisation is followed by a series of repetitive $[Ca^{2+}]i$ transients. Thus, parthenogenetic agents that mimic the naturally occurring $[Ca^{2+}]i$ transients are often used as alternatives to agents that cause a single $[Ca^{2+}]i$ increase. Thimerosal, a thiol reagent that probably acts by oxidising critical sulphydryl groups on intracellular Ca^{2+} release proteins and induces $[Ca^{2+}]i$ transients that are remarkably similar to those at fertilisation with regard to their amplitude, width and attack (Cheek et al., 1993). Thimerosal has been shown to cause $[Ca^{2+}]i$ oscillations in hamster (Swann, 1991), human (Homa and Swann, 1994), mouse (Cheek et al., 1993), bovine (Fissore et al., 1995) and rabbit (Fissore and Robl, 1993) eggs. Although thimerosal treatment of eggs has also been reported to cause cortical granule exocytosis (CGE) it does not cause complete egg activation (Cheek et al., 1993). Thimerosal has been shown to cause meiotic spindle disassembly and since an intact spindle is required for transition from M-phase to interphase, these eggs cannot be released from MII arrest. Disassembly of the meiotic spindle can however be reversed by the reducing agent dithiothreitol (DTT) so that a combined treatment of thimerosal and DTT induces full activation and development to the blastocyst stage in pig eggs (Machaty et al., 1997).

Phorbol ester, an activator of protein kinase C (PKC) has been reported to cause $[Ca^{2+}]i$ oscillations and pronuclear formation in mouse eggs (Cuthbertson and Cobbold,

1985). Other studies have failed to measure any $[Ca^{2+}]i$ increase using phorbol ester and have concluded that phorbol ester can activate PKC in the absence of Ca^{2+} and upon activation PKC can mediate activation-associated processes such as cortical granule exocytosis and cytokinesis (Bement and Capco, 1990). Phorbol ester failed however to activate a significant proportion of eggs, with very few reaching the blastocyst stage compared to when Ca^{2+} ionophore was used as an activating agent (Uranga et al., 1996).

Incubating mouse oocytes in Ca^{2+}-free media containing strontium ions (Sr^{2+}) induces $[Ca^{2+}]i$ oscillations similar to those seen at fertilisation, which in turn causes the associated events of egg activation to occur (Fraser, 1987; Fraser, 1987). Sr^{2+} like Ca^{2+} probably mobilises Ca^{2+} from intracellular stores by increasing the affinity of $InsP_3R$ for $InsP_3$ (Marshall and Taylor, 1994). Sr^{2+} causes the sensitisation of $InsP_3$-stimulated Ca^{2+} release with only three-fold less potency than Ca^{2+} (Marshall and Taylor, 1994). Sr^{2+} has been used in nuclear transfer technology to activate mice oocytes which have then successfully developed to term (Wakayama et al., 2005). Sr^{2+} treatment does not however cause $[Ca^{2+}]i$ oscillations in human, pig (unpublished observations) and domestic animal eggs.

Electrical stimulation (electroporation) of mammalian oocytes has been shown to cause $[Ca^{2+}]i$ oscillations and a high proportion of activation. Electrical-field pulses cause the formation of transient pores in the plasma membrane which allows Ca^{2+} ions present in the extracellular media to enter the cell. The main benefit of this technique is that it allows complete control over the $[Ca^{2+}]i$ transients exhibited by the eggs. This technique has been successfully used to show that the amplitude, frequency and number of $[Ca^{2+}]i$ transients affect rabbit postimplantation embryo development (Ozil and Huneau, 2001).

1.2.11 Ca^{2+}-independent parthenogenetic egg activation

One way to activate eggs in a Ca^{2+}-independent manner is to inhibit MPF activity using broad-range inhibitors of protein synthesis or protein phosphorylation (Fig 1.3B). Incubation of MII arrested eggs for 6 hours or longer in cyclohexamide (CX) or puromycin is sufficient to cause egg activation (Siracusa et al., 1978; Moses and Kline, 1995). Pronuclear formation occurred when protein synthesis was almost totally inhibited and activation was induced when the levels of protein synthesis are depressed by more than 70% (Siracusa et al., 1978). Puromycin has also been reported as an effective inhibitor of human eggs (Balakier and Casper, 1993). In many species such as the pig, these inhibitors are not sufficient to cause egg activation when used alone (Nussbaum and Prather, 1995) but when used in combination with a Ca^{2+} inducing stimulus such as electrical-field pulses, egg activation can be successfully accomplished with high efficiency (Nussbaum and Prather, 1995). The combination of a protein synthesis inhibitor with a Ca^{2+} inducing stimulus is in fact commonly used in nuclear transfer (NT). Activation of bovine eggs with ethanol and CX after NT lead to activation and development to term (Zakhartchenko et al., 1999). A major limitation with using protein synthesis inhibitors such as CX is that they do not just deplete the cell of the proteins that maintain MPF but also from proteins that function in critical processes such as cell cycle progression. A delay in the initiation of protein synthesis has in fact been reported in eggs activated by ethanol and CX (Alberio et al., 2001a). It is unsurprising that abnormalities in postimplantation development such as skeletal malformations, hydroallantios and perinatal death have been shown to occur in embryos activated with CX (Zakhartchenko et al., 1999).

The inhibition of MPF can be carried out by the binding of specific cyclin-dependent kinase inhibitors (cdkI). The non-specific serine/ threonine kinase inhibitor 6-DMAP for example, inhibits the phosphorylation of many proteins. Under normal circumstances, MPF activity is kept high by the action of various kinases that regulate its

phosphorylation status. The cdc25 activates MPF by dephosphorylation of the tyr15 site on cdk1. 6-DMAP inhibits the activation site of cdc25 which inactivates MPF and causes meiotic resumption. 6-DMAP treatment has been reported however as an ineffective treatment for activating many eggs such as those from the mouse and cow (Liu et al., 1998; Szollosi et al., 1993). 6-DMAP has been reported to accelerate many post-fertilisation events such as pronucleus formation and microtubule formation (Szollosi et al., 1993) and is very effective at artificial activation when used in combination with the Ca^{2+} ionophore ionomycin, which has lead to high rates of activation and blastocyst formation in sheep and cow eggs (Loi et al., 1998; Liu et al., 1998). 6-DMAP activation has however been associated with a number of placental and embryonic abnormalities suggesting that it may hinder a number of kinases that are important for development (Cibelli et al., 1998).

Roscovitine (6-benzylamino-9-isopropylpurine) and its analogue bohemine belong to a group of purine derivatives, which specifically inhibit the cyclin-dependent kinases cdc2, cdk2 and cdk5. Roscovitine inhibits MPF activity by targeting its ATP binding site (Meijer et al., 1997) and has thus been used to activate eggs artificially (Phillips et al., 2002). Roscovitine treatment has been reported to cause high rates of egg activation in mouse eggs however very few of these parthenotes develop beyond the 8-cell stage (Phillips et al., 2002). This suggests that the developmental competency of embryos activated by the inhibition of these kinases is limited.

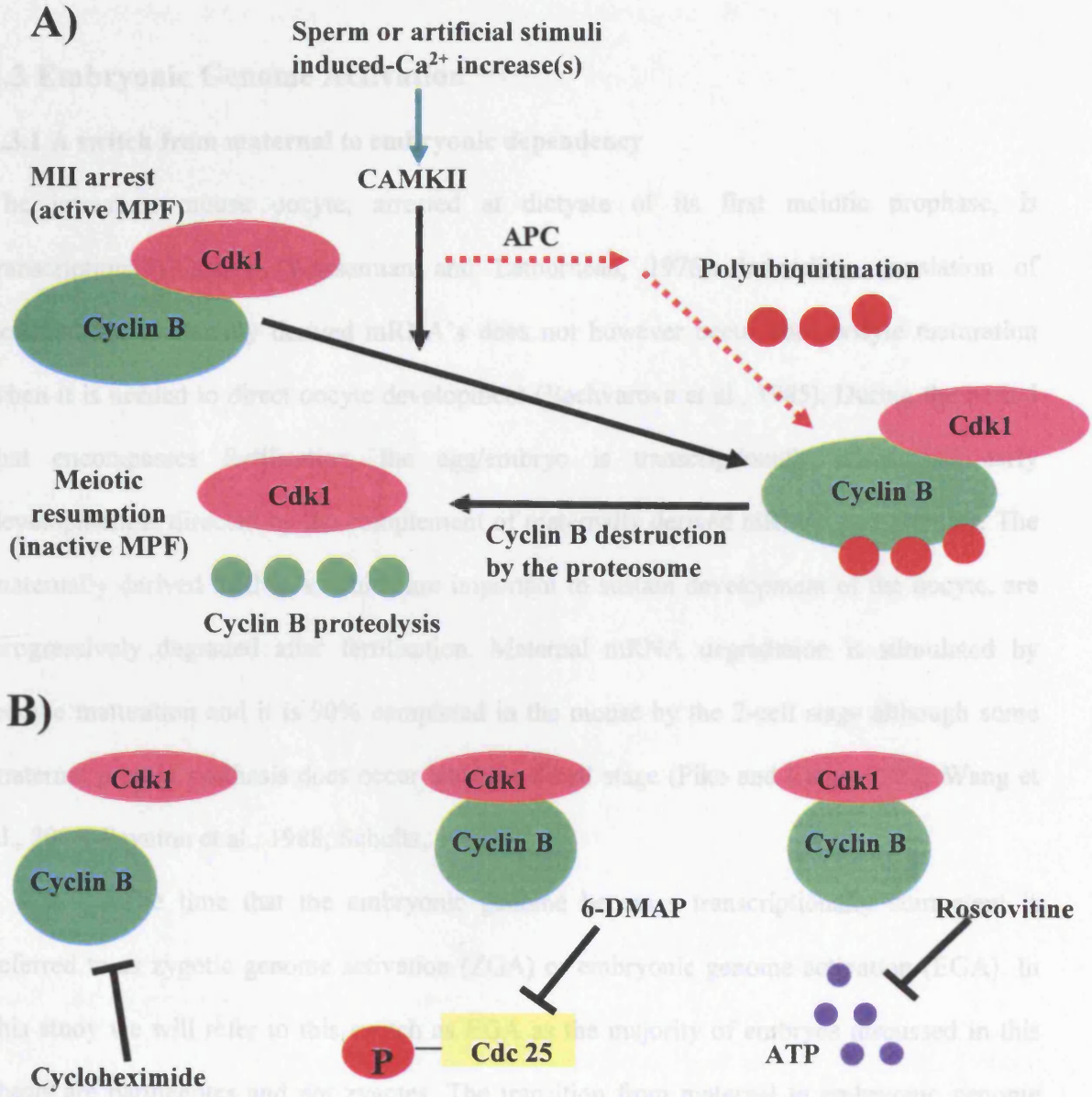

Figure1.3 Mechanisms of inducing artificial egg activation. A) Egg activation using Ca^{2+} dependent means. The egg is arrested in MII by active MPF. Ca2+ increases triggered by stimuli such as sperm, strontium ions or ionomycin are thought to activate CAMKII. CAMKII triggers the activation of the APC which targets cyclin B for destruction by the proteosome by polyubiquitination of its destruction-box. Cyclin proteolysis results in inactive MPF and release from MII arrest. B) Ca^{2+}-independent activation can be induced using stimuli that cause MPF inactivation. Cyclohexamide, a protein synthesis inhibitor works by preventing the synthesis of cyclin B. 6-DMAP inhibits the phosphatase cdc25, which normally acts to keep MPF active.Roscovitine targets the ATP binding site on MPF

1.3 Embryonic Genome Activation

1.3.1 A switch from maternal to embryonic dependency

The immature mouse oocyte, arrested at dictyate of its first meiotic prophase, is transcriptionally active (Wassarman and Letourneau, 1976). Immediate translation of accumulated maternally derived mRNA's does not however occur until oocyte maturation when it is needed to direct oocyte development (Bachvarova et al., 1985). During the period that encompasses fertilisation, the egg/embryo is transcriptionally silent and early development is directed by the complement of maternally derived mRNAs and proteins. The maternally derived mRNA's, which are important to sustain development of the oocyte, are progressively degraded after fertilisation. Maternal mRNA degradation is stimulated by oocyte maturation and it is 90% completed in the mouse by the 2-cell stage although some maternal protein synthesis does occur until the 8-cell stage (Piko and Clegg, 1982; Wang et al., 2004; Paynton et al., 1988; Schultz, 1993).

The time that the embryonic genome becomes transcriptionally competent is referred to as zygotic genome activation (ZGA) or embryonic genome activation (EGA). In this study we will refer to this switch as EGA as the majority of embryos discussed in this thesis are parthenotes and not zygotes. The transition from maternal to embryonic genome dependency has a number of functions that are critical for the continued development of the embryo (Schultz and Worrad, 1995). EGA replaces the degraded maternal transcripts that are common to both the oocyte and embryo, with zygotic transcripts. These transcripts are important for basic cellular functions since preventing the replenishment of maternal transcripts results in developmental arrest (Schultz and Worrad, 1995). EGA is also critical for the generation of novel transcripts that are not present in the oocyte and are therefore

unique to the embryo (Piko and Clegg, 1982; Bachvarova et al., 1989). EGA is characterised by the sensitivity of the embryo to transcription. The treatment of fertilised embryos with α-amanatin, a specific inhibitor of RNA polymerases II and III, result in cell cleavage arrest usually within one cell division.

In the mouse EGA appears to occur in two phases (Fig 1.4). The first phase is evident during G2 of the 1st cell cycle (Latham et al., 1991) and directs the synthesis of approximately 40 proteins (Figure 1.3) (Latham et al., 1991; Schultz, 1993). This 'early' phase involves the synthesis of a relatively small number of novel proteins and is referred to as 'minor EGA'.A much larger increase in embryonic protein synthesis occurs about 10-12 hours later than the minor EGA during the G2 phase of the 2-cell embryos (Flach et al., 1982). This later phase is termed 'major EGA' and is a requirement for further embryo development (Latham et al., 1991; Christians et al., 1995). Many species have a biphasic EGA. The embryonic genome of the cow embryo is for example, fully activated by the 8-cell stage although this is preceded by a minor activation which occurs at the late 1-cell stage (Petzoldt and Muggleton-Harris, 1987).

1.3.2 The Zygotic Clock and initiation of EGA

The onset of minor EGA is governed by a time-dependent mechanism (termed the zygotic clock) rather than by a particular cell cycle event. This is evident in the mouse embryo where minor EGA occurs around 24 hours after fertilisation, independent of whether or not the 1-cell embryo has completed S phase and formed a 2-cell embryo (Schultz, 1993; Bolton et al., 1984). When 1-cell embryos that have not yet formed pronuclei are incubated in aphidocolin (an inhibitor of replicative DNA polymerases), they arrest development when they reach S-phase but minor EGA still occurs at the time corresponding to when they would ordinarily

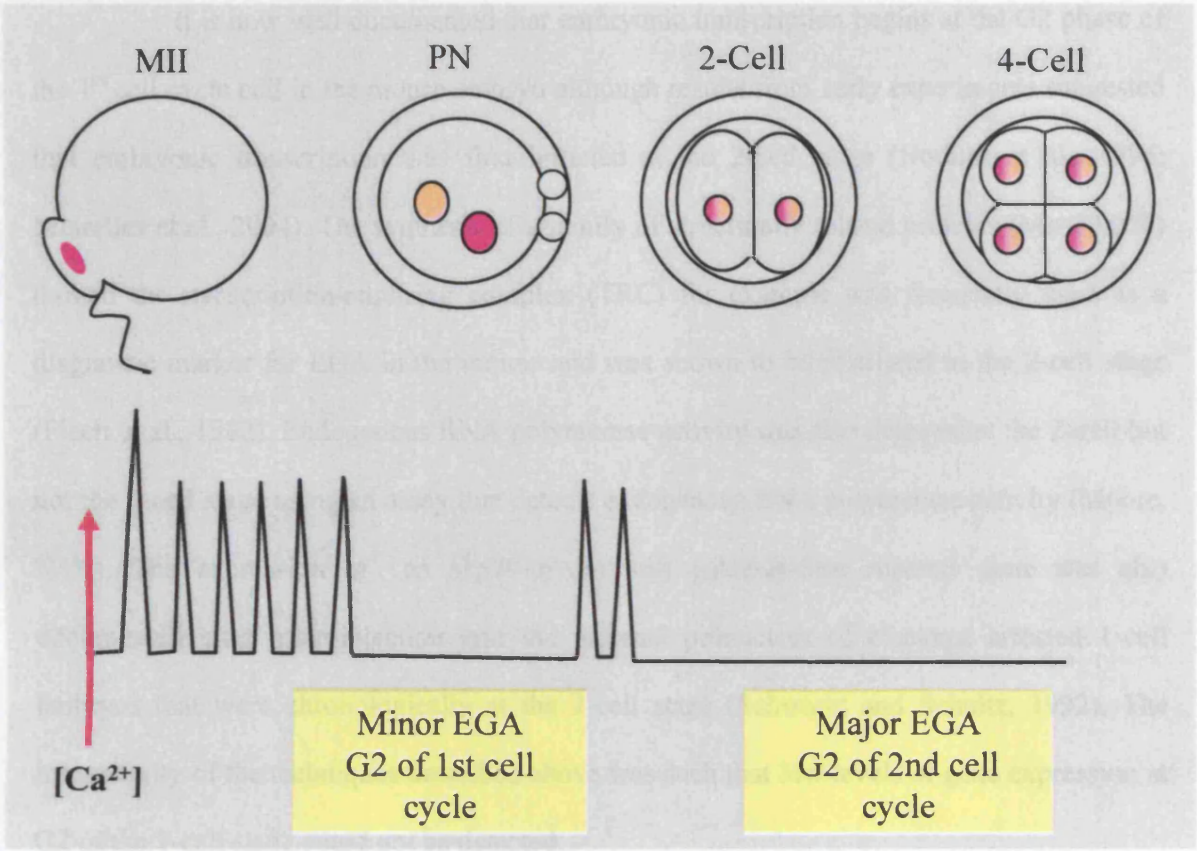

Figure 1.4 Minor and major phases of embryonic genome activation. The egg is arrested at metaphase of the 2nd cell cycle (MII). If fertilisation occurs the egg is released from MII and pronuclei form. During the G2 phase of the first cell cycle the egg a small wave of gene activation occurs. This marks the first event whereby the embryo is transcriptionally competent and is referred to as minor EGA. Minor EGA appears to be governed by a zygotic clock since it is independent of any cell division events. A much larger gene activation event occurs at G2 of the 2nd cell cycle and is referred to as Major EGA. This event is dependent on minor EGA and the first cell division event.

have become 2-cell embryos. In contrast to minor EGA, major EGA is dependent on cell-cycle progression until the 2-cell stage in mice (Howlett, 1986).

It is now well documented that embryonic transcription begins at the G2 phase of the 1st cell cycle cell in the mouse embryo although results from early experiments suggested that embryonic transcription was first initiated at the 2-cell stage (Nothias et al., 1996; Meirelles et al., 2004). The synthesis of a family of structurally related proteins (Mr=70,000) termed the transcription-requiring complex (TRC) for example was frequently used as a diagnostic marker for EGA in the mouse and was shown to be restricted to the 2-cell stage (Flach et al., 1982). Endogenous RNA polymerase activity was also detected at the 2-cell but not the 1-cell stage using an assay that detects endogenous RNA polymerase activity (Moore, 1975). The expression of an hsp70-driven beta galactosidase reporter gene was also documented after microinjection into the paternal pronucleus of cleavage arrested 1-cell embryos that were chronologically at the 2-cell stage (Schwartz and Schultz, 1992). The insensitivity of the techniques described above was such that low levels of gene expression at G2 of the 1-cell stage could not be detected.

The development of highly sensitive techniques provided evidence in support of a transcriptionally permissive state developing at the 1-cell stage. Expression of an Sp1-dependent luciferase reporter gene was readily detected for example at the G2 stage of the first cell cycle (Ram and Schultz, 1993). Consistent with this, luciferase transcripts are detected following fertilisation at the 1-cell stage after using transgenic sperm containing a luciferase transgene driven by β-actin expression (Matsumoto et al., 1994), moreover TRC synthesis was detected at G2 of the 1st cell cycle following transplantation of a 2-cell embryo nucleus treated with α-amanitin into an enucleated 1-cell embryo (Latham et al., 1992). The expression of TRC genes was however much greater following transfer into late rather than early 1-cell stage recipient embryos (Latham et al., 1992). The replacement of inactive RNA

polymerase II from the 2-cell with functional RNA polymerase II from the enucleated 1-cell embryo is likely to be responsible for driving the transcription of TRC.

1.3.3 Measuring EGA

In the past gene expression during the maternal-to-embryonic transition was measured using plasmid-borne reporter genes that encode either luciferase (Ram and Schultz, 1993; Wiekowski et al., 1991) or β-galactosidase (Vernet et al., 1993). The outcome drawn from this method was consistent with the results obtained from expression of integrated transgenes (Christians et al., 1995; Matsumoto et al., 1994) and endogenous genes (Manejwala et al., 1991) regarding the onset of a transcriptionally permissive state. One major disadvantage of these gene expression assay systems is that they have to be measured by destructive analysis (lysis) of eggs taken from cohorts of treated eggs. This prevents a full profile of gene activity from an individual embryo during developmental transition and cannot be measured in real-time. Real time imaging of transcriptional activity has been carried out in live mouse preimplantation embryos that carry a transgene encoding the secreted luminescent reporter, *Vargula* luciferase (Thompson et al., 1995). In this study the culture medium was assayed for luciferase activity so transfers of an embryo to new drops of culture medium for each measurement were required.

Gene expression has been quantitatively analysed in preimplantation mouse embryos using the Green Fluorescent Protein (GFP) reporter gene (Medvedev et al., 2002). GFP is advantageous in monitoring embryos because it requires no substrates apart from oxygen and it is essentially non-toxic and resistant to proteases. The temporal dynamics of gene expression can also be monitored and quantitatively measured in real time. This method is limited though, because UV light is required to measure GFP fluorescence and this is detrimental to the developmental capacity of the embryo. Only two recordings could therefore

be taken every 24 hours, preventing a detailed study of gene expression during a critical time of development, furthermore gene expression could only be detected from the embryonic four-cell stage (Medvedev et al., 2002). In Chapter 5 I will describe a highly sensitive luminescent technique which I employed to measure gene expression in real time during EGA in mouse embryos.

1.3.4 Role of chromatin assembly during EGA

A number of studies have shown that functional differences exist between the maternal and paternal pronuclei to support transcription and which are likely to be due to a chromatin-mediated repression. The maternal pronucleus inherits repression factors from the oocyte which are absent in the male pronucleus. A number of studies support the idea that the maternally-derived pronucleus is transcriptionally repressed in comparison to the paternal pronucleus. The Sp1-dependent luciferase reporter gene is preferentially expressed in G2 of the 1st cell cycle following microinjection of the paternal pronucleus compared to microinjection of the maternal pronucleus (Ram and Schultz, 1993). BrUTP incorporation studies similarly show that transcription is primarily in the paternal pronucleus during this time period (Aoki et al., 1997). These differences in transcriptional activity are concurrent with the finding that nuclear concentration of the transcription factors Sp1 and TATA-box binding protein is greater in the male pronucleus as compared to that of the female pronucleus (Worrad et al., 1994). The nuclear concentrations of these transcription factors increase in a time-dependent fashion during the 1st cell cycle and are dependent on DNA synthesis but not transcription or cytokinesis (Worrad et al., 1994).

The massive reprogramming of gene expression that is initiated at the late 1-cell stage in mice is followed by a transcriptionally repressive state **(Wiekowski et al., 1991)** which is initiated at the 2-cell stage but increases as development proceeds to the 4-cell stage

(Henery et al., 1995). When 1-cell embryos injected with reporter genes are developed to the 2-cell stage the gene expression levels are reduced to less than 1% of that at S-phase in the 1 cell embryo **(Wiekowski et al., 1991)**. The genes of 2-cell embryos require an enhancer sequence for efficient gene expression in the 2–cell but not the 1-cell embryo **(Wiekowski et al., 1991; Majumder et al., 1993)**. This form of repression reduces the activity of any promoter and is initiated sometime between S-phase of the 1st cell cycle and the 2-cell stage. The expression of endogenous genes such as the TRC increases from the 1-cell to late 2 cell but then decreases between the late 2 cell to 4 cell stage. This decrease in TRC expression can be prevented if histone hyperacelylation is induced by butyrate treatment **(Davis et al., 1996)**. This demonstrates that this inhibition of TRC transcription is induced by chromatin-structure assembly. Inhibiting the transcriptionally repressive state by inducing histone hyperacelylation prevents development beyond the 2 cell stage, suggesting that the transcriptionally repressive state directs the correct pattern of gene expression that is vital for the continued development of the embryo. Some genes such as those of the TRC are required to overcome the effect of transcriptional inhibition and undergo expression at the 2-cell stage. It has been suggested that the presence of an enhancer sequence or unusually strong promoter may account for their expression **(Schultz and Worrad, 1995)**.

1.3.5 Developmental block

The embryonic genome of different species is fully activated at different stages in embryo development. In mice this occurs by the 2-cell stage (Flach et al., 1982). In contrast, EGA is complete at the 4-8 cell stage in humans (Braude et al., 1988) and pigs (Tomanek et al., 1989) and at the 8-16 cell stage in sheep (Crosby et al., 1988) and cows (Camous et al., 1986). The timing of developmental block is species-specific and is generally correlated with the stage of development where major EGA begins (De Sousa et al., 1998). The developmental block thus

occurs during the fourth cell cycle in cattle, second in mice and the third to fourth in humans and pigs (Memili and First, 2000).

As the timing of developmental block seems to coincide with the time major EGA begins it has often been assumed that the failure of *in vitro* cultured embryos to undergo EGA is causative of the developmental block. This idea was proposed by a group that demonstrated a decrease in mRNA levels correlating to the critical period for 2-cell block induced by phosphate exposure during the time of EGA (Haraguchi et al., 1999). A more recent study of protein synthesis patterns by two-dimensional gel electrophoresis of [^{35}S] Methionine radiolabeled 2-cell embryos has however shown that it is not a failure but a delay in the initiation of ZGA that may cause the 2-cell block in mice cultured *in vitro* (Qiu et al., 2003). Many mammalian embryos do not accomplish their preimplantation developmental potential when cultured *in vitro* (Yong et al., 2002). With the exception of some inbred and F1 hybrid mice, *in vitro* culture of 1-cell mouse embryos causes them to undergo a single cell division before arresting at the 2-cell stage. This is referred to as the 2-cell block. Developmental block is a phenomenon that occurs when an embryo ceases to cleave during preimplantation development.

Mouse strain, medium components and culture conditions have been shown to affect the development of 1-cell embryos *in vitro* (Chatot et al., 1989). Mouse embryos were first cultured from the 8-cell to blastocyst stage nearly fifty years ago, a simple defined media was used (Whitten, 1956). As media improved it became possible to culture embryos from earlier stages. A simple mouse-designed medium termed CZB was the first media developed in which even blocking type mouse embryos developed from the fertilised egg to the blastocyst stage (Chatot et al., 1989). Simplex-optimized media (SOM) and a version with higher K^+ (KSOM), were subsequently demonstrated to be very successful (Lawitts and Biggers, 1991; Lawitts and Biggers, 1993). Changes in the overall osmolarity or

pyruvate:lactate ratio, decreased NaCl concentration and lowered glucose and phosphate were all factor in the media that were demonstrated to alleviate the 2-cell block in mouse embryos (Biggers, 1998). It is interesting however to note that the developmental block can be rescued by the transfer of cytoplasm from non-blocking strains and this indicates that a cytoplasmic component may be lacking in the 'blocking' strains of mice (Muggleton-Harris et al., 1982).

The inability to react to injuries from the environment and failure to activate transcription of important developmental genes are the main mechanisms that have been suggested to cause embryonic developmental block in mammalian embryos (Betts and King, 2001). The mechanisms behind developmental block are unclear however when mouse embryos from the 'blocking' strain are developed *in vivo* until the 2-cell stage before further *in vitro* culture high numbers of them develop to the blastocyst stage (Whitten and Biggers, 1968; Chatot et al., 1989)

1.4 Gene Expression in the preimplantation embryo

1.4.1 Monitoring global gene expression in the preimplantation embryo

Most research involving gene expression analysis focuses on genes that are differentially expressed between different cell types or similar cells grown in varying conditions. Until relatively recently identification of differentially expressed genes in preimplantation embryos were carried out using complex molecular biology techniques, many of which have major flaws. Differential display for example, was recently used to identify genes that were highly expressed in either oocyte or 8-cell embryo, however it was found to produce a high level of false positives and its detection system was biased towards the more abundant transcripts (Ma et al., 2001).

Expressed Sequence Tag (EST) projects have been undertaken with the purpose to identify genes specifically expressed in egg and preimplantation stage embryos. Thousands of

ESTs have been stored on the public sequence database to date (Ko et al., 2000). One disadvantage of this system however is that it is limited to the quality of the cDNA library and therefore some rare transcripts are likely to be underestimated (Sharov et al., 2003). Quantitative analysis of 2-dimensional protein gels (Latham et al., 1991) and Serial Analysis of Gene Expression (SAGE) (Blomberg le and Zuelke, 2004) have also been used to determine the levels of differentially expressed genes in cohorts of embryos. One relatively new and successful method of identifying specific differentially expressed genes is a PCR-based cDNA subtraction strategy called suppression subtractive hybridization (SSH) (Diatchenko et al., 1996). SSH is advantageous because it detects transcripts that are both high and low in abundance without showing bias and it gives a low incidence of false positives. The system involves a linear amplification step so that even tissues with a relatively small mRNA yield can be used. SSH has successfully been applied to identify oocyte versus 8-cell-embryo-specific cDNA clones (Zeng and Schultz, 2003). One major disadvantage which occurs in all the methods described above is that they are unable to measure large numbers of genes simultaneously. The recent development of large-scale genomic approaches has rescued this problem. The development of large microarrays for example, has proved particularly useful for embryo development studies (Ko et al., 2000) and has been used to identify global expression differences in all stages of mouse preimplantation embryo development from the unfertilized egg to the late blastocyst stage (Wang et al., 2004; Hamatani et al., 2004a). Microarray analysis has been used to elucidate molecular pathways influencing blastocyst dormancy and activation (Hamatani et al., 2004b) as well as global gene expression differences between the morula and blastocyst stage (Tanaka and Ko, 2004).

1.4.2 Preimplantation development is marked by phased gene expression

Two separate reports recently produced the first detailed studies of global gene expression changes during each stage of preimplantation embryo development using microarray technology (Wang et al., 2004; Hamatani et al., 2004a). Expression profiling revealed that two distinct waves of major gene expression occur in the preimplantation embryo. The first wave corresponds to EGA (described above) which reflects the time when transcription can first be supported by the embryo. The second wave termed Mid-preimplantation Gene Activation (MGA) occurs between the 4-cell to 8-cell stage and involves a significantly large increase in gene expression (Hamatani et al., 2004a). The annotation of many genes expressed during MGA appears to be important for functions relating to the later stages of preimplantation development. For example, Na-K-ATPase and water channel genes are upregulated at this stage and are likely to influence the ionic gradient across the trophectoderm and the formation of the fluid-filled blastocoel (Watson and Barcroft, 2001). Genes involved in the metabolic switch from pyruvate to glucose dependency, DNA methylation and tight junction formation also appear to be expressed at this stage (Wang et al., 2004; Hamatani et al., 2004a).

The transient waves of expression of such large numbers of genes appear to be unique in the preimplantation embryo. The requirement of the embryo to have fixed waves of gene expression could reflect the need for specific groups of genes to be expressed at certain times, furthermore when genes have fulfilled their function, their expression may be harmful to the embryo so inactivation must take place to allow normal development. The waves of activation have also been proposed to act in a stepwise manner such that maternal transcripts and proteins trigger the onset of EGA and the proteins derived from EGA activate MGA (Hamatani et al., 2004a).

1.5 Synopsis

The aim of this thesis is to investigate the role of $[Ca^{2+}]i$ oscillations during egg activation on mammalian preimplantation development. The aim of Chapter 3 was to establish whether the recently discovered sperm factor, PLCζ can cause $[Ca^{2+}]i$ oscillations, egg activation and development to the blastocyst stage in pigs and humans since this has already been shown in mice. In Chapter 4 I investigate the role of $[Ca^{2+}]i$ oscillations more deeply and study how the effects of this signal can impact on embryo cleavage potential, cell allocation in the blastocyst and apoptosis. Chapter 5 describes work using luminescence techniques to examine whether $[Ca^{2+}]i$ signals at activation may be having an effect on global gene expression during embryonic genome activation (EGA). Continuing with this theme, Chapter 6 describes work using microarray technology to examine how $[Ca^{2+}]i$ signals affect gene expression during the 8-cell stage of embryo development. Chapter 7 summarises the overall results from Chapters 3 to 6 and provides a detailed discussion of the findings reported in this thesis.

Chapter 2

Materials and methods

2.1 Mouse egg experiments

2.1.1 Mice

Mice were sourced from Harlan and all procedures were carried out in accordance with Home Office regulations. Ex-breeder F1 (C57xCBA) male mice of proven fertility were used for *in vitro* fertilisation and mating. Oocytes and embryos from 21-24 day old MF1 female mice were used for all other experiments, unless otherwise stated. Embryos and *in vivo* fertilised oocytes were obtained from female mice that had been mated.

2.1.2 Oocyte and embryo collection

To induce ovulation, female mice were administered 7.5I.U pregnant mare serum gonadotrophin (PMSG; Intervet, Milton Keynes, UK) by intraperitoneal injection followed 48 hours later by an injection of 7.5 I.U human chorionic gonadotrophin (hCG; Intervet). Mice were killed by cervical dislocation between 14 and 17 hours post-hCG and oviducts were removed with a fine pair of scissors and forceps. Oviducts were placed in warmed Hepes-buffered KSOM (HKSOM) media (Summers et al., 2000) containing 4mg/ml BSA (Sigma). Approximately 40 mg of BSA were added to 10 mls of HKSOM media to make a working stock of 4 mg/ml. See the appendices for a recipe of HKSOM and KSOM media. HKSOM was made as a 10x stock for frozen storage at -20°C. When 10xHKSOM was removed from the freezer it was kept as a 10x stock at 4°C for a maximum time of 5 days. Just prior to use

the HKSOM was diluted to 1x with fresenius water and amino acids and BSA were added accordingly. Cumulus masses were released into fresh media by tearing the ampulla region of the oviduct with a sterile pair of forceps. Cumulus cells were removed by addition of 300ug/ml hyaluronidaise (Sigma) to the media for approximately 5 minutes. A 1500 Units/ml stock solution of hyaluronidaise was made by dissolving hyaluronidaise in HKSOM media without BSA. A working stock of 150 Units/ml was prepared by adding 100ul of stock solution to 900ul of HKSOM media. Eggs were washed three times through fresh drops of media and left to recover from hyaluronidaise treatment for at least 10 minutes at 37°C before being used for experiments.

2.1.3 Parthenogenetic Activation

Parthenogenetic activation of MII eggs was carried out using a number of different stimuli. Activation took place 15-18 hours post-hCG and all eggs were treated with 2μM cytochalasin D (Sigma) for 2 hours to prevent 2nd polar body extrusion. Stocks of 2mM Cytochalasin D were made by dissolving 0.01g Cytochalasin D powder in 0.985 mL DMSO. Aliquots of stock were stored at -20°C and were diluted 1000x with HKSOM media to make a working stock.

Eggs activated with strontium chloride (Sigma) were first washed three times in Ca^{2+}-free HKSOM and then incubated in Ca^{2+} free HKSOM containing 10mM Sr^{2+} for 2 hours at 37°C. A Strontium chloride stock solution was made by adding 2.67g of $SrCl_2$ to 10ml of fresenius water producing a 1M solution. The stock solution was diluted 100x with HKSOM to make a working stock of 10mM.

Ethanol activation was carried out by placing eggs in HKSOM containing 7% ethanol (Grade V; BDH Analar) for 7 minutes at room temperature.

Artificial activation in a Ca^{2+} independent manner was performed using cycloheximide (Sigma) or roscovitine (Calbiochem). Eggs stimulated with cycloheximide were incubated for a period of 4 hours in HKSOM containing 20ug/mL cycloheximide at 37°C. A 20mg/mL cycloheximide stock solution was prepared in DMSO and was diluted 1000x in HKSOM to make a working stock of 20ug/mL.

Eggs stimulated with roscovitine were incubated for 4 hours in HKSOM containing 50μM roscovitine at 37°C. Roscovitine was prepared as a 50mM stock in DMSO.

When a combined treatment was carried out with Sr^{2+} and either cycloheximide or roscovitine, oocytes were first incubated in cycloheximide or roscovitine alone for two hours followed by 2 hours incubation in Ca^{2+}-free HKSOM containing Sr^{2+} with either cycloheximide or roscovitine. Oocytes activated with ethanol and cycloheximide were first incubated in cycloheximide alone for 2 hours followed by 7% ethanol treatment for 7 mins, before being incubated in cycloheximide for the remaining 2 hours.

2.1.4 Mouse embryo development

Mouse embryos were cultured *in vitro* in drops of equilibrated potassium simplex optimised media containing essential and non-essential amino acids (KSOM/AA) (Summers et al., 2000) under mineral oil (Sigma) in 5% CO2 incubator at 37°C. KSOM media was made weekly and stored at 4°C. See the appendices for details of the recipe. The sizes of the drops used to culture embryos were governed by the number of embryos in each drop, with approximately 3μl of media per embryo. Eggs and embryos were cultured in drops on 30mm plastic petri dishes (Falcon). For scoring embryos during development, embryos were removed briefly from the incubator 24 hours post-activation (2-cell stage), 48 hours post-activation (4-cell stage), 72 hours post-activation (8-cell stage), 96 hours post-activation (morula/early blastocyst stage) and 103 hours post-activation (blastocyst stage).

2.1.5 *In vitro* fertilisation (IVF)

IVF was performed 16-18 hours after administration of hCG. Epididymi were collected from F1 ex-breeder male mice by cutting the vas deferens close to the caudal epididymis using sterile fine scissors and forceps. Sperm were squeezed from the caudal region of the epididymis into a petri-dish with 1ml T6 media (Quinn et al., 1982) containing 15mg/ml BSA (Fraction V, Sigma) and which had been equilibrated in a 5% CO_2 in air incubator overnight at 37°C to pH 7.6. The sperm were given a 20-30 minute swim out period in the T6 media after which time 200µl drops of concentrated sperm media were made under oil and put in the incubator for three hours to allow capacitation of the sperm. In order to monitor Ca^{2+} changes in eggs during IVF, eggs were injected with 1mM Oregon Green BAPTA Dextran and the zona pellucidae were removed by brief exposure to acidified Tyrode's solution (Sigma). The zona-free eggs were washed three times before being transferred to 0.5ml BSA-free HKSOM, which allowed the eggs to stick to the coverslip. After 15 minutes, when the eggs were firmly stuck to the coverslip, 0.5ml of BSA-containing media was added to the chamber. Then 20µl of the sperm-containing media was removed from the edges of the 200ul drops and added to the chamber containing the zona-free eggs. Ca^{2+} measurements commenced when the first sperm was seen attaching to an egg.

2.1.6 Monitoring Embryonic Genome Activation (EGA) with a luciferase reporter gene

Embryonic genome activation was assayed by monitoring luminescence from embryos injected with the firefly luciferase reporter gene pGL3 (Promega) (Ram and Schultz, 1993). Pronuclei of *in vivo* fertilized or *in vitro* activated parthenotes were injected with 50ng/ml of pGL3-control vector DNA (Promega) in buffer containing 120mM KCL and 20mM Hepes. After injection the pronucleate embryos were incubated in HKSOM media containing luciferin (100µM). Luciferin is a natural compound isolated from fireflies and is a substrate

for the enzyme luciferase. Luciferase is encoded by the luc gene, which is widely used as a reporter gene in a variety of cells. Due to the intrinsic low background of the chemiluminescence technique, detection of the luc gene expression can be made at a very low level. The firefly luciferase enzyme is a euglobulin related to the acyl-CoA ligases. It performs a ligase function in step I and an oxygenase function in step II of the assay described below. Firefly luciferin is a benzothiazole. The role of ATP is not as an energy source but instead to combine with luciferin as AMP and allow the formation of the dioxetanone intermediate by providing a leaving group and allowing electrophilic attack of the 4^{th} carbon by molecular oxygen. A chemically initiated intramolecular electron exchange process initiates the spontaneous breakdown of the dioxetanone ring and the formation of oxyluciferin bearing a singlet excited state electron. When this electron rapidly falls to the ground state it releases a photon of light in the process.

$$\text{Luciferin} + \text{MgATP}^{2-} \xrightarrow{\text{I}} \text{adenyl-luciferin} + \text{PPi}$$

$$\text{Adenyl-luciferin} + O_2 \xrightarrow{\text{II}} [\text{peroxyluciferin}] + \text{AMP}$$

$$[\text{peroxyluciferin}] \longrightarrow [\text{oxyluciferin}] + CO_2$$

$$[\text{oxyluciferin}] \longrightarrow \text{oxyluciferin} + \text{light}$$

The luminescence from cohorts of embryos was monitored continuously for up to 25 hours using an imaging photon detector (IPD) system supplied by Science Wares (www.sciencewares.com). The IPD consists of an inverted Zeiss Axiovert microscope with two attached cameras (see figure 2.1). The first is an IPD camera, which is sensitive enough to detects single photon events using a cooled (-10°C) S20 photocathode, a microplate channel and resistive anode (Photek Ltd, St Leonards on Sea, UK). The second is a CCD camera that takes brightfield pictures so that cell morphology can be monitored over the time course of luminescence imaging. An integration time of 5 mins was sufficient to detect a clear photon signal above background for a single embryo when a 10 x 0.5NA objective was used.

2.1.7 Monitoring cyclin-luciferase in control and cycloheximide-treated eggs

The Cyclin-luciferase mRNA was made entirely by Dr. Victoria Nixon and given as a gift. Luciferase cDNA from the pRL vector (Promega) was ligated to the C-terminus of the human form of cyclin B1 and the intact luciferase-cyclin fusion construct was cloned into the pCS2+ vector for in vitro mRNA synthesis using SP6 mMessage mMachine kit (Ambion). A poly-A tail was added using the mMessage kit and poly-A polymerase (Ambion). Cyclin-luciferase mRNA was injected at a pipette concentration of 2.7ug/ul into mouse eggs. The injection was 3-5% of the egg total volume and was estimated from the displacement of a bolus injection. After injection the eggs were incubated in HKSOM media containing luciferin (100μM) for 2 hours. Zonae pellucidae were removed prior to transfer of eggs to the IPD for luminescence measurements (see above and Fig 2.1 for more information on the IPD). For cycloheximide treatment eggs were monitored in HKSOM media for 2 hours followed by HKSOM media containing 20ug/ml cycloheximide. An integration time of 30 seconds was sufficient to detect a clear photon signal above background for a single embryo when a 20 x 0.5NA objective was used.

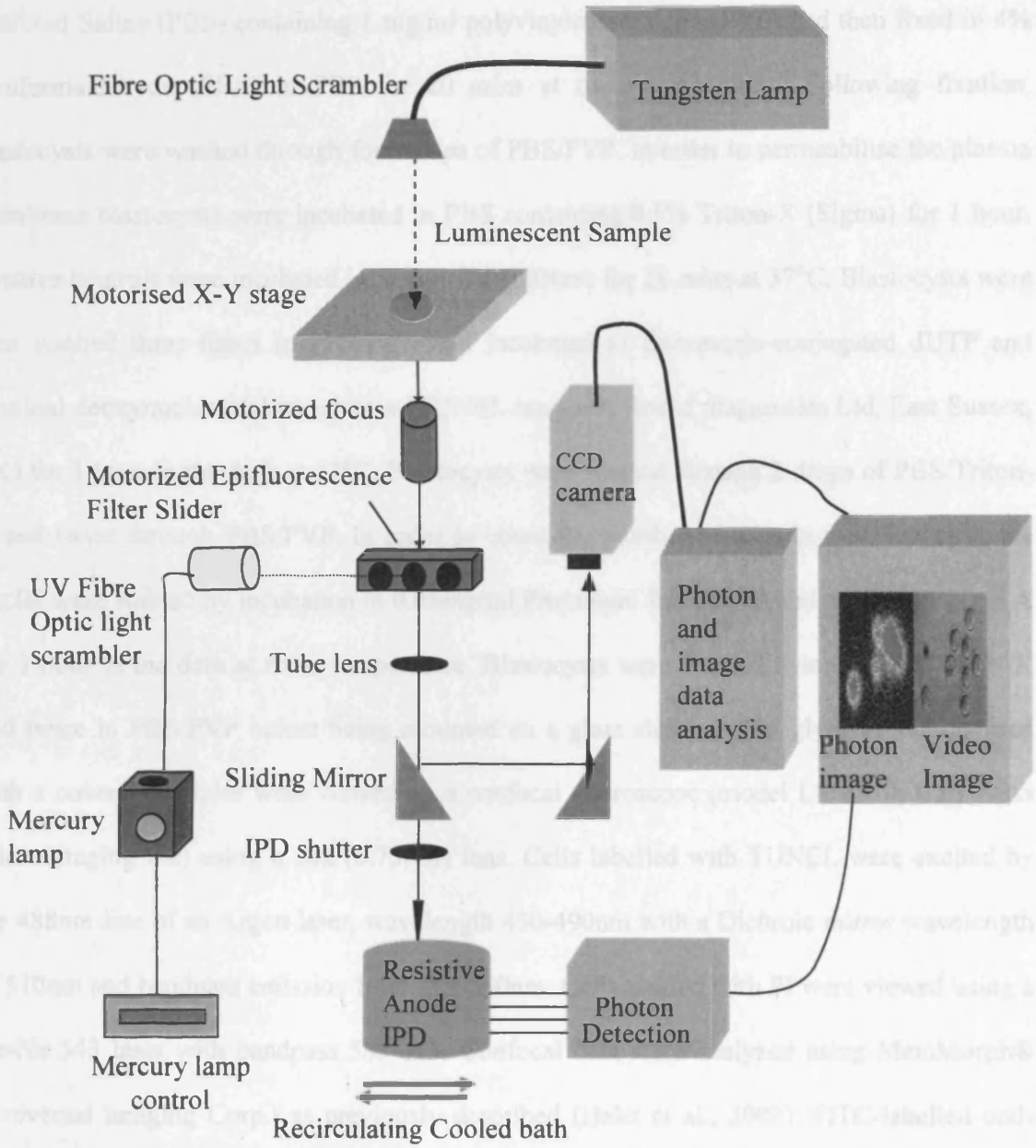

Figure 2.1 Schematic diagram of a Microscope-based Imaging Photon Detector. Photon images are acquired when light from the sample passes the objective, microscope tube lens and a reducing lens before it reaches the Resistive anode-IPD input window. Transmitted or fluorescent light is acquired by the use of a 100% mirror which is placed after the tube lens to reflect light up to the trinoc, where it is then projected to the eyepiece or the CCD camera. Adapted from Sciencewares.com

2.1.8 TUNEL labelling to assay apoptosis in mouse blastocysts

Mouse blastocysts (103 hours post-activation) were washed through three drops of Phosphate Buffered Saline (PBS) containing 1 mg/ml polyvinylpyrrolidone (PVP) and then fixed in 4% paraformaldehyde (PFA) in PBS for 20 mins at room temperature. Following fixation, blastocysts were washed through four drops of PBS/PVP. In order to permeabilise the plasma membrane blastocysts were incubated in PBS containing 0.5% Triton-X (Sigma) for 1 hour. Positive controls were incubated in 5U/ml RQ1 DNase for 20 mins at 37°C. Blastocysts were then washed three times in PBS/PVP and incubated in fluorescein-conjugated dUTP and terminal deoxynucleotidel transferase (TUNEL reagents; Roche diagnostics Ltd, East Sussex, UK) for 1 hour in the dark at 37°C. Blastocysts were washed through 2 drops of PBS/Triton-X and twice through PBS/PVP. In order to count the number of cells in the blastocyst, the nuclei were stained by incubation in 0.05mg/ml Propidium Iodide (PI) and 50µg/ml RNase A for 1 hour in the dark at room temperature. Blastocysts were washed twice in PBS/Triton-X and twice in PBS/PVP before being mounted on a glass slide in 10µl glycerol and covered with a coverslip. Slides were viewed on a confocal microscope (model LSM510; Carl Zeiss MicroImaging Inc) using a 20x (0.75NA) lens. Cells labelled with TUNEL were excited by the 488nm line of an Argon laser, wavelength 450-490nm with a Dichroic mirror wavelength of 510nm and bandpass emission filter 505-530nm. Cells stained with PI were viewed using a He-Ne 543 laser with bandpass 585-615. Confocal data were analyzed using MetaMorph® (Universal Imaging Corp.) as previously described (Halet et al., 2002). FITC-labelled cells were counted as apoptotic cells and PI stained nuclei were counted as total number of live cells. The apoptotic index was calculated by the total number of dead cells divided by the total number of cells (dead cells and live cells) in each blastocyst.

2.1.9 Differential staining of ICM and TE in mouse blastocysts

Zona pellucidae were removed from blastocysts (103 hours post-activation) by a 3-5 minute exposure to acidified Tyrode's solution (Sigma) at 37°C. Zona-free blastocysts were then exposed to 100ug/ml fluorescein isothiocyanate (FITC)- labelled wheat germ lectin (WGA; Sigma) for 20 min at 37°C followed by fixation in 4% paraformaldehyde in PBS at room temperature for 30 mins. Blastocysts were exposed to 0.05% Triton-X in PBS for 1 hour followed by incubated in 5µg/ml propidium iodide for 1 hour. After permeabilisation and staining blastocysts were washed through 3 drops of PBS before being viewed on a confocal microscope (model LSM510: Carl Zeiss Microimaging Inc) using a 20x (0.75NA) lens. Cells stained with PI were viewed using a HE-Ne 543 laser with bandpass 585-615. Cells labelled with FITC-WGA were excited by the 488nm line of an argon laser, wavelength 450-490nm, a dichroic mirror wavelength of 510nm and a bandpass emission filter 505-530nm.

2.2 Pig egg experiments

2.2.1 Collection of Ovaries

Pig ovaries were collected from an abattoir (Fowler Bros Ltd, Burnham-on-Crouch, UK) and transported to the laboratory in Dulbecco's Phosphate Buffered Saline (PBS) (Unipath Ltd., Basingstoke, UK). The PBS was kept at 25-30°C by heated wheat bags in a thermo carrier and the transportation time was 2-3 hours. The ovaries were washed three times in PBS that was warmed to 37°C, before aspiration of the ovarian follicle cells.

2.2.2 Oocyte Collection

Cumulus oocyte complexes (COC's) and pig follicular fluid (pff) were aspirated from ovarian follicles that were 3-6 mm in diameter with a 18 G needle fitted to a 10ml syringe. The COC's were selected out of the pff by applying a thin layer of follicular fluid to a 35mm

petridish and removing them with a mouth pipette. The COC's were collected in 1 ml drops of Hepes-buffered Tyrode albumin lactate pyruvate (PVA-TL-HEPES) medium containing 0.1% polyvinylalcohol (PVA). The COC's were washed through three drops PVA-TL-Hepes. COC's with at least three layers of compact cumulus cells and uniform cytoplasm were selected for culture. The aspirated pff was collected in warm sterile 10ml falcon tubes during COC collection. Following this the pff was put in centrifugal tubes and spun at 3,000 for 30 mins. The supernatant was collected from the tubes and equilibrated in a 35mm petridish at 39°C in 5% C02 in air for 1 hour in preparation for *in vitro* maturation (IVM).

2.2.3 In vitro maturation of pig oocytes

IVM of pig oocytes was carried out in North Carolina State University 23 (NCSU-23) medium that had been equilibrated at 39°C in 5% CO2 in air for 5-6 hours. The NCSU-23 media was supplemented with 10% pff which had been previously aspirated from the ovarian follicles, 1% essential amino acids (B-6766, Sigma), 0.1% non-essential amino acids (M-7145, Sigma), 10 IU/ml equine chorionic gonadotrophin (eCG) (Intervet, Ireland), 10 IU/ml human chorionic gonadotrophin (hCG) (Intervet, Ireland), 1mM dibutyrl cyclic AMP, 10ng/ml Epidermal growth factor and I mM cysteine. The oocytes were washed through 3 droplets of NCSU-23 and then kept in the same media for 22 hours in culture. After 22 hours the oocytes were washed three times in fresh equilibrated NCSU-23 with all supplements except hCG, eCG and db-cAMP. They were cultured for a further 22 hours in this media. Only mature eggs, which had extruded the 1st polar body, were used for further experiments.

2.2.4 Pig embryo development

Pig embryos were cultured in NCSU-23 media containing 10mg/ml BSA at 39°C in 5% CO_2 in air. Embryos were cultured in drops whose size was equivalent to approximately 3-5ul per

embryo. Each day embryos were removed from the incubator briefly and their development was noted.

2.3 Human egg work

2.3.1 Patient treatment prior to oocyte collection

Human eggs were obtained from patients whose gametes had failed to fertilise following ICSI or IVF. Ethical approval for the project was obtained from St Thomas's Hospital Local Research Ethics Committee and from the Human Fertilisation and Embryology Authority (HFEA) who issued a licence for the work (R0147). Prior to their treatment patient's gave their consent for the use of all unfertilised eggs used in this research. For treatment patients underwent pituitary down regulation using buserelin (Suprefact; Hoechst UK Ltd, Middlesex, UK) in a mid-luteal start long protocol. Controlled ovarian hyperstimulation was performed using gonadotrophins following satisfactory pituitary suppression as evidenced by a thin endometrium and absence of follicular activity or ovarian cysts. Ovarian stimulation was achieved using a daily Follicle Stimulating Hormone (FSH) dose of 150-450 IU of recombinant FSH (Gonal F; Serono Laboratories Ltd, Welwyn Garden City, UK). Human chorionic gonadotrophin (HCG) 10,000 IU (Serono laboratories Ltd) was administered when at least 3 follicles had reached a mean diameter of 18mm or more. Transvaginal follicular aspiration was performed 34-36 hours after HCG injection.

Cumulus-oocyte complexes (COC's) were isolated from follicular aspirates, washed and incubated at 37°C in 6% CO2 in air. 3-6 hours post oocyte recovery oocytes were prepared for IVF or ICSI dependant upon earlier semen analysis. Oocytes for IVF were inseminated in a 4 well Nunc dish in G-Fert media (Vitrolife, Falmouth, UK) with 100,000 sperm per 1 ml well. Oocytes for ICSI had their surrounding cumulus cells removed with the minimal exposure to Hyase (Vitrolife) before being injected with a single sperm in G-MOPS

(Vitrolife). Following IVF insemination or ICSI oocytes were cultured overnight in G-Fert (IVF) or G-1 (ICSI) and checked for signs of fertilisation 19-20 hours later. Those oocytes that had fertilised normally were transferred to fresh drops of G-1 media and cultured to embryo transfer. Those oocytes at the metaphase 2 stages that showed no signs of fertilisation were entered into the project. Up until this stage all work on human eggs and oocytes were carried out by embryologists or clinicians at Guys Hospital. These unfertilised eggs were transferred from the Assisted Conception Unit at Guys Hospital to laboratories at University College London. Eggs were kept in G-1 media warmed by heated sterile sand in a thermo carrier. The time taken for the transfer of oocytes was approximately 30 minutes. All experiments in the laboratory were carried out in Hepes-KSOM (HKSOM) media unless otherwise stated.

2.3.2 Embryo culture

Oocytes were cultured in Sydney IVF cleavage medium (COOK) from days 1-3 (up to 8-cell stage) before transfer to Sydney IVF blastocyst medium (COOK) for the remaining culture time. Oocytes were cultured in 20ul drops under mineral oil at 37°C in a 6% CO2 incubator. Each day embryos were removed from the incubator briefly and their development was noted.

2.4 General Egg work

2.4.1 Egg loading and Microinjection.

Mouse eggs were loaded with 2μM Fura-2 (Molecular probes) for about 15 mins whereas pig eggs required a longer loading time of about 30-40 mins due to the larger size of the egg. The loading, manipulation and Ca^{2+} measurement were carried out in media containing 0.25mM sulfinpyrazone (Sigma) to prevent compartmentalisation of the Ca^{2+} indicator dye (Lawrence et al 1997).

For PLCζ injections (Saunders et al., 2002) of mouse and pig eggs, injection pipettes were back-filled with varying concentration of PLCζ cRNA in a buffered salt solution (120mM KCL and 20mM Hepes, pH 7.4) that had been treated with Chelex 100 beads (Sigma) to remove divalent cations. In human eggs PLCζ cRNA was combined with 1mM Oregon Green BAPTA dextran (Molecular Probes, Eugene, OR, USA) as an alternative way to monitor Ca^{2+} changes without prior loading. PLCζ cRNA was stored in aliquots at -80°C and thawed immediately before injection. For developmental purposes, when no Ca^{2+} imaging took place Oregon Green BAPTA was omitted from the injection and no prior loading of pig or mouse eggs in Fura-2 took place. All eggs were also placed in 2μM cytochalasin D (Sigma) for approximately two hours to prevent second polar body extrusion.

Eggs were prepared for injection by transfer to a plastic petri dish with a fresh drop of media covered with mineral oil (Sigma). The Petri-dish was placed on a Nikon Diaphot microscope stage and eggs were manipulated using a micropipette and Narishige manipulators. Each egg was immobilized using a holding pipette and the injection pipette tip was pushed through the zona pellucida to the plasma membrane. Using the pressure injection system a dose of the PLCζ cRNA was injected into the oocyte. The injection was 3-5% of the egg total volume and was estimated from the displacement of a bolus injection.

2.4.2 $[Ca^{2+}]i$ Measurements.

Loaded pig or mouse eggs were transferred to a heated chamber on the stage of a Nikon Diaphot microscope. The heated chamber contained media absent of BSA to ensure the eggs remained stuck to the bottom of the chamber. A Xenon lamp was used to excite the Fura-2 at 340 and 380nm. Emission fluorescence was collected using a 20 x 0.75 objective lens that passed through a 520 long pass filter and detected using a CCD camera. Ca^{2+} measurements of human eggs took place in a heated chamber on the stage of a Zeiss Axiovert microscope,

which was equipped with epifluorescence optics and a 20 x 0.75NA objective lens. Light from a halogen lamp passed through 490nm bandpass filter and emission was collected with a 510nm long-pass filter. Fluorescence measurements were taken for individual eggs using an imaging photon detector (IPD; Photek Ltd, East Sussex, UK) and specialised software developed by Science Wares (Falmouth, MA, USA).

2.5 Microarray work

2.5.1 Collection of 8-cell parthenotes for microarray work

Eggs were activated parthenogenetically using Sr^{2+} or cycloheximide (See 2.1.4). After 60 hours of culture (See 2.1.5), only 8-cell embryos exhibiting excellent morphology were selected for collection. Batches of 34 8-cell embryos were washed four times through drops of M2 media and flash-frozen in 4ul of the same media. 8-cell embryos were shipped on dry ice to the National Institute on Aging (NIA), National Institute of Health (NIH), Baltimore, USA for RNA extraction, hybridisation and microarray analysis. The samples were stored at -80°C until further use.

2.5.2 Extraction and amplification of mRNA

Two collections of 34 x 8-cell embryos were collected for each group of cycloheximide and Sr^{2+} activated 8-cell embryos. Total mRNA was extracted from each group of embryos using a Quickprep micro poly-A RNA Extraction Kit (Amersham Biosciences, Piscataway, MJ) and linear acrylamide as a carrier (Ambion, Austin, Texas). Total RNA samples from each extraction were labeled with Cy3-dye by two-round linear amplification labelling reaction for cRNA targets using a Fluorescent Linear Amplification Kit (Agilent Technologies, Palo Alto, CA). Amplification was necessary due to the small amount of materials and starting mRNA we had extracted. Compared to a single round of amplification, two-round amplification

reduces the sensitivity of differential expression detection to 60%, however detection specificity was retained to 96% (Carter et al., 2003).

Quality (purity) and size distribution of cRNA targets was determined using an Agilent 2100 Bioanalyzer that utilised a 6000 Nano lab-on-chip Assay (Agilent Technologies). Data was displayed as a gel image or an electropherogram. The images and data provided information about how well the probes were labelled, the concentration and quality of total RNA and any impurities that were present in the samples.

2.5.3 RNA labelling and hybridization on the NIA 22K 60-Mer Oligo Microarray

Universal mouse reference RNA (Stratagene, La Jolla, CA) was labelled with Cy5-dye by a one-round amplification labelling reaction and used as a control for all hybridization reactions, allowing cross-comparisons between all data sets. The cRNA targets from both sets of parthenogenetically activated embryos and universal mouse reference RNA were hybridized on the NIA 22k 60-mer oligo microarray (Carter et al., 2003). The NIA 22k 60-mer oligo microarray is enriched with genes suitable for the study of mouse embryo development and is compatible with the small amounts of RNA extracted from preimplantation mouse embryos (Ko et al., 2000).

2.5.4 Analysis of Microarray data

The intensity of 21,045 gene features per array were extracted from scanned microarray images using Feature Extraction 5.1.1 software (Agilent Technologies), which performs background subtraction and dye normalization. Dye normalisation by Feature Extraction 5.1.1 software is targeted at detecting changes in the relative expression of individual genes rather than global expression. Global gene expression was quantitatively analyzed using hierarchical clustering and Principle Component Analysis (PCA). A scatter plot showing the log-ratios of

differentially expressed genes in both groups of embryos was created using the NIA microarray analysis tool (http://lgsun.grc.nia.nih.gov/ANOVA/).

Statistically significant genes were determined quantitatively using the analysis of variance - false discovery rate (ANOVA-FDR) = 10%, which minimises the occurrence of false positives (Sharov et al., 2005). Assignment of gene function was carried out using Gene Ontology (GO) terms (Ashburner et al., 2000) which characterized genes into basic groups such as cell cycle and cell adhesion. GO terms (Ashburner et al., 2000) were used in conjunction with GenMapp/ MAPPFinder (Doniger et al., 2003) to find the genes and functional groups associated with embryos parthenogenetically activated with Sr^{2+} or Cycloheximide. The microarray data are available from the public databases (GEO and ArrayExpress) and the website: http://lgsun.grc.nia.nih.gov/microarray/data.html.

Chapter 3

PLCζ; a sperm specific protein that can activate development in mouse, pig and human eggs

3.1.1 Introduction

Fertilisation in mammalian eggs triggers a series of long-lasting $[Ca^{2+}]i$ oscillations that are paramount for meiotic resumption, pronucleus formation, cortical granule exocytosis and entry into the first mitotic division (Kline and Kline, 1992). These events are collectively referred to as egg activation (Lawrence et al., 1998). In mice, the $[Ca^{2+}]i$ oscillations continue for about 4 hours before they cease at a time corresponding to pronucleus formation (Cuthbertson and Cobbold, 1985; Jones et al., 1995a). The exact pattern of these sperm-induced $[Ca^{2+}]i$ oscillations is unique. Strontium ions (Sr^{2+}) are one of a number of artificial stimuli that can induce [Ca2+]i oscillations, but the patterns with which these $[Ca^{2+}]i$ oscillations occur is easily distinguishable from the highly characteristic oscillations which are actually induced at fertilisation. Many attempts have been made to elucidate the factor responsible for triggering $[Ca^{2+}]i$ oscillations, egg activation and embryo development (Swann et al., 2004).

Recently a novel phospholipase C (PLC), termed PLCζ(zeta) was put forward as a candidate for the sperm factor (Saunders et al., 2002). Microinjection of mouse PLC zeta complementary RNA (mPLCζ cRNA) into mouse eggs triggered a pattern of $[Ca^{2+}]i$ oscillations that were indistinguishable from those induced by fertilisation. Preimplantation embryo development to the blastocyst stage has been triggered in mouse eggs after microinjection of mPLCζ with success rates similar to those after IVF (Saunders et al., 2002). Hamster sperm extracts failed to induce any $[Ca^{2+}]i$ oscillations, egg activation or later

development when microinjected into mouse eggs if they were previously subjected to immunodepletion of PLCζ (Saunders et al., 2002). These results strongly suggest that PLCζ is the sperm factor responsible for activating egg development at fertilisation.

PLCζ genes have been identified in mice, humans, monkeys, chimpanzee, cow, rat, dog and chickens (Saunders et al., 2002; Cox et al., 2002; Coward et al., 2005). The different forms of PLCζ all appear to have a functional similarity and can all cause Ca^{2+} release in mouse eggs. One study has shown that differences exist between mice, human and monkey PLCζ (mPLCζ, hPLCζ and cPLCζ respectively) with regards to their Ca^{2+}-releasing potential in mouse eggs (Cox et al., 2002). $[Ca^{2+}]$i oscillations were generated more effectively from microinjection of hPLCζ cRNA than microinjection of mPLCζ or cPLCζ cRNA (Cox et al., 2002). Studies have so far focused on the nature of different species PLCζ and their differing potential in causing $[Ca^{2+}]$i oscillations (Saunders et al., 2002; Cox et al., 2002; Coward et al., 2005) or on the functionality of the PLCζ molecule as an enzyme (Kouchi et al., 2005; Nomikos et al., 2005). Whilst there have been investigations on the affect of PLCζ in mouse eggs, no studies have investigated variation in the sensitivity of eggs from other species to PLCζ.

The aim of this chapter was to investigate the effectiveness of mPLCζ and hPLCζ in triggering $[Ca^{2+}]$i oscillations, egg activation and development in mouse, pig and aged human eggs. To my knowledge this was the first study to examine the effects of PLCζ cRNA injection on pig and human eggs. The experiments presented here show that differences in sensitivity exist between mouse, pig and human eggs regarding their ability to release Ca^{2+} after stimulation by mPLCζ and hPLCζ.

3.2 Results

3.2.1 Sperm induce repetitive $[Ca^{2+}]i$ oscillations during IVF

In vitro fertilisation (IVF) of mouse eggs was carried out to monitor the different parameters of $[Ca^{2+}]i$ oscillations (frequency, mean interspike interval, amplitude and duration) induced by sperm. Mouse eggs were injected with Oregon green BAPTA Dextran (OGBD) and their Zona-Pellucidae (ZP) were removed prior to fertilisation as the eggs needed to be immobilised before $[Ca^{2+}]i$ recording could begin. $[Ca^{2+}]i$ transients were monitored by increases in OGBD fluorescence. Fluorescent light was measured on an Imaging Photon Detector (IPD) which produced both a bright field and fluorescence image of the eggs (Fig 3.1Ci and ii). The range of colours represented fluorescence intensity, red represents high $[Ca^{2+}]i$ and blue represents basal levels of $[Ca^{2+}]i$ (Fig 3.1Cii).

$[Ca^{2+}]i$ oscillations began less than 5 minutes after adding the capacitated sperm to the media. Initiation of $[Ca^{2+}]i$ oscillations would normally take longer if the ZP was intact because the sperm would need to trigger the acrosome reaction to permit ZP penetration. The sperm induced the characteristic pattern of $[Ca^{2+}]i$ oscillations previously reported to occur at fertilisation (Fig 3.1A) (Miyazaki et al., 1993; Swann and Ozil, 1994). The first transient lasted approximately 6 minutes and at its peak, it exhibited a series of small superimposed high frequency $[Ca^{2+}]i$ spikes (Fig 3.1B). The first $[Ca^{2+}]i$ transient was also characterised by having a distinct shoulder during its rising phase. The subsequent $[Ca^{2+}]i$ oscillations were of much shorter duration (~ 60 seconds) and were of similar amplitude to one another. Each regenerative $[Ca^{2+}]i$ transient began with a slow rise in $[Ca^{2+}]i$ from basal levels, followed by a swift attack to the peak. The five eggs monitored during IVF exhibited $[Ca^{2+}]i$ oscillations that had a mean interspike interval of 10.9 ± 1.29 (standard error mean; s.e.m) mins.

3.2.2 Mouse and human PLCζ triggers long lasting $[Ca^{2+}]i$ oscillations in mouse eggs

PLCζ was used in the form of complementary RNA (cRNA), since it is rapidly translated into protein following microinjection into mouse eggs. PLCζ protein was not used because it is unstable and was not available in a consistently active form. The protein form is also harder to microinject into eggs and can easily be contaminated by other proteins during the protein purification stage. PLCζ cRNA was stored in -80°C and only thawed immediately prior to usage to prevent degradation of PLCζ by RNAses. Mouse eggs were loaded with fura-2 before being injected with various concentrations of mouse or human PLCζ (mPLCζ and hPLCζ respectively). Microinjection of mPLCζ or hPLCζ into mouse eggs triggered repetitive $[Ca^{2+}]i$ oscillations (Fig 3.2) which were indistinguishable from those induced by IVF (Fig 3.1).

The frequency of the $[Ca^{2+}]i$ oscillations was determined by the concentration and type of PLCζ cRNA microinjected into the mouse egg. The highest pipette concentration of mPLCζ used was 2mg/ml which corresponds to a concentration of <0.1mg/ml in the mouse egg after a 3-5% injection volume. Nine eggs were injected with 2mg/ml hPLCζ cRNA and all eggs responded by exhibiting high frequency $[Ca^{2+}]i$ oscillations with a mean interspike interval of 8.8 $\pm$ 0.52 (s.e.m) mins (Table 3.1) that commenced within 20-30 minutes of microinjection (Fig 3.2A). Many of the $[Ca^{2+}]i$ transients had a distinct shoulder during their rising phase. Injecting a ten-fold lower pipette concentration of mPLCζ (200μg/ml) reduced the frequency of $[Ca^{2+}]i$ oscillations (Fig 3.2B) and gave a mean interspike frequency of 15.38 $\pm$ 2.12 (s.e.m) mins (Table 3.1). Nine mouse eggs were injected with this concentration of mPLCζ and eight eggs (89%) exhibited $[Ca^{2+}]i$ oscillations. Consistent with the pattern of IVF-induced $[Ca^{2+}]i$ oscillations, the first $[Ca^{2+}]i$ transient induced by mPLCζ lasted approximately 5 mins and had smaller $[Ca^{2+}]i$ rises superimposed on its peak (Fig 3.2C)

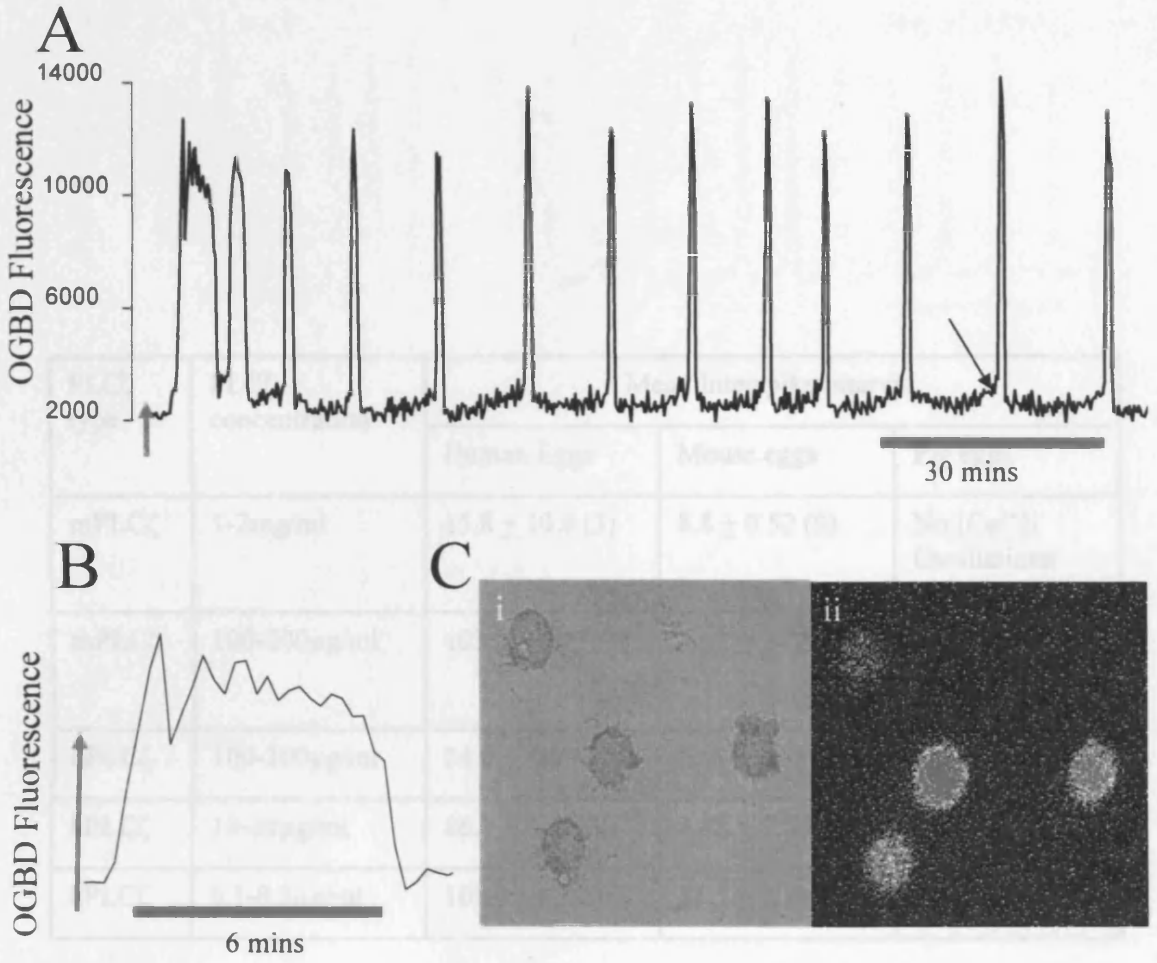

Figure 3.1 Sperm induced $[Ca^{2+}]i$ Oscillations during IVF. A sample $[Ca^{2+}]i$ trace in a single Oregon Green BAPTA dextran (OGBD) loaded MII mouse oocyte. OGBD fluorescence was in arbitrary units. $[Ca^{2+}]i$ oscillations began less than 5 minutes after introduction of sperm into the media, (indicated by the red arrow). The black arrow shows that the $[Ca^{2+}]i$ transient is triggered by an initial gradual rise in basal $[Ca^{2+}]i$. The first $[Ca^{2+}]i$ transient (B) had a duration of about 6.5 mins and contained smaller superimposed increases on top of it's peak. Zona pellucida were removed from eggs prior to IVF as shown on the brightfield image (Ci). Fluorescence was monitored in mouse eggs over time (ii). The range of colours reflect the fluorescence intensity of $[Ca^{2+}]i$ in the eggs with red and blue indicating high and basal cytosolic $[Ca^{2+}]i$ levels respectively. The middle and far right egg are high in cytosolic Ca^{2+} and probably at a peak in the $[Ca^{2+}]i$ transient. The egg above (blue) exhibits resting $[Ca^{2+}]i$ levels and the egg below has rising $[Ca^{2}]i^{+}$ levels probably just prior to an upstroke in $[Ca^{2+}]i$.

PLCζ type	PLCζ concentration	Mean Interspike interval		
		Human Eggs	Mouse eggs	Pig eggs
mPLCζ	1-2mg/ml	15.8 ± 10.0 (3)	8.8 ± 0.52 (9)	No $[Ca^{2+}]i$ Oscillations
mPLCζ	100-200μg/ml	103.0 ± 4.17 (4)	15.3 ± 2.12 (9)	No $[Ca^{2+}]i$ oscillations
hPLCζ	100-200μg/ml	24.0 ± 4.82 (4)	N/A	10.5 ± 9.02 (6)
hPLCζ	10-20μg/ml	86.0 ± 3.29 (9)	3.88 ± 1.54 (12)	78.3 ± 2.4 (9)
hPLCζ	0.1-0.2μg/ml	109.0 ± 4.49 (6)	11.5 ± 2.29 (6)	N/A

Table 3.1 Mean interspike intervals of $[Ca^{2+}]i$ oscillations after mPLCζ or hPLCζ cRNA injection into mouse, pig and human eggs. Brackets denote the number of eggs tested for each concentration of PLCζ. N/A applies to concentrations of PLCζ not tested in eggs

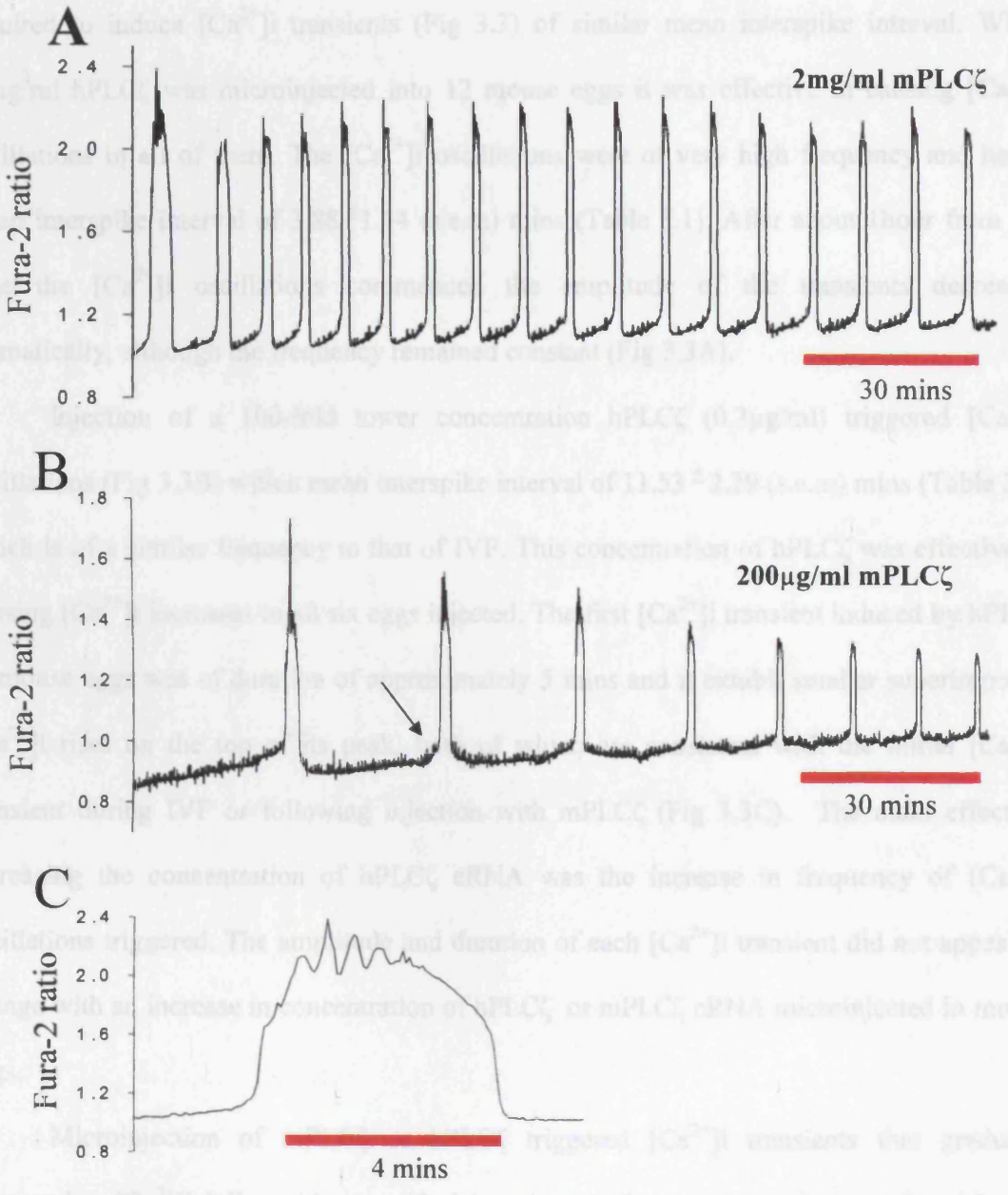

Figure 3.2 Injection of mPLCζ cRNA in mouse eggs. 2mg/ml PLCζ initiated high frequency $[Ca^{2+}]i$ transients with a mean interspike interval of 8.8 mins and which occurred approximately 20-30 mins after injection (A). Lowering he pipette concentration of PLCζ 10-fold (200µg/ml) reduced the frequency of $[Ca^{2+}]i$ oscillations so that the mean interspike interval was 15.38 mins and $[Ca^{2+}]i$ oscillations began 45-60 mins after injection (B). At this frequency the $[Ca^{2+}]i$ oscillations take on a form similar to $[Ca^{2+}]i$ oscillations induced by fertilisation. The arrows show the gradual increase in basal $[Ca^{2+}]i$ initiating the next $[Ca^{2+}]i$ transient. The first $[Ca^{2+}]i$ transient was approximately 4.5 mins long and contained smaller superimposed increases on the top of the peak (C).

Compared to the concentration of mPLCζ used, much lower concentrations of hPLCζ were required to induce $[Ca^{2+}]i$ transients (Fig 3.3) of similar mean interspike interval. When 20μg/ml hPLCζ was microinjected into 12 mouse eggs it was effective in causing $[Ca^{2+}]i$ oscillations in all of them. The $[Ca^{2+}]i$ oscillations were of very high frequency and had a mean interspike interval of 3.88 $\pm$1.54 (s.e.m) mins (Table 3.1). After about 1hour from the time the $[Ca^{2+}]i$ oscillations commenced the amplitude of the transients decreased dramatically, although the frequency remained constant (Fig 3.3A).

Injection of a 100-fold lower concentration hPLCζ (0.2μg/ml) triggered $[Ca^{2+}]i$ oscillations (Fig 3.3B) with a mean interspike interval of 11.53 $\pm$2.29 (s.e.m) mins (Table 3.1) which is of a similar frequency to that of IVF. This concentration of hPLCζ was effective in causing $[Ca^{2+}]i$ increases in all six eggs injected. The first $[Ca^{2+}]i$ transient induced by hPLCζ in mouse eggs was of duration of approximately 5 mins and it exhibit smaller superimposed $[Ca^{2+}]i$ rises on the top of its peak, both of which are consistent with the initial $[Ca^{2+}]i$ transient during IVF or following injection with mPLCζ (Fig 3.3C). The main effect of increasing the concentration of hPLCζ cRNA was the increase in frequency of $[Ca^{2+}]i$ oscillations triggered. The amplitude and duration of each $[Ca^{2+}]i$ transient did not appear to change with an increase in concentration of hPLCζ or mPLCζ cRNA microinjected in mouse eggs.

Microinjection of mPLCζ or hPLCζ triggered $[Ca^{2+}]i$ transients that gradually increased in $[Ca^{2+}]i$ followed by a swift rising phase before an abrupt decay to basal levels. Another gradual increase in $[Ca^{2+}]i$ was observed before the next $[Ca^{2+}]i$ transient and this suggested that a $[Ca^{2+}]i$ pacemaker was in action, leading to regular increases in $[Ca^{2+}]i$ over time (Fig 3.2 and 3.3).

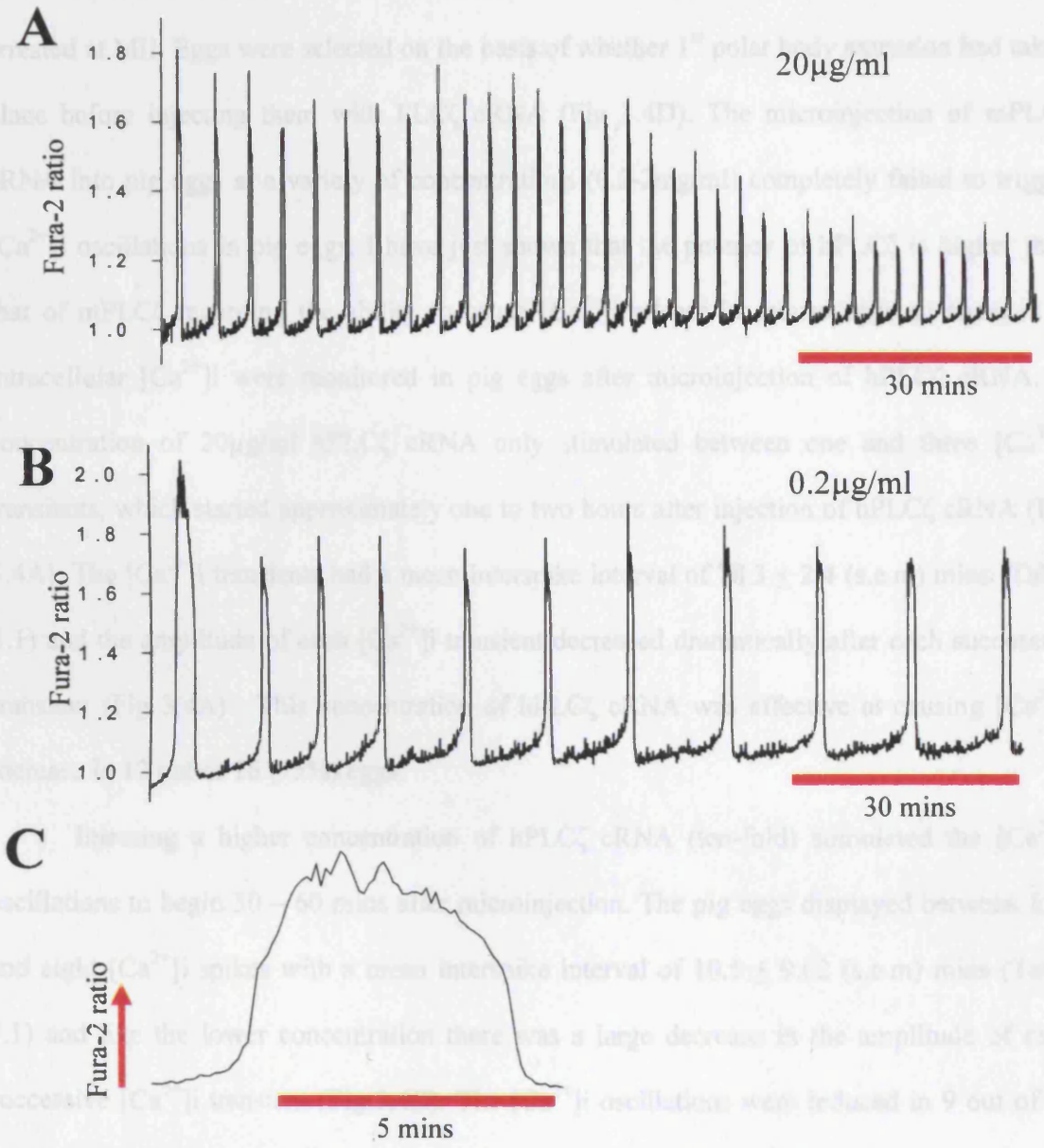

Figure 3.3 – Injection of human PLCζ (hPLCζ) into mouse eggs. PLCζ was injected at concentrations of A) 20µg/ml and B) 0.2µg/ml in mouse eggs. The higher (A) concentration produced very high frequency $[Ca^{2+}]i$ oscillations that reduced in amplitude after the first 1.5 hours. Lowering the pipette concentration (100-fold) of hPLCζ (B) triggered $[Ca^{2+}]i$ oscillations that were indistinguishable from those at IVF, the first transient was longer in duration (~ 5 mins) than the subsequent transients and had smaller peak $[Ca^{2+}]i$ increases on the top (C).

3.2.3 hPLCζ but not mPLCζ is effective at triggering $[Ca^{2+}]i$ oscillations in pig eggs

Immature cumulus enclosed pig eggs were cultured for approximately 48 hours until they arrested at MII. Eggs were selected on the basis of whether 1st polar body extrusion had taken place before injecting them with PLCζ cRNA (Fig 3.4D). The microinjection of mPLCζ cRNA into pig eggs at a variety of concentrations (0.2-2mg/ml) completely failed to trigger $[Ca^{2+}]i$ oscillations in pig eggs. I have just shown that the potency of hPLCζ is higher than that of mPLCζ regarding the ability to cause $[Ca^{2+}]i$ release in mouse eggs so changes in intracellular $[Ca^{2+}]i$ were monitored in pig eggs after microinjection of hPLCζ cRNA. A concentration of 20μg/ml hPLCζ cRNA only stimulated between one and three $[Ca^{2+}]i$ transients, which started approximately one to two hours after injection of hPLCζ cRNA (Fig 3.4A). The $[Ca^{2+}]i$ transients had a mean interspike interval of 78.3 ± 2.4 (s.e.m) mins (Table 3.1) and the amplitude of each $[Ca^{2+}]i$ transient decreased dramatically after each successive transient (Fig 3.4A). This concentration of hPLCζ cRNA was effective at causing $[Ca^{2+}]i$ increase in 12 out of 16 (75%) eggs.

Injecting a higher concentration of hPLCζ cRNA (ten-fold) stimulated the $[Ca^{2+}]i$ oscillations to begin 30 – 60 mins after microinjection. The pig eggs displayed between four and eight $[Ca^{2+}]i$ spikes with a mean interspike interval of 10.5 ± 9.02 (s.e.m) mins (Table 3.1) and like the lower concentration there was a large decrease in the amplitude of each successive $[Ca^{2+}]i$ transient (Fig 3.4B). The $[Ca^{2+}]i$ oscillations were induced in 9 out of 12 (75%) eggs after hPLCζ injection and in these eggs the oscillations lasted approximately one hour before cessation. The first $[Ca^{2+}]i$ transient in the pig egg lasted approximately 90 seconds and did not appear to have any smaller spikes superimposed over the peak (Fig 3.4C).

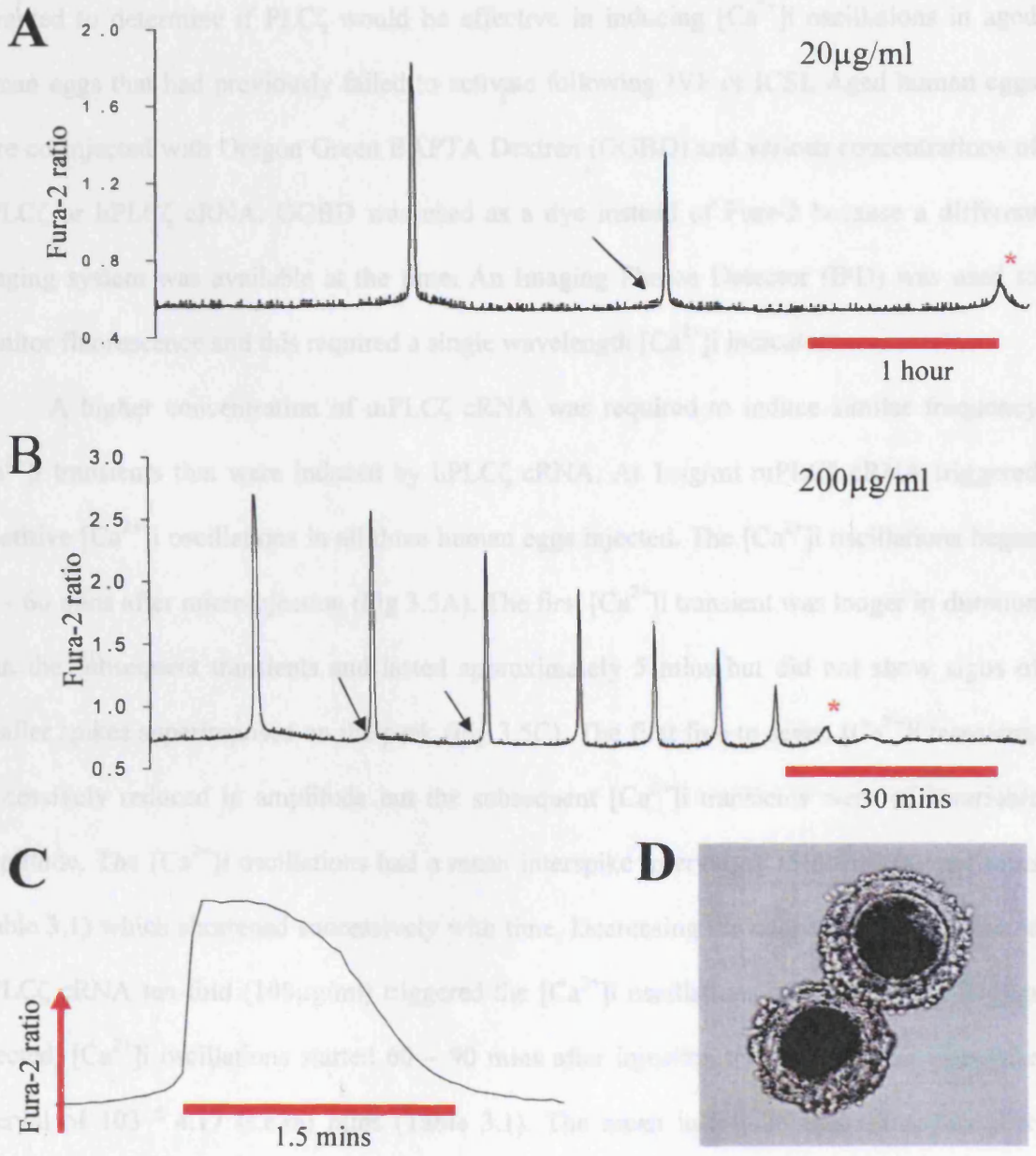

Figure 3.4 $[Ca^{2+}]$i oscillations in pig eggs triggered by microinjection of hPLCζ cRNA. 20µg/ml hPLCζ cRNA triggered two or three $[Ca^{2+}]$i transients that were approximately 60 mins apart (A). 200µg/ml hPLCζ cRNA triggered multiple $[Ca^{2+}]$i oscillations, which lasted for about 1 hour before cessation (B). An arrow indicates the pacemaker Ca^{2+} which was responsible for stimulating sharp $[Ca^{2+}]$i transients. * indicates the time the Ca^{2+} pacemaker fails to initiate a swift increase in $[Ca^{2+}]$i. The first $[Ca^{2+}]$i transient (C) lasted approximately 1.5 mins. Immature cumulus enclosed pig eggs (D) were cultured for approximately 48 hours until they arrested at MII. MII-arrested eggs were subsequently injected with hPLCζ cRNA.

3.2.4 Mouse and human PLCζ induces $[Ca^{2+}]i$ oscillations in aged human eggs

I wanted to determine if PLCζ would be effective in inducing $[Ca^{2+}]i$ oscillations in aged human eggs that had previously failed to activate following IVF or ICSI. Aged human eggs were co-injected with Oregon Green BAPTA Dextran (OGBD) and various concentrations of mPLCζ or hPLCζ cRNA. OGBD was used as a dye instead of Fura-2 because a different imaging system was available at the time. An Imaging Photon Detector (IPD) was used to monitor fluorescence and this required a single wavelength $[Ca^{2+}]i$ indicator.

A higher concentration of mPLCζ cRNA was required to induce similar frequency $[Ca^{2+}]i$ transients that were induced by hPLCζ cRNA. At 1mg/ml mPLCζ cRNA triggered repetitive $[Ca^{2+}]i$ oscillations in all three human eggs injected. The $[Ca^{2+}]i$ oscillations began 30 – 60 mins after microinjection (Fig 3.5A). The first $[Ca^{2+}]i$ transient was longer in duration than the subsequent transients and lasted approximately 5 mins but did not show signs of smaller spikes superimposed on the peak (Fig 3.5C). The first five to seven $[Ca^{2+}]i$ transients successively reduced in amplitude but the subsequent $[Ca^{2+}]i$ transients were of invariable amplitude. The $[Ca^{2+}]i$ oscillations had a mean interspike interval of 15.8 $\pm$ 10 (s.e.m) mins (Table 3.1) which shortened successively with time. Decreasing the concentration of injected mPLCζ cRNA ten-fold (100μg/ml) triggered the $[Ca^{2+}]i$ oscillations in all four human eggs injected. $[Ca^{2+}]i$ oscillations started 60 – 90 mins after injection and had a mean interspike interval of 103 $\pm$ 4.17 (s.e.m) mins (Table 3.1). The mean interspike interval appeared to decrease after each $[Ca^{2+}]i$ transient.

Three different concentrations of hPLCζ cRNA were injected into aged human eggs. 100μg/ml hPLCζ cRNA triggered high frequency $[Ca^{2+}]i$ oscillations within 15 mins of microinjection (Fig 3.5A) in all four eggs microinjected at this concentration. The $[Ca^{2+}]i$ transients had a mean interspike frequency of 24 $\pm$ 4.82 (s.e.m) mins (Table 3.1) and similar amplitude for each transient. A 10-fold decrease in the concentration of injected hPLCζ cRNA

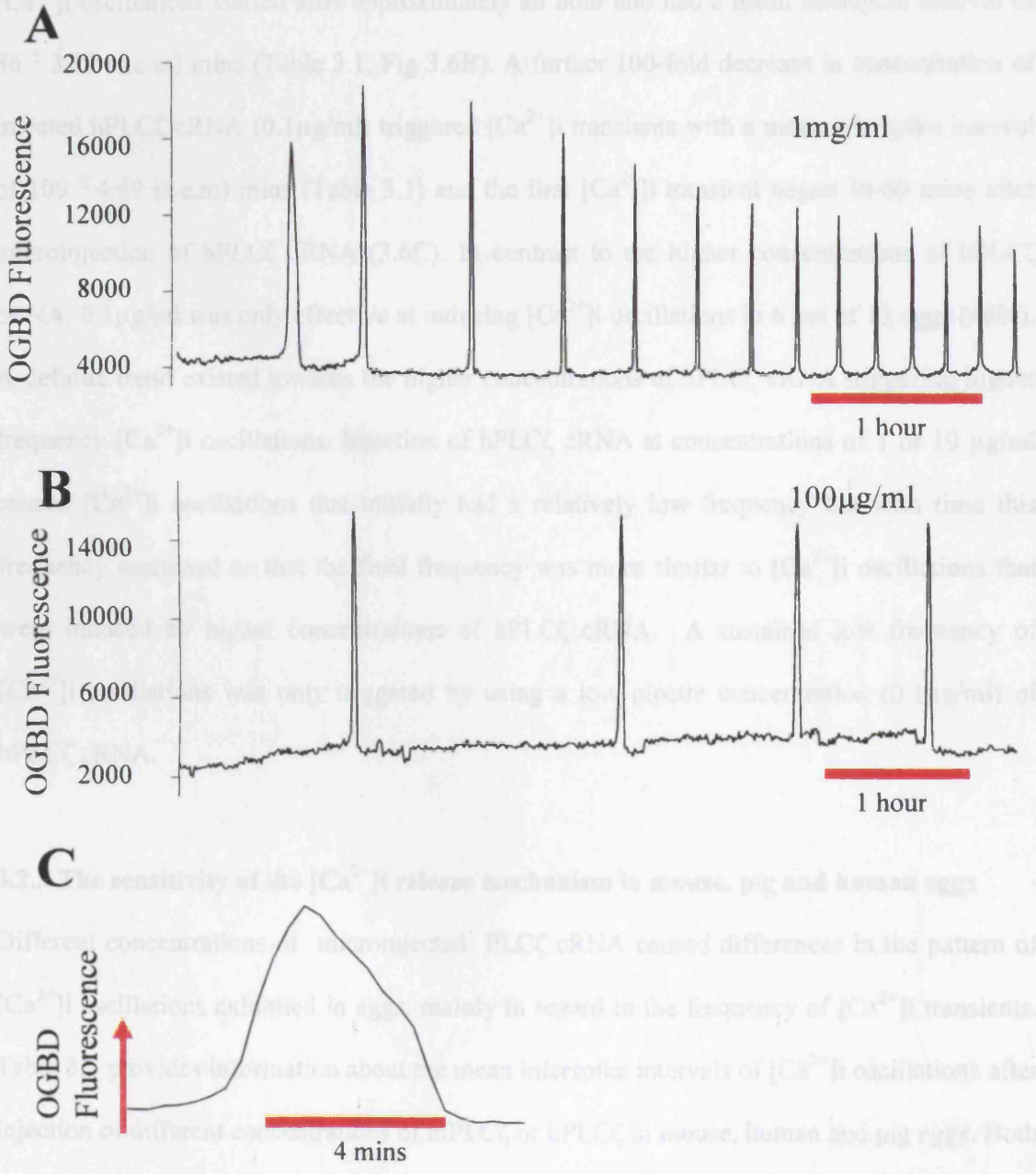

Figure 3.5 Injection of mPLCζ cRNA into aged human eggs. Pipette concentrations of 1mg/ml mPLCζ cRNA triggered high frequency $[Ca^{2+}]i$ oscillations that started about 30 mins after injection (A). 100µg/ml mPLCζ cRNA triggered $[Ca^{2+}]i$ oscillations that were much less frequenct and which started about 90 mins after injection (B). The first $[Ca^{2+}]i$ transient has a distinct peak and lasted for a duration of approximately 5 mins (C). Eggs were co-injected with PLCζ cRNA and Oregon Green BAPTA dextran (OGBD) and $[Ca^{2+}]i$ was monitored using (OGBD) fluorescence.

(10μg/ml) stimulated $[Ca^{2+}]i$ transients in all nine eggs microinjected at this concentration. $[Ca^{2+}]i$ oscillations started after approximately an hour and had a mean interspike interval of 86 ± 3.29 (s.e.m) mins (Table 3.1, Fig 3.6B). A further 100-fold decrease in concentration of injected hPLCζ cRNA (0.1μg/ml) triggered $[Ca^{2+}]i$ transients with a mean interspike interval of 109 ± 4.49 (s.e.m) mins (Table 3.1) and the first $[Ca^{2+}]i$ transient began 30-60 mins after microinjection of hPLCζ cRNA (3.6C). In contrast to the higher concentrations of hPLCζ cRNA, 0.1μg/ml was only effective at inducing $[Ca^{2+}]i$ oscillations in 6 out of 13 eggs (46%). A definite trend existed towards the higher concentrations of hPLCζ cRNA triggering higher frequency $[Ca^{2+}]i$ oscillations. Injection of hPLCζ cRNA at concentrations of 1 or 10 μg/ml caused $[Ca^{2+}]i$ oscillations that initially had a relatively low frequency but with time this frequency increased so that the final frequency was more similar to $[Ca^{2+}]i$ oscillations that were induced by higher concentrations of hPLCζ cRNA. A sustained low frequency of $[Ca^{2+}]i$ oscillations was only triggered by using a low pipette concentration (0.1μg/ml) of hPLCζ cRNA.

3.2.5 The sensitivity of the $[Ca^{2+}]i$ release mechanism in mouse, pig and human eggs

Different concentrations of microinjected PLCζ cRNA caused differences in the pattern of $[Ca^{2+}]i$ oscillations exhibited in eggs, mainly in regard to the frequency of $[Ca^{2+}]i$ transients. Table 3.1 provides information about the mean interspike intervals of $[Ca^{2+}]i$ oscillations after injection of different concentrations of mPLCζ or hPLCζ in mouse, human and pig eggs. Both mPLCζ and hPLCζ appeared to be effective in causing $[Ca^{2+}]i$ oscillations in the mouse and human egg. The human egg and the mouse egg appeared to be less sensitive to mPLCζ and required a 10-fold increase in mPLCζ cRNA concentration to produce similar frequency $[Ca^{2+}]i$ oscillations to those observed in the mouse egg when microinjected with mPLCζ. The

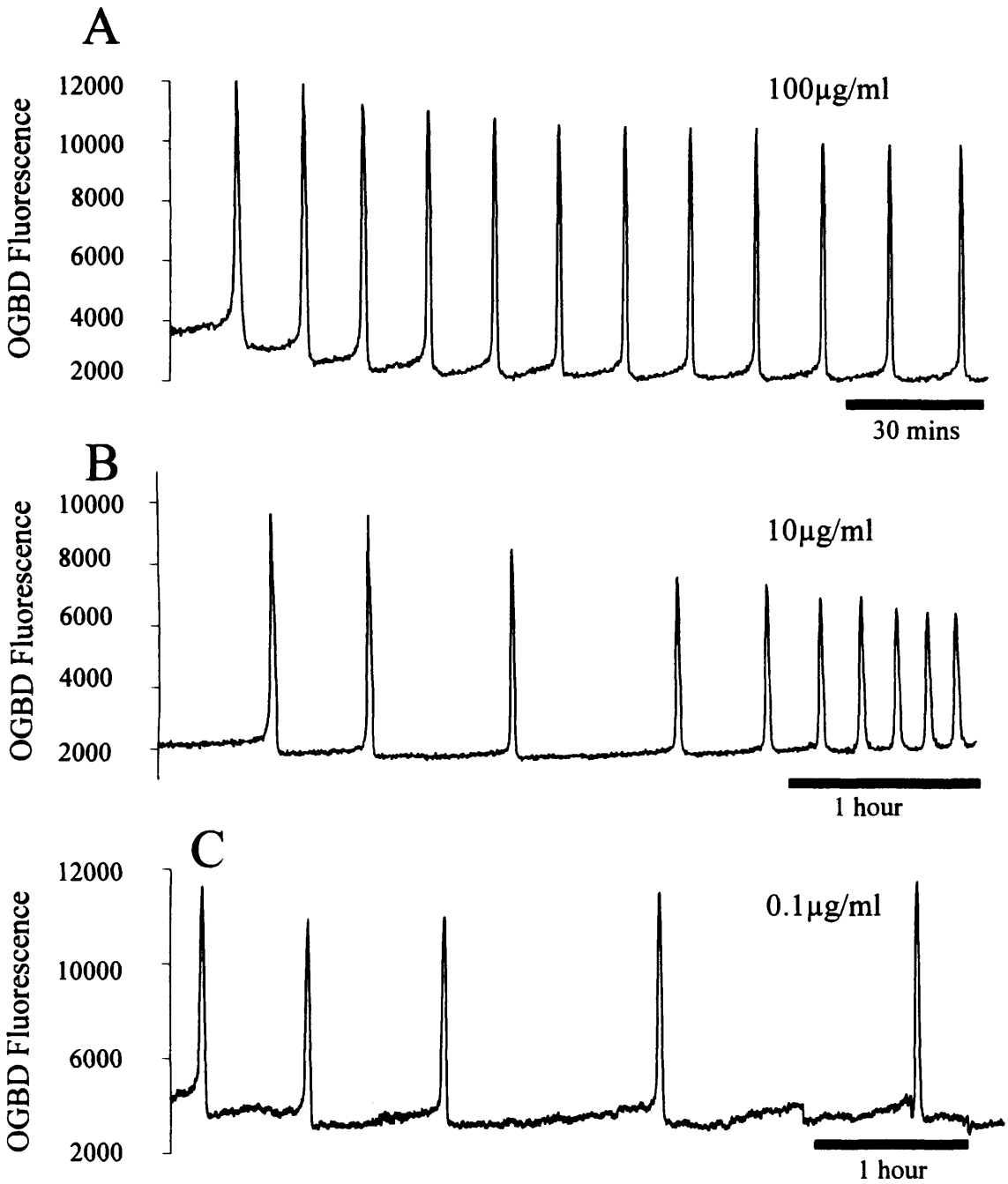

Figure 3.6 $[Ca^{2+}]i$ oscillations triggered by hPLCζ cRNA in aged human eggs. PLCζ cRNA of concentration 100ug/ml (A) , 10ug/ml (B) and 0.1ug/ml (C) were injected into human eggs. The frequency of $[Ca^{2+}]i$ oscillations increased with increased concentration of hPLCζ cRNA injected. The frequency of $[Ca^{2+}]i$ oscillations also increased with time after injection of 10ug/ml hPLCζ cRNA. $[Ca^{2+}]i$ was measured using Oregon Green BAPTA dextran (OGBD) fluorescence. Eggs were co-injected with PLCζ cRNA and OGBD approximately 20 mins before the start of recording. OGBD Fluorescence were measured in arbitrary units.

pig egg was completely unresponsive to injection of mPLCζ cRNA at a concentration of 2mg/ml.

The mouse egg was very sensitive to hPLCζ and produced very high frequency $[Ca^{2+}]i$ oscillations even at low concentrations of hPLCζ (100-0.1μg/ml). The mouse egg appeared to be at least 1000-times more sensitive to hPLCζ than the human egg, since 0.1μg/ml hPLCζ in the mouse egg triggered $[Ca^{2+}]i$ oscillations that were approximately double the frequency of those in human eggs that had been injected with 100μg/ml hPLCζ cRNA.

The pig egg responded to hPLCζ by generating $[Ca^{2+}]i$ transients. Whilst the data in Table 3.1 shows that pig eggs exhibited $[Ca^{2+}]i$ oscillations at a shorter interspike interval than human eggs after microinjection of 10-20 μg/ml hPLCζ cRNA, it does not take into account the short duration of $[Ca^{2+}]i$ oscillations in pig eggs. At 10μg/ml hPLCζ only induced two or three transients which were on average 78 mins apart. Whilst 100μg/ml hPLCζ did produce a much higher frequency of $[Ca^{2+}]i$ oscillations (mean interspike interval = 11.53 mins) the duration only lasted about an hour. The amplitude of each transient also dampened rapidly after each successive $[Ca^{2+}]i$ spike in all pig eggs injected with hPLCζ cRNA..

3.2.6 Embryo development following injection of hPLCζ cRNA

Embryo development was monitored in mouse, pig and human eggs after injection of hPLCζ cRNA (Table 3.2 and Fig 3.8). Changes in $[Ca^{2+}]i$ were not monitored in these embryos since light exposure during fluorescence microscopy can impair embryo development and eggs were injected with hPLCζ cRNA alone. All eggs were treated with cytochalasin D to prevent 2nd polar body extrusion to ensure embryos were diploid. Mouse eggs were injected with 0.2μg/ml hPLCζ cRNA because it had been shown that this concentration of cRNA caused the highest number of embryos reaching the blastocyst stage

of development (38.9%) (Cox et al., 2002). Consistent with this report, I found that 0.2μg/ml hPLCζ cRNA stimulated high percentages of mouse embryos to develop to the 2-cell (82%), 4-cell (67%), 8-cell (55%) and blastocyst (53%) stage (Table 3.2 and Fig 3.8).

I chose to inject human eggs with 10μg/ml or 0.1μg/ml to determine which concentration would generate the best development. 14 human eggs were injected with 10μg/ml hPLCζ cRNA and whilst 10 (71%) formed pronuclei, only 2 (14%) reached the 2-cell stage and arrested development at this stage. A 100-fold decrease in hPLCζ concentration (0.1μg/ml) had a dramatically different affect on embryo development and stimulated high numbers of human eggs to reach the 2-cell (75%), 4-cell (42%), 8-cell (21%) and the blastocyst (17%) stage (Fig 3.7, 3.8 and Table 3.2). Pig eggs were injected with 200μg/ml hPLCζ cRNA because it triggered multiple $[Ca^{2+}]i$ oscillations in the eggs which could not be induced to occur with lesser concentrations (Fig 3.4B). Only 30% of these eggs developed to the 2-cell stage whilst 10% reached the 4-cell stage, 3% reached the 8-cell stage and none developed to the blastocyst stage (Table 3.2 and Fig 3.8).

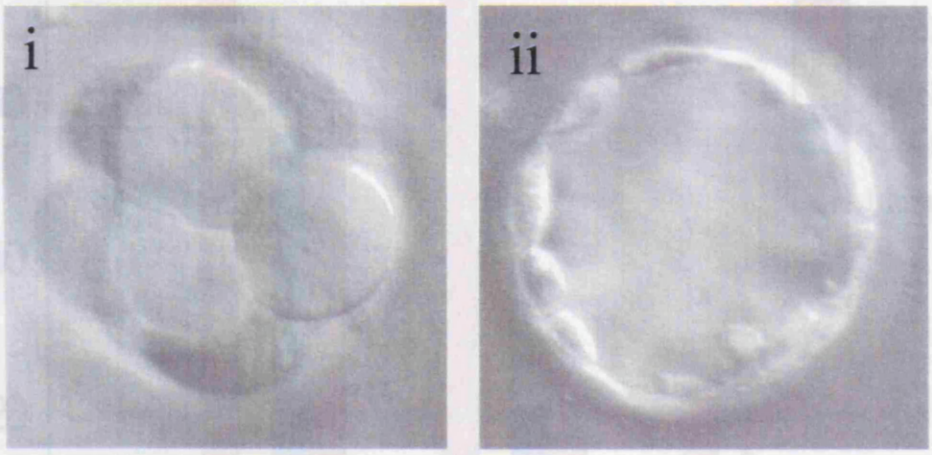

Figure 3.7 Parthenogenetic human embryos. Human eggs that were previously unsuccessful in fertilising during ICSI or IVF were entered into parthenogenetic activation studies using PLCζ cRNA injection. (i) Human 8-cell embryos (21%) and (ii) blastocyst stage embryos (17%) were generated from eggs injected with 0.1μg/ml hPLCζ cRNA. Eggs were treated with cytochalasin D for 2 hours after injection of PLCζ to prevent 2nd polar body emission.

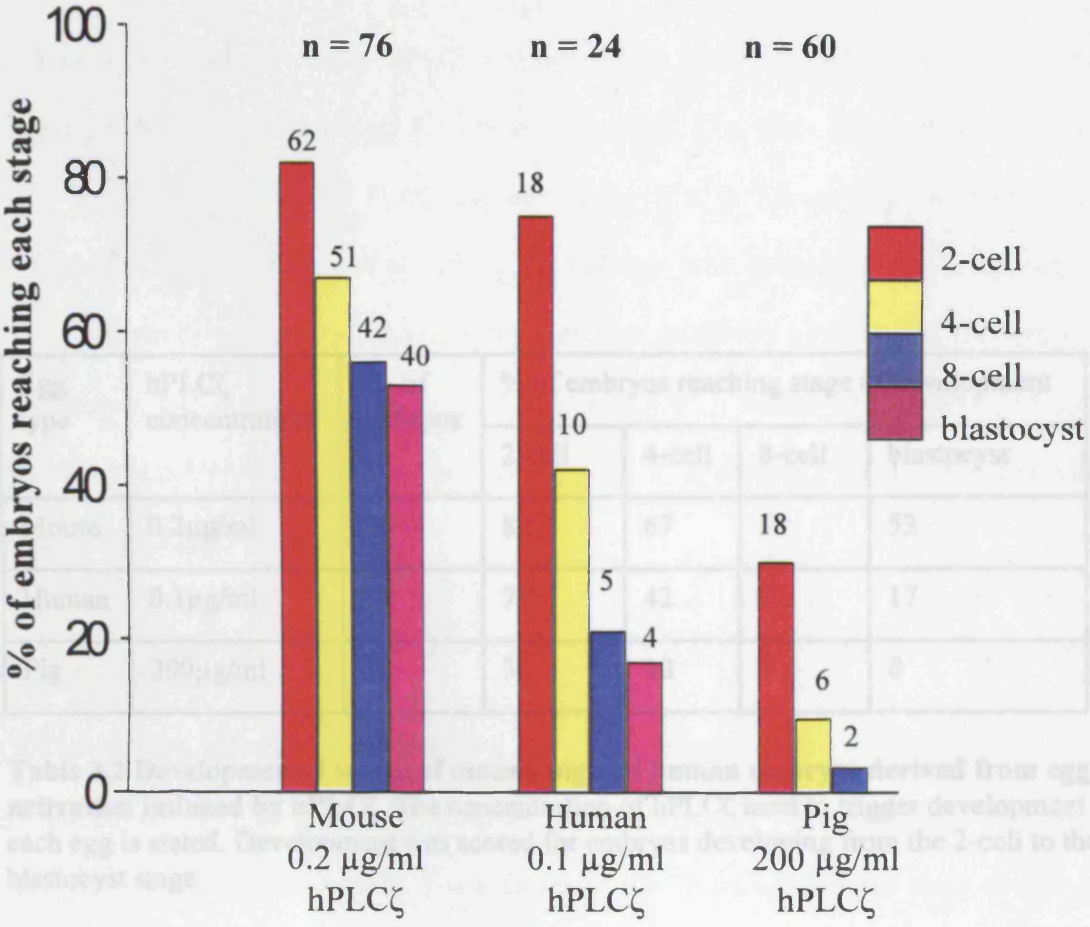

Figure 3.8 Developmental scores of Mouse, human and pig embryos following injection of hPLCζ cRNA. Mouse embryo development was the most successful with 82% and 53% of embryos reaching the 2-cell stage and blastocyst stage, respectively after injection of 0.2µg/ml PLCζ cRNA. Human eggs were injected with 0.1µg/ml hPLCζ which allowed 75% and 17% of human embryos to reach the 2-cell stage and blastocyst stage, respectively. 200µg/ml hPLCζ cRNA allowed only 30% and 3% of pig eggs to reached the 2-cell stage and 8-cell stage (3%) respectively. No pig embryos reached the blastocyst stage. n refers to the total number of embryos that were injected with hPLCζ cRNA in each species group. The number above each bars represents the number of embryos reaching the specified developmental stage. Numbers were derived from 3 or more experiments.

Egg type	hPLCζ concentration	No of embryos	% of embryos reaching stage of development			
			2-cell	4-cell	8-cell	blastocyst
Mouse	0.2μg/ml	76	82	67	55	53
Human	0.1μg/ml	24	75	42	21	17
Pig	200μg/ml	60	30	10	3	0

Table 3.2 Developmental scores of mouse, pig and human embryos derived from egg activation induced by hPLCζ. The concentration of hPLCζ used to trigger development in each egg is stated. Development was scored for embryos developing from the 2-cell to the blastocyst stage.

3.3 Discussion

It has previously been shown that mPLCζ and hPLCζ can cause activation and development to the blastocyst stage in mouse eggs (Saunders et al., 2002; Cox et al., 2002). In this Chapter I show for the first time that PLCζ can also cause $[Ca^{2+}]i$ release egg activation and development in human (Rogers et al., 2004) and pig eggs with different levels of success. I establish that there are clear differences between the sensitivity of different mammalian (mouse, human and pig) eggs regarding PLCζ-induced $[Ca^{2+}]i$ release and confirm previous reports that show that differences in the potency of $[Ca^{2+}]i$ releasing ability exist between mPLCζ and hPLCζ (Cox et al., 2002).

3.3.1 Mouse and human PLCζ can effectively induce $[Ca^{2+}]i$ oscillations in mouse eggs but at different concentrations.

$[Ca^{2+}]i$ oscillations induced by sperm during IVF in mouse eggs were regular, repetitive and long-lasting (Fig 3.1). The first $[Ca^{2+}]i$ transient was about 6.5 mins in duration and contained smaller $[Ca^{2+}]i$ increases on its peak. The subsequent $[Ca^{2+}]i$ transients were much shorter in duration and a gradual increase in basal $[Ca^{2+}]i$ acted as a trigger to initiate the characteristic steep upstroke of each transient. This characteristic pattern of $[Ca^{2+}]i$ oscillations was mimicked by PLCζ cRNA, which induced $[Ca^{2+}]i$ oscillations that were indistinguishable from those induced by IVF. Concentrations of PLCζ cRNA described in the results were injection pipette concentrations. Eggs were injected with pipette concentrations of 2mg/ml – 1 x 10^4 mg/ml PLCζ cRNA, corresponding to <0.1mg/ml – 5 x 10^6 mg/ml PLCζ cRNA in the egg after a 3-5% injection volume.

The main difference between the $[Ca^{2+}]i$ oscillations induced by different pipette concentrations of mPLCζ and hPLCζ was the frequency of the $[Ca^{2+}]i$ oscillations. The higher the pipette concentration of PLCζ cRNA injected into eggs, the higher the frequency of

$[Ca^{2+}]i$ oscillations induced and this matches the same phenomenon observed with different pipette concentrations of PLCζ (Saunders et al., 2002) or sperm extract (Swann, 1990). The amount of PLCζ protein synthesized in mouse eggs has previously been shown to be proportional to the concentration of PLCζ cRNA injected (Saunders et al., 2002). These data suggest that the concentration of PLCζ protein affects the frequency of PLCζ-induced $[Ca^{2+}]i$ oscillations (Rogers et al., 2004). Recently the minimum concentration of PLCζ protein required to induce $[Ca^{2+}]i$ oscillations has been estimated to by different studies to be 300 femptograms (fg)/egg (Kouchi et al., 2004), 44-75 fg/egg (Saunders et al., 2002), 10-40 fg/egg (Yoda et al., 2004) and 50 fg/egg (Nomikos et al., 2005). Differences in the estimated concentrations of PLCζ protein required to induce $[Ca^{2+}]i$ oscillations may be due to modifications of the PLCζ molecule to a more active form in some of the eggs tested. A pipette concentration of 0.02mg/ml mPLCζ cRNA which equates to 44-75fg/egg was reported to induce $[Ca^{2+}]i$ oscillations whose frequency was most like those that occur during IVF. A 10-fold lower concentration (0.002mg/ml) which is equivalent to 4-8 fg/egg did however also cause $[Ca^{2+}]i$ oscillations with a lower frequency than those triggered by IVF (Saunders et al., 2002). A single mouse sperm was calculated to contain about 20-50 fg PLCζ protein which is in the same range as the amount of mPLCζ (4-75 fg of protein or 0.002-0.02 mg/ml cRNA) that is able to generate $[Ca^{2+}]i$ oscillations in a single mouse egg (Saunders et al., 2002) and this is consistent with my data on mPLCζ-induced $[Ca^{2+}]i$ release in mouse eggs.

Injecting a 1000-fold lower pipette concentration of hPLCζ was needed in to cause $[Ca^{2+}]i$ oscillations of a similar frequency to those induced by mPLCζ in mouse eggs. A concentration of 0.2μg/ml hPLCζ or 200μg/ml mPLCζ cRNA was sufficient to induce $[Ca^{2+}]i$ transients with a similar mean interspike interval to those induced by IVF (table 3.1). This data is supported by previous reports that show hPLCζ has a much higher potency than mPLCζ with regard to $[Ca^{2+}]i$ releasing ability in mouse eggs (Cox et al., 2002). The pipette

concentration of hPLCζ and mPLCζ that triggered egg activation and development of mouse embryos to the blastocyst stage in these experiments were similar to previous reports (Saunders et al., 2002; Cox et al., 2002). The reasons for such a difference in $[Ca^{2+}]i$ releasing potency are unclear but it may be that as the volume of the human egg is greater than that of the mouse egg, The diameter of a human egg is approximately 150μm compared to the mouse egg which is approximately 80μm. This makes the human egg around seven times larger in volume than the mouse egg. The dilution of PLCζ from the sperm into the cytoplasm would be larger and therefore may require a more vigorous PLCζ to trigger Ca^{2+} release (Cox et al., 2002). Differences in mouse and human PLCζ may also be due to the fact that different amounts of PLCζ may be present in human and mouse species sperm. The mouse and human egg may alternatively have different sensitivities to the sperm factor as is the case in the hamster egg for example, where it has been reported that the egg is much less sensitive to sperm extract than the mouse egg (Parrington et al., 1996). The sensitivities of mouse, pig and human eggs were investigated with regard to $[Ca^{2+}]i$ -releasing ability following microinjection of mPLCζ and hPLCζ cRNA. This was the first study carried out to investigate the effects of mPLCζ and hPLCζ on pig and human eggs.

3.3.2 Differences in sensitivity to different PLCζ's exist between mouse and human eggs

The concentration of hPLCζ that triggers $[Ca^{2+}]i$ oscillations in mouse eggs (0.2μg/ml) is 1000 times lower than the amount of hPLCζ (200μg/ml) that was used to generate $[Ca^{2+}]i$ oscillations of a similar frequency in aged human eggs (table 3.1). This difference may in part be due to the fact that aged human eggs may not translate the injected PLCζ cRNA into protein as efficiently as the freshly ovulated mouse eggs that were used.

The concentration of mPLCζ that triggers $[Ca^{2+}]i$ oscillations in human eggs (1mg/ml) was only five times higher than the amount used to produce $[Ca^{2+}]i$ oscillations of a similar frequency in mouse eggs (200ug/ml) so any inefficiency of aged human eggs to translate

cRNA to protein must be minimal (figs 3.2 and 3.5). These results show that whilst mouse eggs are much more sensitive to hPLCζ than human eggs (~1000 times), mouse eggs are only slightly more sensitive to mPLCζ than human eggs (~5 times). This suggests that the eggs have different thresholds of sensitivity for different PLCζ's since the mouse egg is highly sensitive to hPLCζ but only slightly more sensitive to mPLCζ compared to that of the human egg.

There appears to be a fine balance between the amount and type (species) of PLCζ and type (species) of egg required to effectively induce $[Ca^{2+}]i$ oscillations. The injection of some intermediate concentrations of hPLCζ cRNA into aged human eggs caused $[Ca^{2+}]i$ oscillations that increased in frequency over time. This is probably due to the gradual increase of translated PLCζ protein over time that in turn causes a frequency of $[Ca^{2+}]i$ oscillations that would normally be observed when higher concentrations of PLCζ cRNA are injected into an egg.

The human eggs used in these experiments were either failed-ICSI or failed-IVF eggs which lead to a number of limitations that must be discussed. Firstly, the procedure of ICSI involves the injection of a single sperm into an egg and this procedure could therefore lead to parthenogenetic activation of the egg since disruption of the egg membrane can cause an increase in $[Ca^{2+}]i$. This could mean that injection of PLCζ into the human eggs may be required in a bigger dose to initiate further $[Ca^{2+}]i$ transients following the initial parthenogenetic activation after ICSI.

It is also possible that some of the eggs that failed to fertilise after ICSI/IVF were diploid. A number of studies have shown that eggs that have failed to fertilise contain both female and male chromosomes (Kunathikom et al, 2001; Zhivkova, 2003). One study has shown that in many failed IVF eggs either decondensed sperm heads (~5% of eggs) were present or premature sperm chromosome condensation (~ 34% of eggs) had occurred

(Kunathikom et al, 2001). Approximately 18% of failed-ICSI eggs were found to contain decondensed sperm heads and 57% showed intact sperm heads (Kunathikom et al, 2001). These results show that many eggs that have failed to fertilise with IVF or ICSI are diploid and this is likely to be reflected in my studies on human eggs. Eggs were checked for the presence of a single pronucleus or two pronuclei approximately 17 hours post ICSI/IVF which would indicate if parthogenetic activation due to the ICSI procedure or fertilisation due to ICSI/IVF had occurred. Any embryos with a single pronucleus or two pronuclei were destroyed immediately in ethanol. The age of the human eggs (>17 hours post ICSI/IVF) may also have been a factor that impeded the development of human eggs after injection of PLCζ. It would be interesting to carry out these same experiments on freshly ovulated human eggs to determine how affective PLCζ is at triggering development to the blastocyst stage in human embryos.

3.3.3 Rapid cessation of $[Ca^{2+}]i$ transients may reflect faulty Ca^{2+}-release mechanism in IVM pig eggs

hPLCζ but not mPLCζ was effective in causing $[Ca^{2+}]i$ oscillations and triggering development in pig eggs. The potency of hPLCζ has been reported to be higher than mPLCζ with regard to causing $[Ca^{2+}]i$ release in mouse eggs (Cox et al., 2002) so it is likely that this is the case in pig eggs.

The highest concentration of mPLCζ cRNA injected into pig eggs was 2mg/ml and this did not trigger a $[Ca^{2+}]i$ response. Pig eggs did respond to hPLCζ cRNA by exhibiting $[Ca^{2+}]i$ oscillations, although they were characteristically short in duration (lasting about 1 hour) and the amplitude of each $[Ca^{2+}]i$ transient was shortened successively until the transients ceased. A gradual increase in basal $[Ca^{2+}]i$ was observed before each $[Ca^{2+}]i$ spike in pig eggs and it appeared that a spike was triggered only when the basal $[Ca^{2+}]i$ reached a threshold level. This is a characteristic that has been previously reported in pig eggs (Sun et

al., 1992). As the PLCζ-induced $[Ca^{2+}]i$ oscillations gradually decreased in amplitude they also exhibited a slower rate of rise, until eventually the increase in basal $[Ca^{2+}]i$ still occurred but was not sufficient to initiate a full $[Ca^{2+}]i$ spike (Fig 3.4A and B). The $[Ca^{2+}]i$ oscillations then ceased. The short duration of hPLCζ-induced $[Ca^{2+}]i$ oscillations in pig eggs was in contrast to the hPLCζ-induced $[Ca^{2+}]i$ oscillations in human and mouse eggs that continued for more than 3 hours. $[Ca^{2+}]i$ recordings of fertilisation in pig eggs has previously shown that sperm-induced $[Ca^{2+}]i$ oscillations last for more than 3 hours and exhibit regular amplitude and frequency $[Ca^{2+}]i$ oscillations (Sun et al., 1992). $[Ca^{2+}]i$ oscillations in pig eggs that had been triggered following injection of crude extract isolated from boar sperm were similar to those seen at fertilisation and the transients did not exhibit rapid reduction in the amplitude of $[Ca^{2+}]i$ transients, instead the time leading to each transient increased until $[Ca^{2+}]i$ transients ceased about 90 mins after injection (Machaty et al., 2000). Recently it has been established that pig sperm have a greater ability to induce $[Ca^{2+}]i$ oscillations in mouse eggs than mouse sperm (Kurokawa et al., 2005) so it would seem reasonable to suggest that the pig egg is more insensitive than the mouse egg. This does not, however account for the fact that the pig eggs exhibited $[Ca^{2+}]i$ oscillations that were both short in duration and showed a rapid decrease in amplitude following each successive $[Ca^{2+}]i$ transient.

The rapidly diminishing hPLCζ-induced $[Ca^{2+}]i$ rises in pig eggs could be due to incomplete oocyte maturation. Dramatic changes in $[Ca^{2+}]i$ release mechanisms have been reported to occur during oocyte maturation (Mehlmann and Kline, 1994; Fujiwara et al., 1993; Carroll et al., 1994; Jones et al., 1995b) and the ability of eggs to generate multiple long-lasting $[Ca^{2+}]i$ oscillations is dependent on successful progression through oocyte maturation (Jones et al., 1995b). Fertilization of immature oocytes induces $[Ca^{2+}]i$ transients that are significantly less in number, are markedly smaller and have a slower rate of rise than mature eggs (Jones et al., 1995b; Cheung et al., 2000; Jones et al., 1995b). These affects are

consistent with the $[Ca^{2+}]i$ response of the IVM pig eggs to hPLCζ cRNA in the experiments presented. This suggests that the pig eggs have not undergone complete development of $[Ca^{2+}]i$ release mechanisms due to poor cytoplasmic maturation.

It has been demonstrated that the ability of a spermatozoa to cause $[Ca^{2+}]i$ oscillations is dependent on the stage of maturation of the oocyte. This was first observed in the starfish oocyte, where the Ca^{2+} release in response to ten fertilizing sperm was less than that seen after a single sperm entry in a mature starfish egg (Chiba et al., 1990). Around 100 times as much $InsP_3$ was required to generate the same Ca^{2+} release in immature oocytes as mature starfish eggs however saturating $InsP_3$ levels caused a the same Ca^{2+} release in both immature oocyte and mature egg (Chiba et al., 1990). Studies on hamster oocytes showed that oocyte maturation caused an increased sensitivity to $InsP_3$ and that mature eggs had an all-or-nothing $[Ca^{2+}]i$ release in response to low $InsP_3$ levels (Fujiwara et al., 1993). The pig eggs did respond to PLCζ albeit not as strongly as human or mouse eggs, which suggests that whilst $[Ca^{2+}]i$ release mechanisms were in place they had a weakened ability to release $[Ca^{2+}]i$ causing a rapid damping of each successive $[Ca^{2+}]i$ transient (fig 3.4). Immature pig oocytes were selected for maturation based on exhibition of a uniform cytoplasm and at least three layers of compact cumulus cells around them. Pig eggs were only selected for hPLCζ microinjection if 1st polar body extrusion had occurred, however more selectivity may be necessary to determine how high quality pig eggs respond to PLCζ with respect to $[Ca^{2+}]i$-releasing ability.

The amount of Ca^{2+} released after stimulation with spermatozoa, ionomycin, $InsP_3$, ryanodine and the Ca^{2+}-ATPase inhibitor thapsigargin, has been shown to increase during oocyte maturation (Tombes et al., 1992; Jones et al., 1995b; Carroll et al., 1996). Previous reports have shown that immature mouse oocytes respond to sperm fusion by generating two to three successful $[Ca^{2+}]i$ transients before $[Ca^{2+}]i$ flux ceases in less than an hour (Jones et

al., 1995b). This is consistent with the results obtained from injection of 20μg/ml hPLCζ cRNA into pig eggs. $[Ca^{2+}]i$ can cause regenerative $[Ca^{2+}]i$ increases by activating neighboring Ca^{2+} channels to release $[Ca^{2+}]i$ by a process called Calcium-Induced Calcium Release (CICR). The gradual reduction of $[Ca^{2+}]i$ being released from the stores may be hindering further $[Ca^{2+}]i$ uptake and hence $[Ca^{2+}]i$ release. The duration of the first $[Ca^{2+}]i$ transient in the pig egg was approximately 90 seconds, which is of much shorter duration than the first transient exhibited in $[Ca^{2+}]i$ oscillations of the human or mouse egg which lasted around five to six minutes. Failure of intracellular $[Ca^{2+}]i$ stores to sequester $[Ca^{2+}]i$ may have caused fast $[Ca^{2+}]i$ depletion during the first $[Ca^{2+}]i$ transient.

The experiments carried out on pig eggs were subject to a number of limitations other than that of the detrimental affects of *in vitro* maturation. The pig oocytes had for example to remain in the ovary for at least 2 hours during transportation of the ovaries from the slaughter-house to the lab. A previous study investigating how temperature changes and time intervals caused by handling and transport of mare ovaries from the slaughterhouse to the laboratory revealed an adverse affect on the rate of oocyte recovery and their quality after IVF and maturation (Guignot et al, 1999). It therefore seems likely that the development of the pig eggs and embryos following activation with PLCζ may be influenced by the stress placed on the oocytes during the time following slaughter of the corresponding gilts.

Another factor affecting the pig eggs' ability to respond to PLCζ mRNA may be their ability to translate mRNA. It is unclear how the translational efficiency of pig eggs varies from that of human and mouse eggs but this may be significantly different. One way to test this hypothesis would be to inject the PLCζ protein rather than the mRNA form into the pig, human and mouse eggs.

3.3.4 hPLCζ can trigger development to the blastocyst stage in human and mouse eggs.

It has previously been shown that hPLCζ cRNA can cause Ca^{2+} oscillations and development to the blastocyst stage when injected into mouse eggs (Cox et al., 2002). Here I confirm that the same concentration of hPLCζ cRNA (0.2μg/ml) can trigger development to the blastocyst stage (53%) in mice with high success (fig 3.8). This finding also demonstrates that the pattern of $[Ca^{2+}]i$ oscillations induced by PLCζ is efficient in causing high levels of development.

A number of chemical treatments have been used to successfully parthenogenetically activate mouse eggs, but human eggs appear to be insensitive to most of these treatments. Artificial stimuli have been reported to trigger egg activation and development up to the blastocyst stage in freshly ovulated eggs but not in aged human eggs. Ca^{2+} ionophore A23187 and puromycin have for example been shown to trigger activation in aged human eggs with 20% of eggs reaching development to the four-cell stage however no development was observed beyond this stage in this study (Nakagawa et al., 2001). Other studies using aged human eggs reported cell cleavages after parthenogenetic activation but not blastocyst formation (Winston et al., 1991; Balakier and Casper, 1993). Freshly ovulated human eggs have in contrast been reported to reach the eight-ten cell stage (Cibelli et al., 2001) and blastocyst stage (Lin et al., 2003; Hwang et al., 2004) after artificial activation stimulated by Ca^{2+} ionophore and 6-DMAP.

To my knowledge this is the first study to show blastocyst stage development after parthenogenetic activation of aged human eggs. The overall number of human eggs that were used for developmental studies were small however, development to the blastocyst stage occurred in 17% of aged human eggs artificially activated with 0.1μg/ml hPLCζ (Rogers et al., 2004). Successful development of human embryos was dependent on a narrow range of hPLCζ cRNA concentration. The lowest concentration (0.1μg/ml) was effective at inducing

$[Ca^{2+}]i$ oscillations in only 46% of eggs although this concentration was particularly effective at causing high numbers of embryos to cleave and reach later stages of preimplantation development up the blastocyst stage (Fig 3.7 and Table 3.2). A 100-fold increase in the concentration of injected hPLCζ (10μg/ml) triggered high frequency $[Ca^{2+}]i$ oscillations in all eggs injected, however this concentration was detrimental to embryo development since no embryos developed past the two-cell stage (data not shown). This result is consistent with a previous study which showed high frequency $[Ca^{2+}]i$ oscillations are detrimental to mouse embryo development, especially after the two-cell stage (Cox et al., 2002).

$[Ca^{2+}]i$ oscillations were first measured in human eggs during fertilization using the calcium-sensitive photo-protein aequorin and this study showed that the Ca^{2+} transients were of low frequency and occurred at different frequencies in different eggs but at regular frequency in individual eggs (Taylor et al., 1993). It is likely therefore that low concentrations of hPLCζ which induce low frequency $[Ca^{2+}]i$ oscillations are more effective at stimulating development of human eggs to the blastocyst stage (Rogers et al., 2004).

One explanation of the success in developing the human eggs to blastocyst stage may lie in the nature of the activation stimulus. Repetitive $[Ca^{2+}]i$ oscillations can be induced by PLCζ in human eggs (Rogers et al., 2004) and these are similar to those that have been observed previously during fertilization in human eggs (Taylor et al., 1993) (Fig 3.6). Many stimuli that cause multiple $[Ca^{2+}]i$ transients in other species eggs (such as Sr^{2+}) are ineffective in human eggs. I exposed human (n = 2 eggs) and pig (n = 5 eggs) to 10 mM Sr^{2+} and found that neither egg exhibited any $[Ca^{2+}]i$ oscillations with this treatment (data not shown). Artificial stimuli that cause a single $[Ca^{2+}]i$ wave are commonly used to activate human and pig eggs for this reason.

Studies on rabbit eggs where the number of $[Ca^{2+}]i$ increases were controlled by electrical pulsing have shown that repetitive $[Ca^{2+}]i$ oscillations can improve the success of

preimplantation (Ozil, 1990) and postimplantation (Ozil and Huneau, 2001) development compared to a single $[Ca^{2+}]i$ increase. Results from a separate study also using electrical-field pulses to induce $[Ca^{2+}]i$ transients in human eggs that failed to fertilize after ICSI, found that the frequency of $[Ca^{2+}]i$ transients applied had an affect on fertilization efficiency as well as embryo development (Zhang et al., 1999).

One study showed that fertilization failure after Intracytoplasmic Sperm Injection (ICSI) was due to incomplete egg activation in approximately 40% of cases (Rawe et al., 2000). This suggests that an inactive factor in the sperm (potentially PLCζ) may be responsible for fertilization failure. The fact that hPLCζ cRNA microinjection caused high rates of egg activation (75%) and development to the blastocyst stage (17%) in human eggs that previously failed to fertilize after Assisted Reproduction Technologies (ART) including ICSI suggests that hPLCζ cRNA could have clinical implications for couples suffering from this form of infertility, called male factor infertility. A small number of cases have shown that egg activation, successful pregnancy and development to term can be achieved in situations where failed fertilization repeatedly occurs after ICSI, by inducing a single $[Ca^{2+}]i$ increase using Ca^{2+} ionophore following the ICSI procedure (Murase et al., 2004; Eldar-Geva et al., 2003). One of the pregnancies did however end with a second trimester miscarriage due to fetal anomaly (Eldar-Geva et al., 2003) which suggests that Ca^{2+} ionophore activation may cause defects later on in embryo development. It is also unclear as to how efficiently Ca^{2+} ionophore works to facilitate later development in human embryos.

These experiments demonstrate that hPLCζ has the ability to trigger activation and development of human eggs at high efficiency and could be used specifically in this way to ensure high levels of egg activation. PLCζ may also be applied as a method to activate recipient eggs during Nuclear Transfer (NT) since it provides a 'natural' mechanism of $[Ca^{2+}]i$ release and may therefore be effective at activating a wide range of mammalian eggs.

Generation of parthenogenetic human embryos for the production of totipotent stem cells using hPLCζ could provide a more ethically acceptable way of producing stem cells from human embryos (Lin et al., 2003).

3.3.5 Summary

In this Chapter I have demonstrated that PLCζ can be used to effectively cause $[Ca^{2+}]i$ oscillations, activation and development in human, mouse and pig eggs. Clear differences in sensitivity exist between the three types of eggs and this was observed by the different amounts and types (mouse or human) of PLCζ needed to cause $[Ca^{2+}]i$ release in these eggs. Mouse eggs appeared to be the most sensitive egg. I have shown for the first time that aged human eggs that had failed to fertilize through ICSI or IVF can be effectively stimulated to activate and develop with reasonable success to the blastocyst stage by injecting them with hPLCζ cRNA. Lower scores of successful development were observed in pig eggs injected with hPLCζ cRNA and this is probably because of incomplete development of $[Ca^{2+}]i$ release mechanisms during oocyte maturation. I have also confirmed the findings of previous reports that show hPLCζ is a more potent Ca^{2+} releasing PLC then mPLCζ (Cox et al., 2002).

Chapter 4

$[Ca^{2+}]i$ oscillations during egg activation affect preimplantation development and blastocyst quality

4.1 Introduction

In Chapter 3 I showed that PLCζ the natural proteinaceous factor found in the sperm, induces repetitive $[Ca^{2+}]i$ oscillations in mice, pigs and human eggs. In this Chapter I demonstrate that repetitive $[Ca^{2+}]i$ oscillations at egg activation have important post-activation effects on preimplantation development.

A number of studies have concluded that $[Ca^{2+}]i$ oscillations at egg activation have a role in longer term embryonic events. Manipulation of $[Ca^{2+}]i$ transients (controlled by electrical field pulse) has been used to show that the pattern of $[Ca^{2+}]i$ transients influence the number of embryos undergoing compaction, forming blastocysts and implanting (Ozil, 1990; Ozil and Huneau, 2001). Blastocyst composition has been shown to be affected by the pattern of $[Ca^{2+}]i$ oscillations during egg activation. Increasing the duration of Sr^{2+}-induced $[Ca^{2+}]i$ oscillations during parthenogenetic activation from two to four to twenty-four hours increased the Inner Cell Mass (ICM) cell number sequentially (Bos-Mikich et al., 1997). Ethanol activation which induces a single $[Ca^{2+}]i$ transient was shown to generate blastocysts with the lowest ICM and the highest Trophectoderm (TE) cell number compared to IVF or Sr^{2+}-activated embryos (Bos-Mikich et al., 1997) and this suggests that $[Ca^{2+}]i$ oscillations have an important role beyond stimulating meiotic resumption. At present it is unclear how $[Ca^{2+}]i$ oscillations during egg activation can influence embryos several cell divisions later then the blastocyst stage

Improved mouse embryo development has been observed when stimuli that increase basal $[Ca^{2+}]i$ levels are added to culture media. The addition of 0.1% ethanol in culture media during the one or two-cell stage has been shown to significantly increase blastocyst cell numbers, rates of blastocyst formation, numbers of successfully hatching blastocysts and earlier formation of adhesive trophoblasts (Leach et al., 1993). Stimulation of mouse morulae with ethanol or Ca^{2+} ionophore was similarly reported to accelerate the rate of fluid accumulation during blastocyst cavitation (Stacheki et al., 1994a) and this was interpreted as an indication that fluctuations in $[Ca^{2+}]i$ may act as a signal to promote cell growth and differentiation as well as to regulate preimplantation embryo development. Studies on somatic cells have shown that the $[Ca^{2+}]i$ oscillations reduce the effective $[Ca^{2+}]i$ threshold for activating transcription factors (Dolmetsch et al., 1998; Li et al., 1998). The frequency of $[Ca^{2+}]i$ oscillations has been reported to increase gene expression specificity so while rapid $[Ca^{2+}]i$ oscillations may stimulate a large number of transcription factors, infrequent $[Ca^{2+}]i$ oscillations may stimulate only a small number (Dolmetsch et al., 1998).

The aim of this Chapter was to examine the role of $[Ca^{2+}]i$ oscillations during post-activation preimplantation development. One major hurdle in attempting to study the affects of $[Ca^{2+}]i$ oscillations on later development is the fact that the earlier events associated with egg activation are dependent on $[Ca^{2+}]i$ increases. One method of separating the affects of $[Ca^{2+}]i$ oscillations on activation from the affects on later embryo development is to trigger egg activation by Ca^{2+}-independent means. Protein synthesis inhibitors such as cycloheximide do not induce a $[Ca^{2+}]i$ increase (Moses and Kline, 1995) but stimulate meiotic resumption by blocking the otherwise continuous synthesis of cyclin B, which is essential for stimulating cyclin dependent kinase (cdk1) and ensuring cell-cycle arrest. The protein synthesis inhibitors cycloheximide and puromycin have both been used to successfully activate mouse eggs in the past and have been reported to cause pronuclei formation and cell cleavage in mouse embryos

(Siracusa et al., 1978). Protein kinase inhibitors such as roscovitine (Phillips et al., 2002) have also been used to activate mouse eggs without stimulating a $[Ca^{2+}]i$ increase. The long-term development of embryos activated with protein synthesis or protein kinase inhibitors alone has not been monitored. In this study I used cycloheximide or roscovitine to activate eggs without a $[Ca^{2+}]i$ increase. Cycloheximide was chosen to activate eggs because it is a commonly used agent for activating eggs (although it is almost always used in combination with an agent that induces a $[Ca^{2+}]i$ increase). As cycloheximide inhibits the synthesis of all proteins in the cell it was a possibility that it may have caused long term developmental damage regardless of the fact that its effects are reversible after its removal. I chose to use roscovitine as an another way of activating eggs in a Ca^{2+} independent manner to safeguard against any detrimental affects on development that may have occurred with cycloheximide treatment. Roscovitine is an inhibior of cyclin-dependent kinase 1 (cdk1) and to a lesser extent of cyclin-dependent kinase 5 (cdk5) and was therefore used because of its higher specificity in translational inhibition than that of cycloheximide. The development of these eggs was compared to eggs that were parthenogenetically activated using strontium ions (Sr^{2+}), ethanol or a combination of Sr^{2+} plus cycloheximide, ethanol plus cycloheximide or roscovitine plus Sr^{2+} (See Fig 4.4 for experimental design). In this Chapter I show that $[Ca^{2+}]i$ increases at egg activation play an important role in cell-cleavage events up to the blastocyst stage and may mediate processes important in establishing blastocyst composition.

4.2 Results

4.2.1 $[Ca^{2+}]i$ measurements during parthenogenetic activation in mouse eggs

To stimulate parthenogenetic activation, eggs were treated using cycloheximide alone or in combination with Sr^{2+} or ethanol, roscovitine alone or in combination with Sr^{2+}, Sr^{2+} alone or ethanol alone. All Sr^{2+} treatments were carried out in Ca^{2+}-free media. Sr^{2+} treatment triggered a series of repetitive $[Ca^{2+}]i$ oscillations that did not change in frequency or amplitude over the duration of two hours in 13/14 eggs tested (Fig 4.1A). Cycloheximide treatment alone did not cause any $[Ca^{2+}]i$ change whatsoever in any of the 14 mouse eggs treated (Fig 4.1B). Treatment of eggs for 2 hours with cycloheximide followed by a further 2 hours treatment in cycloheximide and Sr^{2+} caused repetitive $[Ca^{2+}]i$ oscillations that were similar to those caused by Sr^{2+} alone (Fig 4.1C). $[Ca^{2+}]i$ transients of a similar nature were observed in all 16 eggs tested with this treatment.

In contrast to Sr^{2+} treatment, ethanol (7%) treatment triggered a large single $[Ca^{2+}]i$ transient (Fig 4.1D). The single transient consisted of an initial rapid rise in $[Ca^{2+}]i$ followed by a steady peak before a gradual drop back to basal $[Ca^{2+}]i$ as ethanol was replaced by regular HKSOM media. The gradual decrease was likely to be due to the slow replacement of ethanol with media. For developmental studies eggs were removed rapidly from the ethanol-containing media into regular media which in theory causes a more rapid decline in $[Ca^{2+}]i$.

Roscovitine treatment alone did not induce any $[Ca^{2+}]i$ changes whatsoever in all mouse eggs tested (Fig 4.2A). Treatment of eggs for 2 hours with roscovitine followed by a further 2 hours treatment in roscovitine and Sr^{2+} caused repetitive $[Ca^{2+}]i$ oscillations that were similar to those caused by Sr^{2+} alone (Fig 4.2B).

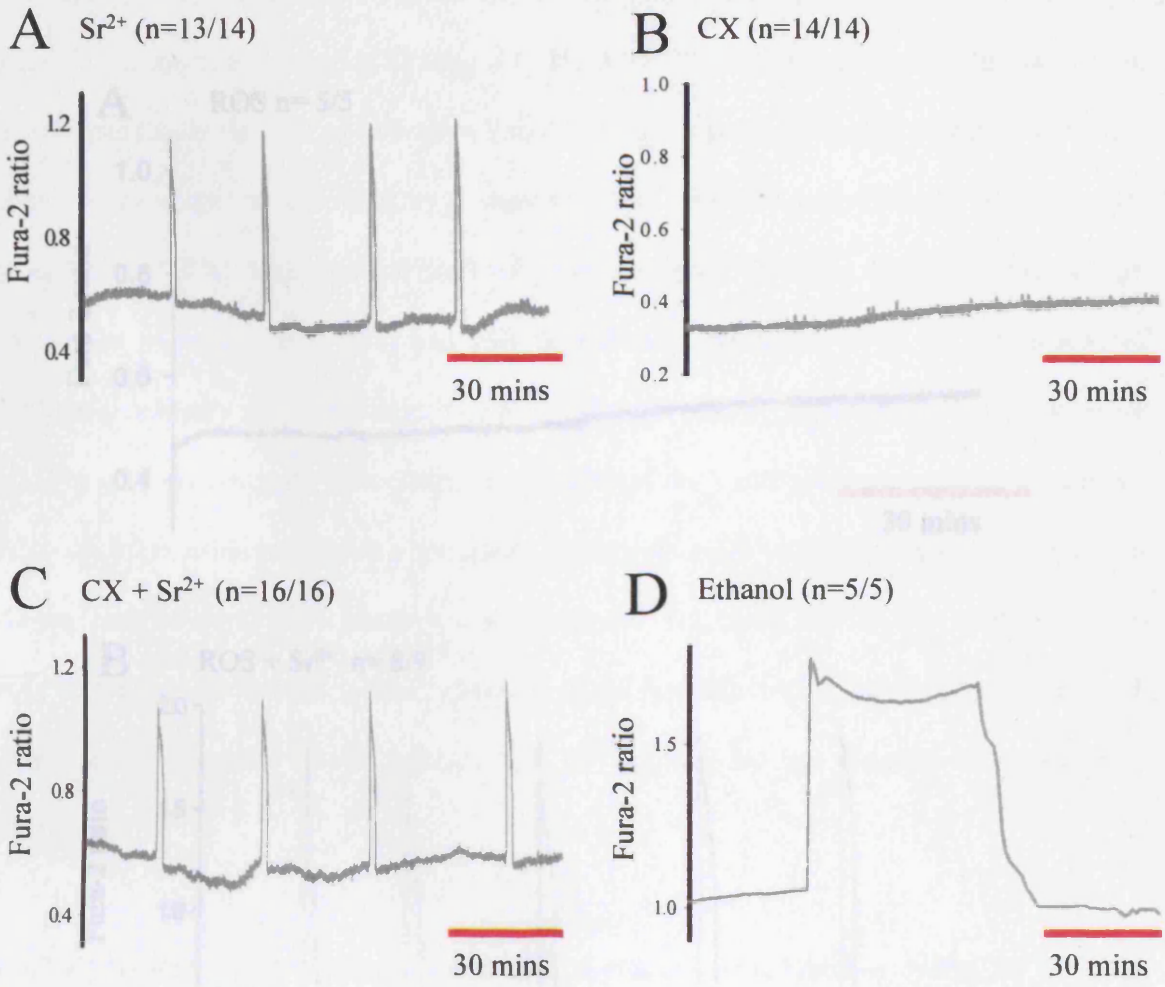

Figure 4.1 [Ca^{2+}]i changes during parthenogenetic activation. [Ca^{2+}]i was monitored in eggs by changes in the fura-2 fluorescence ratio. In (A) a sample trace is shown of an egg undergoing [Ca^{2+}]i oscillations when incubated in media containing 10mM Sr^{2+} from the start of recording. (B) is an example of an egg showing no [Ca^{2+}]i changes in media containing 20µg/ml cycloheximide (CX), in (C) an egg had been exposed to CX for 2 hours before being placed in media containing both Sr^{2+} and CX at the start of recording. (D) is a sample trace of an egg exposed to 7% ethanol for 7 mins. The ethanol-containing media was slowly pipetted off after the 7 min treatment and replaced with fresh media causing a gradual decrease in [Ca^{2+}]i. The n in each sample trace refers to the number of eggs exhibiting [Ca^{2+}]i changes similar to that of the sample trace.

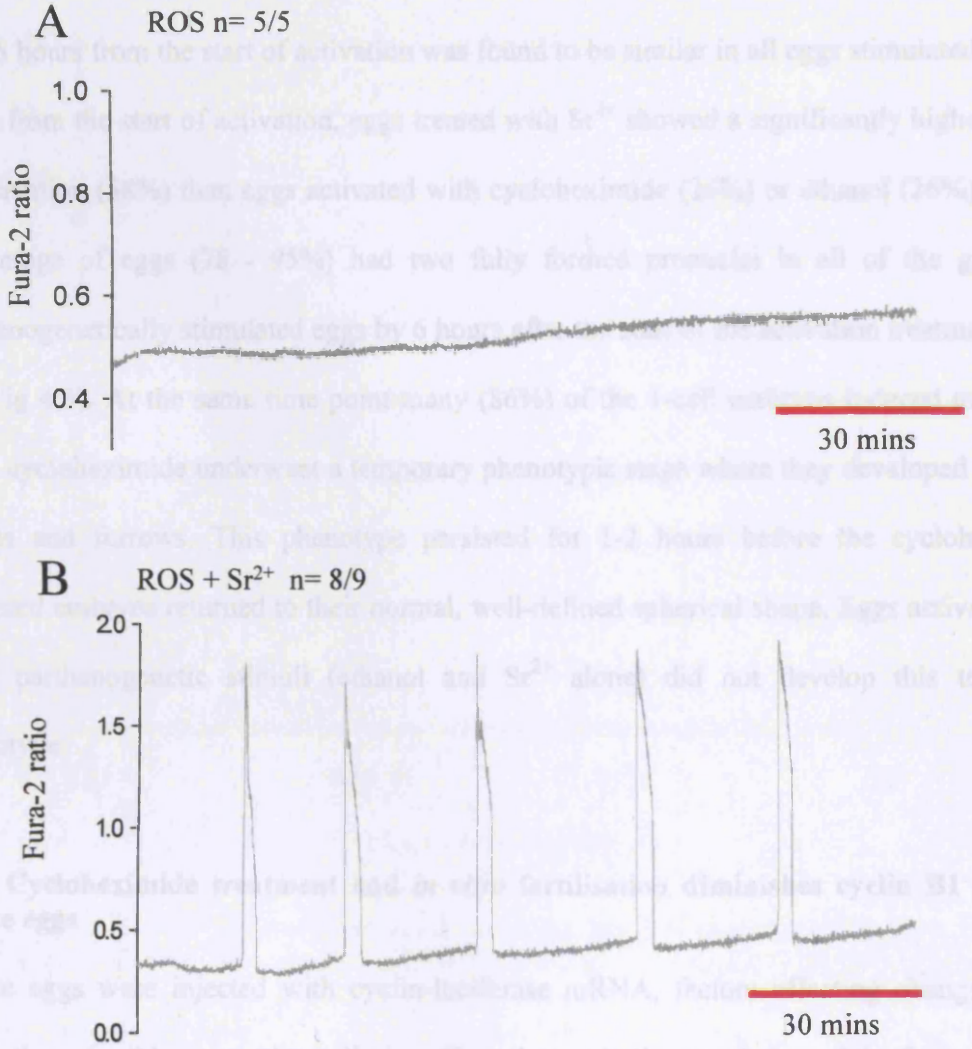

Figure 4.2 [Ca^{2+}]i changes during roscovitine treatment. [Ca2+]i was monitored in eggs by changes in the fura-2 fluorescence ratio. (A) is a sample traces of an egg exhibiting no [Ca2+]i changes in media containing 50μM roscovitine (ROS). In (B) an egg had been exposed to 50μM ROS for 2 hours before being placed in media containing roscovitine and Sr^{2+} at the start of recording. The N in each sample trace refers to the number of eggs exhibiting [Ca2+]i changes similar to that of the sample trace

4.2.2 Pronuclear formation in embryos generated from parthenogenetic activation

The timing of egg activation in parthenogenetically activated eggs was judged by the time taken for pronuclear formation (Table, 4.1, Fig 4.3). The overall amount of egg activation after 6 hours from the start of activation was found to be similar in all eggs stimulated. After 4 hours from the start of activation, eggs treated with Sr^{2+} showed a significantly higher degree of activation (58%) than eggs activated with cycloheximide (26%) or ethanol (26%). A high percentage of eggs (78 - 95%) had two fully formed pronuclei in all of the groups of parthenogenetically stimulated eggs by 6 hours after the start of the activation treatment (table 4.1, Fig 4.3). At the same time point many (86%) of the 1-cell embryos induced to activate using cycloheximide underwent a temporary phenotypic stage where they developed irregular shapes and furrows. This phenotype persisted for 1-2 hours before the cycloheximide-activated embryos returned to their normal, well-defined spherical shape. Eggs activated with other parthenogenetic stimuli (ethanol and Sr^{2+} alone) did not develop this temporary phenotype.

4.2.3 Cycloheximide treatment and *in vitro* fertilisation diminishes cyclin B1 levels in mouse eggs

Mouse eggs were injected with cyclin-luciferase mRNA, factors affecting changes in the translation of wild-type cyclin will also affect change in the translation of the fusion mRNA. The levels of cyclin-luciferase protein in a single egg were measured by the amount of light output from a single egg. The levels of cyclin-luciferase in control eggs (n = 19 eggs) remained in general very steady, often with a slight decrease in cyclin-luciferase over time (Fig 4.4A). Eggs treated with cycloheximide exhibited a rapid decrease in cyclin-luciferase during the first 2 hours of treatment and the levels continued to drop gradually to baseline levels during the last 2 hours of the 4-hour treatment (Fig 4.4B). A time of 57.4 $\pm$ 3.1 minutes (s.e.m) from the start of cycloheximide treatment was required for 90% cyclin-luciferase

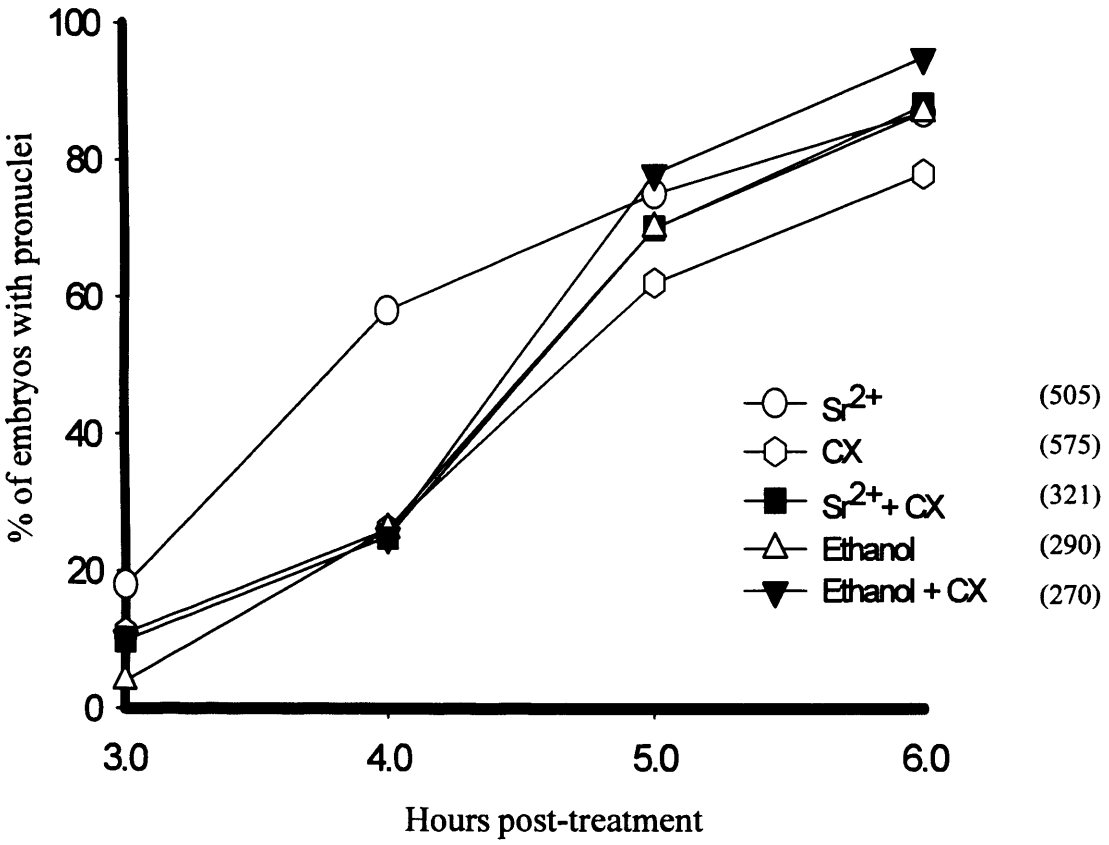

Figure 4.3. Rate of pronuclei formation during parthenogenetic activation. The timing of pronucleus formation from the start of activation treatment with Sr^{2+}, cycloheximide (CX), CX+ Sr^{2+}, Ethanol and CX + Ethanol. The number of embryos with pronuclei were scored every hour from 3 to 6 hours after activation treatment began. Sr^{2+} treatment involved a 2 hour incubation in 10mM Sr^{2+}, CX treatment was a 4 hour incubation in 20µg/ml CX. The combined Sr^{2+} + CX treatment began with 2 hour incubation in CX-containing media followed by 2 hour incubation in media containing both CX + Sr^{2+}. Ethanol treatment was a 7 minute exposure to 7% ethanol at room temperature. The combined CX and ethanol treatment involved ethanol exposure in the middle of a 4 hour treatment in CX. All eggs were cultured in media containing 2µg/ml cytochalasin D for 2 hours during their activation protocol to ensure parthenotes were diploid. The data in the brackets denote the total number of eggs used for each activation protocol. At least 10 biological replicates were used for each egg activation protocol.

Activation Treatment	Number of eggs	Pronuclear formation rate (hours post-treatment)			
		3	4	5	6
Sr^{2+}	505	92 (18)	294 (58)	377 (75)	438 (87)
CX	575	61 (11)	151 (26)	359 (62)	447 (78)
Sr^{2+} + CX	321	33 (10)	81 (25)	224 (70)	281 (88)
Ethanol	290	11 (4)	76 (26)	202 (70)	252 (87)
Ethanol + CX	270	28 (10)	68 (25)	212 (78)	256 (95)

Table 4.1 Pronuclear formation rates after parthenogenetic egg activation. Pronuclear formation was assessed 3-6 hours after the start of egg activation. The numbers in brackets indicate the % of eggs with 2 fully formed pronuclei. Embryos were used from 10 biological replicates. CX = cycloheximide

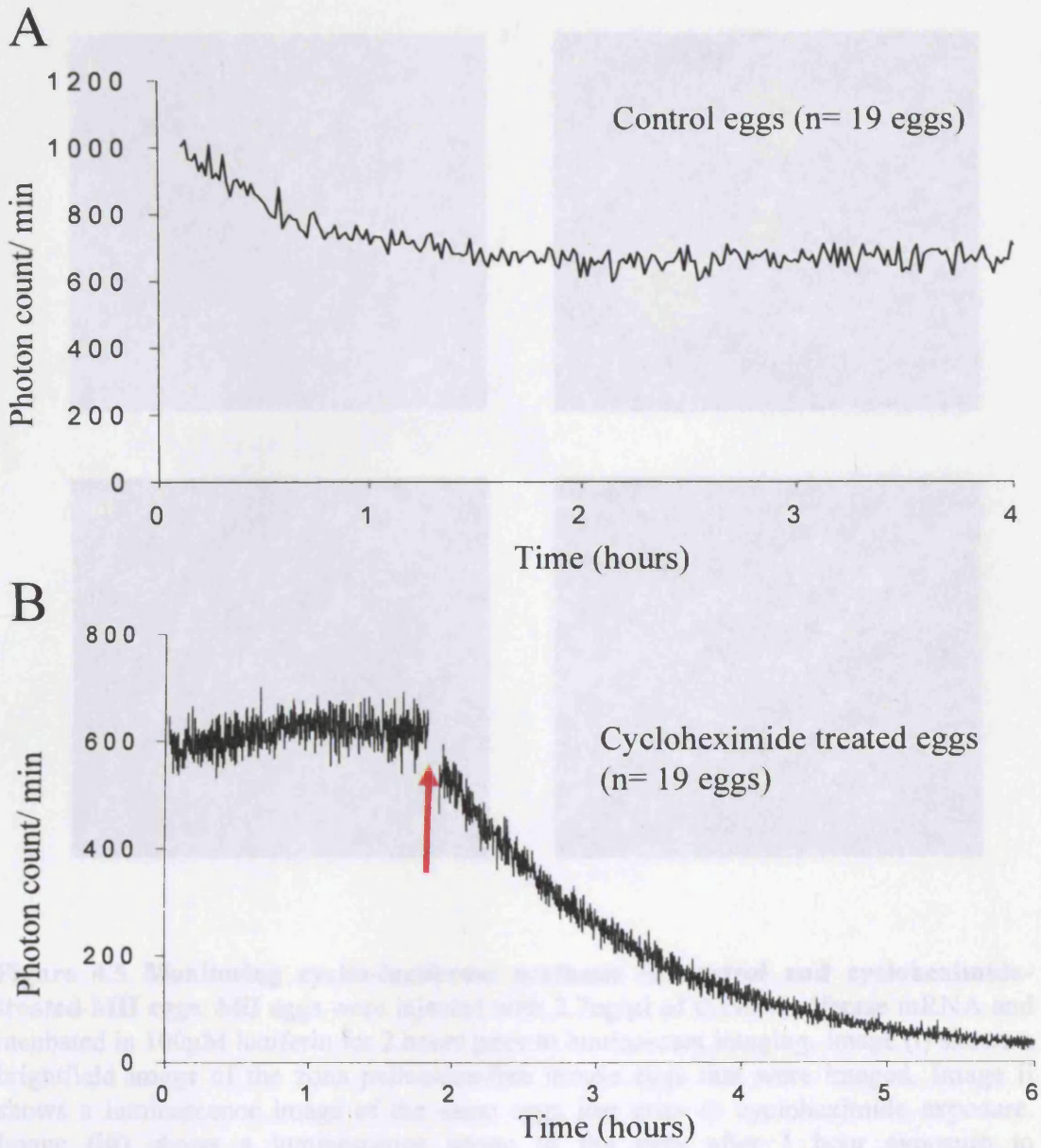

Figure 4.4 Cyclin-luciferase measurements in control and cycloheximide treated mouse eggs. Cyclin-luciferase levels were monitored in control (A) and cycloheximide treated (B) MII mouse eggs (A). Control eggs exhibited levels of cyclin-luciferase that remained high during a four hour period although a gradually reduction in cyclin B levels did occur in the first hour of monitoring. Cycloheximide treatment caused the levels of cyclin-luciferase to decrease drastically in the first hour and these levels continued to reduce during the four hour incubation. The red arrow indicates the point eggs were first exposed to cycloheximide. An integration time of 10 seconds was used to collect photon counts and a 20 x 0.5NA objective was used.

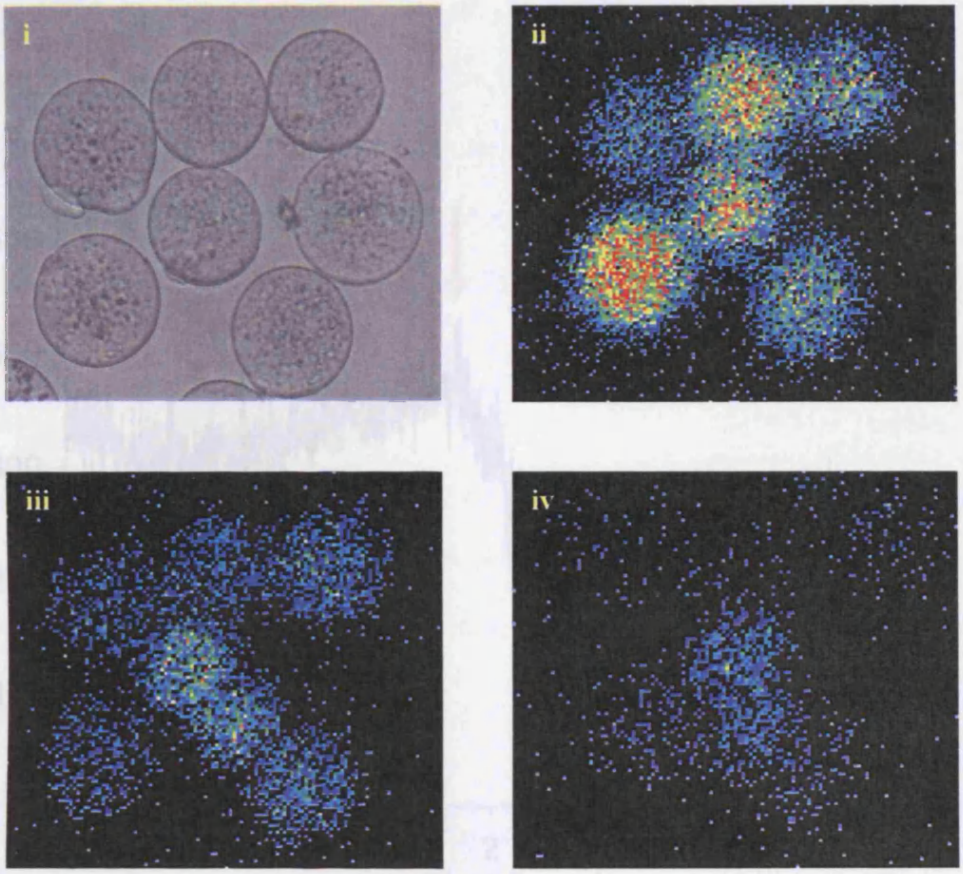

Figure 4.5 Monitoring cyclin-luciferase synthesis in control and cycloheximide-treated MII eggs. MII eggs were injected with 2.7ng/µl of cyclin-luciferase mRNA and incubated in 100µM luciferin for 2 hours prior to luminescent imaging. Image (i) shows a brightfield image of the zona pellucidae-free mouse eggs that were imaged. Image ii shows a luminescence image of the same eggs just prior to cycloheximide exposure. Image (iii) shows a luminescence image of the eggs after 1 hour exposure to cycloheximide and (iv) after 4 hours of exposure to cycloheximide. An integration time of 10 seconds was used to collect photons when a 20 x 0.5NA objective was used. The egg in the middle right of the image did not luminesce as it was dying.

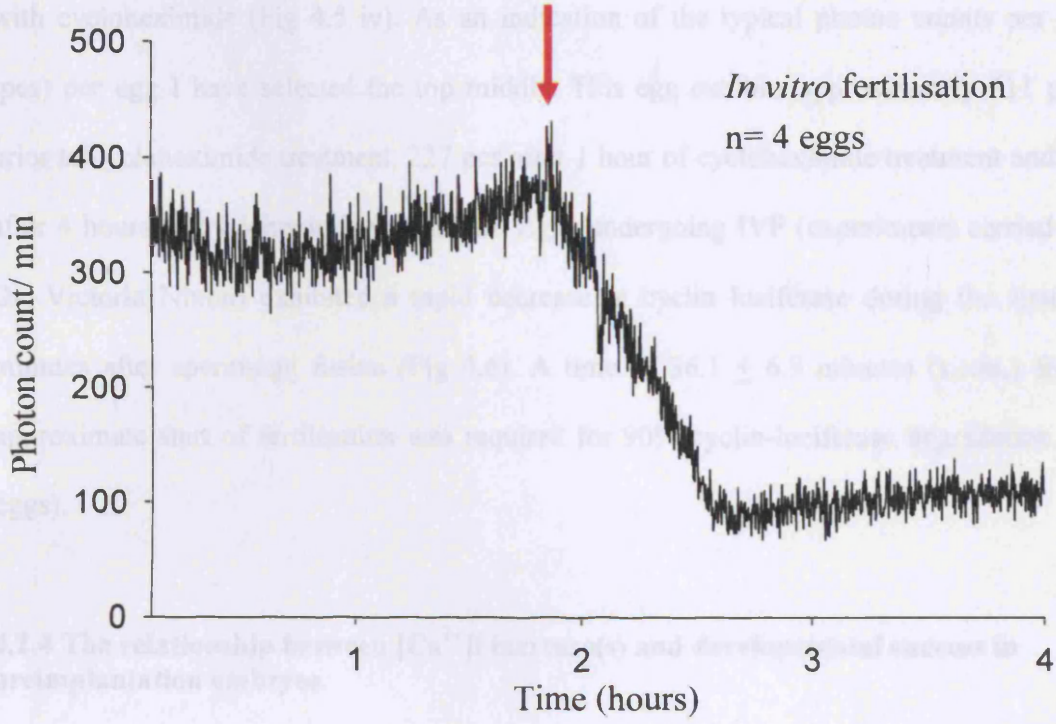

Fig 4.6 Cyclin-luciferase measurements in fertilised mouse eggs. Cyclin-luciferase levels were monitored in mouse eggs undergoing IVF. Cyclin-luciferase measurements were taken in eggs for approximately 2 hours prior to addition of sperm to the media. After sperm-egg fusion the levels of cyclin-luciferase decreased drastically during the first 30-40 minutes and then remained at a constant level for the next few hours. The red arrow indicates the time of fertilisation. An integration time of 10 seconds was used to collect photon counts and a 20 x 0.5NA objective was used.

degradation (n = 19 eggs). Fig 4.5 shows luminescence images of single eggs during different time-points during treatment with cycloheximide. Prior to cycloheximide treatment the eggs exhibited high amounts of cyclin-luciferase protein (Fig 4.5 ii) but after 1 hour of cycloheximide treatment, the amount of luminescence is reduced (Fig 4.5 iii). The luminescent intensity of each egg can be seen to be further reduced after the 4-hour treatment with cycloheximide (Fig 4.5 iv). As an indication of the typical photon counts per second (pcs) per egg I have selected the top middle. This egg exhibits approximately 611 pcs just prior to cycloheximide treatment, 227 pcs after 1 hour of cycloheximide treatment and 87 pcs after 4 hours of cycloheximide treatment. Eggs undergoing IVF (experiments carried out by Dr. Victoria Nixon) exhibited a rapid decrease in cyclin luciferase during the first 30-40 minutes after sperm-egg fusion (Fig 4.6). A time of 36.1 $\pm$ 6.9 minutes (s.e.m.) from the approximate start of fertilisation was required for 90% cyclin-luciferase degradation (n = 4 eggs).

4.2.4 The relationship between $[Ca^{2+}]i$ increase(s) and developmental success in preimplantation embryos.

Parthenogenetic activation was carried out using different combinations of stimuli (See Fig 4.7 for experimental design). Development of parthenogenetically activated eggs was scored from the egg to the blastocyst stage. Sr^{2+}-activation triggered a high percentage of embryos to reach the blastocyst stage and confocal imaging showed that most of these embryos were of good-excellent morphology (Fig 4.8). DNA staining using Hoechst dye also revealed that large nuclei were present in each of the blastomeres of these embryos and that compaction occurred at approximately the 16-cell stage. Around 36% of blastocysts that had previously undergone Sr^{2+} induced egg activation were recorded as hatching.

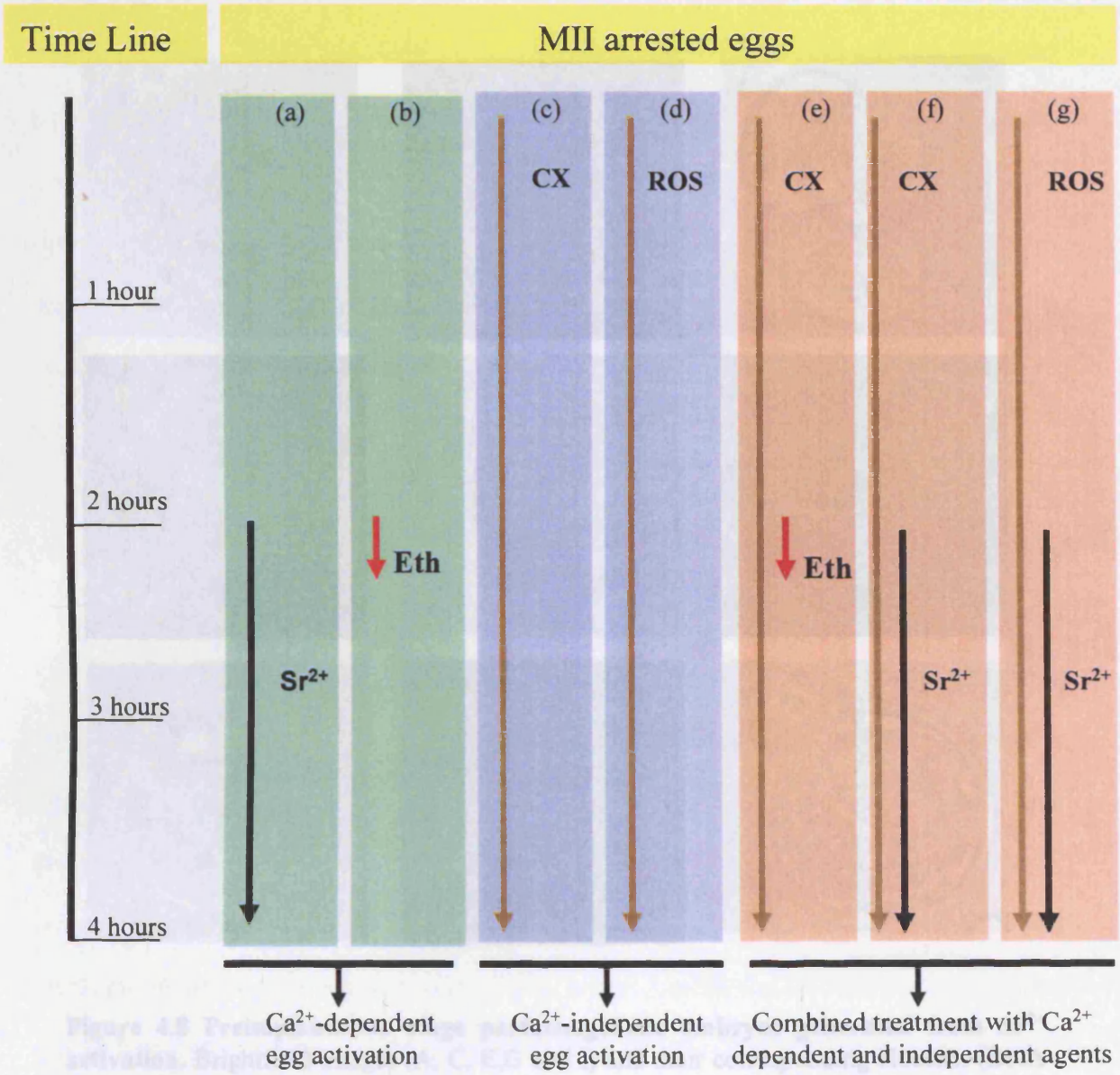

Figure 4.7 Experimental design for parthenogenetic egg activation protocol. Eggs were activated in a Ca^{2+} dependent manner with a two hour incubation in media containing (a) Sr^{2+} or a 7 minute exposure to media containing (b) 7% ethanol (Eth). Eggs were activated in a Ca^{2+} independent manner with a 4 hour incubation in media containing either (c) cycloheximide (CX) or (d) roscovitine (ROS). Combined treatments were carried out by exposing eggs to media containing (e) CX for 4 hours with a 7 min exposure to Eth after 2 hours from the start of CX treatment. Eggs were also incubated in media containing (f) CX for 2 hours followed by treatment in CX plus Sr^{2+} for a further 2 hours. This same treatment was also carried out in eggs but where (g) ROS replaced CX treatment.

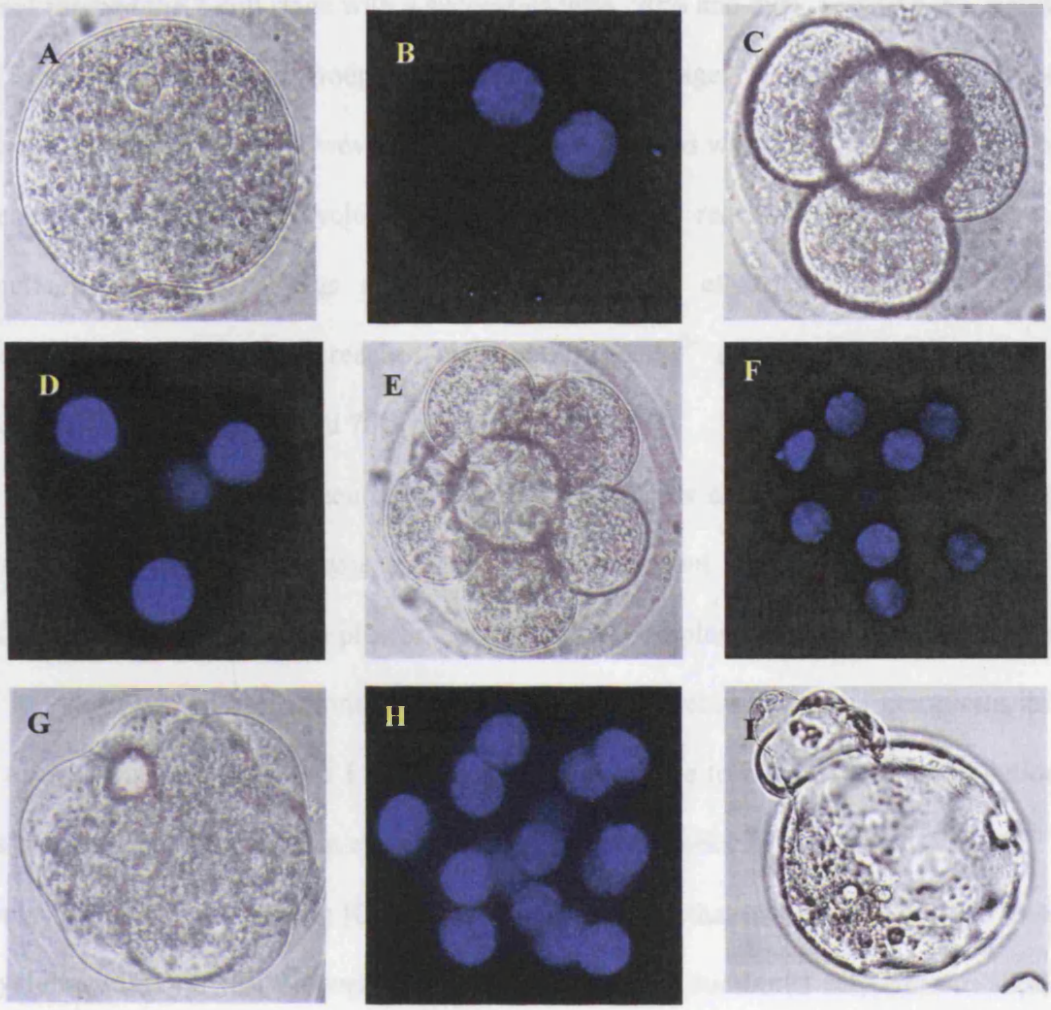

Figure 4.8 Preimplantation stage parthenogenetic embryos generated from Sr^{2+} activation. Brightfield images (A, C, E,G and I) and their corresponding Hoechst (DNA specific images (B,D,F,H) taken by confocal microscopy. Pronuclei form 3-6 hours after Sr^{2+} treatment (A,B). The first and second cell cleavage occurred 18-20 and 45-50 (C,D) hours post-activation. The 8-cell embryo was formed 60-65 hours post-activation (E,F). Approximately 72 hours post activation the embryo formed a compact ball of cells so that the cells were no longer distinguishable from one another (G,H). Formation of a blastocoel is first observed about 96 hours after activation and the embryo is now called a blastocyst. As the blastocoel enlarges the blastocyst expands. The final stage of development *in vitro* is blastocyst hatching (I) when the blastocyst escapes its zona pellucida through a small hole that it has lysed through a process called focal lysis.

A similar percentage of all parthenotes activated using various stimuli (see above) reached the 2 -cell stage of development (Table 4.2, Fig 4.9). Eggs activated with Sr^{2+}, cycloheximide and ethanol reached the 2-cell stage with a success of 90%, 90% and 89%, respectively. Similarly high percentages of these groups reached the 4-cell stage. A significant difference in developmental growth was however observed when embryos were cultured beyond the 4-cell stage. The percentage of cycloheximide-activated eggs reaching the 8-cell stage was dramatically lower than eggs activated with Sr^{2+} and ethanol. Whilst only 38% of cycloheximide-activated eggs reached the 8-cell stage, Sr^{2+} and ethanol eggs reached this stage with a success of 74% and 70% respectively (Fig 4.9).

To test whether the occurrence of $[Ca^{2+}]i$ increases could improve development of cycloheximide-activated embryos I monitored development in embryos activated with a combination of cycloheximide plus Sr^{2+} or cycloheximide plus ethanol. The effectiveness of Sr^{2+} to induce $[Ca^{2+}]i$ oscillations has been reported to decrease as the egg completes its first cell cycle. Consistent with this I found that Sr^{2+} was unable to induce $[Ca^{2+}]i$ oscillations in eggs that had been incubated in cycloheximide for 4 hours prior to exposure to Sr^{2+}. Sr^{2+} was however effective in triggering $[Ca^{2+}]i$ oscillations, in eggs that had previously been exposed to cycloheximide for just 2 hours (Fig 4.1C) and thus this combined activation method was employed to activate eggs. Eggs activated with cycloheximide and Sr^{2+} or ethanol exhibited similar levels of activation and development to the 2-cell (96% and 94% respectively) and 4-cell (88% and 80% respectively) stage (Fig 4.9). Treatment of eggs with cycloheximide for 2 hours followed by Sr^{2+} plus cycloheximide for 2 hours caused the number of embryos developing to the 8-cell stage (77%) to be comparable to embryos activated with Sr^{2+} (74%) alone. Parthenogenetic egg activation using cycloheximide plus ethanol also produced similar success to the 8-cell stage (75%). The developmental success of embryos beyond the 4-cell stage was much higher in eggs activated with these combined $[Ca^{2+}]i$ dependent treatments

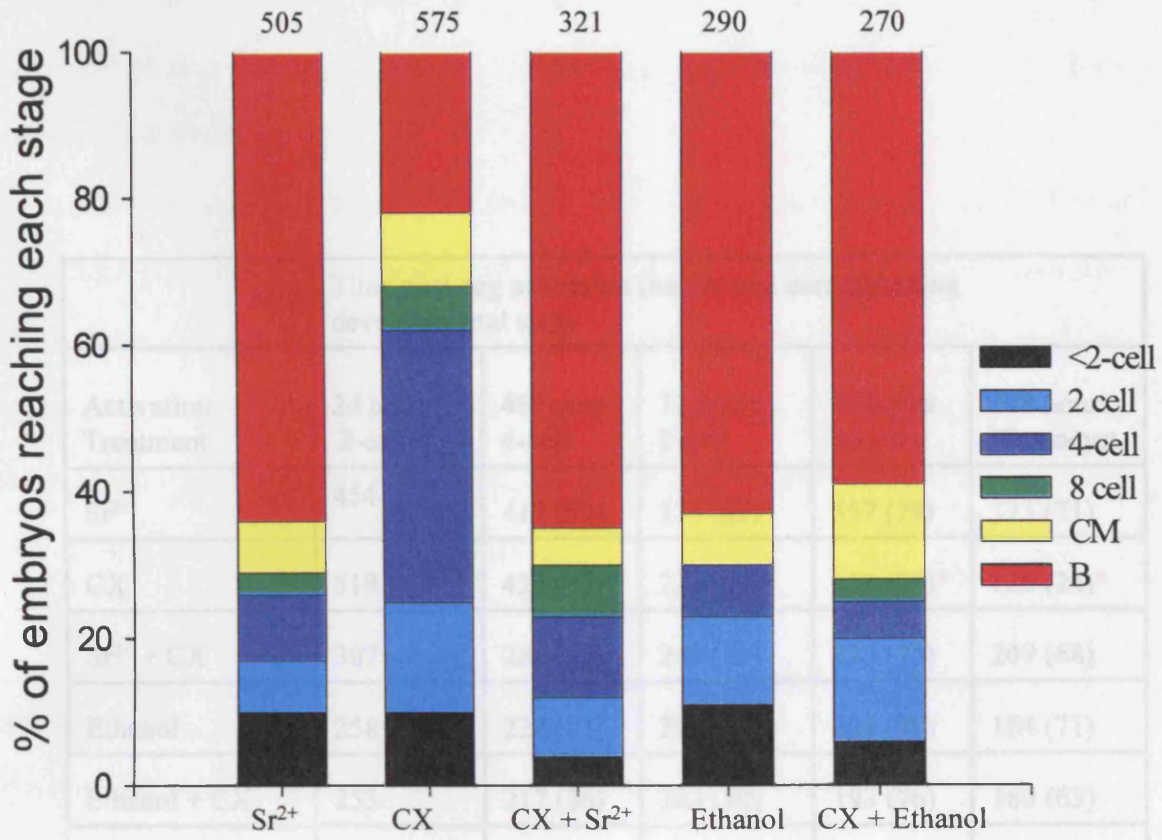

Figure 4.9 Developmental stages reached by eggs parthenogenetically activated by different stimuli. Stacked bar chart showing developmental phases from egg to the blastocyst stage that embryos reach after each type of parthenogenetic activation treatment. The black section of each bar represents the % of eggs that did not undergo 1st cell cleavage to the 2-cell stage. The combined activation treatment of Sr^{2+} and cycloheximide (CX) was the most successful activation stimulus with regard to % of successful egg activation and blastocyst formation. The number of embryos reaching the 8-cell stage dropped dramatically in CX-activated embryos when compared to embryos that had been activated by other stimuli. Total number of mouse eggs used for each treatment are denoted over each of the bars. CM represents compacted morulae and B refers to blastocysts.

	Time post egg activation (hours) and corresponding developmental stage				
Activation Treatment	24 hours 2-cell	48 hours 4-cell	72 hours 8-cell	96 hours Morula	103 hours Blastocyst
Sr^{2+}	454	417 (92)	374 (82)	357 (79)	323 (71)
CX	519	432 (83)	221 (43)*	183 (35)*	126 (24)*
Sr^{2+} + CX	307	281 (92)	248 (81)	223 (73)	209 (68)
Ethanol	258	224 (87)	204 (79)	204 (79)	184 (71)
Ethanol + CX	253	217 (86)	203 (80)	193 (76)	160 (63)
ROS	278	200 (72)*	132 (47)*	83 (30)*	39 (14)*
Sr^{2+} + ROS	236	197 (83)	148 (63)	98 (42)	66 (28)

Table 4.2 Developmental scores of embryos derived from different parthenogenetic stimuli. The numbers in brackets indicate the % of embryos that reached each developmental stage. Embryos were scored for developmental stage after the time (hours post-activation) indicated in the table. Embryos were used from 10 biological replicates. * denotes a significant difference in the group of activated embryos compared to groups without a *. CX= cycloheximide and ROS = roscovitine

than activation using cycloheximide alone. This data shows that $[Ca^{2+}]i$ elevation during egg activation appears to first show a real developmental effect during the 3rd cell cleavage, some time between the 4 and 8-cell stage. Only 22% of cycloheximide-activated eggs developed to the blastocyst stage compared to 65% of Sr^{2+} plus cycloheximide and 59% of cycloheximide plus ethanol activated eggs.

The development of embryos derived from egg activation using roscovitine or roscovitine plus Sr^{2+} was also compared (table 4.2). Roscovitine-induced egg activation allowed 72% of eggs to develop to the 2-cell stage, 47% to the 4-cell stage, 30% to the 8-cell stage and 14% to the blastocyst stage. The combined activation treatment of roscovitine plus Sr^{2+} allowed a significantly higher number of embryos to develop to the 2-cell (83%), 4-cell (63%), 8-cell (42%) and blastocyst stage (28%).

4.2.5 Blastocyst composition after parthenogenetic egg activation with Sr^{2+} or cycloheximide

The numbers of cells in the inner cell mass (ICM) and trophectoderm (TE) of blastocysts generated from cycloheximide and Sr^{2+}-induced parthenogenetic egg activation were assessed using a differential staining technique. The outer cells (TE) of live Zona Pellucida-free blastocysts were artificially labelled with fluorescein-5-isothiocynate (FITC)-labeled Wheat Germ Agglutinin (WGA). The blastocysts were subsequently fixed, permeabilised and stained with propidium iodide (PI). The TE cells fluoresce with green cytoplasm and cell surface and red nuclei whereas the ICM cells will only exhibit red nuclei. Blastocysts were viewed on a confocal microscope and images of 3μm slices were taken from the top to the bottom of each blastocyst in order to carry out cell counts. An example of sections though differentially stained parthenogenetic blastocysts can be seen in Fig 4.10.

The mean total cell number, ICM number, TE number and TE/ICM ratio were calculated (table 4.3, Fig 4.11) in 22 blastocysts generated from Sr^{2+}-induced activation and

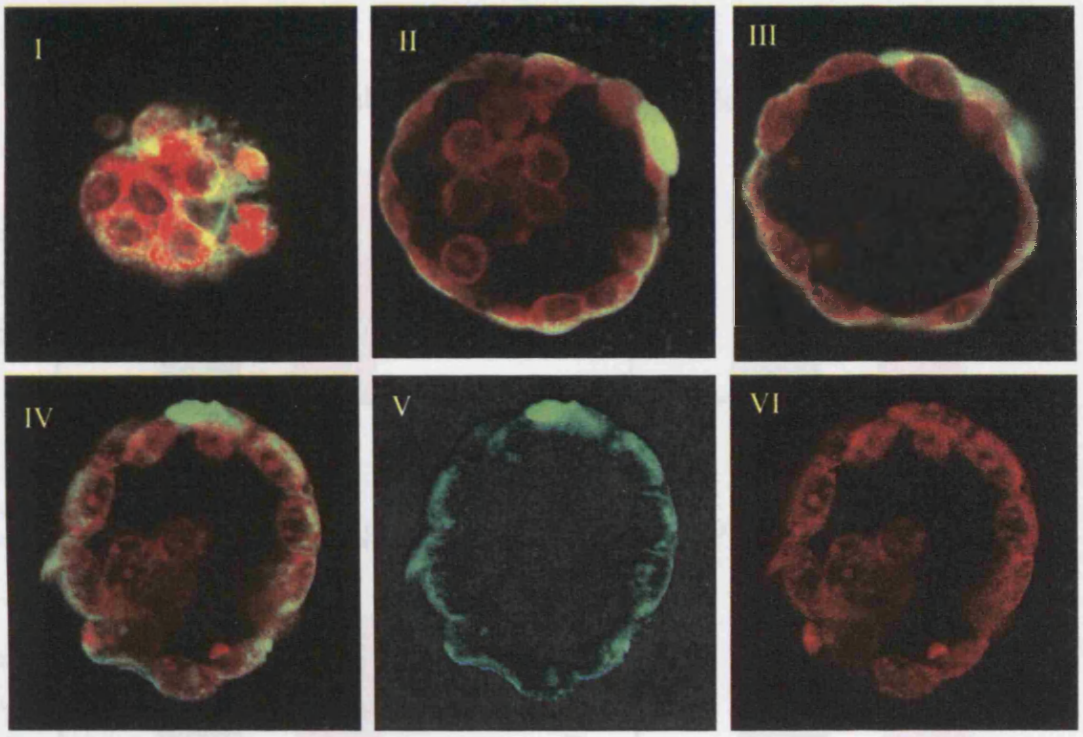

Figure 4.10 Confocal images of differentially stained blastocysts derived from parthenogenetically activated eggs. Exposure of live zona-free blastocysts to FITC-labeled WGA causes the exclusive labeling of the TE cell surface. Phagocytic activity in TE cells also contributes to the FITC labeling on the TE epithelium. Blastocysts are then fixed and permeabilised before being counterstained with Propidium Iodide (PI), which stains the nuclei of both ICM and TE red. The TE cell surface and cytoplasm consequently fluoresces green and the nuclei red from PI staining. Blastomeres allocated to the ICM were readily distinguishable as they were exclusively labeled by the PI and had no green fluorescence. Images I-III show 5μm sections taken from the top and middle of a blastocyst generated from Sr^{2+}-induced egg activation. At the top TE can be seen and consist of red nuclei with green cytoplasm surrounding it (I). Through the middle of the blastocyst, the ICM can be seen in the middle of the blastocyst and is exclusively labeled red (II). Past the ICM another section shows a large cavity and only TE cells can be seen (III). Images IV-VI show sections through a different blastocyst derived from an egg activated by cycloheximide. The red and green colours representing PI and FITC-WGA staining, respectively can be selectively highlighted or removed using MetaMorph 2 imaging software in order to easily establish the cell-type of individual cells.

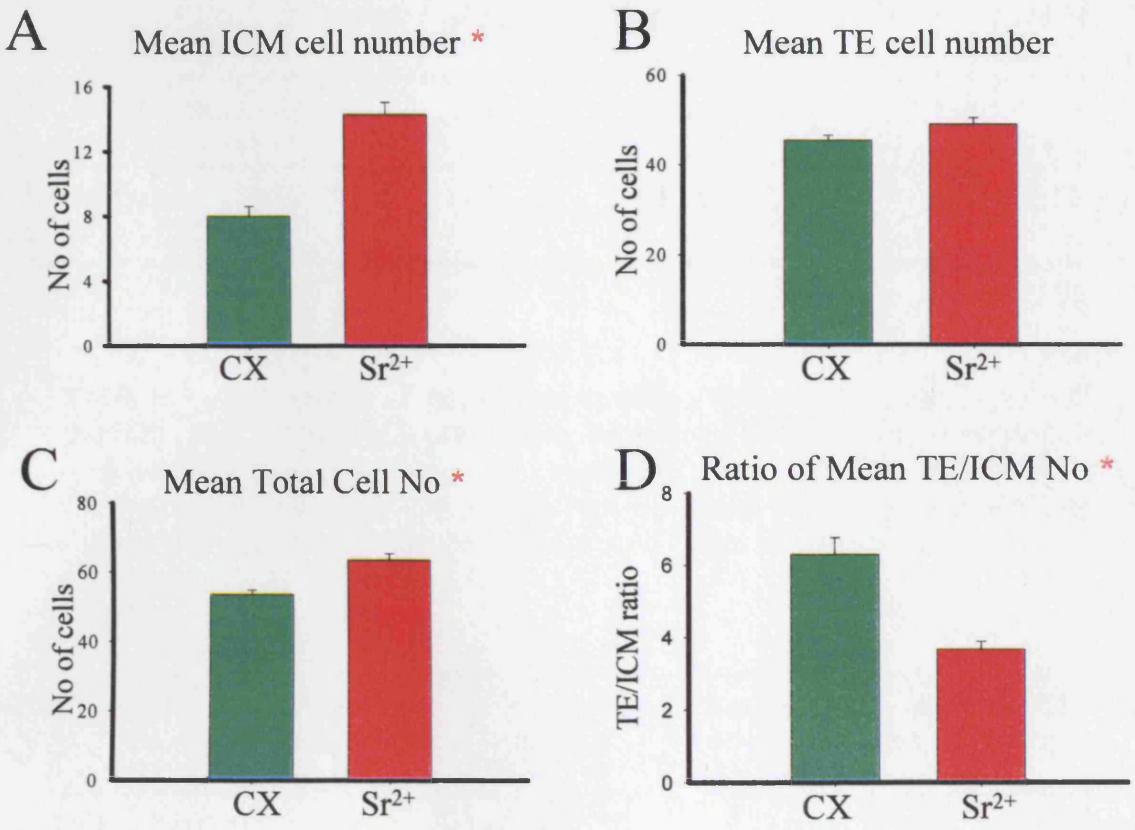

Figure 4.11 Blastocyst composition in blastocysts derived from cycloheximide and Sr^{2+}-induced egg activation. Bar charts with standard error mean (s.e.m) bars showing differences in mean ICM (A), mean TE (B), Mean total cell number (C) and ratio of TE/ICM (D) in blastocysts generated from either Sr^{2+} or cycloheximide (CX)-induced parthenogenetic activation. * indicates that Sr^{2+} and CX groups are significantly different (student's t test, $P<0.01$). B). The data represents mean numbers for 4 replicate experiments.

Fig 4.11

Treatment	No of blastocysts	Mean ICM number *	Mean TE number	Mean Total cell number *	Mean TE/ICM ratio *
Cycloheximide (CX)	21	8 (0.62)	45 (1.16)	53 (1.27)	6.3 (0.48)
Strontium (Sr^{2+})	22	14 (0.76)	49 (1.52)	63 (1.8)	3.67 (0.22)

Table 4.3 Composition of blastocysts resulting from cycloheximide or Sr^{2+}-induced egg activation. Parthenote blastocysts which were generated by cycloheximide (CX) or Sr^{2+} activation were differentially stained using FITC-WGA labelling and the mean ICM, TE, total cell number and ICM/TE ratio was calculated. * denotes a significant difference between the Sr^{2+} and CX treated group. Brackets show the standard error of each group.

Treatment	No of Blastocysts	Mean no of cells *	Mean no of apoptotic cells per blastocyst *	Apoptotic index *
Cycloheximide (CX)	26	46.77 (1.17)	6.42 (0.62)	0.14 (0.01)
Strontium (Sr^{2+})	19	62.68 (3.52)	3.00 (0.37)	0.05 (0.01)

Table 4.4. Apoptotic index in blastocysts derived from cycloheximide or Sr^{2+}-induced egg activation. Table of results showing mean numbers of cells, apoptotic cells and apoptotic index. Apoptotic index (%) is calculated by the equation – (dead cells)/ (live cells + dead cells) x 100. * represents significant difference between Sr2+ and CX activated groups of blastocysts (calculated by students t test, $P<0.05$).

21 blastocysts generated from cycloheximide-induced egg activation. Blastocysts were obtained from 4 treatment groups. The total cell number was significantly smaller (Fig 4.11C) in the blastocysts produced from cycloheximide-induced egg activation (53 cells) compared to those produced from Sr^{2+}-induced egg activation (63 cells). The difference in TE cell numbers in blastocysts generated from cycloheximide (45 cells) and Sr^{2+} - activated (49 cells) eggs were not significant (Fig 4.11B). A significant difference was observed however in the number of cells in the ICM where blastocysts produced from cycloheximide-induced activation had an average of 8 ICM cells and blastocysts generated from Sr^{2+}-induced activation had 14 ICM cells (Fig 4.11A). Analysis of the ratio of TE to the ICM cells revealed that blastocysts derived from eggs activated by Sr^{2+} had 3.67 times more TE than ICM cells. Blastocysts derived from eggs activated by cycloheximide had 6.3 times more TE than ICM (table 4.3, Fig 4.11D).

4.2.6 Apoptosis in blastocysts derived from eggs activated with Sr^{2+} or cycloheximide

TUNEL (Terminal deoxynucleotidyl Transferase Biotin-dUTP Nick End Labeling) staining was used to assay the degree of apoptosis in blastocysts derived from eggs activated with cycloheximide or Sr^{2+}. Extensive DNA degradation is a characteristic event that occurs in the late stages of apoptosis. DNA cleavage or degradation leads to strand breaks within the DNA. The TUNEL method identifies apoptotic cells by using terminal deoxynucleotidyl transferase (TdT) to transfer fluorescein-dUTP to the free 3'-OH termini on the strand breaks of cleaved DNA. Blastocysts were imaged under a fluorescence microscope to detect cells with DNA breaks. A total cell count was made possible by exposing blastocysts to Propidium Iodide (PI) which stains the nuclei of each cell. Cells that contained green fragments were classified as apoptotic.

Fig 4.12A shows examples of blastocysts that have been stained with TUNEL reagents and PI. The apoptotic index was calculated by dividing the number of apoptotic cells by the number of total cells (apoptotic and healthy) (table 4.4, fig 4.12B). The degree of apoptosis (apoptotic index) in blastocysts derived from eggs after cycloheximide-induced activation was almost 3 times higher than when blastocysts were derived from Sr^{2+}-induced egg activation. The mean number of apoptotic cells per blastocyst generated from cycloheximide activation was 6.42 compared to a significantly lower 3.0 apoptotic cells per blastocyst generated from Sr^{2+} activation. Significantly more cells were present in blastocysts derived from Sr^{2+} compared to cycloheximide-induced egg activation and this was consistent with previous results from the differential staining protocol (Fig 4.11C).

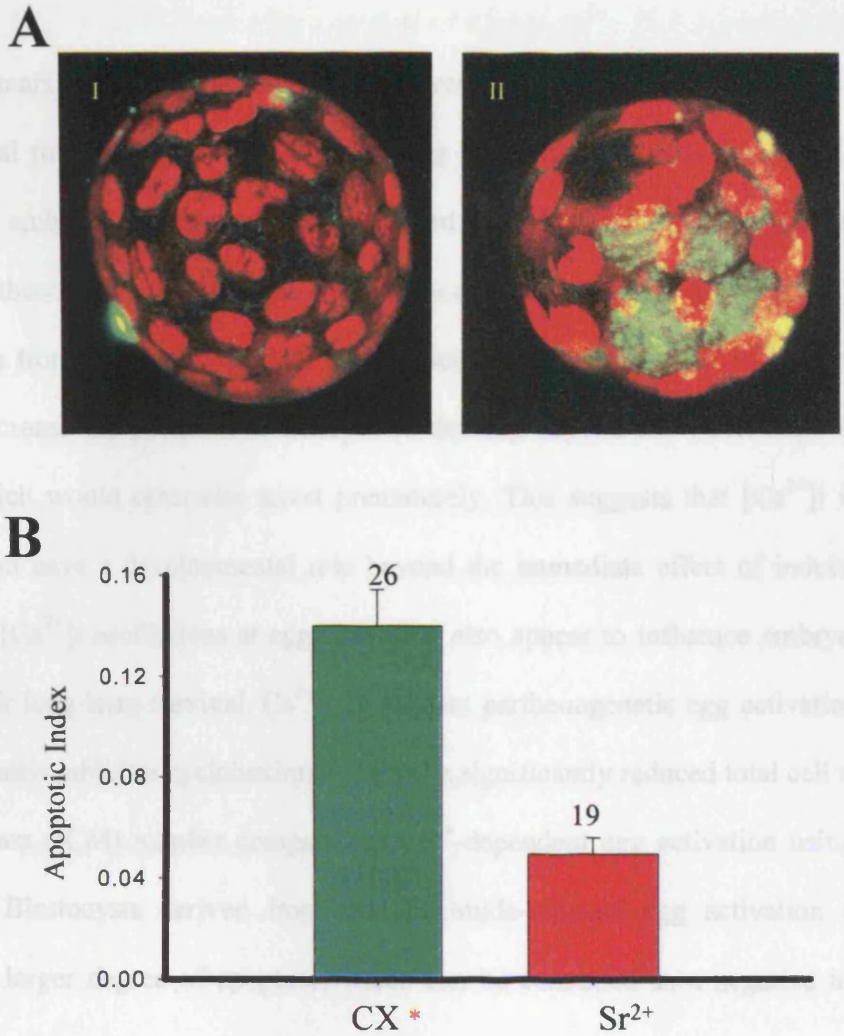

Figure 4.12 Measuring apoptosis in blastocysts. Blastocysts were fixed, permeabilised and incubated in fluorescein-conjugated dUTP and Terminal Deoxynucleotidyl Transferase Biotin-dUTP Nick End Labeling (TUNEL). In order to assess the proportion of apoptosis in the blastocyst all cell nuclei were stained red with propidium iodide (PI) which counted as the total number of cells. Fluorescein-labelled cells (green) were counted as apoptotic cells. Slices (5μM) through the blastocyst from the top to bottom were imaged. Compressed images of TUNEL stained blastocysts derived from eggs activated with (AI) Sr^{2+} and (AII) Cycloheximide (CX). (B) Bar chat representing the apoptotic index of blastocyst parthenotes. A significantly larger apoptotic index occurs in blastocysts derived from CX compared to Sr^{2+} activation (denoted by *). Numbers above the standard error mean (s.e.m) bars show the number of blastocysts used for each treatment group. Blastocysts from 3 biological replicates were used.

4.3 Discussion

The experiments presented in this Chapter were designed to determine the long-term developmental role of $[Ca^{2+}]i$ oscillations at egg activation in mouse embryos. In order to address this, embryo development was compared in embryos derived from eggs that were activated parthenogenetically by stimuli that do or do not trigger $[Ca^{2+}]i$ increase(s). The main interpretation from this work was that $[Ca^{2+}]i$ oscillations or a single $[Ca^{2+}]i$ increase at egg activation increase the potential of embryos to develop beyond the 4-cell stage by rescuing embryos which would otherwise arrest prematurely. This suggests that $[Ca^{2+}]i$ increases at egg activation have a developmental role beyond the immediate effect of inducing meiotic resumption. $[Ca^{2+}]i$ oscillations at egg activation also appear to influence embryo quality in terms of their long term survival. Ca^{2+}-independent parthenogenetic egg activation using the protein synthesis inhibitor cycloheximide caused a significantly reduced total cell number and inner cell mass (ICM) number compared to Ca^{2+}-dependent egg activation using strontium ions (Sr^{2+}). Blastocysts derived from cycloheximide-induced egg activation also had a significantly larger degree of apoptosis which can be construed as a negative influence on embryo survival.

4.3.1 $[Ca^{2+}]i$ changes during parthenogenetic egg activation

Sr^{2+} treatment has been shown to induce repetitive $[Ca^{2+}]i$ oscillations in mouse eggs that are similar but distinguishable to those that occur at fertilisation (Kline and Kline, 1992; Bos-Mikich et al., 1997) and my data is consistent with these observations. Sr^{2+} treatment has been reported to be less effective in triggering $[Ca^{2+}]i$ oscillations as embryos develop through the 1st cell cycle. I found that prior treatment of eggs with cycloheximide for 4 hours prevented

$[Ca^{2+}]i$ oscillations from occurring when eggs were then treated with Sr^{2+} (data not shown). The prior treatment of eggs for 2 hours in cycloheximide did not however prevent the generation of $[Ca^{2+}]i$ oscillations after exposure of eggs to Sr^{2+}. This infers that eggs become insensitive to stimuli that cause $[Ca^{2+}]i$ release if treated with cycloheximide for between 2 and 4 hours. It has previously been shown that at fertilisation sperm-induced $[Ca^{2+}]i$ oscillations are cell-cycle dependent and cease when the egg enters interphase and form pronuclei (Jones et al., 1995a). It therefore appears that sperm can only induce $[Ca^{2+}]i$ oscillations during metaphase and not interphase. My results show that a 4 hour treatment of eggs in cycloheximide is sufficient to cause pronuclei formation in 26% of parthenotes and therefore this time correlates with the time eggs are entering interphase.

According to Bos-Mikich et al, exposure of mouse eggs for 2 hours in 10mM Sr^{2+} caused 96% of eggs to activate (Bos-Mikich et al., 1995). The activation success rate was slightly higher than that which I obtained (87%) using the same protocol. Activation using Sr^{2+} plus cycloheximide triggered a very similar activation rate (88%).

The effectiveness of parthenogenetic agents depends heavily on the post-ovulatory age of the egg and freshly ovulated eggs for example are normally activated at lower rates than aged oocytes (Siracusa et al., 1978; Swann and Ozil, 1994). A combined treatment of Sr^{2+} and cycloheximide has previously been shown to significantly increase the rate of activation in freshly ovulated eggs compared to Sr^{2+}-treatment alone (Bos-Mikich et al., 1995). It has been shown that cycloheximide reduces Maturation Promoting Factor (MPF) (Bos-Mikich et al., 1995) and since MPF decreases spontaneously during aging in eggs it is probable that the eggs I used (16 hours post-hCG) for Sr^{2+} activation did not require an extra stimulus such as cycloheximide to decrease MPF levels further. Cycloheximide has previously been shown to activate eggs without inducing a $[Ca^{2+}]i$ increase (Siracusa et al., 1978; Moses and Kline, 1995; Moos et al., 1996). In support of these findings I found that mouse eggs incubated in

cycloheximide for 4 hours formed pronuclei but failed to exhibit any $[Ca^{2+}]i$ changes (Fig 4.1B).

4.3.2 Cycloheximide and sperm-induced egg activation efficiently cause cyclin degradation

I used cyclin-luciferase mRNA to give an indication of what affect cycloheximide would have on endogenous cyclin B1 in mouse eggs. Cycloheximide is a non-specific eukaryotic protein synthesis inhibitor which works by inhibiting the ribozyme peptidlytransferase an essential enzyme in the elongation reaction during protein synthesis. The amount of cyclin B1-luciferase protein being translated from cyclin-luciferase mRNA in single mouse eggs was related to the amount of light output during luminescence imaging. The levels of cyclin-luciferase protein were fairly steady in control mouse eggs although many eggs exhibited a slight decrease in the levels of protein over time. This was probably due to a small amount of degradation of cyclin B1-luciferase mRNA over time and therefore a smaller yield of overall translated cyclin-luciferase protein. Cycloheximide caused a rapid decline in the amount of cyclin-luciferase protein. These experiments show that cycloheximide can effectively inhibit the levels of cyclin-luciferase synthesis in eggs over the time course of 4 hours. Prior to cycloheximide exposure eggs exhibited luminescence at approximately 10 photon counts per second which corresponds to about 1-2 pg of luciferase protein (personal communication from Nixon and Swann). It has previously been estimated that approximately 10 pg of endogenous cyclin B exist in meiotically competent eggs (Kanatsu-Shinohara et al., 2000).

Reduced levels of cyclin are required for egg activation to occur and it is through the prevention of the synthesis of this protein that cycloheximide appears to be effective as a Ca^{2+}-independent mediator of parthenogenetic activation of eggs. The effects of cycloheximide are reversible and when the eggs are no longer exposed to it, they resume protein synthesis. Cycloheximide treatment of metaphase II-arrested mouse eggs has been

shown to result in similar temporal decreases in both cdc2/cyclin B1 kinase and MAP kinase activities that also occur following fertilization (Moos et al., 1996). Whilst the use of a cyclin based reporter system demonstrates that the protein inhibitor acts specifically upon cyclin, cycloheximide inhibits all translational activity and changes in the levels of cyclin-luciferase during cycloheximide exposure probably represent the relative changes in the translation of many other proteins in the same cell. Fertilisation of mouse eggs caused a more rapid decline in the amount of cyclin-luciferase protein than cycloheximide treatment with the time taken for 90% degradation of cyclin-luciferase protein being 36.1 ± 6.9 and 57.4 ± 3.1 minutes (s.e.m.) respectively. This difference in time indicates that the presence of $[Ca^{2+}]i$ oscillations during fertilisation increases the rate of cyclin-luciferase degradation. A GFP-based approach to examine real-time cyclin destruction in mouse eggs has previously revealed that the presence of sperm-induced $[Ca^{2+}]i$ oscillations cause a 6-fold increase in cyclin destruction when $[Ca^{2+}]i$ levels are raised above 600nM compared to cyclin degradation in unfertilised eggs (Nixon et al., 2002). This report also showed that discrete drops in cyclin B levels were associated with $[Ca^{2+}]i$ spikes when these spikes were as large as the first $[Ca^{2+}]i$ rise; this did not occur when the subsequent $[Ca^{2+}]I$ spikes were of a smaller magnitude. A progressive decrease in cyclin B did occur in eggs regardless of the magnitude of $[Ca^{2+}]i$ oscillations. I did not monitor changes in $[Ca^{2+}]i$ during the monitoring of cyclin luciferase but I would expect to make similar observations to those described by Nixon et al, 2002. The time taken for cyclin B levels to fall to their lowest levels during fertilisation was comparable in the GFP-based study (Nixon et al., 2002) and in the luciferase-based work I describe in this thesis.

Eggs are activated and pronuclei formation occurs when cycloheximide treatment reduces protein synthesis by more than 70% (Siracusa et al., 1978). If fertilisation-induced $[Ca^{2+}]i$ oscillations do indeed increase the rate of cyclin B degradation, then it is likely that Sr^{2+} treatment (which also induces $[Ca^{2+}]i$ oscillations) will have the same affect and this may

also explain the reason for an increased rate of pronuclei formation in Sr^{2+} activated eggs compared to cycloheximide treatment (which causes no $[Ca^{2+}]$I oscillations) (Fig 4.3). Whilst the rate of cyclin B decrease may impact on early developmental events (pronuclei formation) it is unlikely that it would have an affect on later preimplantation development.

4.3.3 $[Ca^{2+}]$i oscillations and preimplantation embryo development

The importance of $[Ca^{2+}]$i oscillations during mammalian egg activation has been well documented with respect to successful egg activation. The necessity for repetitive $[Ca^{2+}]$i oscillations is demonstrated by the finding that at fertilisation at least 9 Ca^{2+} transients were required for the formation of 2 pronuclei in mouse embryos (Lawrence et al., 1998). The frequency of $[Ca^{2+}]$i transients has also been shown to correlate with pronuclei formation (Vitullo and Ozil, 1992; Lawrence et al., 1998). A single $[Ca^{2+}]$i transient which can be induced by agents such as ethanol or Ca^{2+} ionophore can be sufficient to cause egg activation although the activation success is low in freshly ovulated eggs compared to aged eggs (Xu et al., 1997). A monotonic $[Ca^{2+}]$i change in sheep (Loi et al., 1998) and cow (Fukui et al., 1992) eggs is also sufficient to promote some postimplantation developmental events. Whilst these data demonstrate the usefulness of the monotonic $[Ca^{2+}]$i transient in activating development in some mammalian species it does not provide information about how the dynamics of the Ca^{2+} signal influence long-term embryo development. A number of studies have shown that the pattern of $[Ca^{2+}]$i oscillations at egg activation can have a profound affect on the development of the embryo. One study showed that compared with a single $[Ca^{2+}]$i transient, experimentally controlled $[Ca^{2+}]$i oscillations with a fertilisation-like frequency significantly increase the extent of development in preimplantation embryos (Ozil, 1990).

All studies investigating the developmental impact of $[Ca^{2+}]$i oscillations have so far only slightly altered the parameters of $[Ca^{2+}]$i oscillations in terms of the frequency,

amplitude and number of $[Ca^{2+}]i$ transients allowed to take place. The experiments conducted in this work were extreme in order to discover what affect the absence of any $[Ca^{2+}]i$ increases would have on embryo development. The development of embryos derived by means of Ca^{2+} dependent and Ca^{2+} independent parthenogenetic egg activation was scored according to the developmental stage reached by each embryo. This method provided a simple, effective and reproducible way of studying any possible influences of $[Ca^{2+}]i$ on development and these developmental affects could be separated by any affect of $[Ca^{2+}]i$ upon egg activation. It is well known that diploid parthenotes are less apoptotic and have a greater developmental capacity compared to haploid parthenotes (Liu et al., 2002). All eggs were treated during activation with Cytochalasin D, this prevents 2nd polar body extrusion and hence chromosome expulsion, causing eggs to remain diploid. Haploidy therefore does not explain any differences in developmental potential between different cohorts of parthenogenetically activated embryos.

I*n vitro* cultured parthenogenetic embryos cannot develop beyond the blastocyst stage since later stages of development require the expression of paternally derived imprinted genes which are essential for the normal development of extra-embryonic membranes and the trophoblast (Surani et al., 1984). During one study Ca^{2+} or heavy-metal-ion chelators were used to control the number of spontaneous $[Ca^{2+}]i$ transients at fertilisation (Lawrence et al., 1998) but I required complete abolishment of $[Ca^{2+}]i$ oscillations during egg activation and this technique would not be sufficient to cause egg activation without causing $[Ca^{2+}]i$ increases. For this reason activating eggs using cycloheximide appeared to be one of the most effective ways of causing egg activation without inducing $[Ca^{2+}]i$ oscillations.

The degree of successful egg activation was determined by the proportion of eggs that formed pronuclei and this was similar in eggs that were examined after activation with the five different treatments (Fig 4.3). At 4 hours after activation treatments began, a significantly

higher proportion of Sr^{2+}-activated embryos had 2 pronuclei compared to cycloheximide and ethanol-activated embryos. The reason for there being significantly less eggs with pronuclei after 2 hours from the start of activation with cycloheximide plus Sr^{2+} compared to Sr^{2+} activation alone is unclear. The cycloheximide treatment may inhibit proteins that are required for pronuclei formation. By 6 hours from the start of activation embryos from all five treatment groups had similar percentages of embryos with 2 pronuclei and thus successful activation.

The results from these experiments show that $[Ca^{2+}]i$ rises are not necessary to trigger egg activation and preimplantation embryo development since activation with cycloheximide or roscovitine alone did trigger cell cleavages to occur albeit with reduced success rates compared to embryos generated from egg activation with Ca^{2+}-releasing stimuli (Sr^{2+} and ethanol). More notably a significantly larger group of embryos developed to the 8-cell and blastocyst stages after egg activation with stimuli that cause either single or multiple $[Ca^{2+}]i$ transients.

It could be argued that egg activation by inhibitors of protein synthesis may have detrimental affects on embryo development. The data from embryo culture shows however that when used in combination with Sr^{2+}, cycloheximide does not have a significantly detrimental affect on the number of embryos forming 8-cell embryos compared to eggs activated in Sr^{2+} alone. This shows that cycloheximide does not have a detrimental affect on early stage embryos with regard to cell cleavage but instead it suggests that there in a link between the induction of $[Ca^{2+}]i$ oscillations at egg activation and better developmental potential.

The protein kinase inhibitor roscovitine was found to be sufficient at activating eggs with a similar efficiency to other stimuli (~72%) however further preimplantation development was severely impaired with only 14% of roscovitine-activated eggs developing

to the blastocyst stage. Consistent with my data, results from a published study showed roscovitine-induced egg activation caused similar numbers of embryos to develop to each preimplantation stage, although this study did not report any blastocyst formation (Phillips et al., 2002). The addition of Sr^{2+} treatment to roscovitine-treated eggs improved the numbers of embryos developing from the 2-cell to the blastocyst stage. This improvement was however not as pronounced as that of Sr^{2+} and cycloheximide treatment which suggests that roscovitine may cause inhibition of kinases that function around the time of egg activation and which may as a result of inhibition impact detrimentally on early preimplantation development. For this reason roscovitine-induced egg activation was not used for further studies.

4.3.4 Differential staining

Monochromatic or fluorochrome staining is a commonly used method for assessing total cell numbers in blastocysts. Further developmental information can however be obtained by assessing the relative numbers ICM and TE cells in blastocysts (Van Soom et al., 2001). I will briefly explain some of the methods that have previously been used to differentially stain blastocysts and explain the reasons for the staining protocol I used. The first approach that allowed selective labelling of TE and ICM used antibody complement-mediated membrane lysis (Handyside and Hunter, 1984). The outer TE cells form tight junctions to one another and are lysed by complement after being labelled with antibodies and PI whilst ICM cells are protected from lysis by the TE cells. The embryos are then fixed and all nuclei labelled with bisbenzimide. This technique is labour intensive and somewhat tedious as the antiserum must be prepared and tested for variability. A different method which involves labelling the outer cell surface proteins with benzenesulphonic acid (TNBS) has been used and is advantageous since the TNBS-labelled cells are recognised by antiserum that is commercially available (Hardy et al., 1989). I tested this procedure on mouse blastocysts and found that the

complement activity was highly variable and often resulted in incomplete lysis of the outer cells. TE cells can be permeabilised by rapid treatment with the ionic detergent Triton X-100 in combination with PI, followed by fixation in ethanol and bisbenzimide (Thouas et al., 2001). I used this technique but found that slight overexposure of blastocysts to Triton X-100 for even a few seconds caused permeabilisation of the ICM cells. The most successful technique I used involved labelling the outer cells of zona-free mouse blastocysts with fluorescein-5-isothiocynate (FITC)-labeled Wheat Germ Agglutinin (WGA) which binds to saccharide residues on the plasma membrane of TE cells. The blastocysts are then fixed, permeabilised and stained with PI. The cytoplasm of the TE cells fluoresce green and nuclei stain red whereas the ICM nuclei only show red (Fig 4.10). This technique has been used successfully in mouse blastocysts (De La Fuente and King, 1998). I found this technique to be very simple to carry out, fast, effective and accurate in differentially staining mouse blastocysts.

4.3.5 $[Ca^{2+}]i$ oscillations at egg activation influence blastocyst composition

Analysis of total cell number, inner cell mass (ICM) and trophectoderm (TE) number in blastocysts are an accurate indicator of embryo quality in terms of implantation viability (Thouas et al., 2001). A significant number of cow blastocysts with low ICM cell numbers have been shown to be derived from embryos of poor morphology (Van Soom et al., 1997) and increases in the number of ICM and total cells have been reported in cattle embryos cultured under favourable conditions (Narula et al., 1996).

The total number of cells in my Sr^{2+} and cycloheximide activated blastocysts (103 hours post-activation) were 63 and 53 cells respectively. There appears to be considerable variation between reported total cell numbers in parthenogenetic activated with various studies reporting 46 cells (Bos-Mikich et al, 1997), 62 cells (Brison and Schultz, 1997) and

104 cells (Liu et al, 1998) 96 hours post-egg activation. The variation in total cell number may reflect the differences in mouse strain, culture conditions and also the time point at which total cell numbers were evaluated post-egg activation. The parthenogenetic blastocysts in my experiments were within the reported range of total cell number described in other studies although it is hard to make direct comparisons with other studies when blastocyst cell numbers from my experiments were evaluated at different times post- egg activation. The total cell numbers of *in vivo* fertilised mouse blastocysts have also been reported in many published papers but again variation is observed in different studies and means of 65 cells (Jurisicova et al, 1998), 69 cells (Brison and Schultz, 1997) and 73 cells (Lin et al, 2003) have been reported in different studies on mouse blastocysts (96 hours post-hCG injection).

My results show that the nature of the activation stimulus during egg activation also has an impact on cell allocation in the blastocyst. I found that the total and ICM cell numbers were significantly reduced in blastocysts derived from eggs activated in a Ca^{2+}-independent manner compared to eggs activated in a Ca^{2+}-dependent manner. This suggests that $[Ca^{2+}]i$ increases during egg activation don't just influence egg activation but also events that take place a number of cell divisions later at the blastocyst stage. The pattern of $[Ca^{2+}]i$ oscillations at egg activation has previously been shown to affect blastocyst composition. One study reported that increasing the duration of Sr^{2+}-induced $[Ca^{2+}]i$ oscillations increased the number of ICM cells in mouse blastocysts (Bos-Mikich et al., 1997). Egg activation using different concentrations of Sr^{2+} or duration of treatment has also been shown to affect blastocyst formation and composition (Ma et al., 2005). An optimised treatment of 10mM Sr^{2+} for 2.5 hours was shown to be the most effective at generating high numbers of blastocysts with large ICM and total cell numbers (Ma et al., 2005). Both total and ICM cell numbers have been shown to be significantly lower in diploid parthenogenetic blastocysts derived from Sr^{2+}-induced egg activation than fertilised embryos that had been cultured *in vivo* or *in vitro* (Ma et

al., 2005). It would therefore be useful to compare the composition of blastocysts derived from PLCζ-induced egg activation with Sr^{2+}-induced egg activation. The sperm-specific protein PLCζ induces Ca^{2+} oscillations with a pattern indistinguishable from those induced by sperm (Saunders et al., 2002). Sr^{2+}-induced $[Ca^{2+}]i$ responses are not equivalent to those induced by fertilisation, which suggests that difference in stimulation of the egg activation signalling pathway can modify cellular and molecular events that impact upon later developmental events.

Knowledge of how different activation stimuli will affect cell allocation in blastocysts is of considerable importance since a minimal number of ICM cells are required to obtain a pregnancy. It has also been suggested that allocation of a disproportionate number of ICM cells could result in an abnormally large foetus and large-offspring syndrome (Leese et al., 1998).

4.3.6 Apoptotic index is reduced in blastocysts derived from Sr^{2+} compared to cycloheximide-induced activation.

The lower cell number in blastocysts generated from cycloheximide compared to Sr^{2+}-induced egg activation may be due to higher levels of apoptosis. Apoptosis is an important mechanism for removing defective cells that would otherwise be detrimental to the embryos survival. High levels of apoptosis have also been observed in embryos of excellent morphology, suggesting that apoptosis may control embryo cell number (Hardy et al., 2003). It has recently been reported that minimal and moderate levels of fragmentation in human blastocysts reduced cell numbers in blastocysts but this was mainly confined to TE cells since an invariable number of ICM cells were maintained (Hardy et al., 2003). The same study did however show that extensive fragmentation (>25%) causes cell numbers to reduce in both lineages. The findings presented in this chapter indicate that apoptosis may have a different

affect on TE/ICM cell numbers since blastocysts derived from egg activation by cycloheximide have around three times as much apoptosis compared to blastocysts derived from Sr^{2+}-activation but this appears to only cause a reduced ICM cell number and not a reduced TE cell number. It is unclear however if apoptosis in these parthenogenetic blastocysts is the major factor contributing to a reduction in ICM cell number. A combined differential staining and apoptosis assay would determine if apoptosis is more prevalent in ICM cells than TE cells. One way of investigating if the blastocyst composition and degree of apoptosis are due to a positive effect by Sr^{2+} or a negative affect by cycloheximide would be to study blastocysts derived from egg activation treatment using a combination of Sr^{2+} plus cycloheximide compared with blastocysts generated from cycloheximide treatment alone. A number of previously published reports have revealed the level of apoptosis in *in vivo* and *in vitro* cultured mouse embryos. One study showed that mouse blastocysts cultured in vivo or *in vitro* from the 2-cell stage showed approximately 2% and 6% of dead cells respectively (Brison and Schultz, 1997). Other studies have shown that blastocysts that have been derived from culture *in vitro* contain approximately 3-8% apoptotic nuclei (Handyside and Hunter, 1986; Fabian et al, 2003; Fabian et al, 2004) whereas a 1-5 % occurrence of apoptosis has been documented from *in vivo* derived mouse blastocysts (Jurisicova et al, 1998; Liu et al, 1999). In comparison to these data the incidence of apoptosis in my *in vitro* cultured Sr^{2+}-activated blastocysts appears to be comparable to blastocysts derived from *in vitro* culture in other studies. The blastocysts derived from cycloheximide-activation in my experiments exhibited 14% apoptotic cells, which appears to be higher than has been observed in previously published reports on *in vitro* cultured blastocysts. This suggests that the mechanism of parthenogenetic egg activation may later influence the level of apoptosis in embryos. A previous study has shown however that the level of apoptosis in blastocysts is not increased in parthenogenetically activated blastocysts but by haploidy (Liu et al, 1998). In this

elegant study, the level of apoptosis in diploid Sr^{2+}-activated blastocysts (4% apoptotic cells) was not found to be significantly different from blastocysts derived from *in-vitro* fertilisation (3% apoptotic cells) but both groups were found to be significantly different from haploid Sr^{2+}-activated blastocysts (7% apoptotic cells).

It is unclear how $[Ca^{2+}]i$ rises may positively affect embryo development. It has been suggested that developmentally-important information is encoded in the pattern of $[Ca^{2+}]i$ oscillations imparted into the egg by the activating sperm factor. Consistent with this idea, rapid superfusion of immobilized Ca^{2+}- and calmodulin-dependent protein kinase II (CaMKII) *in vitro* showed that the enzyme can decode the frequency of $[Ca^{2+}]i$ spikes into distinct amounts of kinase activity (De Koninck and Schulman, 1998). The pattern of $[Ca^{2+}]i$ oscillations has also been shown to modify gene expression (Dolmetsch et al., 1998; Li et al., 1998) although transcriptional activity in mammalian embryos is minor at the time of egg activation. $[Ca^{2+}]i$ rises may induce a long-term affect on gene expression by altering the chromatin structure, which may in turn promote expression of developmentally-important genes (Ozil and Huneau, 2001). $[Ca^{2+}]i$ oscillations may also modify gene expression by affecting protein synthesis during the 1st cell cycle. Recruitment of maternal mRNA and post-translational protein modifications are characteristic of fertilisation (Howlett, 1986) and it is therefore likely that frequency and duration of fertilisation-induced $[Ca^{2+}]i$ oscillations act to modify protein synthesis machinery. In support of this idea, data from a recent study showed that the number of $[Ca^{2+}]i$ transients at fertilisation determines the translation of specific proteins (Ducibella et al., 2002). In Chapter 6 I investigate what impact the presence or absence of $[Ca^{2+}]i$ oscillations has on gene expression levels in preimplantation stage embryos

Abnormalities in postimplantation development such as skeletal malformation and hydroallantois have been reported to occur in a high number of nuclear transfer (NT) embryos activated with cycloheximide (Zakhartchenko et al., 1999). Initiation of DNA synthesis and

cell cleavage have also been reported to be delayed in NT embryos activated with ethanol and cycloheximide (Alberio et al., 2001a; Wang and Latham, 1997) and it is feasible that the activating agents used may contribute to later embryonic abnormalities. Most abnormalities associated with NT are likely however to be associated with inaccurate nuclear reprogramming of the injected nuclei. The studies that showed a delay in embryonic transcription used cycloheximide treatments for duration of 6-14 hours whereas in this study I only exposed eggs to cycloheximide for 4 hours. More importantly I showed that inducing single or multiple Ca^{2+} increases can reverse the poor development observed in embryos derived from egg activation with CX alone. In Chapter 5 I examine whether egg activation with Sr^{2+} or cycloheximide affects the onset of embryonic transcription or embryonic genome activation (EGA) and amount of global gene expression that takes place at this time to determine whether cycloheximide affects the timing or amount of embryonic transcription.

Chapter 5

Embryonic Genome Activation in parthenogenetic embryos

5.1 Introduction

In order for an embryo to progress through preimplantation development it must become transcriptionally active. The acquisition of transcriptional competency occurs when there is a switch from maternal to embryonic transcriptional dependency and this is referred to as Embryonic Genome Activation (EGA). EGA has a number of crucial functions such as the replacement of degraded maternal transcripts, expression of which are common to both egg and embryo with transcripts of embryonic origin. Preventing the occurrence of EGA results in a developmental block, usually within one cell division (Schultz and Worrad, 1995), this demonstrates that early embryonic transcripts encode proteins that have a basic cellular function. EGA also triggers the synthesis of novel transcripts that are not present in the egg prior to EGA but are required for later embryo development (Piko and Clegg, 1982; Bachvarova et al., 1989).

EGA in many species is biphasic. In the mouse embryo a 'minor' phase of activation occurs during the late one-cell stage (Latham et al., 1991; Ram and Schultz, 1993; Latham et al., 1992) and is characterised by a low level of gene activation. At this stage approximately 40 proteins are synthesized (Latham et al., 1991). The onset of the minor EGA is controlled by a time-dependent mechanism known as the zygotic clock and not by any particular cell-

cycle event. EGA begins approximately 24 hours after activation regardless of whether the one-cell embryo has divided to form a two-cell embryo (Bolton et al., 1984; Schultz, 1993).

A 'major' phase of EGA is initiated during the late two-cell stage and involves a much larger burst of gene activation which is necessary for further embryo development (Latham et al., 1991). In contrast to the minor phase, the major phase of EGA is cell-cycle dependent and does not occur unless a two-cell embryo has formed (Howlett, 1986).

In this Chapter I assay gene expression during EGA in parthenogenetic embryos. Previous assays of gene expression in embryos have included the monitoring of plasmid-borne reporter genes (Wiekowski et al., 1991; Ram and Schultz, 1993; Vernet et al., 1993), integrated transgenes (Christians et al., 1995) and endogenous genes (Manejwala et al., 1991). The methods described there involved the destructive analysis of embryos taken from large cohorts and as a result of the methods used a full profile of gene expression in individual embryos could not be generated.

The temporal dynamics of gene expression have been quantitatively measured using a Green Fluorescent Protein (GFP) reporter gene (Medvedev et al., 2002), which is advantageous since it does not require destruction of the embryo. GFP gives a much less sensitive measure of gene expression than reporter systems based upon firefly luciferase expression and gene expression could not be detected until the embryonic 4-cell stage when using GFP. This makes GFP unsuitable for the monitoring of EGA.

To monitor global gene expression during EGA I have combined aspects of previous assays and injected the pGL3-control vector DNA (Promega, Madison, Wisconsin) into a single pronucleus of *in vivo* fertilised or *in vitro* parthenogenetically activated one-cell embryos (Ram and Schultz, 1993). This plasmid contains the luciferase gene and SV40 enhancer and SV40 promoter sequences. The replication and expression of genes encoded in extra-chromosomal DNA respond to the same signals that regulate these processes in

endogenous DNA (Majumder et al., 1993) and the expression of the embryonic genome consequently initiates the transcription of the luciferase from the vector template. Luciferase assays involve the oxidation of luciferin by the enzyme luciferase, the product of which is oxyluciferin which bears an excited electron. When the electron falls to the ground state the molecule loses the energy in the form of light. The quantum yield of the reaction is very high (~90%), with around one photon being released for every molecule of luciferin undergoing oxidation. The luciferin can simply be added to the culture media rather than injected into the egg since it is membrane permeable. It is the esterification of the D-luciferin carboxyl group as an ethyl ester that allows the uptake of the substrate by the egg. After entering the egg, the ethyl ester is quickly removed by ubiquitous esterase activity inside the egg, rendering the molecule incapable of leaving the egg. We can measure the extent of transcription by the rate at which photons are emitted from the reaction. The Imaging Photon Detector (IPD, Photek, St Leonard-on-sea, UK) was suitable for measuring gene expression during EGA as it is sensitive enough to detect luminescence over a dynamic range of 50 - 5 x 10^4 photons/second/pixel (See Fig 2.1 for schematic diagram of IPD). Gene expression could also be monitored continuously since no destructive analysis was required for luminescent measurements on the IPD, thus allowing a full gene activity profile of individual embryos to be made.

The embryos of many species are subject to a time during preimplantation development when they are vulnerable to developmental arrest. Developmental arrest occurs when preimplantation embryonic cells fail to cleave and is often referred to as the developmental block. Developmental block normally correlates with the time that major EGA is initiated in that species (De Sousa et al., 1998) and by way of an example,(Memili and First, 2000) developmental block occurs in mice at the two-cell stage. It has been suggested that embryos undergo developmental block as a result of failure to complete EGA (Haraguchi

et al., 1999) though more recent evidence suggests that a delay, rather than a failure of EGA is more likely to be causative of the developmental block (Qiu et al., 2003). Developmental block can be alleviated by alteration of the culture media (Biggers, 1998) but the mechanisms regulating this phenomenon remain unclear.

EGA is one of the major molecular events to occur (<24 hours) following the $[Ca^{2+}]i$ signals that trigger egg activation. The purpose of this work was to determine if $[Ca^{2+}]i$ oscillations at egg activation influence the onset and amount of gene expression during EGA. Gene expression was monitored in parthenogenetic embryos generated from eggs activated by triggering Sr^{2+}-induced $[Ca^{2+}]i$ oscillations or without any $[Ca^{2+}]i$ changes by using the protein synthesis inhibitor, cycloheximide. The data from luminescent imaging experiments described in this chapter revealed that $[Ca^{2+}]i$ oscillations at egg activation are not required for the onset of, or affect the duration or total amount of gene expression occurring during EGA.

5.2 Results

5.2.1 EGA can be measured with luciferase reporter genes and an Imaging Photon detector.

Gene expression during Embryonic Genome Activation (EGA) was monitored continuously by luminescence imaging of one-cell embryos using an Imaging Photon Detector (IPD). A single pronucleus was injected in pronuclear stage 1-cell embryos with a mixture of pGL3 luciferase reporter gene and fluorescein dextran. Fluorescein dextran was a necessary constituent of the injection mixture since I could verify that the injection mixture had entered the pronucleus by exciting the injected egg with fluorescent light. Fig 5.1A shows an example of a bright-field (i) and fluorescent (ii) image of an injected 1-cell pronucleate embryo. The pronuclei can be difficult to identify under bright-field imaging. The fluorescent image reveals however that whilst a small amount of injection mixture has entered the cytoplasm from the microinjection pipette (faint green background) one pronucleus has clearly been microinjected successfully since it fluoresces a much brighter colour of green. The dark circle on the far right of the fluorescence micrograph represents the uninjected pronucleus. In parthenogenetic embryos a single pronucleus was choosen at random for injection. In fertilised embryos it was the female pronucleus that was injected as transcriptional activity could be compared to the pronuclei in parthenogenetic embryos that were both maternally derived. It is also known that the male pronucleus has a different level of transcriptional activity than the female pronucleus and therefore injection of the male pronucleus would prevent an accurate comparison of transcriptional activity in fertilised and parthenogenetic embryos.

The IPD was used to measure changes in luminescence of embryos injected with the luciferase reporter gene. An integration time of five minutes was sufficient to produce a clear

luminescence signal above background noise. Typical luminescence (Fig 5.1Bi) and bright-field (Fig 5.1Bii) images of one-cell parthenogenetic embryos derived from Sr^{2+}-activation can be observed in Fig 5.1B. The light emission intensity is represented by the colours on the luminescence image which are proportional to the level of gene expression. When no photon signal above background noise can be observed this means that no gene expression is taking place, blue signals (~30 photon counts /min) show that low/moderate amounts of gene expression are taking place and a yellow-red signal (~100-120 photon counts/ min) indicate a high level of gene expression is taking place. The IPD is a very sensitive photon detector because of the very low background photon count. I measured the background photon count of an area the same size as an egg from a sample data set and found that this area exhibited ~10 photons /min. The bright-field images could be overlaid on the luminescent images in order to monitor any morphological changes in embryo development (such as cell death or cleavage) whilst measuring gene expression in the same embryos. Luminescence in embryos was measured for duration of approximately 25 hours to capture the time of gene expression during EGA.

5.2.2 Minor and major EGA in *in vivo* fertilised embryos

The time of onset of gene expression in fertilised 1-cell embryos varied between different embryos although it always began in the time frame of 15-21 hours post-fertilisation (Table 5.1, Fig 5.2) in all embryos tested [n=14 embryos]. The timing of fertilisation can only be approximated since variations of a few hours exist in the timing of mating and ovulation. Gene expression in all fertilised embryos occurred with an initial slow increase which was then followed by a swift attack to the maximum peak. The decrease in gene expression following the peak of expression exhibited a lower gradient than that of the attack phase.

A)

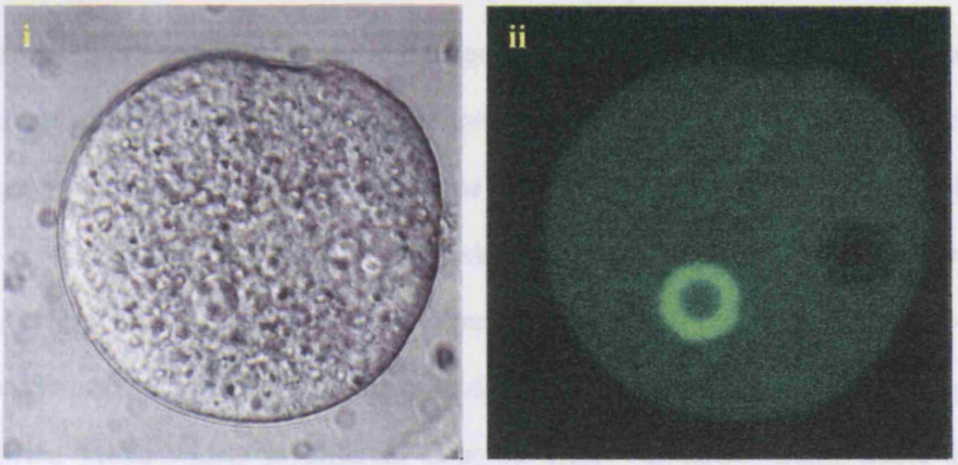

B)

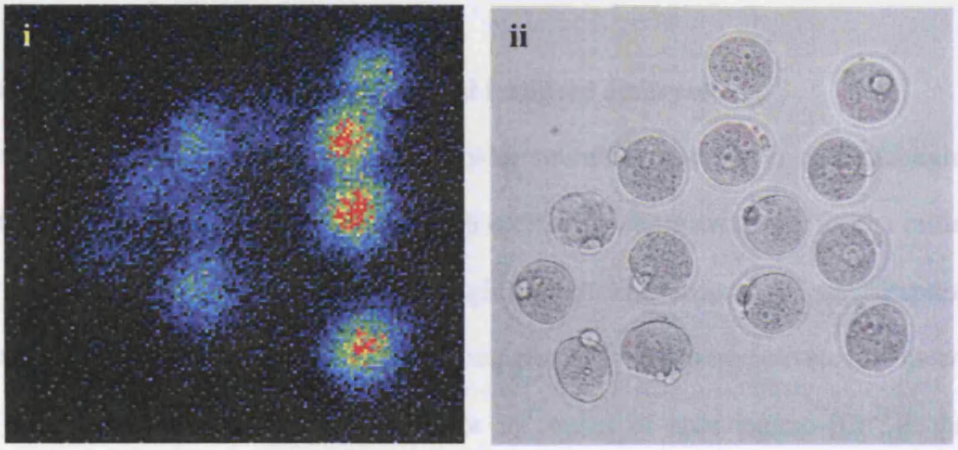

Figure 5.1 Monitoring EGA using firefly luciferase reporter gene pGL3-control vector DNA. (Ai) The pronuclei of *in vivo* fertilized or *in vitro* activated parthenotes were injected with 50ng/ml of pGL3-control vector DNA and (Aii) fluorescein dextran in order to check pronuclei were injected successfully using fluorescence microscopy. After injection, the pronucleate embryos were incubated in HKSOM media containing luciferin (100μM). (Bi) The luminescence from embryos was measured for approximately 25 mins using an Imaging Photon detector (IPD). The luminescent image represents the photon count during an integration time of Brightfield images were taken throughout recording to monitor development (Bii)

Minor EGA lasted approximately 20 hours (Fig 5.2). The peak of expression in embryos derived from *in vivo* fertilisation ranged from 36-64 photons/ min (Fig 5.2)

Gene expression was also monitored during the major phase of EGA. Embryos (n= 9 embryos) at the 2-cell stage were obtained from pregnant female mice approximately 38 hours after fertilisation. The nucleus from one blastomere was microinjected with the luciferase reporter gene prior to imaging the embryo on the IPD. The onset of major EGA began about 40 hours post-fertilisation and lasted for approximately 20 hours in all nine embryos tested (Table 5.1, Fig 5.3). The maximum peak of expression was up to ten times higher in embryos during the major EGA compared to embryos during minor EGA however the maximum peak of expression varied widely in different embryos. Gene expression during major EGA occurred in a wave-like pattern which was similar to that observed during minor EGA.

5.2.3 Minor EGA is similar in parthenotes and fertilised embryos

Parthenotes were derived from egg activation with strontium ions (Sr^{2+}) or cycloheximide treatment. I wanted to investigate whether $[Ca^{2+}]i$ oscillations were necessary for the initiation of minor EGA or if they had an affect on the global pattern or amount of gene expression taking place at this phase. In order to do this I compared eggs that were activated by means of inducing $[Ca^{2+}]i$ oscillations (Sr^{2+} treatment) or by means of inducing no $[Ca^{2+}]i$ change whatsoever using cycloheximide. This method was used in the experiments described in Chapter 4 to investigate whether $[Ca^{2+}]i$ oscillations affect development and embryo quality during preimplantation development.

A 2 hour treatment in cytochalasin D was used during artificial egg activation to prevent extrusion of the 2nd polar body and therefore allow formation of 2 pronuclei. Sr^{2+}-activated embryos [n = 32 embryos] and cycloheximide-activated embryos (n = 35 embryos) were microinjected approximately 6 hours after the start of development of pronuclei (~12

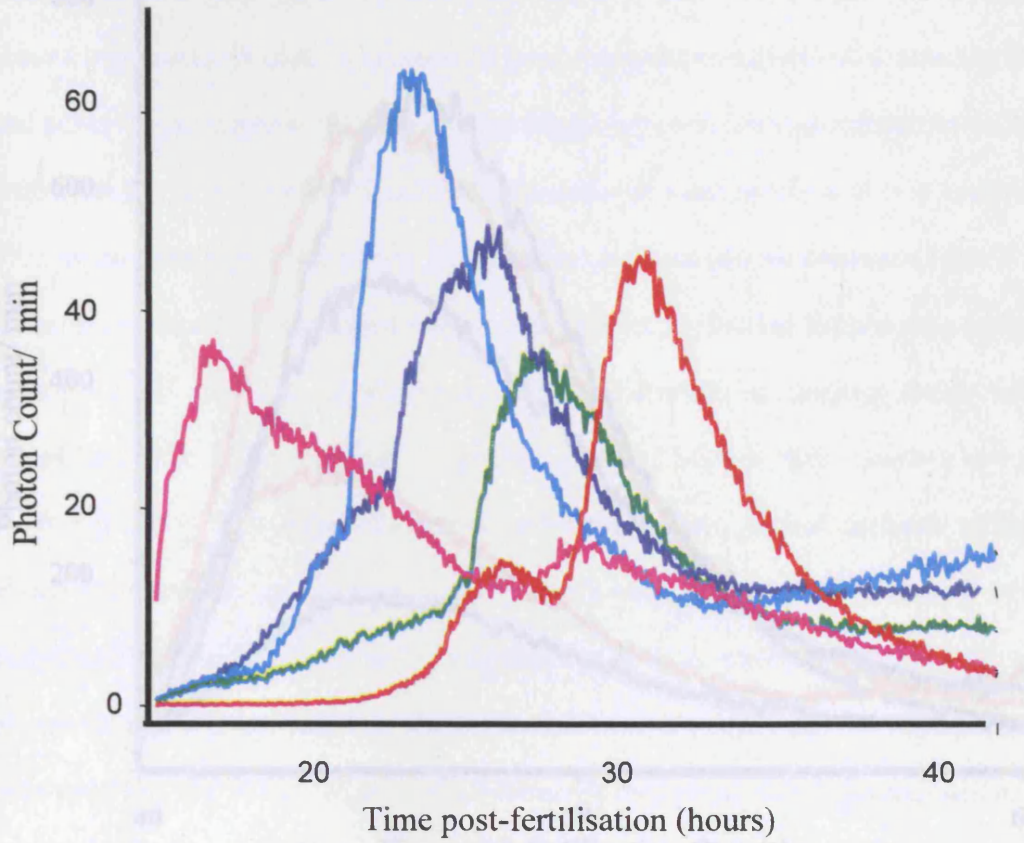

Figure 5.2 Minor EGA measurements in 5 *in vivo* fertilised embryos. The overall peak of expression varied widely amongst different eggs although EGA onset began in all eggs 15-21 hours post-fertilisation and lasted for approximately 20 hours. Gene expression increased gradually to begin with and then at began to rise very rapidly. A more gradual decrease in expression occurred following peak gene expression. An integration time of 5 minutes was sufficient to collect a photon signal above background signals. Maximum peaks ranged from 36-62 photon counts/ min.

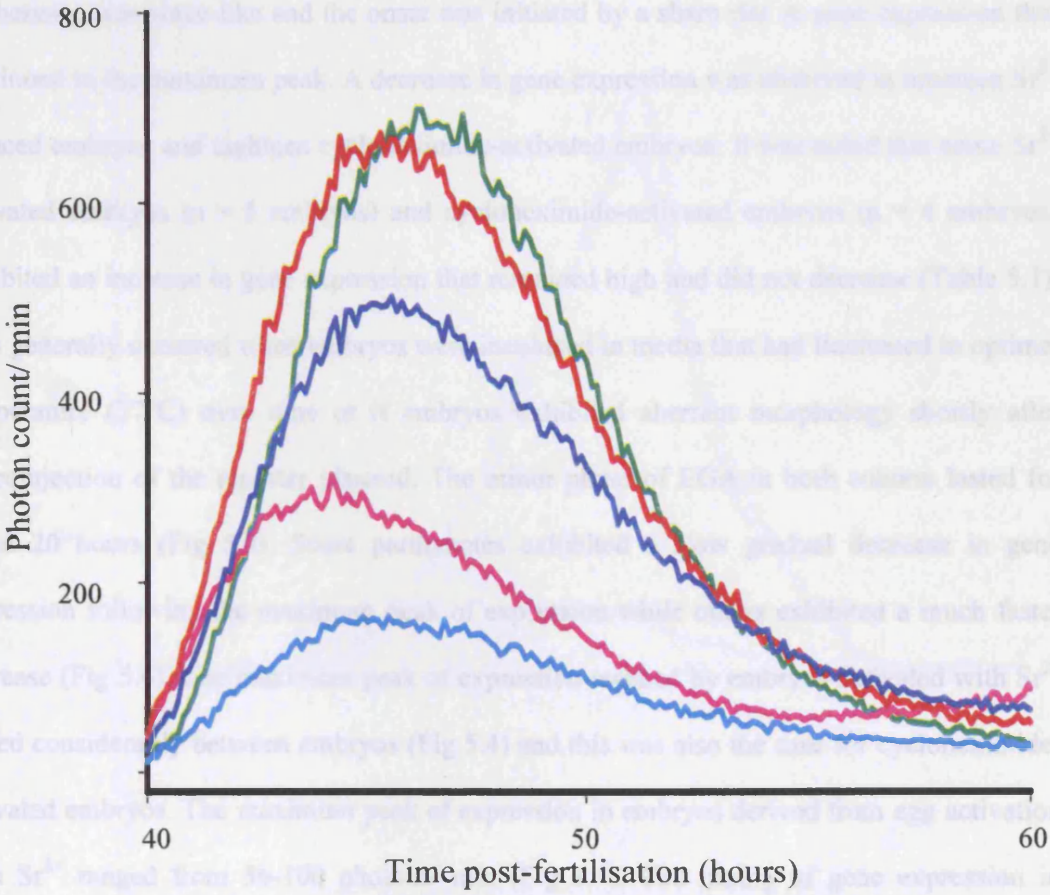

Figure 5.3 Major EGA measurements in 5 *in vivo* fertilised 2-cell mouse embryos. The degree of gene expression varied largely between individual 2-cell mouse embryos however the onset of major EGA was very similar in different eggs and occurred approximately 40 hours post-fertilisation. The onset of EGA was marked by a steep rise in expression to the peak followed by a slower decline. Maximal peak expressions ranged from 160-700 photon counts / min. Major EGA lasted about 20 hours.

hours post-treatment). Gene expression in twenty-three 1-cell embryos derived from Sr^{2+} induced egg activation and twenty-two embryos derived from cycloheximide-induced activation was initiated approximately 18 hours after the start of parthenogenetic treatment. The pattern of gene expression during minor EGA in Sr^{2+} and cycloheximide activated parthenotes was wave-like and the onset was initiated by a sharp rise in gene expression that continued to the maximum peak. A decrease in gene expression was observed in nineteen Sr^{2+} induced embryos and eighteen cycloheximide-activated embryos. It was noted that some Sr^{2+} activated embryos (n = 5 embryos) and cycloheximide-activated embryos (n = 4 embryos) exhibited an increase in gene expression that remained high and did not decrease (Table 5.1). This generally occurred when embryos were incubated in media that had fluctuated in optimal temperature (37°C) over time or if embryos exhibited aberrant morphology shortly after microinjection of the reporter plasmid. The minor phase of EGA in both cohorts lasted for about 20 hours (Fig 5.4). Some parthenotes exhibited a slow gradual decrease in gene expression following the maximum peak of expression while others exhibited a much faster decrease (Fig 5.4). The maximum peak of expression reached by embryos activated with Sr^{2+} varied considerably between embryos (Fig 5.4) and this was also the case for cycloheximide-activated embryos. The maximum peak of expression in embryos derived from egg activation with Sr^{2+} ranged from 36-100 photons/ min (Fig 5.4). The timing of gene expression in embryos activated with cycloheximide was not significantly different to embryos activated with Sr^{2+} (see section 5.2.4 for details).

I attempted to monitor major EGA in parthenotes derived from Sr^{2+} and cycloheximide to determine if differences in the pattern of expression could be determined during this phase of higher gene expression levels. Whilst the onset of gene expression during major EGA was recorded in all parthenogenetic Sr^{2+}-activated (N = 8 embryos) and cycloheximide (N = 11 embryos) 2-cell stage embryos, a decrease in gene expression was

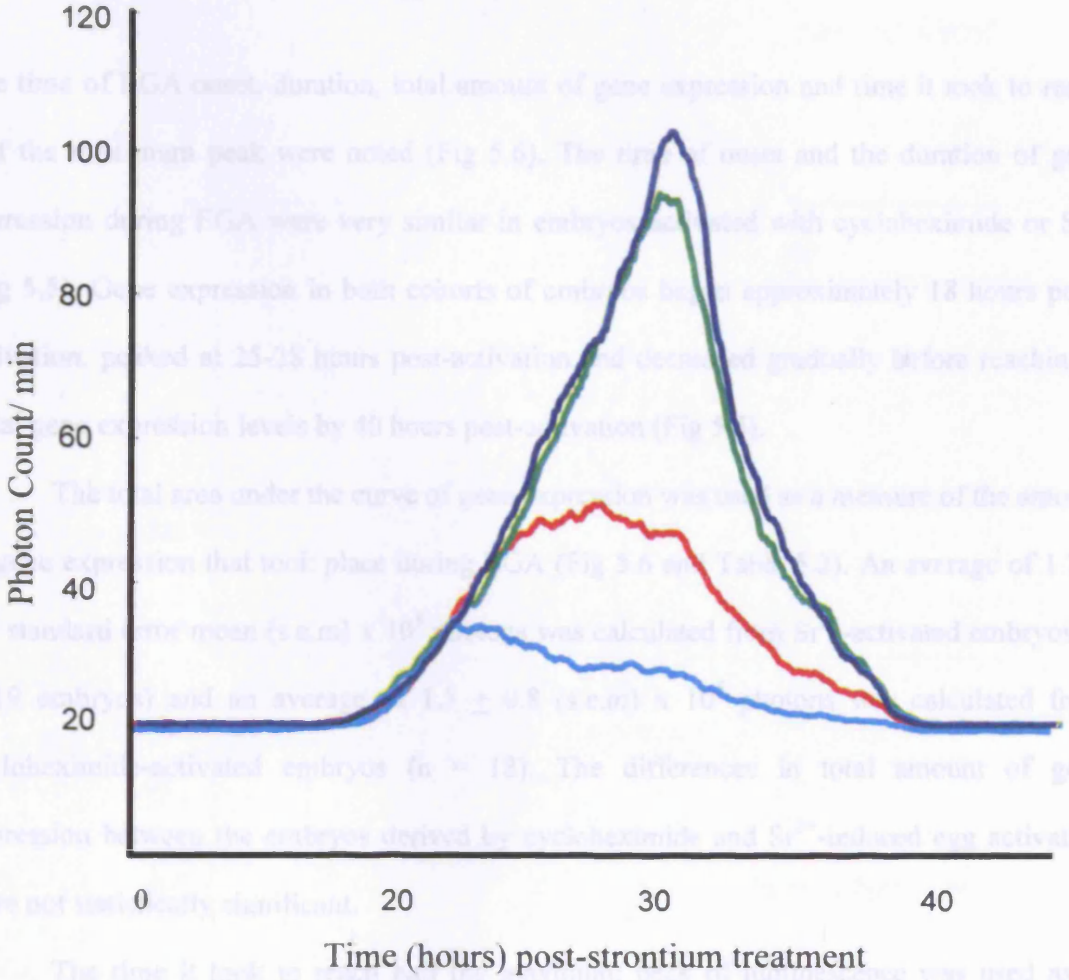

Figure 5.4 Minor EGA in embryos generated from Sr^{2+}-induced egg activation. The degree of gene expression during EGA varied largely amongst eggs activated with $Sr^{2+}$with the maximal peaks of gene expression ranging from 32-104 photon counts/ min. Minor EGA lasted for approximately 20 hours. In general the pattern of gene expression was similar to that of a bell-shaped curve. Some eggs exhibited a rapid increase in gene expression to the peak followed by a slower decline (blue and red curve) whilst others showed a more-or-less similar rate of attack and decay producing a more symmetrical curve (green and navy curve).

observed in only two Sr^{2+}-activated embryos and 4 cycloheximide embryos. None of these 2-cell embryos cleaved to the 4-cell stage (Table 5.1).

5.2.4 The time of EGA onset and duration is similar in embryos derived from cycloheximide and Sr^{2+} induced egg activation

The time of EGA onset, duration, total amount of gene expression and time it took to reach half the maximum peak were noted (Fig 5.6). The time of onset and the duration of gene expression during EGA were very similar in embryos activated with cycloheximide or Sr^{2+} (Fig 5.5). Gene expression in both cohorts of embryos began approximately 18 hours post-activation, peaked at 25-28 hours post-activation and decreased gradually before reaching a basal gene expression levels by 40 hours post-activation (Fig 5.5).

The total area under the curve of gene expression was used as a measure of the amount of gene expression that took place during EGA (Fig 5.6 and Table 5.2). An average of 1.7 $\pm$ 0.7 standard error mean (s.e.m) x 10^5 photons was calculated from Sr^{2+}-activated embryos (n = 19 embryos) and an average of 1.5 $\pm$ 0.8 (s.e.m) x 10^5 photons was calculated from cycloheximide-activated embryos (n = 18). The differences in total amount of gene expression between the embryos derived by cycloheximide and Sr^{2+}-induced egg activation were not statistically significant.

The time it took to reach half the maximum peak of luminescence was used as a measure of the rate of EGA onset (Fig 5.6 and Table 5.2) as this point represents the best measure of the effective gradient of the initiation of transcription. The time it took to reach half the maximum peak of EGA was 9.6 $\pm$ 0.8 (s.e.m) hours for Sr^{2+} activated embryos (n = 19 embryos) and 10.9 $\pm$ 0.9 (s.e.m) hours for cycloheximide-activated embryos (n = 18 embryos). The time it took to reach half the maximum peak of gene expression during EGA in cohorts that were generated by Sr^{2+} or cycloheximide-induced egg activation was not significantly different.

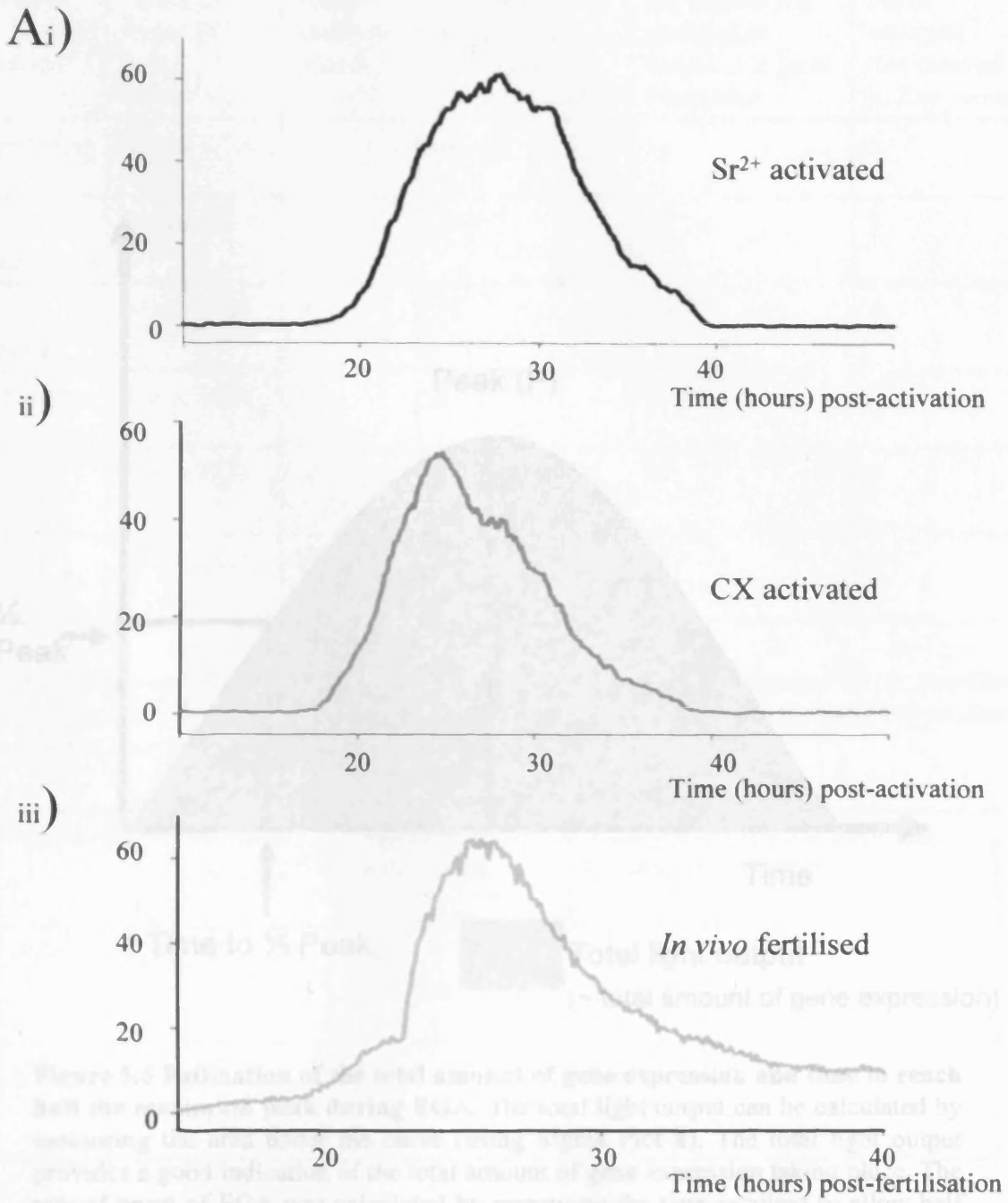

Figure 5.5 Minor EGA in embryos derived from fertilisation, Sr^{2+} or cycloheximide-induced egg activation. The graphs show that minor EGA begins approximately 20 hours post-activation or fertilisation and the duration of which lasts for about 20 hours. The shapes of the curves are similar to bell-shaped curves. The onset of EGA appears to occur at a faster rate than the rate of decrease as gene expression levels fall. Cycloheximide = CX.

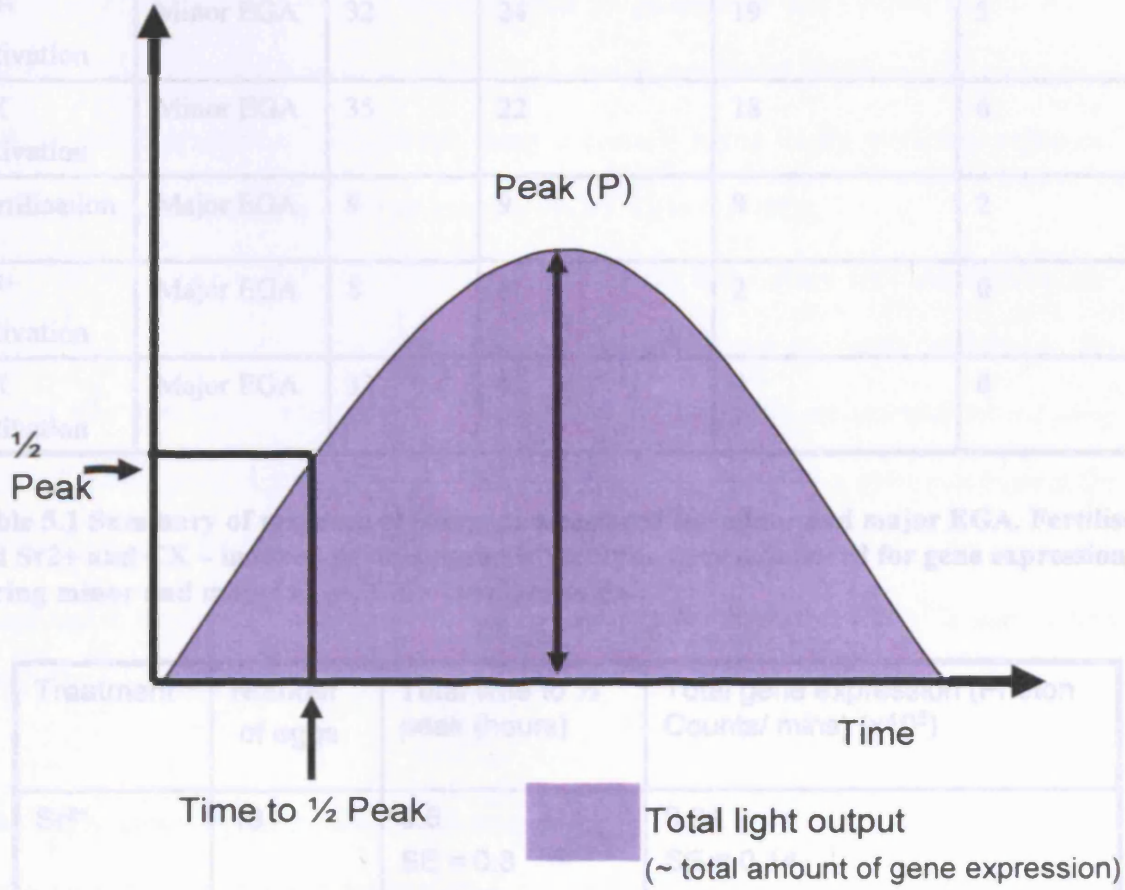

Figure 5.6 Estimation of the total amount of gene expression and time to reach half the maximum peak during EGA. The total light output can be calculated by measuring the area under the curve (using Sigma Plot 8). The total light output provides a good indication of the total amount of gene expression taking place. The rate of onset of EGA was calculated by measuring the time required to allow half the maximum peak of gene expression to occur.

Method of egg activation	Minor or major EGA being monitored	No of embryos tested	No of embryos showing an increase in gene expression	No of embryos showing an decrease in gene expression	No of embryos that cleaved to 2 or 4-cell
Fertilisation	Minor EGA	14	14	14	5
Sr^{2+} activation	Minor EGA	32	24	19	5
CX activation	Minor EGA	35	22	18	6
Fertilisation	Major EGA	9	9	9	2
Sr^{2+} activation	Major EGA	8	8	2	0
CX activation	Major EGA	11	11	4	0

Table 5.1 Summary of response of embryos monitored for minor and major EGA. Fertilised and Sr2+ and CX – induced parthenogenetic embryos were monitored for gene expression during minor and major EGA. CX = cycloheximide.

Treatment	Number of eggs	Total time to ½ peak (hours)	Total gene expression (Photon Counts/ mins) ($x10^5$)
Sr^{2+}	19	9.6 SE = 0.8	0.34 SE = 0.14
CX	18 **P value**	10.9 SE = 0.9 **0.89**	0.3 SE = 0.16 **0.27**

Table 5.2 Rate of EGA onset and total gene expression during minor EGA in embryos derived from parthenogenetic egg activation using Sr^{2+} and Cycloheximide. SE denotes standard error. The total gene expression was measured as total photon counts over an integration time of 1 minute. P values from student unpaired ttest show that there is no significant difference ($P<0.05$) between cycloheximide (CX) and Sr^{2+} activated eggs.

5.3 Discussion

Embryonic genome activation (EGA) marks the switch of an embryo's dependency from maternally derived transcripts to embryonic transcripts. The occurrence of EGA at the correct time is essential for the embryo's developmental progression. In this Chapter I demonstrate that low levels of gene expression during EGA can be monitored continuously in real time without the destruction of the embryo using a plasmid borne firefly luciferase enhancer-promoter- reporter gene assay and an Imaging Photon Detector (IPD).

EGA is one of the first major molecular events that occurs after the fertilisation-induced $[Ca^{2+}]i$ signal during egg activation. The purpose of the experiments described in this chapter was to elucidate whether $[Ca^{2+}]i$ increases at egg activation are essential for initiating EGA. The data from this work shows that minor EGA does not have a strict requirement for the occurrence of $[Ca^{2+}]i$ oscillations at egg activation since EGA occurred in the same time frame and in a similar amount in parthenogenetic embryos activated in a $[Ca^{2+}]i$ independent or $[Ca^{2+}]i$ dependent manner.

5.3.1 EGA occurs in waves of gene expression

Measurements of minor and major phases of EGA (Fig 5.2 and 5.3) in fertilised embryos revealed that changes in the levels of gene expression occurred in a bell-shaped pattern and each phase lasted approximately 20 hours. The onset of minor EGA began 15-21 hours post-fertilisation and major EGA began at approximately 40 hours post-fertilisation. The main difference between the two phases of EGA in fertilised embryos was the that the peak of gene expression was up to ten times higher in the major phase of EGA than the minor phase of EGA. This data complements previously reported data that has shown that the minor phase of EGA involves a limited amount of transcription (resulting in the synthesis of approximately

40 proteins) whilst the major phase of EGA involves a much larger amount of transcription (Latham et al., 1991; Bolton et al., 1984; Christians et al., 1995).

The time that a photon signal was first detected in fertilised embryos during minor EGA ranged from 15-21 hours post-fertilisation between different *in vivo* fertilised mouse embryos. This probably reflects the fact that in the mouse, eggs are ovulated over a time period of 2-3 hours, so the timing of fertilisation will vary among eggs in the same mouse. Eggs were also obtained from a number of female mice that were introduced to different male mice at the same time so variations in the timing of mating and ovulation in different mice may also add to the variation in fertilisation times.

The onset of major EGA appeared to be much more synchronous than the onset of minor EGA in different *in vivo* fertilised embryos although the reasons for this are unclear. *In vivo* signalling mechanisms may play a role in synchronising early embryo development at this stage.

5.3.2 Parthenotes and fertilised embryos have a similar gene expression phase during EGA.

To my knowledge this is the first time EGA has been monitored in parthenogenetic embryos. The onset of EGA in Sr^{2+} activated parthenotes was over a very narrow time frame (Fig 3.4) and occurred about 18 hours after Sr^{2+} treatment began. This is likely to be due to the fact that eggs were all exposed to Sr^{2+} treatment at precisely the same time and therefore activated simultaneously in contrast to *in vivo* fertilised eggs (Fig 3.2). The timing of gene expression during minor EGA was however similar in parthenotes compared to embryos which had been fertilised. This data clearly demonstrates that the paternal genome is not required for EGA although this information is also clear from previous studies that show parthenogenetic egg activation can trigger embryo development up to the blastocyst stage as exemplified by Kaufman (Kaufman, 1979).

The pattern of global gene expression during the rising phase of minor EGA did appear to differ between fertilised embryos and parthenogenetically activated embryos. The gene expression in zygotes began with a slow but gradual increase in expression which was followed by a rapid increase to the peak (Fig 5.2). The pattern of gene expression during EGA in zygotes appeared to be dependent on a minimum threshold level of global gene expression in order for a much higher level of expression to be triggered. There was no initial slow rising phase in parthenotes during EGA but a steep increase in expression from the beginning of EGA onset. It is unclear why there appears to be a difference in the pattern of onset of gene expression between fertilised and parthenogenetic embryos. The pattern of $[Ca^{2+}]i$ oscillations has been shown to determine expression levels and gene specificity in somatic cells (Dolmetsch et al., 1998). The $[Ca^{2+}]i$ oscillations triggered by Sr^{2+}-activation are distinguishable from those of fertilisation and it may be that specific patterns of sperm induced $[Ca^{2+}]i$ oscillations encode information for the egg that changes the degree of expression and specificity of genes expression during early EGA. In order to test out this theory individual genes that are known to be expressed during minor EGA, such as heat shock protein 70 (Christians et al., 1995) could be monitored to determine how their expression patterns change over the time course of EGA in fertilised and parthenogenetic embryos. Paternal influences may also be involved in changing the pattern of gene expression at this stage and although these differences are clearly not required for the progression of embryos through the preimplantation stages of development, their affects may be exerted some time after this stage during postimplantation development. A number of studies have shown that the maternally-derived pronucleus is transcriptionally repressed in comparison to the paternal pronucleus because the maternal pronucleus inherits repression factors from the oocyte which are absent in the male pronucleus. For this reason, only the maternal pronucleus (and not the male pronucleus which is visibly larger in size) was injected with the pGL3-control vector

DNA when minor EGA was monitored so that comparisons could be made between in-vivo fertilised and parthenogenetic embryos.

5.3.3 EGA is not dependent on $[Ca^{2+}]i$ increases during egg activation

EGA is a major molecular event during preimplantation development and as it is a proximal event to $[Ca^{2+}]i$ signalling at egg activation, it is logical to explore any affects that $[Ca^{2+}]i$ oscillations may have on this phase. In order to investigate whether $[Ca^{2+}]i$ oscillations are essential for EGA, I compared EGA in embryos activated by Ca^{2+}-dependent (Sr^{2+}-activation) means to those activated by Ca^{2+}- independent (cycloheximide activation) means. These methods of activation have been used as a basis for artificially activating eggs in much of the work described in this thesis and can be read in detail in Chapter 4.

Luminescence measurements revealed that minor EGA lasted for the same duration (~ 20 hours) in both cycloheximide and Sr^{2+}-activated parthenogenetic embryos and fertilised embryos. The time of onset of minor EGA was also similar in the two groups of parthenogenetic embryos and this correlated with the onset of EGA in fertilised embryos. This data clearly shows that the initiation and timings of EGA are not strictly dependent on the presence of $[Ca^{2+}]i$ oscillations during egg activation since parthenotes activated dependently or independently of $[Ca^{2+}]i$ appeared to exhibit similar patterns of gene expression.

To further investigate the affects of $[Ca^{2+}]i$ on the global pattern of gene expression in these parthenogenetic embryos, I calculated the overall photon signal which gives a good indication of the total amount of gene expression and I also determined the time it took to reach half the maximum peak and compared these parameters in both groups of parthenotes. The values for the total photon signal and time taken to reach the peak were not significantly different between the two groups, indicating again that $[Ca^{2+}]i$ does not exert any global affects on gene expression during minor EGA. Considerable variation did however exist

between eggs from the same cohorts regarding the degree of expression and rate of onset of EGA, so small differences in EGA between the two cohorts cannot be excluded without further analysis and larger numbers of embryos. This data demonstrates that the initiation of EGA is not the result of a $[Ca^{2+}]i$ signalling pathway and may be due to a genome-wide release of gene expression from inhibition of transcription (Schultz, 1993) by some other factor.

As a much larger degree of gene expression occurs during the major phase of EGA compared to the minor phase, it was possible that any large difference may become apparent at this stage. I attempted to monitor major EGA in parthenotes to determine if differences in the global pattern of expression could be determined during major EGA. In contrast to *in vivo* fertilised embryos which exhibited wave-like gene expression that fell to baseline levels as major EGA finished, in the majority of parthenogenetic 2-cell stage embryos gene expression increased to high levels but then failed to decrease back to baseline levels. I previously observed this pattern of gene expression in morphologically impaired embryos or those that were cultured under sub-optimal conditions. It may be argued that gene expression did not decrease back to baseline levels during major EGA in parthenotes because they have a weaker developmental potential than those of *in vivo* fertilised embryos. This is unlikely though, since completion of major EGA is necessary for development to progress beyond the 2-cell stage and under optimised *in vitro* culture conditions many parthenotes do develop beyond this stage and up to the blastocyst stage. A failure of gene expression to decrease in parthenotes is probably due to the fact that parthenogenetic 2-cell embryos were cultured *in vitro* from the MII stage egg and they may therefore have a reduced developmental capacity compared to fertilised embryos that were not removed from female mice until a few hours prior to the monitoring of major EGA onset and did exhibit a decrease in gene expression after peak expression (Fig 5.3). To test out this theory *in vivo* fertilised embryo could be

removed from oviducts and cultured *in vitro* prior to imaging for gene expression during major EGA. The imaging of parthenogenetic 2-cell embryos in KSOM culture media with the use of a CO_2 chamber would enable longer-term studies to be carried out and as the conditions would be more optimal in KSOM than HKSOM media it is likely that these embryos would exhibit wave-like gene expression that falls back to baseline levels during major EGA and be of a high quality with regards to developmental potential.

Previous work from Chapter 4 demonstrated that embryos derived from cycloheximide-induced egg activation had a reduced developmental capacity compared to those derived from Sr^{2+}-induced egg activation; that work also showed however that the addition of Sr^{2+}-induced $[Ca^{2+}]i$ oscillations significantly improved successful cleavages and development from the 4-cell to the blastocyst stage in embryos activated with cycloheximide. This indicated that it was a lack of $[Ca^{2+}]i$ oscillations that had a negative impact on development rather than detrimental affects caused by cycloheximide-activation. Previous reports have in contrast shown that parthenogenetic egg activation involving cycloheximide causes a delay in the initiation of DNA synthesis and cell division during the first cell cycle (Wang and Latham, 1997; Alberio et al., 2001a) and it has also been suggested that postimplantation abnormalities in cycloheximide-activated embryos may be due to this early delay in transcriptional activity (Zakhartchenko et al., 1999). My results do not support these findings since no significant difference in the timing of EGA were recorded between embryos derived from cycloheximide-induced egg activation and Sr^{2+}-induced egg activation or fertilisation.

A major limitation with the luminescent reporter gene technique used to measure EGA was that only global measures of gene expression could be taken. This does not reveal any information about the changing patterns of specific genes that occur in embryos during EGA. Changes in the expression levels of genes having an important affect can be masked by

balancing changes in other genes. Genes expressed at low levels which are highly potent in their effect or highly expressed yet relatively impotent genes can also cause problems when only global expression changes are monitored. The differential expression of some genes may be causing the developmental arrest observed at the 4-cell stage in the cycloheximide-activated eggs and which is described in Chapter 4. In Chapter 6 I investigate differences in gene expression between Sr^{2+} and cycloheximide-activated parthenotes during the 8-cell embryo stage. Instead of monitoring global gene expression which has limitations regarding the absence of information on individual gene activity, I used microarray technology to monitor the activity of 21,045 genes specific to stem cells and preimplantation development embryonic cells.

5.3.4 Summary

In this Chapter I have, for the first time used a plasmid borne firefly luciferase reporter gene assay to monitor EGA in parthenotes. This assay provided a sensitive, accurate and simple means of monitoring gene expression during EGA. My data clearly shows that a similar pattern of gene expression during EGA occurs in fertilised and parthenogenetically activated embryos. More significantly in regard to previous work carried out in this thesis, I have demonstrated that EGA is not strictly dependent on the $[Ca^{2+}]i$ oscillations that occur at egg activation. A more detailed examination of specific genes during both phases of EGA will help to elucidate whether $[Ca^{2+}]i$ oscillations have an impact on a small number of developmentally important genes, which would not be notable in whole genome expression studies.

Chapter 6

Gene expression in 8-cell mouse embryos derived from strontium or cycloheximide-induced egg activation.

6.1 Introduction

In this Chapter I determine whether $[Ca^{2+}]i$ oscillations at egg activation have any influence on the expression of specific genes during preimplantation development. A number of studies have shown that the pattern of $[Ca^{2+}]i$ oscillations can exert specific affects on gene expression. Repetitive $[Ca^{2+}]i$ oscillations in somatic cells for example have been shown to be more efficient at inducing gene expression and were able to trigger expression of a higher number of transcription factors compared to a monotonic rise in $[Ca^{2+}]i$ (Dolmetsch et al., 1998). The optimisation of gene expression in somatic cells has also been shown to be dependent on the frequency of $[Ca^{2+}]i$ oscillations (Li et al., 1998) but no data reported so far has shown that the pattern of $[Ca^{2+}]i$ oscillations at egg activation can affect the pattern of gene expression in mammalian embryonic cells.

In order to investigate whether $[Ca^{2+}]i$ oscillations affect gene expression in embryos I utilised strontium ions (Sr^{2+}) and the protein synthesis inhibitor cycloheximide. Both chemicals are capable of activating eggs but whilst Sr^{2+} ions induce repetitive $[Ca^{2+}]i$ oscillations, cycloheximide does not induce any $[Ca^{2+}]i$ changes in eggs (Fig 4.2). I chose to investigate differences in the expression of individual genes at the embryonic 8-cell stage, mainly because the differential expression of genes at this stage should reflect some of the major events that take place at the blastocyst stage and genes involved in apoptosis and cell differentiation were likely to be of particular interest.

A recent study investigating phased gene expression in the preimplantation embryo reported that the transition from the 4 to 8-cell embryo is characterised by a period in which an enormous number of genes undergo a dramatic change in gene expression (Hamatani et al., 2004a). Studying embryos at this stage is likely to reveal more notable differences in gene expression between the two groups of embryos than would be seen at any other stage of preimplantation embryo development

Until relatively recently the isolation of differentially expressed genes in early stage embryos was elucidated using differential display technology (Ma et al., 2001), EST projects (Ko et al., 2000), 2-dimensional protein gels (Latham et al., 1991) Serial Analysis of Gene Expression (SAGE) (Blomberg le and Zuelke, 2004) and a PCR-based cDNA subtraction strategy called Suppression Subtractive Hybridization (SSH) (Diatchenko et al., 1996). These methods are all limited because they cannot measure large numbers of genes simultaneously. The use of microarray technology solves this problem and has very rapidly become an invaluable tool in the study of developmental genomics (Ko et al., 2000). Microarrays have been used to determine patterns of gene expression during different phases of preimplantation embryo development (Wang et al., 2004; Hamatani et al., 2004a). I utilised microarray analysis to quantify differences in gene expression between Sr^{2+} and cycloheximide-activated 8-cell parthenogenetic embryos. Gene expression studies on early stage mammalian embryo development have previously been hindered by the difficulties in obtaining large numbers of embryos to produce sufficient quantities of mRNA. This hurdle was crossed by using an optimized labelling reaction with two rounds of cRNA linear amplification suitable for tiny amounts of extracted mRNA (Carter et al., 2003). The lack of available microarray platforms containing genes unique to early stage embryos has also been a hindrance. A 60-mer oligo microarray platform enriched in genes expressed in stem cells and preimplantation stage embryonic cells was recently produced

(Hamatani et al., 2004a) and I was given access to this microarray by Dr Ko, of the National Institute of Aging (NIA), National Institute of Health (NIH), Baltimore.

Here I show that gene expression in 8-cell embryos derived from parthenogenetic egg activation using either Sr^{2+} or cycloheximide exhibit differences in the expression levels of specific genes. Differentially expressed genes were clustered into functional groups in order to obtain some idea of the biological significance of these changes. High expression of genes associated with the cell-cycle, apoptosis and cell differentiation were found to be characteristic of 8-cell embryos generated from cycloheximide-induced parthenogenetic egg activation. High expression of genes associated with ion transport, cell adhesion and cell proliferation pathways were found to be characteristic of 8-cell embryos generated from Sr^{2+}-induced egg activation. The results from this study on gene expression suggest that the presence or absence of $[Ca^{2+}]i$ oscillations during egg activation have an affect on developmentally important genes and pathways during preimplantation embryo development.

These experiments were carried out in the laboratories of the NIA, NIH, Baltimore and were in collaboration with Dr Minoru Ko, Dr Yulan Piao, Dr Kazuhiro Aiba and Dr Alexi Sharov.

6.2 Results

6.2.1 Experimental design for cRNA microarray work

Embryos that were activated using cycloheximide or Sr^{2+} were developed to the 8-cell stage and collected in groups of 34 before being frozen at -80°C. Experiments were done in duplicate. The mRNAs from cycloheximide and Sr^{2+} activated 8-cell embryos were labeled with Cyanine 5 (Cy5) fluorochrome by fluorescent linear amplification (Fig 6.1a). In order to identify differential gene expression using microarray platforms, an experimental design is required which is suitable for the type of samples being tested. Two types of 2-colour array experimental designs exist and are referred to as the "loop" and "reference" designs. In the "loop" design, samples are compared to one another in circular or multiple-pairwise fashion. This is a useful design when small numbers of samples are being compared however it becomes inefficient with large numbers of samples. In the "reference" design each sample is compared to a common RNA reference sample which serves as a common denominator between different microarray hybridizations (Fig 6.1b). Reference markers also reduce the incidence of laboratory mistakes because each sample is handled the same way and thus all comparisons are made with equal efficiency.

Microarray analyses of cycloheximide and Sr^{2+} -activated 8-cell embryos were carried out using a reference design based upon the Universal Mouse Reference RNA (UMRR; Strategene). This is comprised of total RNA from 11 pooled mouse cell lines of different tissue origins including embryo, testis, kidney and mammary gland. UMRR was labeled with Cyanine 3 (Cy3) fluorochrome and upon stimulation the Cy5/Cy3 intensities from each of the 4 microarray platforms (cycloheximide duplicates CX1, CX2 and Sr^{2+} duplicates $Sr^{2+}1$, $Sr^{2+}2$)

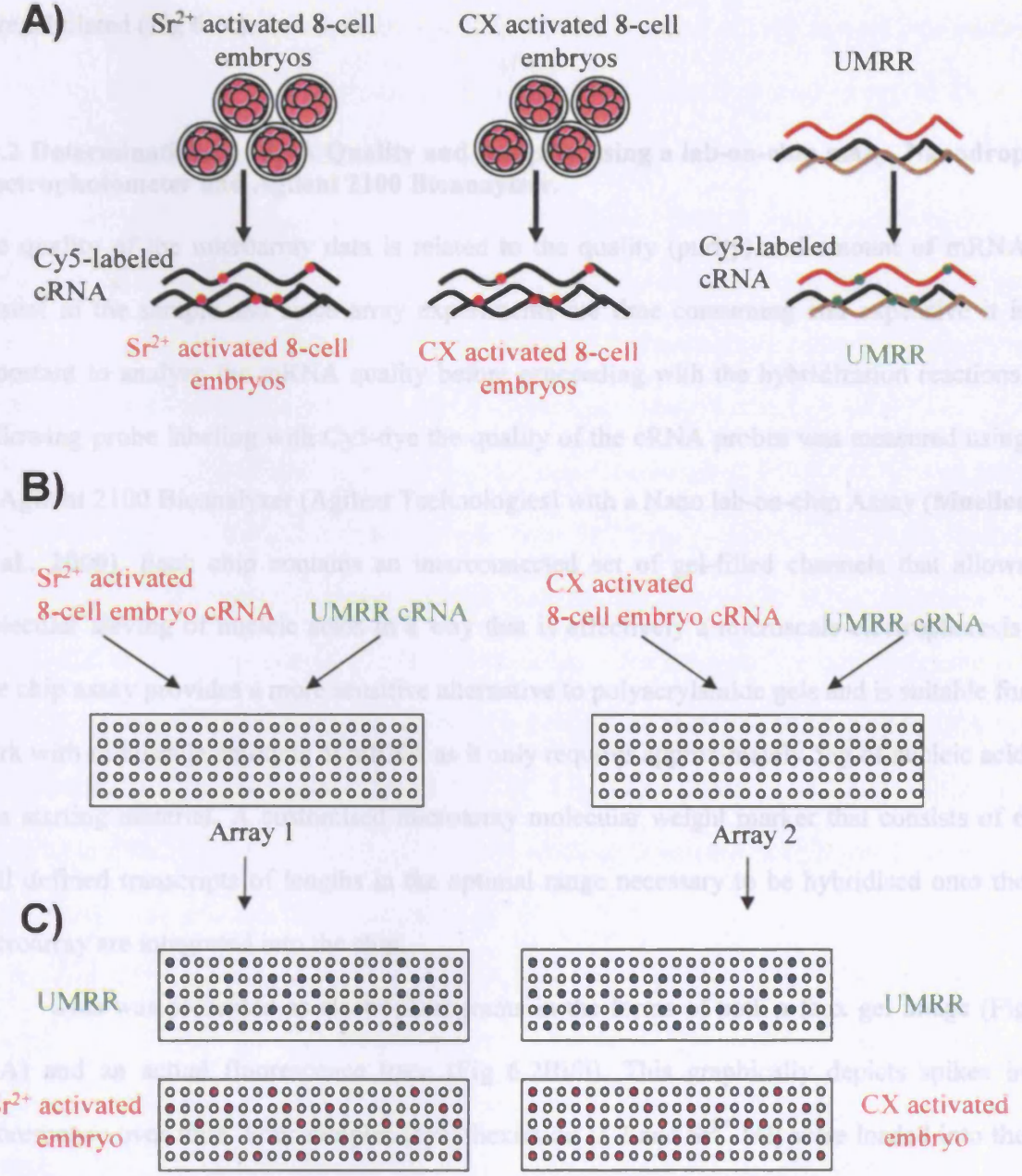

Fig 6.1 Experimental design for microarray work. Comparison of gene expression in Sr^{2+} and cycloheximide (CX)-activated 8-cell embryos using universal mouse reference RNA (UMRR) as a common reference sample. Total RNA isolated from 8-cell embryos was labeled with Cy5 during cRNA synthesis. UMRR cRNA was labeled with Cy3 (a) Each experimental Cy5-labeled cRNA was co-hybridized with Cy3-labeled cRNA from UMRR onto a 22,000-spot cRNA microarray (b). Ratios of Cy5/Cy3 intensities were compared to each other and differentially expressed genes tabulated (c).

were compared to one another. Differentially expressed genes from each group of embryos were tabulated (Fig 6.1c).

6.2.2 Determination of cRNA Quality and integrity using a lab-on-chip assay, Nanodrop spectrophotometer and Agilent 2100 Bioanaylzer.

The quality of the microarray data is related to the quality (purity) and amount of mRNA present in the sample and since array experiments are time consuming and expensive it is important to analyze the mRNA quality before proceeding with the hybridization reactions. Following probe labeling with Cy5-dye the quality of the cRNA probes was measured using an Agilent 2100 Bioanalyzer (Agilent Technologies) with a Nano lab-on-chip Assay **(Mueller et al., 2000)**. Each chip contains an interconnected set of gel-filled channels that allows molecular sieving of nucleic acids in a way that is effectively a microscale electrophoresis. The chip assay provides a more sensitive alternative to polyacrylamide gels and is suitable for work with minuscule amounts of mRNA as it only requires approximately 5ng of nucleic acid as a starting material. A customised microarray molecular weight marker that consists of 6 well defined transcripts of lengths in the optimal range necessary to be hybridised onto the microarray are integrated into the chip.

Data was presented as electropherograms in the forms of both a faux gel image (Fig 6.2A) and an actual fluorescence trace (Fig 6.2Bi/ii). This graphically depicts spikes in fluorescence over time. Four samples (cycloheximide 1/ 2 and Sr^{2+} 1/2) were loaded into the chip wells and allowed to run for 3 minutes. A high number of cRNA transcripts with lengths similar to that of the customised molecular weight markers were observed (Fig 6.2A). The large number of cRNA transcripts all of which were of different lengths in the samples prevented visualisation of distinct bands in the gel. The gel did confirm however that the cRNA transcripts were fragmented to suitable lengths that were in the optimal range for hybridization onto the microarray platform.

Degradation of total RNA by RNAases can be easily detected by a shift in the RNA transcript size distribution towards smaller fragments. Inspection of each sample lane on the gel showed that there was no increase in the amount of smaller fragments in any of the gel lanes and this indicated that mRNA degradation was minimal.

The Agilent 2100 bioanalyzer software automatically detects ribosomal RNA (rRNA) contamination by looking for bands of characteristic size which represent the major rRNA species (18S and 28S) which tend to electrophorese in a characteristic pattern. Results from the bioanalyzer show that there was no rRNA contamination in any of the samples.

The Agilent 2100 bioanalyzer produced an electropherogram of cRNAs derived from each sample (See Fig 6.2Bi and ii for examples from $Sr^{2+}1$ and cycloheximide2 respectively). The area under the curve is directly proportional to the amount of cRNA although the relationship is only semi-quantitative due to the nature of the assay and the non-representative nature of such a small test volume of macromolecules. The total amounts of mRNA for cycloheximide1, cycloheximide 2, $Sr^{2+}1$ and $Sr^{2+}2$ were as follows; 607ng/µl, 670ng/µl, 478ng/µl and 430 ng/µl respectively. The cRNA obtained from each sample was in sufficient quantities to allow efficient hybridisation.

The cRNA from each sample was labelled with Cy5 and co-hybridised with Cy3-labelled UMRR onto the NIA 22k microarray. Ratios of Cy5 and Cy3 intensities were compared to one another. Fig 6.3 shows an example of a scanned image from a microarray platform after hybridisation of cRNA obtained from the $Sr^{2+}1$ cohort of embryos. The intensity of the colour of each spot reflects the amount of expression occurring in the gene represented by each spot; the higher the intensity of red in a spot, the higher the expression of the represented gene in the test sample compared to that of the UMRR. The higher the intensity of green in a spot the higher the expression of the represented gene in the UMRR

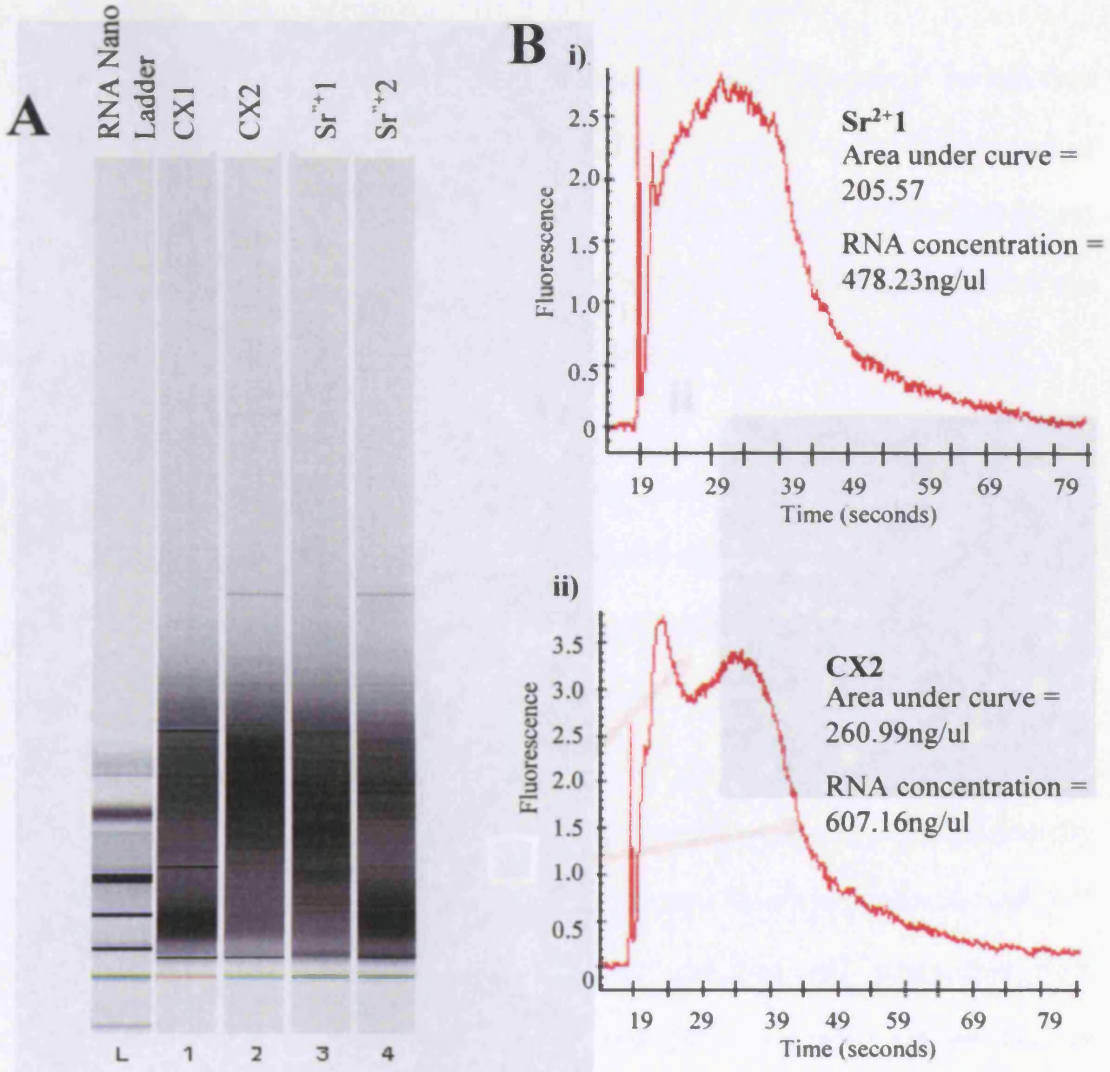

Figure 6.2. Determination of cRNA quality and quantity prior to hybridisation. Digitally generated gel image of Cy3-labelled cRNA's from the 4 samples (CX1, CX2, $Sr^{2+}1$ and $Sr^{2+}2$) (A). The lengths of cRNA transcripts in all samples are of similar size to that of the ladder (L) indicating their suitability for microarray work. Bioanalyzer electropherograms of cRNA from $St^{2+}1$ (Bi) and CX1 (Bii) samples were carried out to analyze the integrity of cRNA. To calculate the concentration of total RNA, the area under the entire RNA electropherogram is determined and compared to the area under the ladder and this value is directly related to the cRNA concentration. CX = cycloheximide.

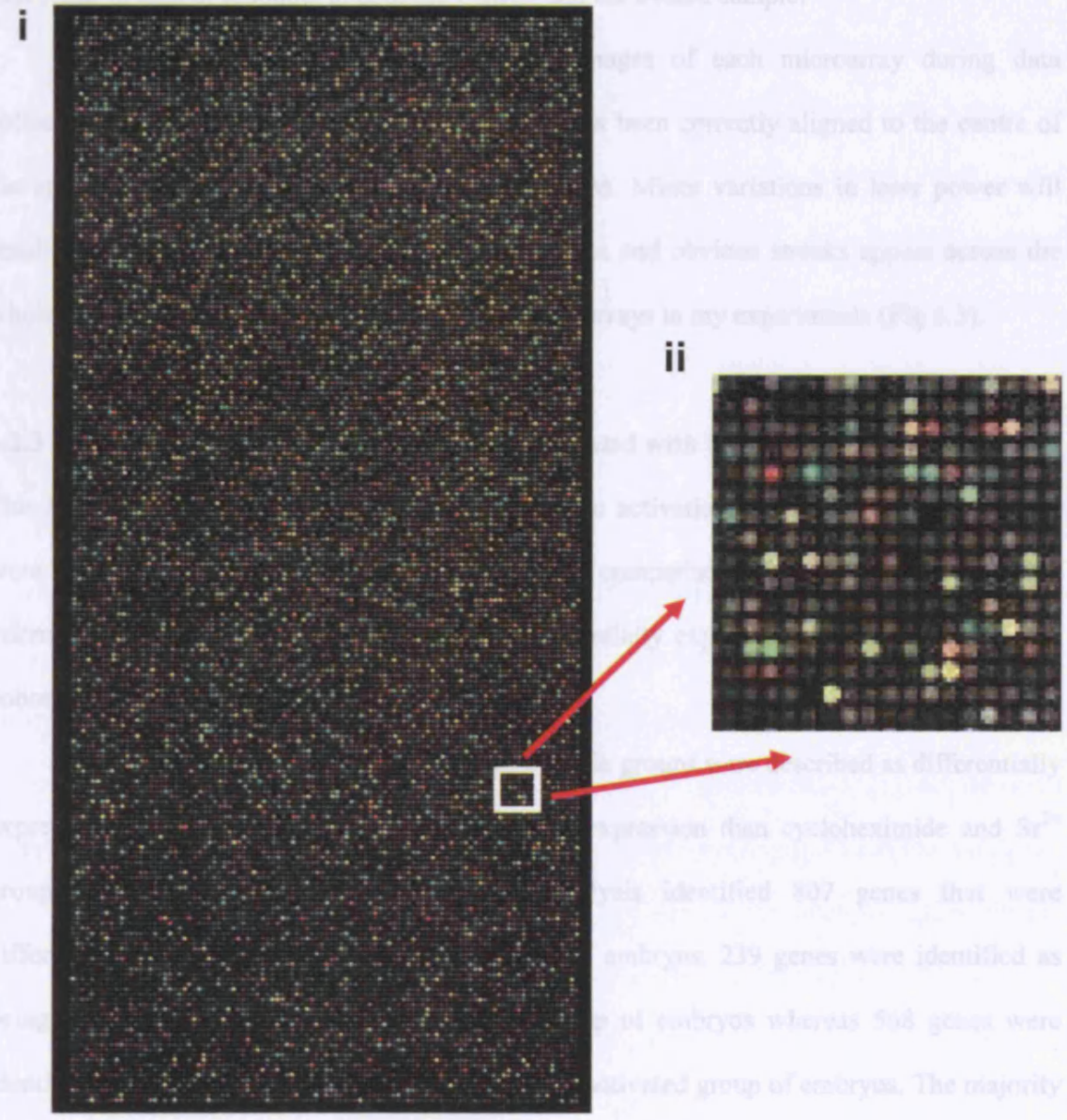

Figure 6.3 NIA 22K 60-Mer Oligo Microarray. Image of a whole microarray after hybridisation of cy3-labeled cRNA from $Sr^{2+}1$ sample group and cy5-labeled UMRR (i). Magnification of a small area of the microarray showing distinct green, red and yellow spots that vary in intensity (ii). A red spot indicates that the represented gene in the cohort of embryos is more highly expressed compared to the expression of the gene in the UMRR A green spot indicates that the represented gene in the UMRR is more highly expressed compared to the gene in the cohort of embryos. A yellow spot indicates that there is no significant differences in gene expression levels of the represented gene in either the cohort of embryos or UMRR.

compared to that of the test sample. When the spot is yellow it indicates that the gene is expressed in similar amounts in both the UMRR and the treated sample.

It is important to analyse the scanned images of each microarray during data collection, this is to ensure that the scanner laser has been correctly aligned to the centre of the spots and there have been no power fluctuations. Minor variations in laser power will result in apparent brightness variations in the images and obvious streaks appear across the whole image. No streaks were present on any of the arrays in my experiments (Fig 6.3).

6.2.3 Pairwise comparison of 8-cell embryos activated with Sr^{2+} or cycloheximide.

The 8-cell embryos generated from parthenogenetic activation with Sr^{2+} or cycloheximide were used for expression profiling. A pairwise comparison of gene expression using microarray data was carried out to highlight differentially expressed genes between the two cohorts of 8-cell embryos.

Genes expressed in the Sr^{2+} and cycloheximide groups were described as differentially expressed when they exhibited a 1.5-fold higher expression than cycloheximide and Sr^{2+} groups, respectively. Quantitative statistical analysis identified 807 genes that were differentially expressed between the two groups of embryos. 239 genes were identified as being highly expressed in the Sr^{2+}- activated group of embryos whereas 568 genes were identified as highly expressed in the cycloheximide-activated group of embryos. The majority of differentially expressed genes in both groups had a log intensity of approximately 2.5-3.5 and a log-ratio value of 0.4-0.6 which revealed that most differentially expressed genes exhibited a 1.5-2 fold difference in gene expression (Fig 6.4). As the comparison of gene expression between the two groups of embryos was a pairwise comparison genes were described as highly expressed with respect to the other group and could not be described as under expressed with respect to the same group. A table of all the differentially expressed

genes (fold changes > 1.5) and their fold-changes can be observed in the appendices (Tables 8.1 and 8.2).

A scatter plot of the log intensities versus log ratio was generated using the NIA array analysis tool (http://lgsun.grc.nia.nih.gov/ANOVA/) (Fig 6.4). Each differentially expressed gene was represented by a single point on the scatter plot. The log intensity refers to the logarithm of intensity of fluorescent light for each dye on each spot of the array. Log-ratios are usually used for microarray data analysis to facilitate the calculation of fold change, where a 2 fold up-regulation of a gene corresponds to a log ratio of 1. Highly variable genes that had a high signal to noise ratio were treated with caution.

6.2.4 A perspective on global gene expression by Principle Component Analysis

I used Principle Component Analysis (PCA), a common tool used in microarray analysis, as a cluster analysis tool to compare common global gene expression patterns in datasets of cycloheximide and Sr^{2+} activated parthenogenetic eggs to unfertilized eggs and fertilised embryos at the 1 cell, 2 cell, 4 cell, 8 cell, morula and blastocyst stages. I used the NIA array analysis tool (http://lgsun.grc.nia.nih.gov/ANOVA/) to identify any common global theme that might be representative of my treated embryos during preimplantation development **(Sharov et al., 2005)**. PCA is useful because it breaks down the complexity of large datasets and characterizes the most abundant themes of gene expression.

In a situation where two variables are to be compared, we would normally draw a two dimensional chart or graph where the first variable represents the first dimension (x) and the second variable represents the second dimension (y). If we were comparing three variables simultaneously we could still draw a graph including a third dimension (z). Each covariate point in this three dimensional space has a co-ordinate value (x,y,z). The addition of a fourth variable in the comparison causes problems as we cannot perceive or draw a fourth spatial

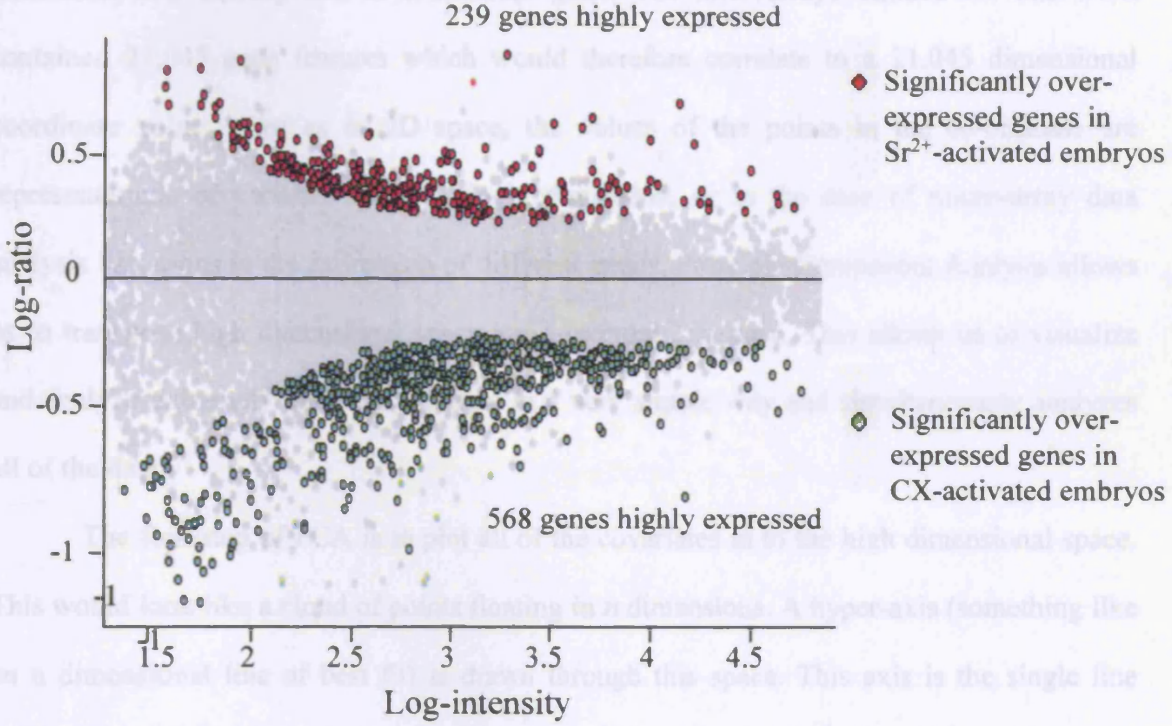

Figure 6.4 Scatter plot showing log intensity and ratio of differentially expressed genes. The horizontal axis represents the averaged log (intensity) of genes and the vertical axis represents the log-ratio of signal intensity for each genes. The coloured dots represent genes that have passed statistical analysis by false rate discovery (FDR) =10%. Highly expressed genes from Sr^{2+} activated 8-cell embryos are denoted by red dots and those from cycloheximide (CX)- activated embryos are denoted by green dots. Highly variable (noisy) genes (shown in a lighter green or red colour) were present in our results and were treated with caution. In total 807 genes were differentially expressed between the 2 groups of parthenogenetic 8-cell embryos.

dimension; this does not however prevent the plotting of a four point co-ordinate value (x,y,z,a). With *n* variables, this principle is extrapolated into *n* dimensional space and each point in this space is described by an *n* dimensional coordinate value (x,y,z,a,b,c...*n*). Each dimension thus corresponds to a different gene. The microarrays utilized for this work contained 21,045 gene features which would therefore correlate to a 21,045 dimensional coordinate value. Just as in 3D space, the values of the points in the co-ordinate are representations of variance along a single dimension, or in the case of micro-array data analysis variations in the expression of different genes. Principle Component Analysis allows us to transpose high dimensional space into a normal 3D space. This allows us to visualize and analyze extremely complex data sets in a very simple way and simultaneously analyzes all of the data.

The first step of PCA is to plot all of the covariates in to the high dimensional space. This would look like a cloud of points floating in *n* dimensions. A hyper-axis (something like an n dimensional line of best fit) is drawn through this space. This axis is the single line which can be drawn through the cloud that gives us the best one dimensional idea of the shape of the cloud in that it passes through more points than any other line, this is Principle Component 1 (PC1). The next step is to draw a second hyper-axis at right angles (just like in normal co-ordinates) to PC1 and this gives us the next best, one-dimensional idea of the shape of the cloud and is Principle Component 2. By plotting PC1 against PC2 we now can identify the basic two-dimensional outline of the cloud as if its shadow had been cast on a wall. This principle can be continued until such a point as most of the variation has been described by the principle components used (i.e. one of the principle components passes through the majority of points in the cloud. In normal situations we would hope that almost all of the variation would be described by the first three principal components as they can be simply graphed in normal space. The principle components are averages of the summative effect of

all of the covariates. The final stage of PCA is to plot each individual set of covariates (i.e. the data from each developmental stage, see Fig 6.5) individually onto the principle components and assess how they vary from the average. For any given grouping (here the type of embryos used), small differences in any number of dimensions in the co-ordinate system will have a knock-on effect on the position of the point representing that grouping along the axes of the principle components. The result is a graph that shows how the gene expression at each developmental stage varies from the average and is without scale or value. The proximity of each set of covariates to one another when graphed along the Principle Components describes in a low dimensional form how they compare to one another in the high dimensional form. In these experiments we can describe how the different sets of embryos compare to one another in terms of the expression of many genes, but in a simple two-dimensional form that describes all, or most of the expression data from the micro-array simultaneously.

PCA revealed that 8-cell embryos generated by activation with Sr^{2+} or cycloheximide followed a similar developmental path to that of the *In vivo* fertilised embryos (Fig 6.5A). Fig 6.5A shows that the gene expression of unfertilized and fertilised oocytes is very different from the gene expression of 2-cell, 4-cell, 8-cell, morulae and blastocyst stages. This has previously been described **(Hamatani et al., 2004a)**. Both groups of 8-cell parthenogenetic embryos exhibited an expression pattern that was in a phase between that of the 4-cell and 8-cell/morula stages of *in vivo* fertilised embryos (Fig 6.5A). Further analysis of PC1 and PC2 revealed that subtle differences existed between Sr^{2+} and cycloheximide-activated embryos (Fig 6.5B). PC1, which represented the most common global gene expression patterns, revealed that Sr^{2+} activated 8-cell embryos showed more resemblance to *In vivo*-fertilised 8-cell, morula and blastocyst stage embryos than any other preimplantation stage (Fig 6.5 Bi). Cycloheximide-activated 8-cell embryos had expression patterns that were most similar to a

Fig 6.5

phase between the 4 and 8-cell preimplantation stages of *In vivo-* fertilised embryos (Fig 6.5 Bi).

PC2 analysis which represented the 2nd most common gene expression pattern, demonstrated that Sr^{2+} and cycloheximide-activated embryos were more similar to one another than to any stage of *in vivo*-fertilised preimplantation embryos (Fig 6.5ii).

6.2.5 Assignment of functional categories to differentially expressed genes.

MAPPFinder **(Doniger et al., 2003)** was used in conjunction with GenMAPP in order to assign functional categories to differentially expressed genes by identifying the major Gene Ontology (GO) terms **(Ashburner et al., 2000)** associated with them. The microarray data are available from the public databases (GEO and ArrayExpress) and the website http://lgsun.grc.nia.nih.gov/microarray.data.html.

To assess possible biological significance, only functional categories that had three or more differentially expressed genes in either the Sr^{2+} or cycloheximide-activated group of embryos were selected. Overall functional groupings were quite different between embryos generated from cycloheximide and Sr^{2+}-induced egg activation. 8-cell embryos derived from cycloheximide-activation were characterized by genes such as those associated with the GO-terms "cell cycle, microtubule-based processes, ATP binding, apoptosis and cell differentiation" (Table 6.1). The 8-cell embryos resulting from Sr^{2+} activation were represented by genes such as those associated with the GO-terms "cell proliferation, cell adhesion and ion transport" (Table 6.2). It is important to note that a single gene can be common to more than one biological process, for example RAD21 is associated with both the cell cycle and apoptosis pathways and Gadd45g is associated with apoptosis and cell differentiation.

Table 6.1 - Genes more highly expressed in 8-cell cycloheximide-activated embryos compared to Sr^{2+} activated 8-cell embryos.

Gene Ontology classification	Gene Name	Protein Name	Fold change
Cell cycle	*Spin*	spindlin	2.092
	Ccnb3	cyclin B3	1.883
	Cdc6	cell division cycle 6	1.858
	Cdk7	cyclin-dependent kinase 7	2.225
	Cdk9	cyclin-dependent kinase 9	1.961
	Cdkn2d	cyclin-dependent kinase inhibitor 2D	1.711
	Mapk4	mitogen-activated protein kinase 4	1.786
	Plk4	polo-like kinase 4	1.731
	Rad21	Double-strand-break repair protein rad21 homolog	1.716
Microtubule based processes	*Dnclc1*	cytoplasmic , light chain 1	1.739
	Kif11	kinesin family member 11	2.399
	Kif1b	kinesin family member 1b	1.772
	Kif2c	kinesin family member 2c	1.879
	Kif3c	kinesin family member 3C	1.704
	Tuba4	tubulin, alpha 4	1.81
	Tubb3	tubulin, beta 3	2.097
Cytoskeleton dependent intracellular transport	*Bicd2*	bicaudal D homolog 2	2.093
	Dnclic1	dynein, light intermediate chain 1	1.951
	Bicd2	bicaudal D homolog 2	2.093
	Dnclc1	Dynein, cytoplasmic , light chain 1	1.739
	Dnclic1	dynein, light intermediate chain 1	1.951
	Tuba4	tubulin, alpha 4	1.81
Microtubule motor activity	*Kif11*	kinesin family member 11	2.399
	Kif1b	kinesin family member 1b	1.772
Apoptosis	*Faf-1*	Fas-associated factor 1	2.421
	Dapk2	Death associated protein kinase 2	1.691
	Jak2	Janus kinase 2	1.778
	Rad21	Double-strand-break repair protein rad21 homolog	1.716
	Zfp346	zinc finger protein 346	1.752
	Gadd45g	growth arrest and DNA-damage-inducible 45 gamma.	2.358
	Cebpb	CCAAT/enhancer binding protein (C/EBP), beta	1.871
	Card4	caspase recruitment domain 4	1.841
Cell growth	*Socs1*	suppressor of cytokine signaling 1	1.772
	Socs2	Suppressor of cytokine signaling 2	1.919
	Socs3	Suppressor of cytokine signaling 3	1.942
Cell proliferation	*Cdk9*	cyclin-dependent kinase 9	1.961
Organic acid transporter activity	*Slc1a7*	Solute carrier family 1 (glutamate transporter), member 3	1.753
	Slc38a4	Solute carrier family 38, member 4	2.033
	Slc1a3	Solute carrier family 1 (glial high affinity glutamate transporter), member 3	1.913
Morphogenesis of epithelium	*Xdh*	Xanthine dehydrogenase	1.778
	Celsr1	Cadherin EGF LAG seven-pass G-type receptor 1 precursor	1.889
	Jag1	Jagged 1	2.07
Protein phosphorylation	*Akt3*	Thymoma viral proto-oncogene 3	1.751
	Cdk7	cyclin-dependent kinase 7	2.225
	Cdk9	cyclin-dependent kinase 9	1.961
	Dapk2	Death associated kinase 2	1.691

	Ddr1	discoidin domain receptor family, member 1	2.007
	Eifak3	eukaryotic translation initiation factor 2 alpha kinase 3	2.054
	JAK2	Janus kinase 2	1.778
	Mapk14	mitogen activated protein kinase 14	1.937
	Mapk4	mitogen-activated protein kinase 4	1.786
	Nek4	NIMA (never in mitosis gene a)-related expressed kinase 4	2.357
	Prkcb	protein kinase C, beta	1.882
	Prkar2a	protein kinase, cAMP dependent regulatory, type II alpha	1.77
	PLK4	polo-like kinase 4	1.731
	Abcb9	ATP-binding cassette, sub-family B (MDR/TAP), member 9	2.031
	Abcc10	ATP-binding cassette, sub-family C	1.726
	Acly	ATP citrate lyase	1.705
	Akt3	thymoma viral proto-oncogene 3	1.751
	D1Pas1	DNA segment, Chr 1, Pasteur Institute 1	1.666
ATP binding	***Dapk2***	Death associated kinase 2	1.691
	Dck	deoxycytidine kinase	2.059
	Ddr1	discoidin domain receptor family, member1	2.007
	Ddx27	DEAD box polypeptide 27	1.857
	Ddx28	DEAD box polypeptide 28	1.976
	Cdc6	cell division cycle 6,	1.858
	Cdk7	cyclin-dependent kinase 7	2.225
	Cdk9	cyclin-dependent kinase 9	1.961
	Edaradd	ectodysplasin-A receptor	2.129
Cell differentiation	***Gadd45g***	growth arrest and DNA-damage-inducible 45 gamma.	2.358
	Jak2	Janus kinase 2	1.778
	Xdh	xanthine dehydrogenase	1.254
	Sp3	Trans-acting transcription factor 3	1.884
	Icsbp1	interferon consensus sequence binding protein 1	1.808
	Cebpb	CCAAT/enhancer binding protein, beta	1.871
	Socs2	Suppressor of cytokine signaling 2	2.118
	Mrap	melanocortin 2 receptor accessory protein	1.7
Integral to membrane	***1300007B12Rik***	RIKEN cDNA 1300007B12 gene	2.222
	1700018O18Rik	RIKEN cDNA 1700018O18 gene	2.403
	1810055G02Rik	RIKEN cDNA 1810055G02 gene	2.399
	4732495E13Rik	RIKEN cDNA 4732495E13 gene	1.959
	5031400M07Rik	RIKEN cDNA 5031400M07 gene	2.045
Extracellular space	***Art5***	ADP-ribosyltransferase 5	1.873
Morphogenesis of an epithelium	***Celsr1***	Cadherin EGF LAG seven-pass G-type	1.889
	Jag1	Jagged1	2.07
	Ank1	ankyrin,1 erythriod	1.803
	Edaradd	EDAR (ectodyplasin-A receptor-associated death domain	2.129
Signal transduction	***Fgf18***	Fibroblast growth factor 18	2.274
	Gng7	G protein, gamma 7 subunit	1.908
	Hivep2	Human immunodeficiency virus type enhancer protein 2	2.328
	Prkar2a	protein Protein kinase, cAMP dependent regulatory, type II	1.77
	Rgs17	alpha	1.916
	Rtkn	regulator of G-protein signaling 17	2.115
	Socs1	Rhotekin	1.772
	Socs2	Suppressor of cytokine signalling 1	1.919
	Socs3	Suppressor of cytokine signaling 2	1.942
		Suppressor of cytokine signaling 3	
	2410005k20Rik	RIKEN cDNA 2410005K20	1.749
Protein biosynthesis	***Eif2ak3***	Eurakyotic translation initiation factor 2 alpha kinase 3	2.054
	Gadd45g	growth arrest and DNA-damage-inducible 45 gamma	1.894
	Rad21	Double-strand-break repair protein rad21 homolog	1.716
	Rps271	ribosomal protein S27-like	1.993
	RpL17	ribosomal protein L17	1.706

Table 6.2 Genes more highly expressed in Sr^{2+}-activated 8-cell embryos than in CX activated 8-cell embryos

Gene Ontology classification	Gene Name	Protein (or gene) of interest	Fold change
	Muc 2	mucin 2	1.81
Apoptosis	***Nfkb1***	Nuclear factor of kappa light chain gene	2.208
	Btg1	B-cell translocation gene 1, anti-proliferative	2.015
Cell proliferation	***Pdgfa***	platelet derived growth factor, alpha	1.681
	Prkar1a	Protein kinase, cAMP dependent regulatory, type I, alpha	2.001
	Uhrf1	ubiquitin-like, containing PHD and RING finger domains	1.763
Organic acid transporter activity	***Slc12a7***	solute carrier family 12, member 7	1.831
ATP binding	***Axl***	AXL receptor tyrosine kinase	1.612
Cell differentiation	***Mdfi***	MyoD family inhibitor	1.886
	DOCK2	dedicator of cyto-kinesis 2	2.089
	Tgfbr2	transforming growth factor, beta receptor II	2.679
	CD36	CD36 antigen	1.801
Cell adhesion	***Cntnap2***	Contactin associated protein 1	2.039
	Dsc1	Dermatopontin	3.477
	Gpnmb	Glycoprotein (transmembrane) nmb	2.114
	Pcdh7	Protocadherin 7	1.875
	Pcdha1	Protocadherin alpha 1	1.677
	Trpc7	transient receptor potential cation channel, subfamily C,	3.698
	Slc12a7	member 7	1.831
	Scn8a	solute carrier family 12, member 7	2.295
Ion transport	***Kcnj11***	sodium channel, voltage-gated, type VIII, alpha polypeptide	1.967
		potassium inwardly rectifying channel J 11	
Signal Transduction	***Rgs9***	regulator of G-protein signaling 9	1.935
	Nfkb1	Nuclear factor of kappa light chain gene	2.208
	Gab1	growth factor receptor bound protein 2-associated protein 1	2.434
	Prkar1a	Protein kinase, cAMP dependent regulatory, type I, alpha	2.001
	Eif3s10	Eurakyotic translation initiation factor 3,subunit 10 (theta)	3.271
Protein biosynthesis	***Mrpl15***	mitochondrial ribosomal protein L15	1.886
	Rpl10	ribosomal protein L10	2.32
	Rpl9	ribosomal protein L9	2.628
	Rpl29	ribosomal protein L29	2.031
	Rp9	ribosomal protein L9	2.628
	Scyel	small inducible cytokine subfamily E, member 1	1.956
	Rps3a	ribosomal protein S3a	1.946
	Rps27a	ribosomal protein S27a	2.35

6.3 Discussion

The aim of the work presented in this chapter was to investigate whether $[Ca^{2+}]i$ oscillations at egg activation have an impact on gene expression during preimplantation embryo development. To further examine the affects of $[Ca^{2+}]i$ oscillations on development I used embryos obtained from parthenogenetic activation using Sr^{2+} (which induces activation by inducing $[Ca^{2+}]i$ oscillations) and cycloheximide (does not cause any $[Ca^{2+}]i$ changes). The data from microarray analysis reveals that the occurrence of $[Ca^{2+}]i$ oscillations during egg activation may affect the expression of genes associated with biological processes such as apoptosis, cell cycle, ion transport, cell proliferation, cell differentiation and cell adhesion.

6.3.1 High expression of genes associated with the cell-cycle, apoptosis and cell differentiation are characteristic of cycloheximide-activated 8-cell embryos.

Microarray analysis data revealed that 8 genes associated with the cell cycle (Table 6.1) were more highly expressed in 8-cell embryos generated from cycloheximide-activation compared to Sr^{2+} activation. Of particular interest was the high expression of *Ccnb3*, which codes for the regulatory protein subunit cyclin B3. Cyclins are commonly known to be positive regulatory subunits of the cyclin-dependent kinases (cdks) which regulate mitotic cell cycle transitions. The degradation of cyclins is necessary for the progression of the cell cycle through mitosis. Preventing cyclin B3 degradation by using a stable version of the protein has been shown to prevent normal spindle organization and blocks other events such as chromosome decondensation (Parry, 2001). High expression of non-degradable cyclin B3 has also been reported to cause cell-cycle arrest in anaphase and at higher doses interferes with progression through G1 and entry into S phase **(Nguyen et al., 2002)**. It is evident that high expression levels of cyclin B3 may have detrimental effects on the cell cycle and this may therefore be an

explanation of why premature developmental arrest occurs in many of the cycloheximide-activated 4-cell embryos (Chapter 4).

Cycloheximide-activated 8-cell embryos were also characterised by the high expression of *Spin*, which encodes the protein Spindlin. Spin is involved in the progression of the meiotic and first mitotic cell cycles and it is highly expressed in the growing oocyte where it persists through embryogenesis until the 4-cell stage after which time it degrades **(Oh et al., 2005)**. Under normal circumstances 8-cell embryos would not express *Spin*, in cycloheximide-activated 8-cell embryos however, *Spin* is overexpressed 2.1 fold compared to Sr^{2+} activated 8-cells. It appears that there is no requirement for the expression of *Spin* following the first mitotic cell cycle and that a high level probably interferes with developmental progression through later mitotic cell-cycles, which is consistent with the observations made in cycloheximide-activated embryos.

Cell cycle arrest has also been reported to occur in cells after overexpression of other cell cycle related genes which were highly expressed in cycloheximide-activated 8-cell embryos. *Cdk7* **(Nishiwaki et al., 2000)** and *Cdkn2d* **(Okuda et al., 1995)** overexpression for example causes premature cell cycle arrest in different somatic cell types. There was no high expression of cell-cycle related genes in Sr^{2+}-activated 8-cell embryos compared to cycloheximide-activated embryos. Previous experiments have shown that Sr^{2+}-activated embryos progress through preimplantation development to the blastocyst stage without any major hurdles (Chapter 4) and since cycloheximide-activated embryos (which often arrest prematurely) exhibit high levels of cell-cycle related gene expression, this suggests that high levels of expression of these genes has a detrimental effect on embryo development.

Apoptosis related genes were found to be differentially expressed in both cycloheximide and Sr^{2+} activated embryos. Only two apoptosis-related genes, *Muc 2* and *Nfkb1* (Table 6.2) were found to be highly expressed in 8-cell embryos generated from Sr^{2+}

activation. More apoptosis-related genes were however discovered to be more highly expressed in 8-cell embryos activated by cycloheximide (Table 6.1). High expression levels of *DAPK2 (Death Associated Kinase 2)* were present in cycloheximide-activated embryos and have been reported to significantly induce the morphological changes characteristic of apoptosis in skeletal muscle cells **(Kawai et al., 1999)**. DAPK2 binds directly to calmodulin and is activated in a Ca^{2+}/Calmodulin-dependent manner. It is surprising that *DAPK2* is overexpressed in cycloheximide-activated embryos because cycloheximide-induced egg activation occurs in the absence of $[Ca^{2+}]i$ oscillations.

A number of genes which were found to be more highly expressed in cycloheximide-activated embryos and whose function is associated with apoptosis also appear to be related to the cell cycle. In fact there is mounting evidence that apoptosis regulatory proteins themselves can directly impinge on the cell-cycle machinery. The gene *Rad21 (Double-strand-break repair protein 21)* for example plays a critical role in cell division by regulating sister chromatid cohesion and separation at the metaphase-to-anaphase transition but also has a further role in the regulation of apoptosis by repairing double-strand DNA breaks. High expression levels of *Rad21* cause an increased incidence of apoptosis in Molt4 and 293T cells **(Pati et al., 2002)** and could mean that *RAD21* overexpression leads to an increase in apoptosis in other cell types. The 8-cell embryos activated with cycloheximide were indeed found to have a 1.7-fold increase in *RAD21* expression compared to those embryos derived from Sr^{2+} activation which may account for the higher degree of apoptosis observed in these parthenogenetic embryos.

Gadd45g is another gene which was originally identified to be a gene involved in negative regulation of the cell cycle and growth control however over expression of this gene has recently been shown to cause apoptosis and cell cycle arrest *In vitro* ***(Mak and Kultz, 2004)***. *Gadd45g* is also expressed approximately 2.4 fold higher in cycloheximide-activated

embryos than in Sr^{2+} activated embryos. The *Cdk9* protein which is associated with the cell division phase of the cell cycle has also been shown to render cells lines sensitive to apoptosis when expressed in high levels **(Foskett et al., 2001)**. The highest incidence of apoptosis in blastocysts as determined by TUNEL occurred in embryos generated from cycloheximide compared to Sr^{2+} activation and high levels of cell cycle and apoptosis-related genes may therefore induce this effect. Further work will be needed to elucidate any apoptosis-related pathways that may be in action and are triggered by the lack of $[Ca^{2+}]i$ signals at activation. Unfortunately it is still unclear how most apoptosis genes work and how high expression can lead to eventual programmed cell death. It was surprising that some genes known to be activated via classical effector pathways such as the pro-apoptotic *bcl-2* family members, *bax* and *caspase-1* were not found to be highly expressed in cycloheximide when compared to Sr^{2+}-activated embryos. It has been suggested that various apoptosis regulatory factors may enhance or inhibit the function of a gene and in this way the ratio of activators to inhibitors may determine if the cell undergoes apoptosis or not (korsmeyer et al, 1995).

The 8-cell embryos generated with cycloheximide had high expression of genes associated with the GO-term "cell differentiation" (Table 6.1). Overexpression of *Sp3 (Trans-acting transcription factor 3)* was particularly interesting as it has been reported to cause down-regulation of N-cadherin expression in human osteoblasts **(Le Mee et al., 2005)**. Members of the cadherin family function by facilitating cell-cell adhesion, which is a vital process for preimplantation stage embryos, especially during the process of compaction. *Socs2 (Suppressor of cytokine signaling 2)* is a growth control gene with inhibitory functions and therefore high expression of this gene would lead to a growth inhibiting affect on the embryo, which may explain the incidence of less Inner Cell Mass (ICM) cells in blastocysts derived from cycloheximide-activation.

6.3.2 High expression of genes associated with ion transport, cell adhesion and cell proliferation pathways are characteristic of Sr^{2+}-activated 8-cell embryos.

8-cell embryos resulting from Sr^{2+}-induced egg activation has differential expression of genes associated with the GO term "ion transport" (Table 6.2). The overexpression of *Trpc7* (*Transient receptor potential cation channel, subfamily C, member 7*) was interesting as it functions as a Ca^{2+} permeable cation channel which is activated by diacyglycerol (DAG) and Ca^{2+} store depletion (Hoffmann et al., 1999). The $[Ca^{2+}]i$ rises that are stimulated by Sr^{2+} lead to the synthesis of DAG which in turn may lead to activation of the channel. Egg activation by cycloheximide-stimulation in contrast, occurs in a Ca^{2+} dependent manner without the production of DAG, which may prevent activation of the channels.

The expression of *Scn8a* and *kcnj11*, which code for a voltage gated Na^+ and K^+ channel respectively may be relevant to the formation of the blastocoel cavity. Although the exact mechanisms of blastocoel formation are unclear it appears to be mediated by Na/K-ATPase-generated trans-trophectoderm ion gradient that promotes the accumulation of water across the epithelium (Watson and Barcroft, 2001). The expression of genes associated with Na^+ and K^+ ion channels appears to have an important role in the maintenance and later development of the embryo during preimplantation development, especially during the blastocyst stage.

Genes associated with the GO-term "cell adhesion" were identified as being differentially expressed in Sr^{2+} and cycloheximide-activated groups of 8-cell embryos. The 8-cell embryos derived from cycloheximide-induced egg activation were characteristed by the high expression levels of 3 cell adhesion related genes (Table 6.1) however 6 cell adhesion related genes (Table 6.2) were highly expressed in 8-cell embryos resulting from Sr^{2+}-induced activation. The two protocadherins *Pcdh7 (Protocadherin 7)* and *Pcdha1 (Protocadherin alpha 1)* which work by Ca^{2+}-dependent cell-cell adhesion were both highly expressed in 8-cell embryos activated by Sr^{2+} and their overexpression may aid the cell

adhesion events in the 8-cell embryo. Further analysis by antibody staining or protein assays is necessary to be clearer about the exact function of these adhesion genes in the preimplantation embryo.

Overexpression of genes relating to cell proliferation was found in 8-cell embryos that were generated by Sr^{2+} and cycloheximide activation. Only 1 cell proliferation gene (*cdk9*) was found to be highly expressed in the cycloheximide-activated group (Table 6.1) whereas 4 genes (Table 6.2) were found to be highly expressed in the Sr^{2+}-activated group. *Pdgfa (Platelet derived growth factor alpha)* is a potent mitogen that has a major role in wound healing by stimulating neighboring cells to grow. *Uhrf1 (Ubiquitin-like, containing PHD and RING finger domains)* which has been shown to suppress expression of tumor suppressor genes in breast cancer cells has also been reported to be involved in cell proliferation-associated events (Unoki et al., 2004). High expression levels of these proliferation genes in Sr^{2+} activated embryos may explain why the resulting blastocysts have an increased number of cells in their ICM.

The majority of differentially expressed genes in both cohorts of embryos were only differentially expressed 1.5 – 2.5 fold however it is becoming widely accepted that even small differences in gene expression can have profound consequences for the cell. Expression studies on human breast cancer for example, revealed that as little as a 1.25- to 2.5-fold increase in expression of *RAD21* was present in several human breast cancer cell lines as compared with normal breast cell lines (Atienza et al., 2005), although this may not be the only aberrant gene in these cancerous cells.

6.3.3 Experimental limitations and future directions

Analysis of gene expression in cycloheximide and Sr^{2+}-activated parthenotes would ideally not have been restricted to the 8-cell stage but extended through all stages of preimplantation

development from the 1-cell pronucleate to the blastocyst stage. This would have provided a much more detailed view of how $[Ca^{2+}]i$ oscillations at egg activation can change the expression patterns of individual genes throughout preimplantation development. During development in the fertilised embryo for example, the gene *Spin* is only expressed until the 4-cell stage after which time the protein is degraded (Oh et al., 2005). High expression levels of Spin occur however in 8-cell embryos generated from cycloheximide-induced activation. The opportunity to follow the expression pattern of *Spin* throughout preimplantation development would reveal when this gene first becomes differentially expressed with respect to Sr^{2+} activated parthenotes or fertilised embryos. The high costs (~$1000 per array) and time associated with this work prevented me from examining the different cohorts of parthenotes during each stage of preimplantation development. The 8-cell stage of development was however a suitable stage to examine gene expression in the groups of parthenotes since any major events taking place around the time of blastocyst formation, such as compaction and cell differentiation would be reflected by the pattern of gene expression at this stage.

It could be argued that any deleterious affects on gene expression could be due to the affect of cycloheximide which has previously been shown to delay cell division and embryonic transcription (Zakhartchenko et al., 1999; Alberio et al., 2001b). I have previously shown however that cycloheximide does not affect the timing or amount of gene expression that occurs during minor embryonic genome activation (Chapter 5) and moreover, it is the advantageous affect of Sr^{2+} and not the detrimental affect of cycloheximide that causes a high number of embryos to reach the blastocyst stage after egg activation when a combined treatment of cycloheximide plus Sr^{2+} is used (Chapter 4). It will be useful to carry out microarray analysis of embryos treated with the combined treatment (Sr^{2+} plus cycloheximide) to rule out the possibility that differential gene expression was due to the detrimental affects of cycloheximide rather than by the $[Ca^{2+}]i$ oscillations induced by Sr^{2+}

activation. Again it was the high costs of testing a larger number of microarrays that prevented me from testing the combined activation treatment.

PCA was performed to compare global gene expression patterns in the 8-cell parthenogenetic embryos with fertilised embryos from all stages of preimplantation development (Fig 6.5). I compared the results from the gene expression database from 8-cell parthenotes in my experiments with the results of gene expression datasets from fertilised embryos which have been published previously (Hamatani et al., 2004a). Two main differences between the cohorts of embryos from each database prevented me from being able to make direct comparisons between the two datasets. Firstly, I had to compare my global gene expression results from parthenogenetic embryos with fertilised embryos, so any influence the sperm or its DNA has over gene expression during preimplantation development would not be observed in parthenogenetic 8-cell embryos. In the future it may be possible to inject a male pronucleus into each egg prior to parthenogenetic activation to ensure complete paternal input. This was however unnecessary as the main aim of the work was to investigate the affect $[Ca^{2+}]i$ signaling had on gene expression by comparing eggs that had been activated in a $[Ca^{2+}]i$ dependent or independent manner.

The second parameter that prevented me from making direct comparisons of my 8-cell embryos with the fertilised embryo gene expression datasets was the fact that the fertilised embryos were developed under *In vivo* conditions and only removed prior to microarray analysis. The 8-cell parthenotes from my work on the other hand were cultured *in vitro* from the time of activation. The environmental conditions that the embryo is subjected to are a big determinant of embryo quality and viability. Many studies have concluded that it is during the first few cleavages of preimplantation development that the embryo is particularly sensitive to environmental conditions, which have been reported to influence the relative abundance of embryonic transcripts at these stages (Rizos et al., 2003). Studies on bovine embryos have

shown that *In vitro*-cultured embryos have a higher incidence of chromosomal abnormalities (Viuff et al., 1999) compared to embryos cultured *In vivo*. In fact even altering the supplemental ingredients of cell culture media such as amino acids has been shown to have an effect on the gene expression and cavitation rates of blastocysts (Rinaudo and Schultz, 2004). Analysis of Principle Component 1 (PC1) from the Principle Component Analysis (PCA) results nevertheless revealed that embryos from the two groups of parthenotes were more similar to other preimplantation stages of *in vivo* fertilised embryos than to one another (Fig 6.5Bi). The gene expression of cycloheximide-activated 8-cell embryos were most similar to a stage between the 4 and 8-cell stage of *in vivo* fertilised embryos and the gene expression of Sr^{2+} activated 8-cell embryos were most similar to a time between the 8-cell, morula and blastocyst development of *in vivo* fertilised embryos (Fig 6.5i). This global gene expression data indicates that cycloheximide-activated 8-cell embryos were developmentally less advanced then Sr^{2+} activated embryos and that the method of activation and possibly the presence or absence of $[Ca^{2+}]i$ oscillations at this time has important implications for gene expression and perhaps more so than the extent of *in vitro* culture systems.

The analysis of PC2 from the PCA revealed there were similar patterns of gene expression between the 2 sets of parthenotes compared to other stages of *in vivo* fertilised embryos. This is likely to reflect the fact that the embryos were cultured under identical *in vitro* conditions that were very different from the optimal *in vivo* conditions that the *in vivo* fertilised embryos were subject to.

One interesting result from the analysis of gene expression was the larger number of highly expressed genes in the cycloheximide-activated group (568) compared to that of the Sr^{2+}-activated group (239). This could be happening for a number of reasons. Firstly, a large number of overexpressed genes in cycloheximide-activated embryos may be negative regulators of important processes such as the cell cycle and cell growth, which may explain

why many of the embryos arrest development prematurely and have a smaller blastocyst cell number (See Chapter 4). Secondly, if 8-cell embryos activated with Sr^{2+} were at a more advanced stage of development than embryos activated with cycloheximide, the maternal mRNA that exists in the embryos until degradation some time during the 8-cell stage may the cause the amount of gene expression in many genes to be higher. Choosing a single time point to study gene expression is not as accurate as using different time points to make direct conclusions about gene expression activity. In the future an investigation of gene expression after parallel morphological stages rather than specific times may provide better quality results.

6.3.4 Summary

The work described in this chapter provided information on gene activity during a snapshot moment of development during the 8-cell stage in parthenotes activated with cycloheximide and Sr^{2+}. The data from these results demonstrate that the methods used for artificial egg activation can have profound implications for the embryo with regards to specific gene expression. The results also imply that the occurrence of $[Ca^{2+}]i$ oscillations during egg activation may influence gene expression which is associated with biological processes such as apoptosis, cell differentiation and the cell cycle.

Chapter 7

General Conclusions

In this thesis I have presented the data from a number of studies that have investigated the occurrence of $[Ca^{2+}]i$ oscillations at egg activation and their impact on preimplantation development. A number of original findings have resulted from this work. I have shown that the human form of phospholipase C zeta (hPLCζ) cRNA can be used to activate aged human eggs that have previously failed to fertilise after ICSI or IVF and that this procedure permits development up to the blastocyst stage. I have shown that hPLCζ cRNA can be used to activate pig eggs, which as a consequence can develop up to the 8-cell stage. I have demonstrated that $[Ca^{2+}]i$ oscillations or a single $[Ca^{2+}]i$ increase at egg activation vastly improves the number of parthenogenetic embryos cleaving beyond the 4-cell stage compared to embryos derived from $[Ca^{2+}]i$ independent egg activation. This shows that the nature of the parthenogenetic stimulus has an affect on the cellular composition and degree of apoptosis in blastocysts and there are indications, although not conclusive proof, that the presence of $[Ca^{2+}]i$ oscillations at egg activation influences these events. I have also demonstrated that the initiation and degree of gene expression during the minor phase of Embryonic Genome Activation (EGA) is independent of the presence of $[Ca^{2+}]i$ oscillations at egg activation. Finally, I have revealed that $[Ca^{2+}]i$ oscillations at egg activation are likely to influence specific expression of genes during the embryonic 8-cell stage. Fig 7.1 is a diagrammatic representation of the novel findings I have presented in this thesis. These findings are of particular relevance to understanding the relationship between $[Ca^{2+}]i$ oscillations and preimplantation embryo development. This final chapter will discuss a number of important

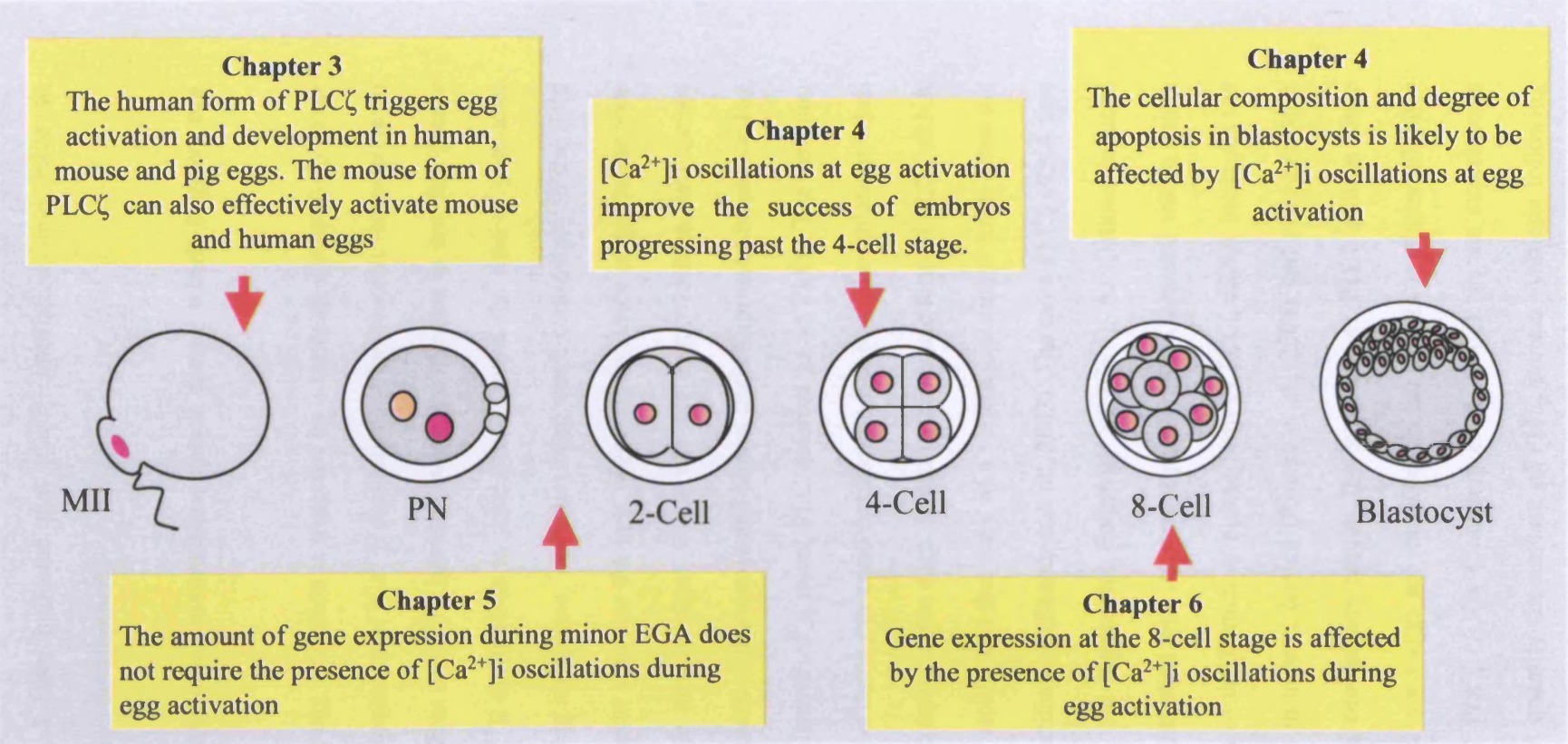

Figure 7.1 Overall conclusions about the affect of $[Ca^{2+}]i$ oscillations on preimplantation development. The human form of PLCζ (hPLCζ) can trigger $[Ca^{2+}]i$ oscillations and egg activation in pig, mouse and human eggs. There does not appear to be a requirement for the presence of $[Ca^{2+}]i$ oscillations at egg activation for the initiation and amount of global gene expression during the minor phase of Embryonic Genome Activation (EGA). Using different parthenogenetic activation stimuli to induce $[Ca^{2+}]i$ oscillations or a single $[Ca^{2+}]i$ increase, I demonstrated that $[Ca^{2+}]i$ increases at egg activation improves the developmental success of embryos beyond the 4-cell stage compared to embryos that are activated independently of $[Ca^{2+}]i$. Microarray analysis of gene expression in embryos activated by Sr^{2+} or Cycloheximide revealed that $[Ca^{2+}]i$ oscillations affect the expression of genes associated with processes such as apoptosis and the cell-cycle at the 8-cell stage. The results from TUNEL staining and differential staining also indicate that the presence of $[Ca^{2+}]i$ oscillations at egg activation affect the degree of apoptosis and cellular composition of blastocysts, respectively. Cycloheximide-activation caused blastocysts to have a significantly larger degree of apoptotic cells and a smaller total and Inner Cell Mass cell number.

developmental processes which I have indicated that $[Ca^{2+}]i$ oscillations may have an influence on during preimplantation development.

7.1.1 PLCζ appears to be a universal mammalian sperm factor which triggers egg activation.

During fertilisation in mammals, egg activation is triggered by a series of distinctively long-lasting $[Ca^{2+}]i$ oscillations. The frequency of $[Ca^{2+}]i$ oscillations at fertilisation varies between different species and can range from a $[Ca^{2+}]i$ increase every few minutes to one that occurs every hour. Sperm-induced $[Ca^{2+}]i$ oscillations in mice cease around the time of pronuclei formation when the egg is entering interphase. There has been much controversy in the field of fertilisation about how the sperm activates the egg. Mounting evidence supports the idea that the sperm induces a soluble proteinaceous factor into the egg, which in turn causes $[Ca^{2+}]i$ oscillations to occur. A search of the mouse and human testis Expressed Sequence Tag (EST) database revealed the existence of a novel PLC referred to as PLCζ. The defining characteristic of the sperm factor is that it can cause fertilisation-like $[Ca^{2+}]i$ oscillations when it is injected in the form of sperm extracts into eggs. Injecting the mouse form of PLCζ cRNA in mouse eggs triggered $[Ca^{2+}]i$ oscillations that were of a pattern indistinguishable from the $[Ca^{2+}]i$ oscillations induced by fertilisation (Saunders et al., 2002). The more PLCζ cRNA that was injected into mouse eggs, the higher the frequency of $[Ca^{2+}]i$ oscillations induced (Saunders et al., 2002). This is consistent with the work I presented in Chapter 3 which shows that increasing the concentration of the human or mouse form of PLCζ cRNA increases the frequency of $[Ca^{2+}]i$ oscillations in mouse, human (Rogers et al., 2004) and pig eggs. It is clear that PLCζ-induced $[Ca^{2+}]i$ oscillations require the synthesis of PLCζ protein since $[Ca^{2+}]i$ oscillations are prevented when eggs are incubated in the protein synthesis inhibitor cycloheximide after injection of PLCζ cRNA (Saunders et al., 2002). In the experiments presented in Chapter 3 I did not quantify the amount of PLCζ protein synthesis following

injection of PLCζ cRNA however other groups have done so by using PLCζ tagged with Venus fluorescent protein (Yoda et al., 2004) or luciferase (Nomikos et al., 2005) to show ~50 pg/egg PLCζ protein causes a series of $[Ca^{2+}]i$ oscillations. Recently a study has shown that reducing sperm PLCζ protein by transgenic RNA interference significantly perturbs the $[Ca^{2+}]i$ oscillations exhibited by eggs after insemination of these sperm (Knott et al., 2005). This data provided the first direct evidence that PLCζ works as the physiological sperm factor *in vivo*.

The discovery of PLCζ has prompted further functional studies on the PLCζ molecule (Kouchi et al., 2005; Nomikos et al., 2005) and investigations on how effective the PLCζ is at causing $[Ca^{2+}]i$ oscillations and egg activation in other species (Cox et al., 2002). Sperm extract has previously been documented to trigger $[Ca^{2+}]i$ oscillations across a broad range of species (Dong et al., 2000; Jones et al., 1998b; Knott et al., 2002; Wu et al., 1997) and support for PLCζ as the sperm factor is galvanised by the work presented in this thesis, showing that hPLCζ is effective at causing $[Ca^{2+}]i$ oscillations in pig and mice eggs and that mPLCζ can effectively cause $[Ca^{2+}]i$ oscillations in human eggs. There is evidence for the existence of the PLCζ gene in many species including humans, mice, rats, chimpanzee, pigs, dogs, cows, monkeys and chickens. This data indicates that different versions of mammalian PLCζ would cause fertilisation-like $[Ca^{2+}]i$ oscillations in all mammalian eggs. Recent reports have also demonstrated that chicken PLCζ cRNA can trigger $[Ca^{2+}]i$ oscillations when injected into mouse eggs (Coward et al., 2005) indicating that PLCζ may have a universal role in stimulating egg activation in vertebrates.

It has recently been shown that pig and bull sperm contain significantly more PLCζ than mouse sperm (Kurokawa et al., 2005) which suggests that pig eggs require a larger amount of PLCζ. My findings support this idea because a higher concentration of hPLCζ was required to induce $[Ca^{2+}]i$ oscillations in pig eggs than in mouse eggs. Studies on pig sperm

have shown that PLCζ is present in cytosolic sperm extracts as well as the pellets of extracts that contain the sperm heads. The 70kD full length version of PLCζ was found not to correlate with PLCζ's ability to cause $[Ca^{2+}]i$ oscillations in eggs. This suggests that a proteolytically cleaved version of PLCζ may exist in pigs (Kurokawa et al., 2005). I have demonstrated that differences in the potency of hPLCζ and mPLCζ with regard to causing $[Ca^{2+}]i$ release in eggs exist, since ~1000 times less hPLCζ than mPLCζ cRNA was required to induce similar-frequency $[Ca^{2+}]i$ oscillations in mouse eggs. Differences in the degree of solubility, amount and potency of PLCζ with regard to Ca^{2+}-releasing ability appear to occur in the sperm of different species. I have demonstrated that eggs from different species (human, mouse and pig eggs) also vary in their ability to exhibit PLCζ-induced $[Ca^{2+}]i$ oscillations and this may be due to the differing sensitivities of the different eggs to PLCζ since it has previously been shown that the hamster egg is much less sensitive to sperm extracts than the mouse egg (Parrington et al., 1996). The variation in size of different species' eggs will reflect differences in the efficiency of PLCζ at causing $[Ca^{2+}]i$ oscillations; the human egg for example is several times larger than that of a mouse egg and this may be the reason for the hPLCζ being more potent in its Ca^{2+}-releasing ability than mPLCζ. The fine-tuning of the effective dose of PLCζ during fertilisation thus appears to be species-specific and appropriate to match the size and sensitivity of the egg so that the sperm can induce robust, long-lasting $[Ca^{2+}]i$ oscillations.

The experiments I have presented in chapter 3 indicated that pig eggs were more insensitive to PLCζ than either the mouse or human egg and mPLCζ was in fact completely ineffective at triggering $[Ca^{2+}]i$ oscillations in pig eggs. The $[Ca^{2+}]i$ oscillations in pig eggs that were triggered by hPLCζ were short-lived and successively reduced in amplitude after each $[Ca^{2+}]i$ transient. The inability of hPLCζ to induce long-lasting, higher frequency $[Ca^{2+}]i$ oscillations in pig eggs could be due to the developmental failure of Ca^{2+} release machinery,

hindered by the process of *in vitro* maturation (IVM). Despite advances of *in vitro* culture techniques, IVM has been shown to reduce the quality of the oocyte drastically. A previous investigation studying the developmental competency of IVM pig oocytes after subzonal sperm injection concluded that ooplasmic incompetence was the major cause of limited developmental competence (Nagashima et al., 1996). In order to best study the affects of PLCζ on pig embryo development, IVM techniques will need to be drastically improved to ensure successful development of Ca^{2+} stores and release mechanisms. Measuring the effectiveness of pig PLCζ in inducing $[Ca^{2+}]i$ transients in mouse and human eggs would also help to elucidate what level of potency is required to effectively induce $[Ca^{2+}]i$ oscillations in pig eggs and this would also reflect the relative sensitivity of the pig egg compared to the human and mouse egg.

7.2 $[Ca^{2+}]i$ oscillations and preimplantation embryo development

Pre and post-implantation studies have shown that the pattern of the activating $[Ca^{2+}]i$ signal has an impact on the developmental potential of mouse and rabbit embryos (Ozil, 1990; Ozil and Huneau, 2001; Bos-Mikich et al., 1997; Vitullo and Ozil, 1992). Increasing the frequency of $[Ca^{2+}]i$ oscillations has for example been shown to increase the number of embryos successfully undergoing compaction (Ozil, 1990) and $[Ca^{2+}]i$ transients can be manipulated in rabbit eggs to optimize postimplantation embryo development such as the extent of somite and heart formation (Ozil and Huneau, 2001). The pattern of $[Ca^{2+}]i$ oscillations has been reported to change the cellular composition of developing blastocysts (Bos-Mikich et al., 1997) with an increasing duration from 2 to 4 to 6 hours causing a successive increase in the ICM cell number in blastocysts. A recent study was undertaken to investigate whether or not ICSI-initiated fertilisation causes alterations in $[Ca^{2+}]i$ responses and affects pre-implantation development compared to IVF-initiated fertilisation. ICSI-induced $[Ca^{2+}]i$ oscillations

occurred more infrequently and ceased significantly earlier compared with IVF-induced $[Ca^{2+}]i$ oscillations and were also associated with a reduced developmental capacity to reach the blastocyst stage and reduced blastocyst cell numbers (Kurokawa et al., 2005). In the work presented in this thesis I have shown that the short-lived $[Ca^{2+}]i$ oscillations induced by hPLCζ in pig eggs leads to the poor development of pig embryos with only 3% progressing to the 8-cell stage. This is in contrast to the much more successful development of human and mouse embryos that exhibited long-lasting PLCζ-induced $[Ca^{2+}]i$ oscillations. This data indicates that the duration of $[Ca^{2+}]i$ oscillations at egg activation correlates with the developmental success of the embryo and supports the data of Kurokawa et al, 2005 (Kurokawa et al., 2005). A transgenic RNAi approach was used to reduce production of the sperm-specific PLCζ protein during spermatogenesis showed that sperm extracts from transgenic male mice contained approximately 60% of the amount of PLCζ compared to sperm extract from non-transgenic littermates. More importantly the pattern of $[Ca^{2+}]i$ oscillations was different in eggs fertilised with sperm from transgenic and non-transgenic mice, for example eggs fertilised with sperm from transgenic mice oscillated for substantially shorter periods of time than fertilised control eggs. The reduced duration of $[Ca^{2+}]i$ oscillations induced by sperm from transgenic mice also caused a significantly lower incidence of egg activation as monitored by the incidence of pronuclei formation compared to the longer duration $[Ca^{2+}]I$ oscillations induced by sperm from non-transgenic mice and as a consequence of this, fewer 1-cell embryos cleaved and formed blastocysts. PLCζ also plays an important role in shaping the amplitude and duration of the $[Ca^{2+}]i$ transients at fertilisation. Genotypic analysis of the offspring of the transgenic founder revealed that no transgenic offspring were born, suggesting that the eggs fertilised by transgenic sperm (which fail to exhibit normal $[Ca^{2+}]i$ oscillations) do not develop to term. This is supportive of other

data which has been interpreted as indicating that the oscillatory behaviour of $[Ca^{2+}]i$ has a long-term role in development (Ozil and Huneau, 2001).

Whilst parthenogenetic stimuli such as Sr^{2+} trigger repetitive $[Ca^{2+}]i$ oscillations in eggs they are distinguishable from those at fertilisation and probably lack the ability to encode specific information that may influence gene expression or the activation of certain kinases that play a role in embryo development. More studies are required to elucidate the real long-term affects of the fertilisation-like $[Ca^{2+}]i$ signal compared to the $[Ca^{2+}]i$ signal induced by other parthenogenetic agents.

Human eggs that have previously failed to activate during ART due to a faulty sperm factor are often activated with chemicals (such as ionomycin) that induce a single $[Ca^{2+}]i$ transient. Previous studies have shown that parthenogenetic activation of freshly ovulated human eggs by inducing a single $[Ca^{2+}]i$ transient can result in development to the blastocyst stage (Cibelli et al., 2001; Lin et al., 2003). Parthenogenetic activation of aged human eggs using a protein synthesis inhibitor such as cycloheximide or puromycin in conjunction with stimuli that cause a single $[Ca^{2+}]i$ transient can stimulate early cleavage events but has never been reported to cause development to the blastocyst stage (Winston et al., 1991; Nakagawa et al., 2001). In this thesis I showed for the first time that aged human eggs can be parthenogenetically activated and induced to develop to the blastocyst stage following PLCζ cRNA injection (Rogers et al., 2004). It is possible that the repetitive nature of the $[Ca^{2+}]i$ signal which was induced by PLCζ and which is exhibited normally during human egg fertilization may have been causative of higher success of parthenogenetic development in the embryos. More extensive studies are required to elucidate any influence that $[Ca^{2+}]i$ patterns (oscillations versus single transient) at egg activation can have on the developmental potential of human embryos. The single $[Ca^{2+}]i$ increase that can be used to induce egg activation may also have consequences for sheep, pig or cattle embryo development since these stimuli are

used frequently on these animals during the Nuclear Transfer (NT) procedure. Whilst the activation of cattle eggs using single $[Ca^{2+}]i$ wave stimuli has been shown to work with moderate efficiency if used in conjunction with a protein synthesis inhibitor, the efficiency of NT technology is still very low and the long term consequences of this activation method are unclear. Artificial stimuli that cause single $[Ca^{2+}]i$ transients will need to be studied further to establish what long-term affects it may be triggering

Details of the downstream targets of $[Ca^{2+}]i$ oscillations are unclear, however mounting evidence suggests that $[Ca^{2+}]i$ oscillations activate a number of protein kinases that are relevant to embryo development and they are Calmodulin-dependent Kinase II (CAMKII) and Protein Kinase C (PKC). The process of egg activation is dependent on $[Ca^{2+}]i$ oscillations which act to destroy maturation promoting factor (MPF) and the cohesion that holds the two sister chromatids together (Madgwick et al., 2004) and this is achieved by the destruction of cyclin B and securin respectively. $[Ca^{2+}]i$ oscillations activate CAMKII which stimulates ubiquitin-dependent degradation of Cyclin B (Lorca et al., 1993) by targeting it for destruction by the proteasome, allowing the egg to be released from meiotic arrest. CAMKII is present in all mammalian eggs studied to date and its activity increases immediately after each $[Ca^{2+}]i$ rise associated with fertilization or parthenogenetic activation (Winston and Maro, 1995; Tatone et al., 2002). There is a tight correlation between the $[Ca^{2+}]i$ increase and CAMKII activity with the amplitude of the $[Ca^{2+}]i$ spike determining the relative activity of CAMKII (Markoulaki et al., 2004). CAMKII which has been reported to be the primary downstream target of $[Ca^{2+}]i$ signalling (Madgwick et al., 2005)and has been shown to regulate the activity of more than 20 enzymes such as calcineurin and nitric oxide synthase (Means et al., 1991; Lu and Means, 1993). It is through the action of these enzymes that CAMKII is thought to control a number of critical cellular processes in the early embryo such as cell cycle progression, microtubule formation, cell motility and metabolism (Chafouleas et

al., 1982; Johnson et al., 1998). CAMKII co-localizes with calmodulin (CAM) and MAP kinase following egg activation (Hatch and Capco, 2001). CAM has been found on the mitotic apparatus of yeast cells and mutations in this protein have been reported to cause spindle body defects as well as abnormal chromosome segregation (Davis, 1992). CAM has also been documented to intervene with the cell cycle during the G1 to S boundary, G2 to mitosis phase and the anaphase-metaphase transition (Rasmussen and Means, 1989). Cycloheximide-induced egg activation bypasses the need for any $[Ca^{2+}]i$ rises because it causes the direct degradation of Cyclin B, this however prevents the activation of CAMKII and the regulation of calmodulin-dependent enzymes and may prove detrimental to processes required for cell cycle progression and microtubule associated events. This idea is consistent with my microarray and experimental data that reveal high incidence of premature developmental arrest and high differential gene expression of cell-cycle and microtubule related genes in cycloheximide-activated embryos compared to Sr^{2+}-activated embryos. In recent work investigating the role of CAMKII during meiotic resumption, a constitutively active cRNA construct of CAMKII was shown to induce the same effects on the resumption of meiosis as sperm, since pronucleus formation and 2nd polar body extrusion both occurred, along with the destruction of cyclin B and securin (Madgwick et al., 2005). The use of the spindle poison nocodazole was also shown to block meiotic resumption however the Ca^{2+} chelator BAPTA did not, showing that CAMKII lies downstream of sperm induced $[Ca^{2+}]i$ oscillations but upstream of the spindle check point (Madgwick et al., 2005). In order to study the affects of $[Ca^{2+}]i$ oscillations on embryo development in the future, it would be an idea to inject a constitutively active form of CAMKII which bypasses the need for $[Ca^{2+}]i$ oscillations but is not associated with the detrimental affects of cycloheximide.

Embryonic development requires signals that are transduced through cell surface receptors which upon binding to their ligand initiate signal transduction cascades which alter

the phosphorylation of intracellular components via kinases and phosphatases. The PKC's are a major signal transducer made up of eleven different kinases, many of which are $[Ca^{2+}]i$ and DAG dependent. Some PKC isoforms may in fact serve to decode $[Ca^{2+}]i$ oscillations since stimulation of repetitive $[Ca^{2+}]i$ transients has been shown to cause a parallel repetitive translocation of GFP-tagged PKC gamma to the plasma membrane (Oancea and Meyer, 1998). Recent work using a constitutively active cRNA construct of PKC has revealed that PKC is not a trigger for meiotic resumption (as CAMKII is), but rather has a role in sustaining long-lasting $[Ca^{2+}]i$ oscillations at fertilisation by facilitating store-operated $[Ca^{2+}]i$ entry. In a different study it was also concluded that PKC promotes store refilling and it was shown that PKC overexpression leads to an increased frequency of $[Ca^{2+}]i$ oscillations (Halet et al., 2004).

PKC's may also have a role in later preimplantation development since it has been shown to be involved in mouse embryo compaction since activation of PKC by phorbol ester causes premature compaction of 4-cell embryos within minutes of addition of the ester (Winkel et al., 1990). PKC activation also causes a rapid shift of antibodies to E-cadherin which coincides with the timing of compaction (Winkel et al., 1990). PKC has also been linked to blastocoel formation. Blastocoel formation is dependent on Na^{2+}/K^{+} ATPase activities which help to drive the osmotic transport of water across the epithelium. Na^{2+}/K^{+} activities are believed to be mediated by $[Ca^{2+}]i$ and Ca^{2+}-modulating activities, all of which interact with PKC pathways. While these data suggest that $[Ca^{2+}]i$ rises are responsible for the activation of PKC's, it is unclear if it is these $[Ca^{2+}]i$ rises during activation that function to facilitate blastocoel formation and compaction. The full extent of the role of PKC during preimplantation development has yet to be determined.

7.3 Embryo developmental potential

Developmental arrest is a phenomenon observed in embryos in almost all mammalian species. Suboptimal conditions have often been suggested as the cause of embryonic arrest however one study utilised mathematical modelling and data from experiments to conclude that while environmental factors can influence developmental progression to a limited degree, there will always be a group of embryos that arrest and a group that survives when cultured in suboptimal conditions (Hardy et al., 2001). The mechanisms which cause developmental arrest are unclear however the embryonic stages at which transcription-dependent proteins are first made coincide with the highest incidence of cleavage arrest in most species, suggesting that a delay or failure in the onset of transcription is causative of developmental arrest. A wide range of cellular defects have been observed during cleavage arrest, such as the redistribution of mitochondria (Acton et al., 2004) and abnormal localisation of proteins such as those from the Bcl-2 family.

The developmental progression of fertilised mammalian oocytes is dependent to the successful implementation of specific genetic and developmental programmes. It is not surprising therefore that factors which predispose an embryo to develop normally or to arrest have been suggested to be largely determined at or before the 1-cell zygote stage (Hardy et al., 2001). Chromosomal abnormalities (Munne et al., 1995) and inadequate oocyte maturation (Moor et al., 1998) are some of the commonly suggested causative factors for early embryonic abnormalities (Hardy et al., 2001). The results from studies presented in this thesis reveal that the presence of $[Ca^{2+}]i$ oscillations or a single $[Ca^{2+}]i$ transient during egg activation improve the developmental potential of resulting embryos progressing past the 4-cell stage (See Chapter 4). A recent study has shown that the implantation success of blastocysts are significantly better after oscillatory $[Ca^{2+}]i$ signals rather than a single sustained $[Ca^{2+}]i$ transient during egg activation (Ozil et al., 2005). Whilst I have shown that the presence of $[Ca^{2+}]i$ oscillations at egg activation does not appear to be a requirement for

the initiation of Embryonic Genome Activation (Chapter 5) other processes such as chromatin remodelling may be affected by the presence or absence of oscillatory $[Ca^{2+}]i$ signals

7.4 Apoptosis and cell allocation in mammalian blastocysts

The degree of fragmentation in blastocysts has been used as a good indicator of embryo quality. The presence of minor fragmentation (<10%) has been shown to commonly occur in healthy human embryos which implant and develop to term with a similar success as embryos exhibiting no signs of fragmentation, indicating that the occurrence of fragmentation is a normal process during development. A higher degree of fragmentation (>10-15%) has however has been reported to significantly reduce implantation and pregnancy rates in a number of different studies (Giorgetti et al., 1995; Ziebe et al., 1997). Many factors other than fragmentation have been shown to significantly decrease implantation rates and they include the age of the mother (Giorgetti et al., 1995), embryo growth rate (Cummins et al., 1986), and the number of cells of the Inner Cell Mass (ICM) of blastocysts (Richter et al., 2001). I have demonstrated that the method of parthenogenetic mouse egg activation (Sr^{2+} or cycloheximide-induced egg activation) significantly affects the degree of apoptosis in blastocysts since Sr^{2+} and cycloheximide-induced activation resulted in blastocysts with a 5% and 14% degree of apoptosis respectively. As Sr^{2+} triggers $[Ca^{2+}]i$ oscillations and cycloheximide does not induce any $[Ca^{2+}]i$ changes, it can be ascertained that $[Ca^{2+}]i$ signalling may be responsible, at least in part, for determining the level of fragmentation in blastocysts. Whilst cycloheximide-activated blastocysts did exhibit a significantly larger degree of apoptosis, these blastocysts were still only characterised by an intermediate level of apoptosis (14%). A 10-15% degree of apoptosis has been reported as the threshold of whether apoptosis will reduce the implantation potential of the human embryo or not, so it is unclear if

cycloheximide-derived mouse blastocysts would have a reduced potential to implant due to apoptosis, compared to Sr^{2+}-activated mouse blastocysts.

Parthenogenetic activation of eggs using cycloheximide and Sr^{2+} also had a differential affect on the number of cells forming the ICM and TE in resulting blastocysts. Blastocysts derived from Sr^{2+} activation had significantly larger cell numbers in the ICM but not the TE compared to those activated by cycloheximide. The larger ICM cell number may be due to the occurrence of $[Ca^{2+}]i$ oscillations induced by Sr^{2+} activation. Previous findings have shown that increasing the length of time Sr^{2+}-induced $[Ca^{2+}]i$ oscillations persisted from 2 to 4 to 6 hours successively increased the ICM cell number in blastocysts (Bos-Mikich et al., 1997). The same study did not investigate the cellular composition of blastocysts after egg activation by $[Ca^{2+}]i$ dependent means. Larger ICM cell numbers have been reported to increase the success of implantation and pregnancy potential.

As the ICM but not the TE cell numbers were significantly different between cycloheximide and Sr^{2+}-activated embryos, apoptosis may be occurring predominantly in the ICM group of embryos. This could be quantitatively determined in the future by using a dual-purpose differential staining and apoptosis assay as has previously been described for bovine blastocysts (Fouladi-Nashta et al., 2005). In a number of studies the incidence of apoptosis has been shown to be more prevalent in the ICM when compared to the TE in *in vivo* and *in vitro*-derived mouse blastocysts (Copp, 1978; Brison and Schultz, 1997; Fouladi-Nashta et al., 2005). Minimal and moderate levels of fragmentation in human blastocysts have in contrast been shown to cause a reduction in cell numbers that is largely confined to the TE, whilst a steady number of ICM cells are maintained and only drop in blastocysts exhibiting gross (>25%) fragmentation (Hardy et al., 2003). A homeostatic mechanism in human embryos thus appears to control the numbers of ICM cells up to moderate fragmentation (<25%) levels. Apoptosis has a clear role in regulating ICM cell number in the human blastocyst since

blastocysts with excellent morphology and high cell numbers have higher levels of apoptosis in the ICM than blastocysts of poor morphology with fewer cell numbers (Hardy et al., 2003). It is unclear if this protective mechanism to ensure sufficient ICM cell numbers is specific to some species and not others since it has not been observed in mouse blastocysts. The early mouse embryo has been shown to be equipped with a self-regulating mechanism to stringently maintain the ICM to TE cell ratio and this has been shown to be mediated by a combination of cell interactions, mitotic spindle orientation and changes in cell morphology (Fleming, 1987). The allocation of cell numbers during development is clearly an important factor in development and since the stem cell pool for foetal and extra-embryonic lineages is limited, a depletion of either TE or ICM could influence the pattern of later development.

7.5 $[Ca^{2+}]i$ oscillations and gene expression

Previous studies on somatic cells have demonstrated that changes in $[Ca^{2+}]i$ have an effect on the levels of gene expression in a cell. One study using caged $InsP_3$ to induce $[Ca^{2+}]i$ changes concluded that repetitive $[Ca^{2+}]i$ transients at 1 minute intervals causes significantly more gene expression than transients at intervals of 0.5 or more than 2 minutes (Li et al., 1998). The same study also revealed that a single $[Ca^{2+}]i$ transient causes less gene expression than repetitive transients (Li et al., 1998). A $[Ca^{2+}]i$ clamp technique has previously been used to investigate the effect of the frequency of $[Ca^{2+}]i$ transients on gene expression and it was concluded that repetitive $[Ca^{2+}]i$ oscillations were much more effective at driving gene expression in the transcription factors that were studied (Dolmetsch et al., 1998). High frequency oscillations were also shown to stimulate more transcription factors and increase the specificity of gene expression compared to infrequent oscillations (Dolmetsch et al., 1998). The complete absence of increases in $[Ca^{2+}]i$ during cycloheximide-induced activation

is therefore likely to prevent the expression of genes that may play an important role in later embryo development.

In the future a comparison of gene expression following the use of other artificial activation stimuli would be an interesting study to carry out because of its implications for nuclear transfer and assisted reproductive technologies (ART). Analysis of gene expression following egg activation induced by PLCζ for example, would be valuable for a number of reasons. PLCζ stimulates $[Ca^{2+}]i$ oscillations that are of a pattern that is indistinguishable from those at fertilization (Saunders et al., 2002) and is characterised by features such as the first $[Ca^{2+}]i$ transient being much longer in duration than the proceeding transients and by the presence of smaller sinusoidal $[Ca^{2+}]i$ spikes on top of it. PLCζ-induced activation, like fertilization also causes mitotic Ca^{2+} transients that occur shortly after pronuclear envelope breakdown is initiated (Larman et al., 2004; Marangos et al., 2003) and the cell-cycle dependent manner in which these mitotic $[Ca^{2+}]i$ transients occur could be important in regulating the time-dependent manner in which specific genes are expressed. PLCζ, which provides a natural stimulus to activate eggs, would be a good control for future gene expression experiments conducted on parthenogenetic embryos.

Reference List

1. Acton,B.M., Juriscova,A., Jurisica,I., and Casper,R.F. (2004). Alterations in mitochondrial membrane potential during preimplantation stages of mouse and human embryo development. Mol Hum Reprod *10*, 32.

2. Aizawa,H., Kawahara,H., Tanaka,K., and Yokosawa,H. (1996). Activation of the proteasome during Xenopus egg activation implies a link between proteasome activation and intracellular calcium release. Biochem Biophys Res Commun *218*, 224-228.

3. Alberio,R., Brero,A., Motlik,j., Cremer,T., Wolf,E., and Zakhartchenko,V. (2001a). Remodeling of donor nuclei, DNA-synthesis, and ploidy of bovine cumulus cell nuclear transfer embryos: effect of activation protocol. Mol. Reprod Dev *59*, 371-379.

4. Alberio,R., Zakhartchenko,V., Motlik,j., and Wolf,E. (2001b). Mammalian oocyte activation: lessons from the sperm and implications for nuclear transfer. Int J Dev Biol *45*, 797-809.

5. Alikani,M., Calderon,G., Tomkin,G., Garrisi,J., Kokot,M., and Cohen,J. (2000). Cleavage anomalies in early human embryos and survival after prolonged culture in-vitro. Hum Reprod *15*, 2634-2643.

6. Alikani,M., Cohen,J., Tomkin,G., Garrisi,G.J., Mack,C., and Scott,R.T. (1999). Human embryo fragmentation in vitro and its implications for pregnancy and implantation. Fertil Steril *71*, 836-842.

7. Aoki,F., Worrad,D.M., and Schultz,R.M. (1997). Regulation of transcriptional activity during the first and second cell cycles in the preimplantation mouse embryo. Dev Biol *181*, 296-307.

8. Ashburner,M., Ball,C.A., Blake,J.A., Botstein,D., Butler,H., Cherry,J.M., Davis,A.P., Dolinski,K., Dwight,S.S., Eppig,J.T., Harris,M.A., Hill,D.P., Issel-Tarver,L., Kasarskis,A., Lewis,S., Matese,J.C., Richardson,J.E., Ringwald,M., Rubin.G.M, and Sherlock,G. (2000). Gene ontology:tool for the unification of biology. The Gene Ontology Consortium. Nat Genet *25*, 25-29.

9. Atienza,J.M., Roth,R.B., Rosette,C., Smylie,K.J., Kammerer,S., Rehbock,J., Ekblom,J., and Denissenko,M.F. (2005). Suppression of RAD21 gene expression decreases cell growth and enhances cytotoxicity of etoposide and bleomycin in human breast cancer cells. Mol Cancer Ther *4*, 361-368.

10. Austin,C.R. and Braden,A.W.H. (1953). An investigation of polyspermy in rat and rabbit. Aust J Biol Sci *6*, 674-692.

11. Ayabe,T., Kopf,G.S., and Schultz,R.M. (1995). Regulation of mouse egg activation: presence of ryanodine receptors and effects of microinjected ryanodine and cyclic ADP ribose on uninseminated and inseminated eggs. Development *121*, 2233-2244.

12. Bachvarova,B., Cohen,E.M., De Leon,V., Tokunaga,K., Sakiyama,S., and Paynton,B.V. (1989). Amounts and modulation of actin mRNAs in mouse oocytes and embryos. Development *106(3)*, 561-565.

13. Bachvarova,R., De Leon,V., Johnson,A., Kaplan,G., and Paynton,B.V. (1985). Changes in total RNA, polyadenylated RNA, and actin mRNA during meiotic maturation of mouse oocytes. Dev Biol *108*, 325-331.

14. Balakier,H. and Casper,R.F. (1993). Experimentally induced parthenogenetic activation of human oocytes. Hum Reprod *8*, 740-743.

15. Bavister,B.D. (1995). Culture of preimplantation embryos: facts and artifacts. Hum Reprod Update *1*, 91-148.

16. Bement,W.M. and Capco,D.G. (1990). Protein kinase C acts downstream of calcium at entry into the first mitotic interphase of Xenopus laevis. Cell Regul *1*, 315-326.

17. Berridge,M.J. (1993). Inositol trisphosphate and calcium signalling. Nature *361*, 315-325.

18. Berridge,M.J. and Irvine,R.F. (1989). Inositol phosphates and cell signalling. Nature *341*, 205.

19. Betts,D.H. and King,W.A. (2001). Genetic regulation of embryo death and senescence. Theriogenology *55*, 171-191.

20. Bhatt,R.R. and Ferrell,J.E.j. (1999). The protein kinase p90 rsk as an essential mediator of cytostatic factor activity. Science *286*, 1362-1365.

21. Biggers,J.D. (1998). Reflections on the culture of the preimplantation embryo. Int J Dev Biol *42*, 879-884.

22. Bleil,J.D. and Wassarman,P.M. (1980). Mammalian sperm-egg interaction: identification of a glycoprotein in mouse egg zonae pellucidae possessing receptor activity for sperm. Cell *20*, 882.

23. Blomberg le,A. and Zuelke,K.A. (2004). Serial analysis of gene expression (SAGE) during porcine embryo development. Reprod Fertil Dev *16*, 87-92.

24. Bolton,V.N., Oades,P.J., and Johnson,M.H. (1984). The relationship between cleavage, DNA replication, and gene expression in the mouse 2-cell embryo. J Embryol Exp Morphol *79*, 139-163.

25. Bos-Mikich,A., Swann,K., and Whittingham,D.G. (1995). Calcium oscillations and protein synthesis inhibition synergistically activate mouse oocytes. Mol Reprod Dev *41*, 84-90.

26. Bos-Mikich,A., Whittingham,D.G., and Jones,K.T. (1997). Meiotic and mitotic Ca^{2+} oscillations affect cell composition in resulting blastocysts. Dev. Biol *182*, 172-179.

27. Braude,P., Bolton,V., and Moore,S. (1988). Human gene expression first occurs between the four- and eight-cell stages of preimplantation development. Nature *332*, 459-461.

13. Bachvarova,R., De Leon,V., Johnson,A., Kaplan,G., and Paynton,B.V. (1985). Changes in total RNA, polyadenylated RNA, and actin mRNA during meiotic maturation of mouse oocytes. Dev Biol *108*, 325-331.

14. Balakier,H. and Casper,R.F. (1993). Experimentally induced parthenogenetic activation of human oocytes. Hum Reprod *8*, 740-743.

15. Bavister,B.D. (1995). Culture of preimplantation embryos: facts and artifacts. Hum Reprod Update *1*, 91-148.

16. Bement,W.M. and Capco,D.G. (1990). Protein kinase C acts downstream of calcium at entry into the first mitotic interphase of Xenopus laevis. Cell Regul *1*, 315-326.

17. Berridge,M.J. (1993). Inositol trisphosphate and calcium signalling. Nature *361*, 315-325.

18. Berridge,M.J. and Irvine,R.F. (1989). Inositol phosphates and cell signalling. Nature *341*, 205.

19. Betts,D.H. and King,W.A. (2001). Genetic regulation of embryo death and senescence. Theriogenology *55*, 171-191.

20. Bhatt,R.R. and Ferrell,J.E.j. (1999). The protein kinase p90 rsk as an essential mediator of cytostatic factor activity. Science *286*, 1362-1365.

21. Biggers,J.D. (1998). Reflections on the culture of the preimplantation embryo. Int J Dev Biol *42*, 879-884.

22. Bleil,J.D. and Wassarman,P.M. (1980). Mammalian sperm-egg interaction: identification of a glycoprotein in mouse egg zonae pellucidae possessing receptor activity for sperm. Cell *20*, 882.

23. Blomberg le,A. and Zuelke,K.A. (2004). Serial analysis of gene expression (SAGE) during porcine embryo development. Reprod Fertil Dev *16*, 87-92.

24. Bolton,V.N., Oades,P.J., and Johnson,M.H. (1984). The relationship between cleavage, DNA replication, and gene expression in the mouse 2-cell embryo. J Embryol Exp Morphol *79*, 139-163.

25. Bos-Mikich,A., Swann,K., and Whittingham,D.G. (1995). Calcium oscillations and protein synthesis inhibition synergistically activate mouse oocytes. Mol Reprod Dev *41*, 84-90.

26. Bos-Mikich,A., Whittingham,D.G., and Jones,K.T. (1997). Meiotic and mitotic Ca^{2+} oscillations affect cell composition in resulting blastocysts. Dev. Biol *182*, 172-179.

27. Braude,P., Bolton,V., and Moore,S. (1988). Human gene expression first occurs between the four- and eight-cell stages of preimplantation development. Nature *332*, 459-461.

28. Brind,S., Swann,K., and Carroll,J. (2000). Inositol 1,4,5-trisphosphate receptors are downregulated in mouse oocytes in response to sperm or adenophostin A but not to increases in intracellular Ca^{2+} or egg activation. Dev. Biol. *223*, 251-265.

29. Brison,D.R. and Schultz,R.M. (1997). Apoptosis during mouse blastocyst formation: evidence for a role for survival factors including transforming growth factor alpha. Biol Reprod *56*, 1088-1096.

30. Camous,S., Kopecny,V., and Flechon,J.E. (1986). Autoradiographic detection of the earliest stage of [3H]-uridine incorporation into the cow embryo. Biol Cell *58*, 195-200.

31. Carre,D. and Sardet,C. (1984). Fertilization and early development in Beroe ovata. Dev Biol *105*, 188-195.

32. Carroll,J., Jones,K.T., and Whittingham,D.G. (1996). Ca^{2+} release and the development of Ca^{2+} release mechanisms during oocyte maturation: a prelude to fertilization. Rev Reprod *1*, 137-143.

33. Carroll,J., Swann,K., Whittingham,D., and Whitaker,M. (1994). Spatiotemporal dynamics of intracellular $[Ca^{2+}]i$ oscillations during the growth and meiotic maturation of mouse oocytes. Development *120*, 3507-3517.

34. Carter,M.G., Hamatani,T., Sharov,A.A., Carmack,C.E., Quian,Y., Aiba,K., Ko,N.T., Dudekula,D.B., Brzoska,P.M., Hwang,S.S., and Ko,M.S. (2003). In situ-synthesized novel microarray optimized for mouse stem cell and early developmental expression profiling. Genome Res *13*, 1011-1021.

35. Chafouleas,J.G., Bolton,W.E., Hidaka,H., Boyd,A.E.3., and Means,A.R. (1982). Calmodulin and the cell cycle: involvement in regulation of cell-cycle progression. Cell *28*, 41-50.

36. Chatot,C.L., Ziomek,C.A., Bavister,B.D., Lewis,J.L., and Torres,I. (1989). An improved culture medium supports development of random-bred 1-cell mouse embryos in vitro. J Reprod Fertil *86*, 679-688.

37. Cheek,T.R., McGuinness,O.M., Vincent,C., Moreton,R.B., Berridge,M.J., and Johnson,M.H. (1993). Fertilisation and thimerosal stimulate similar calcium spiking patterns in mouse oocytes but by separate mechanisms. Development *119*, 179-189.

38. Cheung,A., Swann,K., and Carroll,J. (2000). The ability to generate normal Ca^{2+} transients in response to spermatozoa develops during the final stages of oocyte growth and maturation. Hum Reprod *15*, 1389-1395.

39. Chiba,K., Kado,R.T., and Jaffe,J.A. (1990). Development of calcium release mechanisms during starfish oocyte maturation. Dev Biol *140*, 300-306.

40. Christians,E., Campion,E., Thompson,E.M., and Renard,J.P. (1995). Expression of the HSP 70.1 gene, a landmark of early zygotic activity in the mouse embryo, is restricted to the first burst of transcription. Development *121*, 113-122.

41. Ciapa,B., Pesando,D., Wilding,M., and Whitaker,M. (1994). Cell-cycle calcium transients driven by cyclic changes in inositol trisphosphate levels. Nature *368*, 875-878.

42. Ciapa,B. and Whitaker,M. (1986). Two phases of inositol polyphosphate and diacylglycerol production at fertilisation. FEBS Lett *195*, 347-351.

43. Cibelli,J.B., Kiessling,A.A., Cunniff,K., Richards,C., Lanza,R.P., and West,M.D. (2001). Somatic cell nuclear transfer in humans: pronuclear and early embryonic development. e-biomed: the journal of regenerative medicine *2*, 25-31.

44. Cibelli,J.B., Stice,S.L., Golueke,P.J., Kane,J.J., Blackwell,C., Ponce de Leon,F.A., and Robl,J.M. (1998). Cloned transgenic calves produced from nonquiescent fetal fibroblasts. Science *280*, 1256-1258.

45. Collas,P., Fissore,R., Robl,J.M., Sullivan,E.J., and Barnes,F.L. (1993). Electrically induced calcium elevation, activation, and parthenogenetic development of bovine oocytes. Mol Reprod Dev *34*, 212-223.

46. Copp,A.J. (1978). Interaction between inner cell mass and trophectoderm of the mouse blastocyst. I. A study of cellular proliferation. J Embryol Exp Morphol *48*, 109-125.

47. Coward,K., Campos-Mendoza,A., Larman,M.G., Hibbitt,O., McAndrew,B., Bromage,N., and Parrington,J. (2003). Teleost fish spermatozoa contain a cytosolic protein factor that induces calcium release in sea urchin egg homogenates and triggers calcium oscillations when injected into mouse oocytes. Biochem Biophys Res Commun *305*, 299-304.

48. Coward,K., Ponting,C.P., Chang,H.Y., Hibbit,O., Savolainen,P., Jones,K.T., and Parrington,J. (2005). Phospholipase C{zeta}, the trigger of egg activation in mammals, is present in a non-mammalian species. Reproduction *130*, 157-163.

49. Cox,L.J., Larman,M.G., Saunders,C.M., Hashimoto,K., Swann,K., and Lai,F.A. (2002). Sperm phospholipase Czeta from humans and cynomolgus monkeys triggers Ca^{2+} oscillations, activation and development of mouse oocytes. Reproduction *124*, 611-623.

50. Crosby,I.M., Gandolfe,F., and Moor,R.M. (1988). Control of protein synthesis during early cleavage of sheep embryos. J Reprod Fertil *82(2)*, 769-775.

51. Cummins,J.M., Breen,T.M., Harrison,K.L., Shaw,J.M., Wilson,L.M., and Hennessey,J.F. (1986). A formula for scoring human embryo growth rates in in vitro fertilization: its value in predicting pregnancy and in comparison with visual estimates of embryo quality. J In Vitro Fert Embryo Transf *3*, 284-295.

52. Cuthbertson,K.S. and Cobbold,P.H. (1985). Phorbol ester and sperm activate mouse oocytes by inducing sustained oscillations in cell Ca^{2+}. Nature *316*, 541-542.

53. Dale,B., DeFelice,L.J., and Ehrenstein,G. (1985). Injection of a soluble sperm fraction into sea-urchin eggs triggers the cortical reaction. Experientia. 1985 Aug 15;41(8):1068-70. Experientia *41*, 1068-1070.

54. Davis,T.N. (1992). A temperature-sensitive calmodulin mutant loses viability during mitosis. J Cell Biol *118*, 607-617.

55. Davis,W.J., De Sousa,P.A., and Schultz,R.M. (1996). Transient expression of translation initiation factor eIF-4C during the 2-cell stage of the preimplantation mouse embryo:

identification by mRNA differential display and the role of DNA replication in zygotic gene activation. Dev Biol *174*, 190-201.

56. De Koninck,P. and Schulman,H. (1998). Sensitivity of CaM kinase II to the frequency of Ca2+ oscillations. Science *279*, 227-230.

57. De La Fuente,R. and King,R.W. (1997). Use of a chemically defined system for the direct comparison of inner cell mass and trophectoderm distribution in murine, porcine and bovine embryos. Zygote *5*, 309-320.

58. De La Fuente,R. and King,W.A. (1998). Developmental consequences of karyokinesis without cytokinesis during the first mitotic cell cycle of bovine parthenotes. Biol Reprod *58*, 952-962.

59. De Sousa,P.A., Caverney,A., Westhusin,M.E., and Watson,A.J. (1998). Temporal patterns of embryonic gene expression and their dependence on oogenetic factors. Theriogenology *49*, 115-128.

60. Diatchenko,L., Lau,Y.F., Campbell,A.P., Chenchik,A., Moqadam,F., Huang,B., Lukyanov,K., Gurskaya,N., Sverdlov,E.D., and Siebert,P.D. (1996). Suppression subtractive hybridisation:a method for generating differentially regulated or tissue specific cDNA probes and libraries. Proc Natl Acad Sci USA *93*, 6025-6030.

61. Digonnet,C., Aldon,D., Leduc,N., Duman,C., and Rougier,M. (1997). First evidence of a calcium transient in flowering plants at fertilization. Development *124*, 2867-2874.

62. Dolmetsch,R.E., Xu,K., and Lewis,R.S. (1998). Calcium oscillations increase the efficiency and specificity of gene expression. Nature *392(6679)*, 933-936.

63. Dong,J.B., Tang,T.S., and Sun,F.Z. (2000). Xenopus and chicken sperm contain a cytosolic soluble protein factor which can trigger calcium oscillations in mouse eggs. Biochem Biophys Res Commun *268*, 947-951.

64. Doniger,S.W., Salomonis,N., Dahlquist,K.D., Vranizan,K., Lawlor,S.C., and Conklin,B.R. (2003). MAPPFinder: using Gene Ontology and GeneMAPP to create a global gene-expression profile from microarray data. Genome Biology *4:R7*.

65. Doree,M. and Hunt,T. (2002). From Cdc2 to Cdk1: when did the cell cycle kinase join its cyclin partner? J Cell Sci *115*, 2461-2464.

66. Ducibella,T., Huneau,D., Angelichio,E., Xu,Z., Schultz,R.M., Kopf,G.S., Fissore,R.A., Madoux,S., and Ozil,J.P. (2002). Egg-to-embryo transition is driven by differential responses to Ca(2+) oscillation number. Dev Biol *250*, 280-291.

67. Dupont,G. (1998). Link between fertilization-induced Ca^{2+} oscillations and relief from metaphase II arrest in mammalian eggs: a model based on calmodulin-dependent kinase II activation. Biophys Chem *72*, 153-167.

68. Eldar-Geva,T., Brooks,B., Margalioth,E.J., Zylber-Haran,E., Gal,M., and Silber,S.J. (2003). Successful pregnancy and delivery after calcium ionophore oocyte activation in a normozoospermic patient with previous repeated failed fertilization after intracytoplasmic sperm injection. Fertil Steril *79*, 1656-1658.

69. Evans,T., Rosenthal,E.T., Youngblom,J., Distel,D., and Hunt,T. (1983). Cyclin: a protein specified by maternal mRNA in sea urchin eggs that is destroyed at each cleavage division. Cell *33*, 389-396.

70. Fahrudin,M., Otoi,T., Karja,N.W., Mori,M., Murakami,M., and Suzuki,T. (2002). Analysis of DNA fragmentation in bovine somatic nuclear transfer embryos using TUNEL. Reproduction *124*, 813-819.

71. Fissore,R.A., Pinto-Correia,C., and Robl,J.M. (1995). Inositol trisphosphate-induced calcium release in the generation of calcium oscillations in bovine eggs. Biol Reprod *53*, 766-774.

72. Fissore,R.A. and Robl,J.M. (1993). Sperm, inositol trisphosphate, and thimerosal-induced intracellular Ca^{2+} elevations in rabbit eggs. Dev Biol *159*, 122-130.

73. Flach,G., Johnson,M.H., Braude,P.R., Taylor,R.A., and Bolton,V.N. (1982). The transition from maternal to embryonic control in the 2-cell mouse embryo. EMBO J *1(6)*, 681-686.

74. Fleming,T.P. (1986). A quantitative analysis of cell allocation to trophectoderm and inner cell mass in the mouse blastocyst. Dev Biol *119*, 520-531.

75. Fleming,T.P. (1987). A quantitative analysis of cell allocation to trophectoderm and inner cell mass in the mouse blastocyst. Dev Biol *119*, 520-531.

76. Foltz,K.R. and Shilling,F.M. (1993). Receptor-mediated signal transduction and egg activation. Zygote *1*, 276-279.

77. Foskett,S.M., Ghose,R., Tang,D.N., Lewis,D.E., and Rice,A.P. (2001). Antiapoptotic function of cdk9 (TAK/P-TEFb) in U937 promonocytic cells. J Virol *75*, 1220-1228.

78. Fouladi-Nashta,A.A., Alberio,R., Kafi,M., Nicholas,B., Campbell,K.H., and Webb,R. (2005). Differential staining combined with TUNEL labelling to detect apoptosis in preimplantation bovine embryos. Reprod Biomed Online *10*, 497-502.

79. Fraser,L.R. (1987). Strontium supports capacitation and the acrosome reaction in mouse sperm and rapidly activates mouse eggs. Gamete Res *18*, 363-374.

80. Fujiwara,T., Nakada,K., Shirakawa,H., and Miyazaki,S. (1993). Development of inositol trisphosphate-induced calcium release mechanism during maturation of hamster oocytes. Dev Biol *156*, 69-79.

81. Fukui,Y., Sawai,K., Furudate,M., Sato,N., Iwazumi,Y., and Ohsaki,K. (1992). Parthenogenetic development of bovine oocytes treated with ethanol and cytochalasin B after in vitro maturation. Mol Reprod Dev *33*, 357-362.

82. Fulton,B.P. and Whittingham,D.G. (1978). Activation of mammalian oocytes by intracellular injection of calcium. Nature *273*, 151.

83. Galione,A., McDougall,A., Busa,W.B., Willmott,N., Gillot,I., and Whitaker,M. (1993). Redundant mechanisms of calcium-induced calcium release underlying calcium waves during fertilization of sea urchin eggs. Science *261*, 348-352.

84. Gardner,D.K. (1999). Development of serum-free culture systems for the ruminant embryo and subsequent assessment of embryo viability. J Reprod Fertil Suppl *54*, 461-475.

85. Gardner,D.K., Schoolcraft,W.B., Wagley,L., Schlenker,T., Stevens,J., and Hesla,J. (1998). A prospective randomized trial of blastocyst culture and transfer in in-vitro fertilization. Hum Reprod *13*, 3434-3440.

86. Gates,A.H. (1971). Maximising yield and developmental uniformity of eggs. Methods in Mammalian Embryology 64-75.

87. Giorgetti,C., Terriou,P., Auquier,P., Hans,E., Spach,J.L., Salzmann,J., and Roulier,R. (1995). Embryo score to predict implantation after in-vitro fertilization: based on 957 single embryo transfers. Hum Reprod *10*, 2427-2431.

88. Gonzales,D.S. and Bavister,B.D. (1995). Zona pellucida escape by hamster blastocysts in vitro is delayed and morphologically different compared with zona escape in vivo. Biol Reprod *52*, 470-480.

89. Greve,J.M. and Wassarman,P.M. (1985). Mouse egg extracellular coat is a matrix of interconnected filaments possessing a structural repeat. J Mol Biol *181*, 235-264.

90. Grisart,B., Massip,A., and Dessy,F. (1994). Cinematographic analysis of bovine embryo development in serum-free oviduct-conditioned medium. J Reprod Fertil *101*, 257-264.

91. Gulyas,B.J. (1975). A reexamination of cleavage patterns in eutherian mammalian eggs: rotation of blastomere pairs during second cleavage in the rabbit. J Exp Zool *193*, 235-248.

92. Halet,G., Tunwell,R., Balla,T., Swann,K., and Carroll,J. (2002). The dynamics of plasma membrane PtdIns(4,5)P(2) at fertilisation of mouse eggs. J Cell Science *115*, 2139-2149.

93. Halet,G., Tunwell,R., Parkinson,S.J., and Carroll,J. (2004). Conventional PKCs regulate the temporal pattern of Ca^{2+} oscillations at fertilization in mouse eggs. J Cell Biol *164*, 1033-1044.

94. Hamaguchi,Y. and Hiramoto,Y. (1981). Activation of sea urchin eggs by microinjection of calcium buffers. Exp Cell Res *134*, 171-179.

95. Hamatani,T., Carter,M.G., Sharov,A.A., and Ko,M.S. (2004a). Dynamics of global gene expression changes during mouse preimplantation development. Dev Cell *6*, 117-131.

96. Hamatani,T., Daikoku,T., Wang,H., Matsumoto,H., Carter,M.G., Ko,M.S., and Dey,S.K. (2004b). Global gene expression analysis identifies molecular pathways distinguishing blastocyst dormancy and activation. Proc Natl Acad Sci USA *101*, 10326-10331.

97. Handyside,A.H. and Delhanty,J.D. (1997). Preimplantation genetic diagnosis: strategies and surprises. Trends Genet *13*, 270-275.

98. Handyside,A.H. and Hunter,S. (1984). A Rapid Procedure for visualising the Inner Cell Mass and Trophectoderm Nuclei of Mouse Blastocysts In Situ Using Polynucleotide-Specific Flurochromes. J Exp Zool *231*, 429-434.

99. Haraguchi,S., Naito,K., and Sato,E. (1999). Phosphate exposure during the late 1-cell and early 2-cell stages induces a time-specific decrease in cyclin B and cdc25B mRNAs in AKR/N mouse embryos in vitro. Zygote *7*, 87-93.

100. Hardy,K., Handyside,A.H., and Winston,R.M. (1989). The human blastocyst: cell number, death and allocation during late preimplantation development in vitro. Development *107*, 597-604.

101. Hardy,K., Spanos,S., Becker,D., Iannelli,P., Winston,R.M., and Stark,J. (2001). From cell death to embryo arrest: mathematical models of human preimplantation embryo development. PNAS *98*, 1655-1660.

102. Hardy,K., Stark,J., and Winston,R.M. (2003). Maintenance of the inner cell mass in human blastocysts from fragmented embryos. Biol Reprod *68*, 1165-1169.

103. Henery,C.C., Miranda,M., Wiekowski,M., Wilmut,I., and Depamphilis,M.L. (1995). Repression of gene expression at the beginning of mouse development. Dev Biol *169*, 448-460.

104. Hernandez-Ledezma,J.J., Mathialagan,N., Villanueva,C., Sikes,J.D., and Roberts,R.M. (1993). Expression of bovine trophoblast interferons by in vitro-derived blastocysts is correlated with their morphological quality and stage of development. Mol Reprod Dev *36*, 1-6.

105. Hoffmann,T., Obukhov,A.G., Schaefer,M., Harteneck,C., Gudermann,T., and Schultz,G. (1999). Direct activation of human TRPC6 and TRPC3 channels by diacylglycerol. Nature *397*, 259-263.

106. Hogan,B., Beddington,R., Costantini,F., and Lacey,E. (1994). Manipulating the mouse embryo. Second Edition *Cold Spring Harbour Laboratory Press*.

107. Holst,P.A. and Phemister,R.D. (1971). The prenatal development of the dog: preimplantation events. Biol Reprod *5*, 194-206.

108. Homa,S.T. and Swann,K. (1994). A cytosolic sperm factor triggers calcium oscillations and membrane hyperpolarizations in human oocytes. Hum Reprod *9*, 2356-2361.

109. Howlett,S.K. (1986). A set of proteins showing cell cycle dependent modification in the early mouse embryo. Cell *45*, 387-396.

110. Hunter,R.H. (1998). Have the Fallopian tubes a vital role in promoting fertility? Acta Obstet Gynecol Scand *77*, 475-486.

111. Hwang,W.S., Ryu,Y.J., Park,J.H., Lee,E.G., Koo,J.M., Jeon,H.Y., Lee,B.C., Kang,S.K., Kim,S.J., Ahn,C., Hwang,J.H., Park,K.Y., Cibelli,J.B., and Moon,S.Y. (2004). Evidence of a pluripotent human embryonic stem cell line derived from a cloned blastocyst. Science *303*, 1669-1674.

112. Hyslop,L.A., Carroll,M., Nixon,V.L., McDougall,A., and Jones,K.T. (2001). Simultaneous measurement of intracellular nitric oxide and free calcium levels in chordate eggs demonstrates that nitric oxide has no role at fertilization. Dev Biol *234*, 216-230.

113. Igusa,Y. and Miyazaki,S. (1983). Effects of altered extracellular and intracellular calcium concentration on hyperpolarizing responses of the hamster egg. J Physiol *340*, 611-632.

114. Jaffe,L.F. (1991). The path of calcium in cytosolic calcium oscillations: a unifying hypothesis. Proc Natl Acad Sci USA *88*, 9883-9887.

115. Jellerette,T., He,C.L., Wu,H., Parys,J., and Fissore,R.A. (2000). Down-regulation of the inositol 1,4,5-trisphosphate receptor in mouse eggs following fertilization or parthenogenetic activation. Dev Biol *223*, 238-250.

116. Johnson,J., Bierle,B.M., Gallicano,G.I., and Capco,D.G. (1998). Calcium/calmodulin-dependent protein kinase II and calmodulin: regulators of the meiotic spindle in mouse eggs. Dev Biol *204*, 464-477.

117. Jones,K.T., Carroll,J., Merriman,J.A., Whittingham,D.G., and Kono,T. (1995a). Repetitive sperm-induced Ca^{2+} transients in mouse oocytes are cell cycle dependent. Development *121*, 3259-3266.

118. Jones,K.T., Carroll,J., and Whittingham,D.G. (1995b). Ionomycin, thapsigargin, ryanodine, and sperm induced Ca^{2+} release increase during meiotic maturation of mouse oocytes. J Biol Chem *270* , 6671-6677.

119. Jones,K.T., Crutwell,C., Parrington,J., and Swann,K. (1998b). A mammalian sperm cytosolic phospholipase C activity generates inositol triphosphate and causes Ca^{2+} release in sea urchin egg homogenates. FEBS Lett *437*, 297-300.

120. Jones,K.T., Matsuda,M., Parrington,J., Katan,M., and Swann,K. (2000). Different Ca^{2+}-releasing abilities of sperm extracts compared with tissue extracts and phospholipase C isoforms in sea urchin egg homogenate and mouse eggs. Biochem J *346*, 743-749.

121. Jones,K.T., Soeller,C., and Cannell,M.B. (1998a). The passage of Ca^{2+} and fluorescent markers between the sperm and egg after fusion in the mouse. Development *125*, 4627-4635.

122. Jurisicova,A., Varmuza,S., and Casper,R.F. (1996). Programmed cell death and human embryo fragmentation. Mol Hum Reprod *2*, 93-98.

123. Kanatsu-Shinohara,M., Schultz,R.M., and Kopf,G.S. (2000). Acquisition of meiotic competence in mouse oocytes: absolute amounts of p34(cdc2), cyclin B1, cdc25C, and wee1 in meiotically incompetent and competent oocytes. Biol Reprod *63*, 1610-1616.

124. Kaufman,M.H. (1979). Mammalian parthenogenetic development. Reprod *33*, 261-264.

125. Kawahara,H. and Yokosawa,H. (1994). Intracellular calcium mobilization regulates the activity of 26 S proteasome during the metaphase-anaphase transition in the ascidian meiotic cell cycle. Dev Biol *166*, 623-633.

126. Kawai,T., Nomura,F., Hoshino,K., Copeland,N.G., Gilbert,D.J., Jenkins,N.A., and Akira,S. (1999). Death-associated protein kinase 2 is a new calcium/calmodulin-dependent protein kinase that signals apoptosis through its catalytic activity. Oncogene *18*, 3471-3480.

127. Kimura,Y. and Yanagimachi,R. (1995). Intracytoplasmic sperm injection in the mouse. Biol Reprod *52*, 709-720.

128. King,R.W., Peters,J.M., Tugendreich,S., Rolfe,M., Hieter,P., and Kirschner,M.W. (1995). 20S complex containing CDC27 and CDC16 catalyses the mitosis-specific conjugation of ubiquitin to cyclin B. Cell *81*, 279-288.

129. Kline,D. and Kline,J.T. (1992). Repetitive calcium transients and the role of calcium in exocytosis and cell cycle activation in the mouse egg. Dev Biol *149*, 80-89.

130. Kline,D. and Nuccitelli,R. (1985). The wave of activation current in the Xenopus egg. Dev Biol *111*, 471-487.

131. Knott,J.G., Kurokawa,M., Fissore,R.A., Schultz,R.M., and Williams,C.J. (2005). Transgenic RNA interference reveals role for mouse sperm phospholipase Czeta in triggering Ca^{2+} oscillations during fertilization. Biol Reprod *72*, 992-996.

132. Knott,J.G., poothapillai,K., Wu,H., He,C.L., Fissore,R.A., and Robl,J.M. (2002). Porcine sperm factor supports activation and development of bovine nuclear transfer embryos. Biol Reprod *66*, 1095-1103.

133. Ko,M.S., Kitchen,J.R., Wang,X., Threat,T.A., Wang,X., Hasegawa,A., Sun,T., Grahovac,M.J., Kargul,G.J., Lim,M.K., Cui,Y., Sano,Y., Tanaka,T., Liang,Y., Mason,S., Paonessa,P.D., Sauls,A.D., DePalma,G.E., Sharara,R., Rowe,L.B., Eppig,J., Morrell,C., and Doi,H. (2000). Large-scale cDNA analysis reveals phased gene expression patterns during preimplantation mouse development. Development *127*, 1737-1749.

134. Kono,T., Jones,K.T., Bos-Mikich,A., Whittingham,D.G., and Carroll,J. (1996). A cell cycle-associated change in Ca releasing activity leads to the generation of Ca transients in mouse embryos during the first mitotic Division. J. Cell Biol *132*, 915-923.

135. Kouchi,Z., Fukami,K., Shikano,T., Oda,S., Nakamura,Y., Takenawa,T., and Miyazaki,S. (2004). Recombinant phospholipase Czeta has high Ca^{2+} sensitivity and induces Ca^{2+} oscillations in mouse eggs. J Biol Chem *279*, 10408-10412.

136. Kouchi,Z., Shikano,T., Nakamura,Y., Shiakawa,H., Fukami,K., and Miyazaki,S. (2005). The role of EF-hand domains and C2 domain in regulation of enzymatic activity of phospholipase Czeta. J Biol Chem *280*, 21015-21021.

137. Kubiak,J.Z., Weber,M., de Peenart,H., Winston,N.J., and Maro,B. (1993). The metaphase II arrest in mouse oocytes is controlled through microtubule-dependent destruction of cyclin B in the presence of CSF. EMBO J *12*, 3773-3778.

138. Kuo,R.C., Baxter,G.T., Thompson,S.H., Stricker,S.A., Patton,C., Bonaventura,J., and Epel,D. (2000). NO is necessary and sufficient for egg activation at fertilization. Nature *406*, 633-636.

139. Kurokawa,M., Sato,K., Wu,H., He,C., Malcuit,C., Black,S.J., Fukami,K., and Fissore,R.A. (2005). Functional, biochemical and chromatographic characterization of the complete Ca^{2+} oscillation-inducing activity of porcine sperm. Dev Biol ***in press***.

140. Kyozuka,K., Deguchi,R., Mohri,T., and Miyazaki,S. (1998). Injection of sperm extract mimics spatiotemporal dynamics of Ca^{2+} responses and progression of meiosis at fertilization of ascidian oocytes. Development *125*, 4099-4105.

141. Larman,M.G., Saunders,C.M., Carroll,J., Lai,F.A., and Swann,K. (2004). Cell cycle-dependent Ca^{2+} oscillations in mouse embryos are regulated by nuclear targeting of PLCzeta. J Cell Sci. *117(Πτ 12)*, 2513-2521.

142. Latham,K.E., Garrels,J.I., Chang,C., and Solter,D. (1991). Quantitative analysis of protein synthesis in mouse embryos: I. Extensive reprogramming at the one- and two-cell stages. Development *112*, 921-932.

143. Latham,K.E., Solter,D., and Schultz,R.M. (1992). Acquisition of a transcriptionally permissive state during the 1-cell stage of mouse embryogenesis. Dev Biol *149*, 457-462.

144. Lawitts,J.A. and Biggers,J.D. (1991). Optimisation of mouse embryo culture media using simplex methods. J Reprod Fertil *91*, 543-556.

145. Lawitts,J.A. and Biggers,J.D. (1993). Culture of preimplantation embryos. Methods Enzymol *225*, 153-164.

146. Lawrence,Y., Ozil,J.P., and Swann,K. (1998). The effects of a Ca^{2+} chelator and heavy-metal-ion chelators upon Ca^{2+} oscillations and activation at fertilization in mouse eggs suggest a role for repetitive Ca^{2+} increases. Biochem J *335*, 335-342.

147. Lawrence,Y., Whitaker,M., and Swann,K. (1997). Sperm-egg fusion is the prelude to the initial Ca^{2+} increase at fertilization in the mouse. Development *124*, 233-241.

148. Le Mee,S., Fromigue,O., and Marie,P.J. (2005). Sp1.Sp3 and the myeliod zinc finger gene MZF1 regulate the human N-cadherin promoter in osteoblasts. Exp Cell Res *302*, 129-142.

149. Leach,R.E., Stacheki,J.J., and Armant,D.R. (1993). Development of in vitro fertilized mouse embryos exposed to ethanol during the preimplantation period: accelerated embryogenesis at subtoxic levels. Teratology *47*, 57-64.

150. Ledan,E., Polanski,Z., Terret,M.E., and Maro,B. (2001). Meiotic maturation of the mouse oocyte requires an equilibrium between cyclin B synthesis and degradation. Dev Biol *232*, 400-413.

151. Lee,K.W., Webb,S.E., and Miller,A.L. (1999). A wave of free cytosolic calcium traverses zebrafish eggs on activation. Dev Biol *214*, 168-180.

152. Leese,H.J., Donnay,I., and Thompson,J.G. (1998). Human assisted conception: a cautionary tale. Lessons from domestic animals. Hum Reprod *13*, 184-202.

153. Li,S.T., Huang,X.Y., and Sun,F.Z. (2001). Flowering plant sperm contains a cytosolic soluble protein factor which can trigger calcium oscillations in mouse eggs. Biochem Biophys Res Commun *287*, 56-59.

154. Li,W., Llopis,J., Whitney,M., Zlokarnik,G., and Tsien,R.Y. (1998). Cell-permeant caged InsP3 ester shows that Ca^{2+} spike frequency can optimize gene expression. Nature *392*, 936-941.

155. Lin,H., Lei,J., Wininger,D., Nguyen,M.T., Khanna,R., Hartmann,C., Yan,W.L., and Huang,S.C. (2003). Multilineage potential of homozygous stem cells derived from metaphase II oocytes. Stem Cells *21*, 152-161.

156. Lin,J.H., Weigel,H., Cotrine,M.L., Liu,S., Bueno,E., Hansen,A.J., Hansen,T.W., Goldman,S., and Nedergaad,M. (1998). Gap-junction-mediated propagation and amplification of cell injury. Nat Neurosci *1*, 494-500.

157. Lindsay,L.L., Hertzler,P.L., and Clarke,W.H.J. (1992). Extracellular Mg2+ induces an intracellular Ca^{2+} wave during oocyte activation in the marine shrimp Sicyonia ingentis. Dev Biol *152*, 94-102.

158. Liu,L., Ju,J.C., and Yang,X. (1998). Parthenogenetic development and protein patterns of newly matured bovine oocytes after chemical activation. Mol Reprod Dev *49*, 298-307.

159. Liu,L., Trimarchi,J., and Keefe,D. (2002). Haploidy but not parthenogenetic activation leads to increased incidence of apoptosis in mouse embryos. Biol Reprod *66*, 204-210.

160. Loi,P., Ledda,S., Fulka,J.J., Cappai,P., and Moor,R.M. (1998). Development of parthenogenetic and cloned ovine embryos: effect of activation protocols. Biol Reprod *58*, 1177-1187.

161. Lorca,T., Cruzalegui,F.H., Fesquet,D., Cavadore,J.C., Mery,J., Means,A., and Doree,M. (1993). Calmodulin- dependent protein kinase II mediates inactivation of MPF and CSF upon fertilisation of Xenopus eggs. Nature *366*, 270-273.

162. Lorca,T., Galas,S., Fesquet,D., Devault,A., Cavadore,J.C., and Doree,M. (1991). Degradation of the proto-oncogene product p39mos is not necessary for cyclin proteolysis and exit from meiotic metaphase: requirement for a Ca(2+)-calmodulin dependent event. EMBO J *10*, 2087-2093.

163. Lu,K.P. and Means,A.R. (1993). Regulation of the cell cycle by calcium and calmodulin. Endocrine Reviews *14*, 58.

164. Lytton,J., Westlin,M., Burk,S.E., Shull,G.E., and MacLennan,D.H. (1992). Functional comparisons between isoforms of the sarcoplasmic or endoplasmic reticulum family of calcium pumps. J Biol Chem *267*, 14483-14489.

165. Ma,J., Svoboda,P., Schultz,R.M., and Stein,P. (2001). Regulation of zygotic gene activation in the preimplantation mouse embryo: global activation and repression of gene expression. Biol Reprod *64(6)*, 1713-1721.

166. Ma,S.F., Liu,X.Y., Miao,D.Q., Han,Z.B., Zhang,X., Miao,Y.L., Yanagimachi,R., and Tan,J.H. (2005). Parthenogenetic activation of mouse oocytes by strontium chloride: A search for the best conditions. Theriogenology *64*, 1142-1157.

167. Machaty,Z., Bonkl,A.J., Kuhholzer,B., and Prather,R.S. (2000). Porcine Oocyte Activation induced by a cytosolic sperm factor. Mol. Reprod Dev *57*, 290-295.

168. Machaty,Z., Funahashi,H., Mayes,M.A., Day,B.M., and Prather,R.S. (1996). Effects of injecting calcium chloride into in vitro-matured porcine oocytes. Biol Reprod *54*, 316-322.

169. Machaty,Z., Wang,W.H., Day,B.N., and Prather,R.S. (1997). Complete activation of porcine oocytes induced by the sulfhydryl reagent, thimerosal. Biol Reprod *57*, 1123-1127.

170. Madgwick,S., Levasseur,M., and Jones,K.T. (2005). Calmodulin-dependent protein kinase II, and not protein kinase C, is sufficient for triggering cell-cycle resumption in mammalian eggs. J Cell Sci *118*, 3849-3859.

171. Madgwick,S., Nixon,V.L., Chang,H.Y., Herbert,M., Levasseur,M., and Jones,K.T. (2004). Maintenance of sister chromatid attachment in mouse eggs through maturation-promoting factor activity. Dev Biol *275*, 68-81.

172. Majumder,M.M., Wiekowski,M., and Depamphilis,M.L. (1993). Application of firefly luciferase to preimplantation development. Methods Enzymol *225*, 412-433.

173. Mak,S.K. and Kultz,D. (2004). Gadd45 proteins induce G2/M arrest and modulate apoptosis in kidney cells exposed to hyperosmotic stress. J Biol Chem *279*, 39075-39084.

174. Manejwala,F.M., Logan,C.Y., and Schultz,R.M. (1991). Regulation of hsp70 mRNA levels during oocyte maturation and zygotic gene activation in the mouse. Dev Biol *144*, 301-308.

175. Marangos,P., FitzHarris,G., and Carroll,J. (2003). Ca^{2+} oscillations at fertilization in mammals are regulated by the formation of pronuclei. Development *130*, 1461-1472.

176. Markoulaki,S., Matson,S., and Ducibella,T. (2004). Fertilisation stimulates long lasting oscillations of CAMKII activity in mouse eggs. Dev Biol *272*, 15-25.

177. Marshall,I.C. and Taylor,C.W. (1994). Two calcium-binding sites mediate the interconversion of liver inositol 1,4,5-trisphosphate receptors between three conformational states. Biochem J *301*, 591-598.

178. Masui,Y. and Markert,C.L. (1971). Cytoplasmic control of nuclear behavior during meiotic maturation of frog oocytes. J Exp Zool *177*, 129-145.

179. Matsumoto,K., Anzai,M., Nakagata,N., Takahashi,A., Takahashi,Y., and Miyata,K. (1994). Onset of paternal gene activation in early mouse embryos fertilised with transgenic mouse sperm. Mol Reprod Dev *39*, 136-140.

180. McCulloh,D.H. and Chambers,E.L. (1992). Fusion of membranes during fertilization. Increases of the sea urchin egg's membrane capacitance and membrane conductance at the site of contact with the sperm. J Gen Physiol *99*, 137-175.

181. McDougall,A., Levasseur,M., O'Sullivan,A.J., and Jones,K.T. (2000). Cell cycle-dependent repetitive Ca^{2+} waves induced by a cytosolic sperm extract in mature ascidian eggs mimic those observed at fertilization. J Cell Sci *113*, 3453-3462.

182. McDougall,A. and Sardet,C. (1995). Function and characteristics of repetitive calcium waves associated with meiosis. Curr Biol *5*, 318-328.

183. Means,A.R., VanBerkum,M.F., Bagchi,I., Lu,K.P., and Rasmusen,C.D. (1991). Regulatory functions of calmodulin. Pharmacol Ther *50*, 255-270.

184. Medvedev,S.Y., Tokunga,T., Schultz,R.M., Furukawa,T., Nagai,T., Yamaguchi,M., Hosoe,M., and Yakovlev,A.F. (2002). Quantitative analysis of gene expression in preimplantation mouse embryos using green fluorescent protein reporter. Biol Reprod *67*, 282-286.

185. Mehlmann,L.M. and Kline,D. (1994). Regulation of intracellular calcium in the mouse egg: calcium release in response to sperm or inositol trisphosphate is enhanced after meiotic maturation. Biol Reprod *51*, 1088-1098.

186. Meijer,L., Borgne,A., Mulner,O., Chong,J.P.J., Blow,J.J., Inagaki,N., Delcros,J.G., and Moulinoux,J.P. (1997). Biochemical and cellular effects of roscovitine, a potent and selective inhibitor of the cyclin-dependent kinases cdc2, cdk2 and cdk5. Eur J Biochem *243*, 527-536.

187. Meirelles,F.V., Caetano,A.R., Watanabe,Y.F., Ripamonte,P., Carambula,S.F., Merighe,G.K., and Garcia,S.M. (2004). Genome activation and developmental block in bovine embryos. Anim Reprod Sci *82–83*, 13-20.

188. Memili,E. and First,N.L. (2000). Zygotic and embryonic gene expression in cow: a review of timing and mechanisms of early gene expression as compared with other species. Zygote *8*, 87-96.

189. Miyazaki,S., Shirakawa,H., Nakada,K., and Honda,Y. (1993). Essential role of the inositol 1,4,5-trisphosphate receptor/Ca^{2+} release channel in Ca^{2+} waves and Ca^{2+} oscillations at fertilization of mammalian eggs. Dev Biol *158*, 62-78.

190. Miyazaki,S., Yuzaki,M., Nakada,K., Shirakawa,H., Nakanishi,S., Nakade,S., and Mikoshiba,K. (1992). Block of Ca^{2+} wave and Ca^{2+} oscillation by antibody to the inositol 1,4,5-trisphosphate receptor in fertilized hamster eggs. Science *257*, 251-255.

191. Moor,R.M., Dai,Y., Lee,C., and Fulka,J.J. (1998). Oocyte maturation and embryonic failure. Hum Reprod Update *4*, 223-236.

192. Moore,G.P. (1975). The RNA polymerase activity of the preimplantation mouse embryo. J Embryol Exp Morphol *34*, 291-298.

193. Moos,J., Kopf,G.S., and Schultz,R.M. (1996). Cyclohexamide-induced activation of mouse eggs: effects on cdc2/cyclin b and MAP kinase activities. J. Cell. Science *109*, 739-748.

194. Moses,R.M. and Kline,D. (1995). Release of mouse eggs from metaphase arrest by protein synthesis inhibition in the absence of a calcium signal or microtubule assembly. Mol. Reprod Dev *41*, 264-273.

195. Mueller,O., Hahnenberger,K., Dittmann,M., Yee,H., Dubrow,R., Nagle,R., and Iisley,D. (2000). A microfluidic system for high-speed reproducible DNA sizing and quantitation. Electrophoresis *21*, 128-134.

196. Muggleton-Harris,A., Whittingham,D.G., and Wilson,L. (1982). Cytoplasmic control of preimplantation development in vitro in the mouse. Nature *299*, 460-462.

197. Munne,S., Alikani,M., Tomkin,G., Grifo,J., and Cohen,J. (1995). Embryo morphology, developmental rates, and maternal age are correlated with chromosome abnormalities. Fertility and Sterility *64*, 382-391.

198. Murase,Y., Araki,Y., Mizuno,S., Kawaguchi,C., Naito,M., Yoshizawa,M., and Araki,Y. (2004). Pregnancy following chemical activation of oocytes in a couple with repeated failure of fertilization using ICSI: case report. Hum Reprod *19*, 1604-1607.

199. Murray,A.W., Solomon,M.J., and Kirschner,M.W. (1989). The role of cyclin synthesis and degradation in the control of maturation promoting factor activity. Nature *339*, 280-286.

200. Nagashima,H., Grupen,C.G., Ashman,R.J., and Nottle,M.B. (1996). Developmental competence of in vivo and in vitro matured porcine oocytes after subzonal sperm injection. Mol Reprod Dev *45*, 359-363.

201. Nakagawa,K., Yamano,S., Monde,N., Yamashita,M., Yoshizawa,M., and Aono,T. (2001). Effect of activation with Ca^{2+} ionophore A23187 and puromycin on the development of human oocytes that failed to fertilize after intracytoplasmic sperm injection. Fertil Steril *76*, 148-152.

202. Nakano,Y., Shirakawa,H., Mitsuhashi,N., Kuwabara,Y., and Miyazaki,S. (1997). Spatiotemporal dynamics of intracellular calcium in the mouse egg injected with a spermatozoon. Mol Hum Reprod *3* , 1087-1093.

203. Narula,A., Taneja,M., and Totey,S.M. (1996). Morphological development, cell number, and allocation of cells to trophectoderm and inner cell mass of in vitro fertilized and parthenogenetically developed buffalo embryos: the effect of IGF-I. Mol Reprod Dev *44*, 343-351.

204. Neuber,E., Luetjens,C.M., Chan,A.W., and Schatten,G.P. (2002). Analysis of DNA fragmentation of in vitro cultured bovine blastocysts using TUNEL. Theriogenology *57*, 2193-2202.

205. Nguyen,T.B., Manova,K., Capodieci,P., Lindon,C., Bottega,S., Wang,X.Y., Refik-Rogers,J., Pines,J., Wolgemuth,D.J., and Koff,A. (2002). Characterization and

expression of mammalian cyclin b3, a prepachytene meiotic cyclin. J Biol Chem *277*, 41960-41969.

206. Nishiwaki,E., Turner,S.L., Harju,S., Miyazaki,S., Kashiwagi,M., Koh,J., and Serizawa,H. (2000). Regulation of CDK7-carboxyl-terminal domain kinase activity by the tumor suppressor p16(INK4A) contributes to cell cycle regulation . Mol cell Biol *20*, 7726-7734.

207. Nixon,V., Levasseur,M., McDougall,A., and Jones,K.T. (2002). Ca^{2+} oscillations promote APC/C-dependent cyclin B1 degradation during metaphase arrest and completion of meiosis in fertilizing mouse eggs. Curr Biol *12*, 746-750.

208. Nixon,V., McDougall,A., and Jones,K.T. (2000). Ca^{2+} oscillations and the cell cycle at fertilisation of mammalian and ascidian eggs. Biol Cell *92*, 187-196.

209. Nomikos,M., Blayney,L.M., Larman,M.G., Campbell,K., Rossbach,A., Saunders,C.M., Swann,K., and Lai,F.A. (2005). Role of PLC-zeta domains in Ca^{2+}-dependent PIP2 hydrolysis and cytoplasmic Ca2+ oscillations. J Biol Chem.

210. Nothias,J.Y., Miranda,M., and DePampilis,M.L. (1996). Uncoupling of transcription and translation during zygotic gene activation in the mouse. EMBO J *15(20)*, 5715-5725.

211. Nuccitelli,R. (1991). How do sperm activate eggs? Curr Top Dev Biol *25*, 16.

212. Nussbaum,D.J. and Prather,R.S. (1995). Differential effects of protein synthesis inhibitors on porcine oocyte activation. Mol Reprod Dev *41*, 70-75.

213. Oancea,E. and Meyer,T. (1998). Protein kinase C as a molecular machine for decoding calcium and diacylglycerol signals. Cell *95*, 307-318.

214. Oh,B., Hwang,S.Y., Solter,D., and Knowles,B.B. (2005). Spindlin, a major maternal transcript expressed in the mouse during the transition from oocyte to embryo. Development *124*, 493-503.

215. Ohsumi,K., Koyanagi,A., Yamamoto,T.M., Gotoh,T., and Kishimoto,T. (2004). Emi1-mediated M-phase arrest in Xenopus eggs is distinct from cytostatic factor arrest. PNAS *101*, 12531-12536.

216. Okuda,T., Hirai,H., Valentine,V.A., Shurtleff,S.A., Kidd,V.J., Lahti,J.M., Sherr,C.J., and Downing,J.R. (1995). Molecular cloning, expression pattern and chromosomal localization of humans CDKN2D,INK4d, an inhibitor of cyclin D-dependent kinases. Genomics *29*, 623-630.

217. Ola,B., Afnan,M., Sharif,K., Papaioannou,S., Hammadieh,N., and Barratt,C.L. (2001). Should ICSI be the treatment of choice for all cases of in-vitro conception? Considerations of fertilization and embryo development, cost effectiveness and safety. Hum Reprod *16*, 2485-2490.

218. Ozil,J.P., Markoulaki,S., Toth,S., Matson,S., Banrezes,B., Knott,J.G., Schultz,R.M., Huneau,D., and Ducibella,T. (2005). Egg activation events are regulated by the duration of a sustained [Ca^{2+}]cyt signal in the mouse. Dev Biol *282*, 39-54.

219. Ozil,J.P. and Swann,K. (1995). Stimulation of repetitive calcium transients in mouse eggs. J Physiol *483*, 331-346.

220. Ozil,J. (1990). The parthenogenetic development of rabbit oocytes after repetitive pulsatile electrical stimulation. Development *109*, 117-127.

221. Ozil,J. and Huneau,D. (2001). Activation of rabbit oocytes: the impact of the Ca^{2+} signal regime on development.Development. 2001 Mar;128(6):917-28. Development *128*, 917-928.

222. Palermo,G.D., Avrech,O.M., Colombero,L.T., Wu,H., Wolny,Y.M., Fissore,R.A., and Rosenwaks,Z. (1997). Human sperm cytosolic factor triggers Ca^{2+} oscillations and overcomes activation failure of mammalian oocytes. Mol. Reprod Dev *3*, 367-374.

223. Palermo,G.D., Cohen,J., Alikani,M., Adler,A., and Rosenwaks,Z. (1995). Intracytoplasmic sperm injection: a novel treatment for all forms of male factor infertility. Fertil Steril *63*, 1231-1240.

224. Palermo,G.D., Joris,H., Devroey,P., and Van Steirteghem,A.C. (1992). Pregnancies after intracytoplasmic injection of single spermatozoon into an oocyte. Lancet *349*, 17-18.

225. Pampfer,S., Vanderheyden,I., McCracken,J.E., Vesela,J., and De Hertogh,R. (1997). Increased cell death in rat blastocysts exposed to maternal diabetes in utero and to high glucose or tumor necrosis factor-alpha in vitro. Development *124*, 4827-4836.

226. Parrington,J., Lai,F.A., and Swann,K. (2000). The soluble mammalian sperm factor protein that triggers Ca^{2+} oscillations in eggs: evidence for expression of mRNA(s) coding for sperm factor protein(s) in spermatogenic cells. Biol Cell *92*, 267-275.

227. Parrington,J., Swann,K., Shevchenko,V.I., Sesay,A.K., and Lai,F.A. (1996). Calcium oscillations in mammalian eggs triggered by a soluble sperm protein. Nature *379*, 364-368.

228. Pati,D., Zhang,N., and Plon,S.E. (2002). Linking sister chromatid cohesion and apoptosis:role of Rad21. Mol cell Biol *22*, 8267-8277.

229. Paynton,B.V., Rempel,R., and Bachvarova,R. (1988). Changes in state of adenylation and time course of degradation of maternal mRNAs during oocyte maturation and early embryonic development in the mouse. Dev Biol *129(2)*, 304-314.

230. Petzoldt,U. and Muggleton-Harris,A. (1987). The effect of the nucleocytoplasmic ratio on protein synthesis and expression of a stage-specific antigen in early cleaving mouse embryos. Development *99(4)*, 481-491.

231. Peyrieras,N., Hyafil,F., Louvard,D., Ploegh,H.L., and Jacob,F. (1983). Uvomorulin: A non-integral membrane protein of early mouse embryo. Proc. Natl. Acad. Sci. USA *80*, 6274-6277.

232. Phillips,K.P., Petrunewich,M.A., Collins,J.L., Booth,R.A., Liu,X.J., and Baltz,J.M. (2002). Inhibition of MEK or cdc2 kinase parthenogenetically activates mouse eggs and yields the same phenotypes as Mos(-/-) parthenogenotes. Dev Biol *247*, 210-223.

233. Piko,L. and Clegg,K.B. (1982). Quantitative changes in total RNA, total poly(A), and ribosomes in early mouse embryos. Dev Biol *89(2)*, 362-378.

234. Pratt,H.P., Ziomek,C.A., Reeve,W.J., and Johnson,M.H. (1982). Compaction of the mouse embryo: an analysis of its components. J Embryol Exp Morphol *70*, 113-132.

235. Presicce,G.A. and Yang,X. (1994). Parthenogenetic development of bovine oocytes matured in vitro for 24 hr and activated by ethanol and cycloheximide. Mol Reprod Dev *38*, 380-385.

236. Pribnow,D., Muldoon,L.L., Fajardo,M., Theodor,L., Chen,L.Y., and Magun,B.E. (1992). Endothelin induces transcription of fos/jun family genes: a prominent role for calcium ion. Mol Endocrinol *6*, 1003.

237. Psychoyos,A., Nikas,G., and Gravanis,A. (1995). The role of prostaglandins in blastocyst implantation. Hum Reprod 30-42.

238. Qiu,J., Zhang,W.W., Wu,Z.L., Wang,Y.H., Qian,M., and Li,Y.P. (2003). Delay of ZGA initiation occurred in 2-cell blocked mouse embryos. Cell Res *13*, 179-185.

239. Quinn,P., Barros,C., and Whittingham,D.G. (1982). Preservation of hamster oocytes to assay the fertilizing capacity of human spermatozoa. J Reprod Fertil *66*, 161-168.

240. Ram,P.T. and Schultz,R.M. (1993). Reporter gene expression in G2 of the 1-cell mouse embryo. Dev Biol *156*, 552-556.

241. Rasmussen,C.D. and Means,A.R. (1989). Calmodulin is required for cell-cycle progression during G1 and mitosis. EMBO *8*, 73-82.

242. Rawe,V.Y., Olmedo,S.B., Nodar,F.N., Doncel,G.D., Acosta,A.A., and Vitullo,A.D. (2000). Cytoskeletal organization defects and abortive activation in human oocytes after IVF and ICSI failure. Mol Hum Reprod *6*, 510-516.

243. Reimann,J.D. and Jackson,P.K. (2000). Emi1 is required for cytostatic factor arrest in vertebrate eggs. Nature *416*, 850-854.

244. Richter,K.S., Harris,D.C., Daneshmand,S.T., and Shapiro,B.S. (2001). Quantitative grading of a human blastocyst: optimal inner cell mass size and shape. Fertil Steril *76*, 1157-1167.

245. Rinaudo,P. and Schultz,R.M. (2004). Effects of embryo culture on global pattern of gene expression in preimplantation mouse embryos. Reproduction. 2004 Sep;128(3):301-11. Reproduction *128(3)*, 310-311.

246. Rizos,D., Gutierrez-Adan,A., Perez-Gamelo,S., De La Fuente,J., Boland,M.P., and Lonergan,P. (2003). Bovine embryo culture in the presence or absence of serum: implications for blastocyst development, cryotolerance, and messenger RNA expression. Biol Reprod *68*, 236-243.

247. Rizzuto,R., Bastianutto,C., Brini,M., Murgia,M., and Pozzan,T. (1994). Mitochondrial Ca^{2+} homeostasis in intact cells. J Cell Biol *126*, 1183-1194.

248. Rogers,N.T., Hobson,E., Pickering,S., Lai,F.A., Braude,P., and Swann,K. (2004). Phospholipase Czeta causes Ca^{2+} oscillations and parthenogenetic activation of human oocytes. Reproduction *128*, 697-702.

249. Sagata,N., Watanabe,N., Vande Woude,G.F., and Ikawa,Y. (1989). The c-mos proto-oncogene product is a cytostatic factor responsible for meiotic arrest in vertebrate eggs. Nature *342*, 512-518.

250. Sato,M.S., Yoshitomo,M., Mohri,T., and Miyazaki,S. (1999). Spatiotemporal analysis of $[Ca^{2+}]$i rises in mouse eggs after intracytoplasmic sperm injection (ICSI). Cell Calcium *26*, 49-58.

251. Saunders,C.M., Larman,M.G., Parrington,J., Cox,L.J., Royse,J., Blayney,L.M., Swann,K., and Lai,F.A. (2002). PLC zeta: a sperm-specific trigger of Ca^{2+} oscillations in eggs and embryo development. Development *129*, 3533-3544.

252. Schultz,R.M. (1993). Regulation of zygotic gene activation in the mouse. Bioessays. 1993 Aug;15(8):531-8. Bioessays *15*, 531-538.

253. Schultz,R.M. and Kopf,G.S. (1995). Molecular basis of mammalian egg activation. Curr Top Dev Biol *30*, 21-62.

254. Schultz,R.M. and Worrad,D.M. (1995). Role of chromatin structure in zygotic gene activation in the mammalian embryo. Semin Cell Biol *6*, 201-208.

255. Schwartz,D.A. and Schultz,R.M. (1992). Zygotic gene activation in the mouse embryo: involvement of cyclic adenosine monophosphate-dependent protein kinase and appearance of an AP-1-like activity. Mol Reprod Dev *32*, 209-216.

256. Sette,C., Bevilacqua,A., Biancini,A., Mangia,F., Geremia,R., and Rossi,P. (1997). Parthenogenetic activation of mouse eggs by microinjection of a truncated c-kit tyrosine kinase present in spermatozoa. Development *124*, 2267-2274.

257. Sharov,A.A., Dudekula,D.B., and Ko,M.S. (2005). Genome-wide assembly and analysis of alternative transcripts in mouse. Genome Res *15*, 748-754.

258. Sharov,A.A., Piao,Y., Matoba,R., Dudekula,D.B., Qian,Y., VanBuren,V., Falco,G., Martin,P.R., Stagg,C.A., Bassey,U.C., wang,Y., Carter,M.G., Hamatani,T., Aiba,K., Akutsu,H., Sharova,L., Tanaka,T.S., Kimber,W.L., Yoshikawa,T., Jaradat,S.A., Pantano,S., Nagaraja,R., Boheler,K.R., Taub,D., Hodes,R.J., Longo,D.L., Schlessinger,D., Keller,J., Klotz,E., Kelsoe,G., Umezawa,A., Vescovi,A.L., Rossant,J., Kunath,T., Hogan,B.L., Curci,A., D'Urso,M., Kelso,J., Hide,W., and Ko,M.S. (2003). Transcriptome analysis of mouse stem cells and early embryos. PLoS Biol *1*, E74.

259. Siracusa,G., Whittingham,D.G., Molinaro,M., and Vivarelli,E. (1978). Parthenogenetic activation of mouse oocytes induced by inhibitors of protein synthesis. J Embryol Exp Morphol *43*, 157-166.

260. Spanos,S., Becker,D.L., Winston,R.M., and Hardy,K. (2000). Anti-apoptotic action of insulin-like growth factor-I during human preimplantation embryo development. Biol Reprod *63*, 1413-1420.

261. Spitzer,N.C., Gu,X., and Olson,E. (1994). Action potentials, calcium transients and the control of differentiation of excitable cells. Curr Opin Neurobiol *4*, 70-77.

262. Stacheki,J.J., Yelian,F.D., Leach,R.E., and Armant,D.R. (1994b). Mouse blastocyst outgrowth and implantation rates following exposure to ethanol or A23187 during culture in vitro. J Reprod Fertil *101*, 611-617.

263. Stacheki,J.J., Yelian,F.D., Schultz,J.F., Leach,R.E., and Armant,D.R. (1994a). Blastocyst cavitation is accelerated by ethanol- or ionophore-induced elevation of intracellular calcium. Biol Reprod *50*, 1-9.

264. Stephano,J.L. and Gould,M.C. (1997). The intracellular calcium increase at fertilization in Urechis caupo oocytes: activation without waves. Dev Biol *191*, 53-68.

265. Stricker,S.A. (1995). Time-lapse confocal imaging of calcium dynamics in starfish embryos. Dev Biol *170*, 496-518.

266. Stricker,S.A. (1997). Intracellular injections of a soluble sperm factor trigger calcium oscillations and meiotic maturation in unfertilized oocytes of a marine worm. Dev Biol *186*, 185-201.

267. Stricker,S.A. (1999). Comparative biology of calcium signaling during fertilization and egg activation in animals. Dev Biol *211*, 157-176.

268. Stricker,S.A., Swann,K., Jones,K.T., and Fissore,R.A. (2000). Injections of porcine sperm extracts trigger fertilization-like calcium oscillations in oocytes of a marine worm. Exp Cell Res *257*, 341-347.

269. Subramanian,K. and Meyer,T. (1997). Calcium-induced restructuring of nuclear envelope and endoplasmic reticulum calcium stores. Cell *89*, 963-971.

270. Summers,M.C., McGinnis,L.K., Lawitts,J.A., Raffin,M., and Biggers,J.D. (2000). IVF of mouse ova in a simplex optimized medium supplemented with amino acids. Hum Reprod *15*, 1791-1801.

271. Sun,F.Z., Hoyland,J., Huang,X., Mason,W., and Moor,R.M. (1992). A comparison of intracellular changes in porcine eggs after fertilisation and electroactivation. Development *115*, 947-956.

272. Surani,M.A., Barton,S.C., and Norris,M.L. (1984). Development of reconstituted mouse eggs suggests imprinting of the genome during gametogenesis. Nature *308*, 548-550.

273. Swann,K. (1990). A cytosolic sperm factor stimulates repetitive calcium increases and mimics fertilization in hamster eggs. Development *110*, 1295-1302.

274. Swann,K. (1991). Thimerosal causes calcium oscillations and sensitizes calcium-induced calcium release in unfertilized hamster eggs. FEBS Lett *278*, 175-178.

275. Swann,K. (1992). Different triggers for calcium oscillations in mouse eggs involve a ryanodine-sensitive calcium store. Biochem J *287*, 79-84.

276. Swann,K. (1994). Ca^{2+} oscillations and sensitization of Ca^{2+} release in unfertilized mouse eggs injected with a sperm factor. Cell Calcium *15*, 331-339.

277. Swann,K., Larman,M.G., Saunders,C.M., and Lai,F.A. (2004). The cytosolic sperm factor that triggers Ca^{2+} oscillations and egg activation in mammals is a novel phospholipase C: PLCzeta. Reproduction *127*, 431-439.

278. Swann,K. and Ozil,J. (1994). Dynamics of the calcium signal that triggers mammalian egg activation. Int Rev Cytol. *152*, 183-222.

279. Szollosi,M.S., Kubiak,J.Z., Debey,P., de Pennart,H., Szollosi,D., and Maro,B. (1993). Inhibition of protein kinases by 6-dimethylaminopurine accelerates the transition to interphase in activated mouse oocytes. J Cell Sci *104*, 861-872.

280. Tanaka,T.S. and Ko,M.S. (2004). A global view of gene expression in the preimplantation mouse embryo:morula versus blastocyst. Eur J Obstet Gynecol Reprod Biol *115*, 585-591.

281. Tatone,C., Delle Monache,S., Iorio,R., Caserta,D., Di Cola,M., and Colonna,R. (2002). Possible role for Ca^{2+} calmodilin-dependent kinase II as an effector of the fertilisation Ca^{2+} signal in mouse oocyte activation. Mol Hum Reprod *8*, 750-757.

282. Tatone,C., Iorio,R., Francione,A., Gioia,L., and Colonna,R. (1999). Biochemical and biological effects of KN-93, an inhibitor of calmodulin-dependent protein kinase II, on the initial events of mouse egg activation induced by ethanol. J Reprod Fertil *115*, 151-157.

283. Taylor,C.T., Lawrence,Y.M., Kingsland,C.R., Biljan,M.M., and Cuthbertson,K.S. (1993). Oscillations in intracellular free calcium induced by spermatozoa in human oocytes at fertilization. Hum Reprod *8*, 2174-2179.

284. Tesarik,J., Sousa,M., and Testart,J. (1994). Human oocyte activation after intracytoplasmic sperm injection. Hum Reprod *9*, 511-518.

285. Thompson,E.M., Adenot,P., Tsuji,F.I., and Renard,J.P. (1995). Real time imaging of transcriptional activity in live mouse preimplantation embryos using a secreted luciferase. Proc. Natl. Acad. Sci. USA *92*, 1317-1321.

286. Thouas,G.A., Korfiatis,N.A., French,A.J., Jones,G.M., and Trounson,A.O. (2001). Simplified technique for differential staining of inner cell mass and trophectoderm cells of mouse and bovine blastocysts. Reprod Biomed Online *3*, 25-29.

287. Tomanek,M., Kopecny,V., and Kanka,J. (1989). Genome reactivation in developing early pig embryos: an ultrastructural and autoradiographic analysis. Anat Embryol *180*, 309-316.

288. Tombes,R.M., Simerly,C., Borisy,G.G., and Schatten,G. (1992). Meiosis, egg activation, and nuclear envelope breakdown are differentially reliant on Ca^{2+}, whereas germinal vesicle breakdown is Ca^{2+} independent in the mouse oocyte. J Cell Biol *117*, 799-811.

289. Tulsiani,D.R., Yoshida-Komiya,H., and Araki,Y. (1997). Mammalian fertilization: a carbohydrate-mediated event. Biol Reprod *57*, 487-494.

290. Tung,J.J., Hansen,D.V., Ban,K.H., Loktev,A.V., Summers,M.K., Adler Jr,3., and Jackson,P.K. (2005). A role for the anaphase-promoting complex inhibitor Emi2/XErp1, a homolog of early mitotic inhibitor 1, in cytostatic factor arrest of Xenopus eggs. PNAS *102*, 4318-4323.

291. Uehara,T. and Yanagimachi,R. (1977). Activation of hamster eggs by pricking. J Exp Zool *199*, 269-274.

292. Unoki,M., Nishidate,T., and Nakamura,Y. (2004). ICBP90, an E2F-1 target, recruits HDAC1 and binds to methyl-CpG through its SRA domain. Oncogene *23*, 7601-7610.

293. Uranga,J.A., Pedersen,R.A., and Arechaga,J. (1996). Parthenogenetic activation of mouse oocytes using calcium ionophores and protein kinase C stimulators. Int J Dev Biol *40*, 515-519.

294. Van Soom,A., Vanroose,G., and De Kruif,A. (2001). Blastocyst evaluation by means of differential staining: a practical approach. Reproduction *36*, 29-35.

295. Van Soom,A., Ysebaert,M.T., and De Kruif,A. (1997). Relationship between timing of development, morula morphology, and cell allocation to inner cell mass and trophectoderm in in vitro-produced bovine embryos. Mol. Reprod Dev *47*, 47-56.

296. Verlhac,M.H., Kubiak,J.Z., Weber,M., Geraud,G., Colledge,W.H., Evans,M.J., and Maro,B. (1996). Mos is required for MAP kinase activation and is involved in microtubule organization during meiotic maturation in the mouse. Development *122*, 815-822.

297. Vernet,M., Cavard,C., Zider,A., Fergelot,P., Grimber,G., and Briand,P. (1993). In vitro manipulation of early mouse embryos induces HIV1-LTRlacZ transgene expression. Development *119*, 1293-1300.

298. Vitullo,A.D. and Ozil,J. (1992). Repetitive calcium stimuli drive meiotic resumption and pronuclear development during mouse oocyte activation. Dev Biol *151*, 128-136.

299. Viuff,D., Rickords,L., Offenberg,H., Hyttel,P., Avery,B., Greve,T., Olsaker,I., Williams,J.L., Callesen,H., and Thomsen,P.D. (1999). A high proportion of bovine blastocysts produced in vitro are mixoploid. Biol Reprod *60*, 1273-1278.

300. Wagenknecht,T., Grassucci,R., Frank,J., Saito,A., Inui,M., and Fleischer,S. (1989). Three-dimensional architecture of the calcium channel/foot structure of sarcoplasmic reticulum. Nature *338*, 167-170.

301. Wang,Q.T. and Latham,K.E. (1997). Requirement for protein synthesis during embryonic genome activation in mice. Mol. Reprod Dev *47*, 265-270.

302. Wang,Q.T., Piotrowska,K., Ciemerych,M.A., Milenkovic,L., Scott,M.P., Davis,R.W., and Zernicka-Goetz,M. (2004). A genome-wide study of gene activity reveals developmental signaling pathways in the preimplantation mouse embryo. Dev Cell *6(1)*, 133-144.

303. Wassarman,P.M. (1988). Zona pellucida glycoproteins. Annu Rev Biochem *57*, 415-442.

304. Wassarman,P.M. and Letourneau,G.E. (1976). RNA synthesis in fully-grown mouse oocytes. Nature *261*, 73-74.

305. Wasserman,W.J. and Smith,L.D. (1978). The cyclic behavior of a cytoplasmic factor controlling nuclear membrane breakdown. J Cell Biol *78*, R15-R22.

306. Watson,A.J. and Barcroft,L.C. (2001). Regulation of blastocyst formation. Front Biosci *6*, D730.

307. Whitaker,M. (1996). Control of meiotic arrest. Rev Reprod *1*, 127-135.

308. Whitten,W.K. (1956). Culture of tubal mouse ova. Nature *177*, 96.

309. Whitten,W.K. and Biggers,J.D. (1968). Complete development in vitro of the pre-implantation stages of the mouse in a simple chemically defined medium. J Reprod Fertil *17*, 399-401.

310. Wiekowski,M., Miranda,M., and Depamphilis,M.L. (1991). Regulation of gene expression in preimplantation mouse embryos: effects of the zygotic clock and the first mitosis on promoter and enhancer activities. Dev Biol *147*, 403-414.

311. Williams,C.J., Mehlmann,L.M., Jaffe,L.A., Kopf,G.S., and Schultz,R.M. (1998). Evidence that Gq family G proteins do not function in mouse egg activation at fertilization. Dev Biol *198*, 116-127.

312. Winkel,G.K., Ferguson,J.E., Takeichi,M., and Nuccitelli,R. (1990). Activation of protein kinase C triggers premature compaction in the four-cell stage mouse embryo. Dev Biol *138*, 1-15.

313. Winston,N.J., Johnson,M.H., Pickering,S., and Braude,P. (1991). Parthenogenetic activation and development of fresh and aged human oocytes. Fertil Steril *56*, 904-912.

314. Winston,N.J. and Maro,B. (1995). Calmodulin-dependent protein kinase II is activates transiently in ethanol-stimulated mouse oocytes. Dev Biol *170*, 350-352.

315. Winston,N.J., McGuinness,O., Johnson,M.H., and Maro,B. (1995). The exit of mouse oocytes from meiotic M-phase requires an intact spindle during intracellular calcium release. J Cell Sci. *108*, 143-151.

316. Wolosker,H., Kline,D., Bian,Y., Blackshaw,S., Cameron,A.M., Fralich,T.J., Schnaar,R.L., and Snyder,S.H. (1998). Molecularly cloned mammalian glucosamine-6-phosphate deaminase localizes to transporting epithelium and lacks oscillin activity. FASEB J *12*, 91-99.

317. Worrad,D.M., Ram,P.T., and Schultz,R.M. (1994). Regulation of gene expression in the mouse oocyte and early preimplantation embryo: developmental changes in Sp1 and TATA box-binding protein, TBP. Development *120*, 2347-2357.

318. Wu,H., He,C.L., and Fissore,R.A. (1997). Injection of a porcine sperm factor triggers calcium oscillations in mouse oocytes and bovine eggs. Mol. Reprod Dev *46*, 176-189.

319. Xu,K., Abbott,A., Kopf,G.S., Schultz,R.M., and Ducibella,T. (1997). Spontaneous activation of ovulated mouse eggs: time-dependent effects on M-phase exit, cortical granule exocytosis, maternal messenger ribonucleic acid recruitment, and inositol 1,4,5-trisphosphate sensitivity. Biol Reprod *57*, 743-750.

320. Yoda,A., Oda,S., Shikano,T., Kouchi,Z., Awaji,T., Shirakawa,H., Kinoshita,K., and Miyazaki,S. (2004). Ca^{2+} oscillation-inducing phospholipase C zeta expressed in mouse eggs is accumulated to the pronucleus during egg activation. Dev Biol *268*, 245-257.

321. Yong,P., Gu,Z., Wang,J.R., and Tso,J.K. (2002). Antibodies against the C-terminal peptide of rabbit oviductin inhibit mouse early embryo development to pass 2-cell stage. Cell Res *12*, 69-78.

322. Zakhartchenko,V., Alberio,R., Stojkovic,M., Prelle,K., Schernthaner,W., Stojkovic,P., Wenigerkind,H., Wanke,R., Duchler,M., Steinborn,R., Mueller,M., Brem,G., and Wolf,E. (1999). Adult cloning in cattle: potential of nuclei from a permanent cell line and from primary cultures. Mol Reprod Dev *54*, 264-272.

323. Zeng,F. and Schultz,R.M. (2003). Gene expression in mouse oocytes and preimplantation embryos:use of suppression subtractive hybridisation to identify oocyte and embryo-specific genes. Biol Reprod *68*, 31-39.

324. Zhang,J., Wang,C.W., Blaszcyzk,A., Grifo,J.A., Ozil,J., Haberman,E., Adler,A., and Krey,L.C. (1999). Electrical activation and in vitro development of human oocytes that fail to fertilize after intracytoplasmic sperm injection. Fertil Steril. 1999 Sep;72(3):509-12. Fertil Steril *72*, 509-512.

325. Ziebe,S., Peteren,K., Lindenberg,S., Andersen,A.G., Gabrielsen,A., and Andersen,A.N. (1997). Embryo morphology or cleavage stage: how to select the best embryos for transfer after in-vitro fertilization. Hum Reprod *12*, 1545-1549.

Acknowledgments

I must first thank my supervisor Prof. Karl Swann for giving me the opportunity to carry out a Ph.D. in his lab and also for providing guidance and support throughout the last three years.

I am indebted to Dr. John Carroll for 'adopting' me during the final year of my Ph.D. and pulling out all the stops to ensure my time in his lab was happy and productive.

I would also like to thank Dr. Minoru Ko who kindly welcomed me into his laboratory at the National Institute of Heath, Baltimore, MD. for 6 weeks and who allowed me to experience some first class research.

Some excellent people have helped me during the three years of my Ph.D. and they are (in no particular order) Mark Larman, Guillaume Halet, Richard Tunwell, Victoria Nixon, Remi Dumollard, Rachel Webb, Amanda Carr, Helen Owen, David Whitmore, Sung Lim Lee, Kazuhiro Aiba and Alexi Sharov.

During my Ph.D. I have been financially supported by the Medical Research Council (MRC) and have acquired travel scholarships from the Society of Reproduction (SRF) and Bogue fellowship fund, UCL.

A special thanks to my parents, Usha and Norman Rogers and also to my "gotten" parents George and Anita Roberts who have been a never-ending stream of support, encouragement and financial help when times have seemed so bleak.

I am mostly grateful to Chrissy h. Roberts who has supported me throughout my PhD without question and who has never doubted my ability to succeed in what ever I have chosen to do. I hope I have made you proud.

Appendices

KSOM (simplex optimised media: Summers et al., 1995; Lawitts and Biggers, 1998; Summers et al., 2000).

HEPES-KSOM: For embryo collection and stage work

Composition

			lx stock			lOx stock	
	Ingredient	**mM**	**g/L**	**ml/L**		**g/0.5L**	**ml/0.5L**
1	**NaC1**	**95**	**5.55**	**N/A**		**27.75**	**N/A**
2	**KCI**	**2.5**	**0.185**	**N/A**		**0.925**	**N/A**
3	**KH2PO4**	**0.35**	**0.0476**	**N/A**		**0.238**	**N/A**
4	**Sodium Pyruvate**	**0.2**	**0.022**	**N/A**		**0.11**	**N/A**
5	**L-Glutamine**	**1**	**0.146**	**N/A**		**0.73**	**N/A**
6	**Streptomycin Sulfate**	**N/A**	**0.05**	**N/A**		**0.25**	**N/A**
7	**Penicillin G**	**N/A**	**0.063**	**N/A**		**0.315**	**N/A**
8	**EDTA (tetrasodium salt)**	**0.01**	**0.0038**	**N/A**		**0.019**	**N/A**
9	**MgSO4.7H2O**	**0.2**	**0.0493**	**N/A**		**0.2465**	**N/A**
10	**Sodium Lactate (Syrup)**	**10**	**N/A**	**1.474**		**N/A**	**7.37**
11	**NaHCO3**	**4**	**0.0336**	**N/A**		**1.68**	**N/A**
12	**Phenol Red**	**N/A**	**0.011**	**N/A**		**0.055**	**N/A**
13	**HEPES**	**20**	**4.76**	**N/A**		**23.8**	**N/A**
14	**CaC1.2H2O**	**1.71**	**0.251**	**N/A**		**N/A**	**N/A**
15	**Glucose**	**0.2**	**0.036**	**N/A**		**N/A**	**N/A**
16	**BSA**	**N/A**	**N/A**	**1**		**N/A**	**N/A**

lOx stocks containing components 1-13 were prepared, pH was adjusted to 7.3-7.4 using 200-220 µl of 0.5 M NaOH and solution was filter sterilised through a pre-soaked 0.45µM filter.

10x solutions were stored at -20°C. Components 14-16 were added on preparation of lx working solutions.

1.71 M stocks of $CaC1.2H_2O$ were stored -20°C and dilution 1/1000 in final 1X working solutions.

0.2 M Glucose solutions were made weekly and stored at 4-8°C. BSA stocks were kept at 4 mg ml^{-1}

KSOM: used for culturing embryos

		1x stock			10x stock	
	Ingredient	**mM**	**g/L**	**ml/L**	**g/0.5L**	**ml/0.5L**
1	**NaCl**	**95**	**5.55**	**N/A**	**27.75**	**N/A**
2	**KCl**	**2.5**	**0.185**	**N/A**	**0.925**	**N/A**
3	**KH2PO4**	**0.35**	**0.0476**	**N/A**	**0.238**	**N/A**
4	**Sodium Pyruvate**	**0.2**	**0.022**	**N/A**	**0.11**	**N/A**
5	**L-Glutamine**	**1**	**0.146**	**N/A**	**0.73**	**N/A**
6	**Streptomycin Sulfate**	**N/A**	**0.05**	**N/A**	**0.25**	**N/A**
7	**Penicillin G**	**N/A**	**0.063**	**N/A**	**0.315**	**N/A**
8	**EDTA (tetrasodium salt)**	**0.01**	**0.0038**	**N/A**	**0.019**	**N/A**
9	**MgSO4.7H2O**	**0.2**	**0.0493**	**N/A**	**0.2465**	**N/A**
10	**Sodium Lactate (Syrup)**	**11.8**	**N/A**	**1.74**	**N/A**	**8.7**
11	**NaHCO3**	**25**	**2.1**	**N/A**	**10.5**	**N/A**
12	**Phenol Red**	**N/A**	**0.011**	**N/A**	**0.055**	**N/A**
13	**CaC1.2H2O**	**1.71**	**0.251**	**N/A**	**N/A**	**N/A**
14	**Glucose**	**0.2**	**0.036**	**N/A**	**N/A**	**N/A**
15	**BSA**	**N/A**	**N/A**	**1**	**N/A**	**N/A**
16	**Essential amino acids (50x concentrate)**		**10**			
17	**Nonessential amino acids (100x concentrate)**		**5**			

For embryo development in 5% CO_2 environment

1x stocks (made every week) containing components 1-12 were prepared and pH was adjusted to 7.6 using 10-20 µL of 0.5 M NaOH. Solution was filter sterilised through a pre-soaked 0.45µM filter and left to equilibrate to pH 7.4 overnight in a CO_2 incubator.

Components 13-17 were added during the preparation of 1x working solutions. 1.71 M stocks of $CaC1.2H_2O$ were stored -20°C and dilution 1/1000 in final 1X working solutions. 0.2 M Glucose solutions were made weekly and stored at 4-8°C. BSA stocks were kept at 4 mg ml^{-1}. Essential and nonessential amino acids stocks were from Gibco

Table 8.1 Genes overexpressed (>1.5 fold) in 8-cell embryos after parthenogenetic egg activation with Sr^{2+}

Fold change	Common symbol	Gene Name
6.297	3632440L23 Rik	*RIKEN cDNA 3632440L23 gene*
4.848	1500009C09Rik	*Mus musculus cDNA clone IMAGE:4951210, partial cds.*
3.776	A430069L09 Rik	*RIKEN cDNA:A430069L09 gene*
3.698	Trpc7	*transient receptor potential cation channel, subfamily C, member 7*
3.477	Dsc1	*Dermatopontin*
3.271	Eif3s10	*Eurakyotic translation initiation factor 3,subunit 10 (theta)*
3.229	S100a11	*S100 calcium binding protein A11 (calizzarin)*
3.111	LOC328660	*similar to Catechol O-methyltransferase*
3.025	Kera	*keratocan*
2.947	Htr1f	*5-hydroxytryptamine (serotonin) receptor 1F*
2.901	Prtn3	*proteinase 3*
2.857	1700019B01Rik	*RIKEN cDNA 1700019B01 gene*
2.795	Pigf	*phosphatidylinositol glycan, class F*
2.679	Tgfbr2	*Transforming growth factor, beta receptor II*
2.656	Cd97	*CD97 antigen*
2.65	Pink1	*PTEN induced putative kinase 1*
2.628	Rpl29	*ribosomal protein L29*
2.627	2900097C17Rik	*RIKEN cDNA 2900097C17 gene*
2.61	Set	*SET translocation*
2.593	Clmn	*calmin*
2.569	Sqle	*squalene epoxidase*
2.553	1190002C06Rik	*RIKEN cDNA 1190002C06 gene*
2.55	Pcp4l1	*Purkinje cell protein 4-like 1*
2.539	Gabrp	*gamma-aminobutyric acid (GABA-A) receptor, pi*
2.476	Ysg2	*yolk sac gene 2*
2.455	Hdac10	*histone deacetylase 10*
2.436	Sema6b	*sema domain, transmembrane domain (TM), and cytoplasmic domain 6B*
2.435	Hsd17b4	*hydroxysteroid (17-beta) dehydrogenase 4*
2.434	Gab1	*growth factor receptor bound protein 2-associated protein 1*
2.423	Dld	*dihydrolipoamide dehydrogenase*
2.421	Tm4sf1	*transmembrane 4 superfamily member 1*
2.418	1700010M22Rik	*RIKEN cDNA 1700010M22 gene*
2.387	Cri1	*CREBBP/EP300 inhibitory protein 1*
2.365	9430057O19Rik	*RIKEN cDNA 9430057O19 gene*
2.36	Lss	*lanosterol synthase*
2.628	Rpl9	*ribosomal protein L9*
2.343	Bloc1s3	*biogenesis of lysosome-related organelles complex-1, subunit 3*
2.326	Triobp	*TRIO and F-actin binding protein*
2.32	Rnf25	*ring finger protein 25*
2.307	Cpeb1	*cytoplasmic polyadenylation element binding protein 1*
2.304	1810037G04Rik	*RIKEN cDNA 1810037G04 gene*
2.296	Tdh	*L-threonine dehydrogenase*
2.295	Scn8a	*sodium channel, voltage-gated, type VIII, alpha polypeptide*
2.293	Insig2	*insulin induced gene 2*
2.284	Psx2	*placenta specific homeobox 2*

2.271	2310047C04Rik	*RIKEN cDNA 2310047C04 gene.*
2.255	BC027663	*cDNA sequence BC027663*
2.25	Card10	*caspase recruitment domain family, member 10*
2.225	Dscr6	*Down syndrome critical region homolog 6 (human)*
2.213	Muc2	*mucin 2*
2.213	Ube2d3	*RIKEN cDNA G430121H02*
2.208	Ube2d3	*RIKEN cDNA 13.20-3B3*
2.206	Marcks	*myristoylated alanine rich protein kinase C substrate*
2.201	Fbxo3	*F-box only protein 3*
2.193	Srr	*serine racemase*
2.19	Trim8	*tripartite motif protein 8*
2.189	D630045J12Rik	*ATPase, H+ transporting, lysosomal V0 subunit A isoform 4*
2.186	D430038O12 Rik	*RIKEN cDNA D430038O12 gene.*
2.184	Igh	*Mus musculus anti-DNA autoantibody heavy chain variable*
2.159	Tnfrsf18	*tumor necrosis factor receptor superfamily, member 18*
2.158	D630042C05 Rik	*RIKEN cDNA D630042C05 gene*
2.157	2310057D15Rik	*RIKEN cDNA 2310057D15 gene*
2.157	Csmd2, Gm139	*CUB and Sushi multiple domains 2*
2.154	Cldn4	*claudin 4*
2.153	1200013B08Rik	*RIKEN cDNA 1200013B08 gene*
2.153	Gm1873, Hspd1	*heat shock protein 1 (chaperonin)*
2.148	Rap2ip	*Rap2 interacting protein*
2.147	Tebp	*telomerase binding protein, p23*
2.146	Ndp52	*nuclear domain 10 protein 52*
2.137	2810016G10Rik	*RIKEN cDNA 2810016G10 gene*
2.13	Aatk	*apoptosis-associated tyrosine kinase*
2.123	Aqp5	*aquaporin 5*
2.123	Edf1	*endothelial differentiation-related factor 1*
2.115	Rnf14	*ring finger protein 14*
2.114	Gpnmb	*glycoprotein (transmembrane) nmb*
2.109	D930026A11 Rik	*RIKEN cDNA D930026A11 gene*
2.106	Dhrs7	*dehydrogenase/reductase (SDR family) member 7*
2.106	V1re11	*vomeronasal 1 receptor, E11*
2.102	Rap1gds1	*RAP1, GTP-GDP dissociation stimulator 1*
2.089	Dock2	*dedicator of cyto-kinesis 2*
2.082	Rab7l1	*RAB7, member RAS oncogene family-like 1*
2.08	Ly6h	*lymphocyte antigen 6 complex, locus H*
2.076	Zfp235	*zinc finger protein 235*
2.074	D930039E07 Rik	*RIKEN cDNA D930039E07 gene*
2.069	D930046I15 Rik	*RIKEN cDNA D930046I15 gene*
2.068	Icam4	*intercellular adhesion molecule 4, Landsteiner-Wiener blood group*
2.06	Copb1	*coatomer protein complex, subunit beta 1*
2.059	BC021367	*cDNA sequence BC021367*
2.056	D630029K19Rik	*RIKEN cDNA D630029K19*
2.05	Spg20	*spastic paraplegia 20, spartin (Troyer syndrome) homolog (human)*
2.049	E030038G04 Rik	*RIKEN cDNA E030038G04.gene*
2.046	Nfrkb	*nuclear factor related to kappa B binding protein*
2.043	Rps6kb2	*ribosomal protein S6 kinase, polypeptide 2*
2.039	Cntnap2	*contactin associated protein-like 2*
2.032	Ptx3	*pentaxin related gene*
2.32	Rpl10	*ribosomal protein 10*
2.03	Man2b2	*mannosidase 2, alpha B2*
2.026	A530089G01 Rik	*RIKEN cDNA A530089G01 gene*
2.02	Smarca5	*SWI/SNF related, matrix associated, actin dependent regulator of chromatin,*

		subfamily a, member 5
2.015	Btg1	*B-cell translocation gene 1, anti-proliferative*
2.014	2310043N10Rik	*RIKEN cDNA 2310043N10 gene*
2.003	D630050F13 Rik	*RIKEN cDNA D630050F13.gene*
2.001	Prkar1a	*protein kinase, cAMP dependent regulatory, type I, alpha*
1.992	Aldob	*aldolase 2, B isoform*
1.99	Syk	*spleen tyrosine kinase*
1.989	Cldn18	*claudin 18*
1.989	A230086K09 Rik	*RIKEN cDNA A230086K09 gene*
1.983	Cog2	*component of oligomeric golgi complex 2*
1.981	Ckmt1	*creatine kinase, mitochondrial 1, ubiquitous*
1.98	Prlpc3	*prolactin-like protein C 3*
1.976	BC028278	*cDNA sequence BC028278*
1.976	Gm44	*gene model 44, (NCBI)*
1.973	Palmd	*palmdelphin*
1.967	Kcnj11	*potassium inwardly rectifying channel, subfamily J, member 11*
1.966	Ywhae	*tryptophan 5-monooxygenase activation protein, epsilon polypeptide*
1.964	Supt4h	*suppressor of Ty 4 homolog (S. cerevisiae)*
1.958	Xpot	*W093B05 GGTC Gene Trap Library GV03C04 Mus musculus cDNA*
1.956	Scye1	*small inducible cytokine subfamily E, member 1*
1.955	9430047F21 Rik	*RIKEN cDNA 9430047F21 gene*
1.953	Serpinb6c	*serine (or cysteine) proteinase inhibitor, clade B, member 6c*
1.952	Dctn2	*dynactin 2*
1.947	Igvh	*Immunoglobulin heavy chain variable*
1.946	Nek6	*NIMA (never in mitosis gene a)-related expressed kinase 6*
2.35	Rps27a	*ribosomal protein S27a*
1.941	Lrrc15	*leucine rich repeat containing 15*
1.938	Gsc	*goosecoid*
1.935	Rgs9	*regulator of G-protein signaling 9*
1.931	Zfp353	*zinc finger protein 353*
1.927	B530045E10Rik	*RIKEN cDNA B530045E10 gene*
1.923	Otop1	*otopetrin 1*
1.918	Fez2	*fasciculation and elongation protein zeta 2 (zygin II)*
1.918	Has1	*hyaluronan synthase1*
1.917	4932412D23Rik	*RIKEN cDNA 4932412D23 gene*
1.916	Igy	*Mus musculus anti-human apolipoprotein A monoclonal antibody*
1.916	Rhot1	*ras homolog gene family, member T1*
1.912	Clecsf9	*C-type (calcium dependent, recognition domain) lectin, superfamily member 9*
1.908	Per1	*period homolog 1 (Drosophila)*
1.906	Hadhb	*hydroxyacyl-Coenzyme A dehydrogenase*
1.904	Pim1	*proviral integration site 1*
1.9	BC037006	*cDNA sequence BC037006*
1.898	Gzma	*granzyme A*
1.897	LOC381980	*similar to Catechol O-methyltransferase*
1.894	Dyrk1b	*dual-specificity tyrosine-(Y)-phosphorylation regulated kinase 1b*
1.883	Gm1228	*G040G03 GGTC Gene Trap Library GV07C05*
1.881	Cocoacrisp	*Cocoacrisp*
1.875	Pcdh7	*protocadherin 7*
1.875	Trpm2	*transient receptor potential cation channel, subfamily M, member 2*
1.873	Sesn1	*sestrin 1*
1.871	1110049G11Rik	*RIKEN cDNA 1110049G11 gene*
1.866	Mdfi	*MyoD family inhibitor*
1.865	Fcna	*ficolin A*
1.865	Ly6c	*lymphocyte antigen 6 complex, locus C*

1.86	9630015D15Rik	*RIKEN cDNA 9630015D15 gene*
1.86	Rhoq	*ras homolog gene family, member Q*
1.86	Tusc5	*tumor suppressor candidate 5*
1.856	D5wsu178e	*DNA segment, Chr 5, Wayne State University 178, expressed*
1.854	Sc5d	*sterol-C5-desaturase (fungal ERG3, delta-5-desaturase)*
1.852	Ccl4	*chemokine (C-C motif) ligand 4*
1.85	Ky	*kyphoscoliosis*
1.849	Cxcl2	*chemokine (C-X-C motif) ligand 2*
1.849	Zfp111	*zinc finger protein 111*
1.844	Car4	*carbonic anhydrase 4*
1.801	Cd36	*CD36 antigen*
1.831	Slc12a7	*solute carrier family 12, member 7*
1.831	9630005I20 Rik	*RIKEN cDNA 9630005I20 gene*
1.829	Tnfrsf5	*tumor necrosis factor receptor superfamily, member 5*
1.828	2410118I19Rik	*Mus musculus cDNA clone IMAGE:4458730, partial cds.*
1.813	B230399E16Rik	*RIKEN cDNA B230399E16 gene*
1.812	0610007N19Rik	*RIKEN cDNA 0610007N19 gene*
1.886	Mrpl15	*mitochondrial ribosomal protein L15*
1.81	Muc 2	*Mucin 2*
1.809	Hoxa1	*homeo box A1*
1.802	Arid5b	*AT rich interactive domain 5B (Mrf1 like)*
1.802	Wig1	*wild-type p53-induced gene 1*
1.801	Ccpg1	*cell cycle progression 1*
1.801	Trhde	*thyrotropin-releasing hormone degrading ectoenzyme*
1.8	Ncr1	*natural cytotoxicity triggering receptor 1*
1.799	Ccl20	*chemokine (CC motif) ligand 20*
1.786	Large	*like-glycosyltransferase*
1.784	2610209M04Rik	*RIKEN cDNA 2610209M04 gene*
1.782	Phc1	*polyhomeotic-like 1 (Drosophila)*
1.777	Commd8	*COMM domain containing 8*
1.771	Commd9	*COMM domain containing 9*
1.77	A830080H07Rik	*RIKEN cDNA A830080H07 gene*
1.77	Slc39a1	*solute carrier family 39 (zinc transporter), member 1*
1.765	Fbxo15	*A017F06 GGTC Gene Trap Library GV03C04*
1.763	Uhrf1	*ubiquitin-like, containing PHD and RING finger domains, 1*
1.751	Gabarapl1	*gamma-aminobutyric acid (GABA(A)) receptor-associated protein-like 1*
1.751	Muted	*muted*
1.749	Pdcd4	*programmed cell death 4*
1.747	Nudt1	*nudix (nucleoside diphosphate linked moiety X)-type motif 1*
1.745	Coq7	*demethyl-Q 7*
1.741	Sfrs6	*splicing factor, arginine/serine-rich 6*
1.736	Mb	*myoglobin*
1.735	Arpc1a	*actin related protein 2/3 complex, subunit 1A*
1.735	G630071F17 Rik	*RIKEN cDNA G630071F17.gene*
1.726	Idb3	*inhibitor of DNA binding 3*
1.726	Slc34a2	*solute carrier family 34 (sodium phosphate), member 2*
1.721	Grina	*glutamate receptor, ionotropic, N-methyl D-asparate-associated protein 1*
1.72	Svil	*supervillin*
1.716	2810442I22Rik	*RIKEN cDNA 2810442I22 gene*
1.716	Np15	*nuclear protein 15.6*
1.714	Rsbn1	*rosbin, round spermatid basic protein 1*
1.711	5730421E18Rik	*RIKEN cDNA 5730421E18 gene*
1.71	1300006C06Rik	*RIKEN cDNA 1300006C06 gene*
1.709	8030499P14 Rik	*RIKEN cDNA 8030499P14 gene*

1.701	B430201L21 Rik	*RIKEN cDNA B430201L21 gene*
1.699	Pgam1	*phosphoglycerate mutase 1*
1.697	Capn11	*Mus musculus calpain 11 (Capn11) mRNA, complete cds.*
1.694	A430079K02. Rik	*RIKEN cDNA A430079K02.gene*
1.693	F730011C10 Rik	*RIKEN cDNA F730011C10 gene*
1.681	Pdgfa	*platelet derived growth factor, alpha*
1.68	Sec6l1	*SEC6-like 1 (S. cerevisiae)*
1.677	Pcdha1	*protocadherin alpha 1*
1.676	Egr3	*early growth response 3*
1.66	Cxcl12	*chemokine (C-X-C motif) ligand 12*
1.651	Kdelc1	*KDEL (Lys-Asp-Glu-Leu) containing 1*
1.644	Bloc1s1	*biogenesis of lysosome-related organelles complex-1, subunit 1*
1.636	Krt2-8	*keratin complex 2, basic, gene 8*
1.946	Rps3a	*ribosomal protein S3a*
1.627	Klhl17,	*kelch-like 17 (Drosophila)*
1.612	Axl	*AXL receptor tyrosine kinase*
1.61	Eno2	*enolase 2, gamma neuronal*
1.603	Zadh2	*zinc binding alcohol dehydrogenase, domain containing 2*
1.591	BC013529	*cDNA sequence BC013529*
1.586	6330409N04Rik	*RIKEN cDNA 6330409N04 gene*
1.569	Adamts13	*a disintegrin-like and metalloprotease, thrombospondin type 1 motif, 13*
1.568	3930401E15Rik	*RIKEN cDNA 3930401E15 gene*
1.565	2900097C17Rik	*RIKEN cDNA 2900097C17 gene*

Table 8.2 Genes overexpressed (>1.5 fold) in 8-cell embryos after parthenogenetic egg activation with CX

Fold change	Common Symbol	Gene Name
9.774	Cdkn1c	*cyclin-dependent kinase inhibitor 1C (P57)*
8.171	BC030336	*cDNA sequence BC030336*
7.76	Slco3a1	*solute carrier organic anion transporter family, member 3a1*
6.861	Stra8	*stimulated by retinoic acid gene 8*
6.477	Ifnar1	*interferon (alpha and beta) receptor 1*
6.119	Bcan	*brevican*
5.908	Gadd45b	*growth arrest and DNA-damage-inducible 45 beta*
5.344	Aloxe3	*arachidonate lipoxygenase 3*
5.12	Pcdhb9	*protocadherin beta 9*
5.069	Oog1	*oogenesin 1*
5.026	Zcchc8	*zinc finger, CCHC domain containing 8*
4.913	Prlr, AI987712	*Mus musculus prolactin receptor (Prlr), mRNA*
4.896	Dhh	*desert hedgehog*
4.886	Ier5	*immediate early response 5*
4.752	Pdcl	*phosducin-like*
4.608	Tcf3	*transcription factor 3*
4.475	Tfpi	*tissue factor pathway inhibitor*
4.373	Brdt	*bromodomain, testis-specific*
4.359	Plcd4	*phospholipase C, delta 4*
4.133	Ches1	*checkpoint supressor 1*
4.114	Eif2c4	*eukaryotic translation initiation factor 2C, 4*
4.109	Rps6ka6	*ribosomal protein S6 kinase polypeptide 6*
4.108	AF067063	*cDNA sequence AF067063*

4.086	Tiam2	*T-cell lymphoma invasion and metastasis 2*
4.068	Fem1c	*fem-1 homolog c (C.elegans)*
4.056	1300019C06Rik	*RIKEN cDNA 1300019C06 gene*
4.054	Pycard	*PYD and CARD domain containing*
3.995	Nup133	*nucleoporin 133*
3.94	Arg2	*arginase type II*
3.857	Map3k9	*mitogen-activated protein kinase kinase kinase 9*
3.83	Itpr1	*inositol 1, 4, 5-triphosphate receptor 1*
3.824	Evpl	*envoplakin*
3.771	G630049C14Rik	*RIKEN cDNA G630049C14 gene*
3.761	Shmt2	*serine hydroxymethyl transferase 2 (mitochondrial)*
3.727	A430104N18Rik	*RIKEN cDNA A430104N18 gene*
3.706	Smad1	*MAD homolog 1 (Drosophila)*
3.687	Asb4	*ankyrin repeat and SOCS box-containing protein 4*
3.658	5830411E10Rik	*RIKEN cDNA 5830411E10 gene*
3.569	Plxnc1	*plexin C1*
3.566	9830130M13 Rik	*Mus musculus hypothetical protein 9830130M13 (9830130M13), mRNA*
3.535	4932432N11Rik	*RIKEN cDNA 4932432N11 gene*
3.501	2210413P12 Rik	*RIKEN cDNA 2210413P12 gene*
3.443	E430025L02 Rik	*RIKEN cDNA E430025L02 gene*
3.418	Ddx26	*DEAD/H (Asp-Glu-Ala-Asp/His) box polypeptide 26*
3.418	Ripk3	*receptor-interacting serine-threonine kinase 3*
3.407	5730438N18Rik	*RIKEN cDNA 5730438N18 gene*
3.392	Hic2	*hypermethylated in cancer 2*
3.375	1810043M15Rik	*RIKEN cDNA 1810043M15 gene*
3.341	AA536743	*expressed sequence AA536743*
3.291	Map3k5	*mitogen activated protein kinase kinase kinase 5*
3.278	D16Ertd472e	*DNA segment, Chr 16, ERATO Doi 472, expressed*
3.269	Parp9	*poly (ADP-ribose) polymerase family, member 9*
3.261	Cdc25a	*cell division cycle 25 homolog A (S. cerevisiae)*
3.253	Rom1	*rod outer segment membrane protein 1*
3.214	A230054D04Rik,	*W073A02 GGTC Gene Trap Library GV03C04 Mus musculus cDNA clone W073A02,*
3.201	E230022H04Rik	*RIKEN cDNA E230022H04 gene*
3.187	LOC382105	*Mus musculus similar to RIKEN cDNA E330009P21 gene (LOC382105), mRNA*
3.175	Mospd1	*motile sperm domain containing 1*
3.162	Pcdh8	*protocadherin 8*
3.149	Snai1	*snail homolog 1 (Drosophila)*
3.136	Dhx36	*DEAH (Asp-Glu-Ala-His) box polypeptide 36*
3.123	Zfyve20	*zinc finger, FYVE domain containing 20*
3.12	4930555B11Rik	*RIKEN cDNA 4930555B11 gene*
3.12	C330023M02Rik	*RIKEN cDNA C330023M02 gene*
3.112	C230025N18 Rik	*RIKEN cDNA:C230025N18*
3.097	1700081L11Rik	*RIKEN cDNA*
3.092	Osm	*oncostatin M*
3.088	Cul5	*cullin 5*
3.068	3100002L24Rik	*RIKEN cDNA 3010027A04 gene*
3.066	Gdap10	*ganglioside-induced differentiation-associated-protein 10*
3.022	Papln	*papilin, proteoglycan-like sulfated glycoprotein*
3.019	Egr1	*early growth response 1*
3.001	Zfp131	*zinc finger protein 131*
3	Trpm7	*transient receptor potential cation channel, subfamily M, member 7*
2.981	Mkiaa1686	*pleckstrin homology domain containing, family A member 5*
2.966	4931413I07Rik	*RIKEN cDNA 4931413I07 gene*

2.955	Ddit4	*DNA-damage-inducible transcript 4*
2.953	Tac4	*tachykinin 4*
2.951	Mlze	*melanoma-derived leucine zipper, extra-nuclear factor*
2.933	2610511E22Rik	*RIKEN cDNA 2610511E22 gene*
2.932	Pum1	*pumilio 1 (Drosophila)*
2.927	Cbx1	*chromobox homolog 1 (Drosophila HP1 beta)*
2.924	Cables1	*Cdk5 and Abl enzyme substrate 1*
2.92	1700022C02Rik	*RIKEN cDNA 1700022C02 gene*
2.901	Gm92	*gene model 92 , (NCBI)*
2.891	Kcnk4	*potassium channel, subfamily K, member 4*
2.876	Slc38a5	*solute carrier family 38, member 5*
2.862	Sfrs12	*splicing factor, arginine/serine-rich 12*
2.858	Lrp1	*low density lipoprotein receptor-related protein 1*
2.851	Rock1	*Rho-associated coiled-coil forming kinase 1*
2.82	Ell2	*elongation factor RNA polymerase II 2*
2.815	Derl3	*Der1-like domain family, member 3*
2.8	Fgfbp1	*fibroblast growth factor binding protein 1*
2.786	Gdf9	*growth differentiation factor 9*
2.75	Tcea1	*transcription elongation factor A (SII) 1*
2.735	B230218L05Rik	*RIKEN cDNA B230218L05 gene*
2.734	Ercc4	*excision repair cross-complementing rodent repair deficiency, complementation group 4*
2.726	Uxs1, Gm1937	*UDP-glucuronate decarboxylase 1*
2.697	Arid4b	*AT rich interactive domain 4B (Rbp1 like)*
2.688	Gm443	*gene model 443, (NCBI)*
2.671	Smad4	*MAD homolog 4 (Drosophila)*
2.664	Ddx55	*DEAD (Asp-Glu-Ala-Asp) box polypeptide 55*
2.66	Pum2	*pumilio 2 (Drosophila)*
2.632	4930447I22Rik	*RIKEN cDNA 4930447I22 gene*
2.62	Col17a1	*procollagen, type XVII, alpha 1*
2.619	Ero1l	*ERO1-like (S. cerevisiae)*
2.618	Glce	*glucuronyl C5-epimerase*
2.615	A230054D04 Rik,	*RIKEN cDNA A230054D04*
2.613	Adam10	*a disintegrin and metalloprotease domain 10*
2.581	A930019P04 Rik	*RIKEN cDNA A930019P04*
2.579	Shbg	*sex hormone binding globulin*
2.576	4930500O09Rik	*RIKEN cDNA 4930500O09 gene*
2.567	B130054P17 Rik	*RIKEN cDNA B130054P17*
2.559	Zfp68	*zinc finger protein 68*
2.556	Mbd3l2	*methyl-CpG binding domain protein 3-like 2*
2.544	A730025A07 Rik	*RIKEN cDNA A730025A07*
2.542	2410146L05Rik	*RIKEN cDNA 2410146L05 gene*
2.538	B930020H05 Rik	*RIKEN cDNA:B930020H05*
2.537	Pdzrn3	*PDZ domain containing RING finger 3*
2.534	Hmmr	*hyaluronan mediated motility receptor (RHAMM)*
2.532	Lepre1	*leprecan 1*
2.529	A130089I23.Rik	*RIKEN cDNA A130089I23.*
2.524	4833422F06Rik	*RIKEN cDNA 4833422F06 gene*
2.52	4930430J02Rik	*RIKEN cDNA 4930430J02 gene*
2.514	Ankrd17	*ankyrin repeat domain 17*
2.513	4932442K08Rik	*RIKEN cDNA 4932442K08 gene*
2.511	Wdr40a	*WD repeat domain 40A*
2.508	Zc3hdc5	*zinc finger CCCH type domain containing 5*
2.495	Gm978	*gene model 978 , (NCBI)*

2.491	Aif1	*allograft inflammatory factor 1*
2.491	D130064H19Rik	*RIKEN cDNA D130064H19 gene*
2.49	Tcf19	*transcription factor 19*
2.481	Atxn7l3	*ataxin 7-like 3*
2.481	Gsdmdc1	*gasdermin domain containing 1*
2.477	Mafk	*v-maf musculoaponeurotic fibrosarcoma oncogene family, protein K (avian)*
2.474	Cpa1	*carboxypeptidase A1*
2.469	Snrp70	*U1 small nuclear ribonucleoprotein polypeptide A*
2.462	Bcl7a	*B-cell CLL/lymphoma 7A*
2.454	Pramel4	*preferentially expressed antigen in melanoma like 4*
2.45	4933412A08Rik	*RIKEN cDNA 4933412A08 gene*
2.447	Cd7	*CD7 antigen*
2.445	1300013B24Rik	*RIKEN cDNA 1300013B24 gene*
2.445	9230118O19 Rik	*RIKEN cDNA 9230118O19*
2.442	E030047P15 Rik	*RIKEN cDNA:E030047P15*
2.437	4930408F14Rik	*RIKEN cDNA 4930408F14 gene*
2.437	Brd1	*bromodomain containing 1*
2.437	Cdh3	*cadherin 3*
2.433	Sec23a	*SEC23A (S. cerevisiae)*
2.431	AW544865	*expressed sequence AW544865*
2.429	Zfp371	*zinc finger protein 371*
2.421	Faf1	*Fas-associated factor 1*
2.417	Mga	*MAX gene associated*
2.414	3110048E14Rik	*RIKEN cDNA 3110048E14 gene*
2.403	1700018O18Rik	*RIKEN cDNA 1700018O18*
2.399	1810055G02Rik	*RIKEN cDNA 1810055G02 gene*
2.399	Kif11	*kinesin family member 11*
2.396	Gsr	*glutathione reductase 1*
2.388	D130036D15.Rik	*RIKEN cDNA D130036D15.*
2.385	D130020L05Rik	*RIKEN cDNA 1110034C04 gene*
2.385	Mapkbp1	*mitogen activated protein kinase binding protein 1*
2.382	Tap-1, Tap1	*transporter 1, ATP-binding cassette, sub-family B (MDR/TAP)*
2.376	Son	*Son cell proliferation protein*
2.364	Orc1l	*origin recognition complex, subunit 1-like (S.cereviaiae)*
2.361	Siat5	*sialyltransferase 5*
2.359	Map3k6	*mitogen-activated protein kinase kinase kinase 6*
2.359	Syngr3	*synaptogyrin 3*
2.357	Nek4	*NIMA (never in mitosis gene a)-related expressed kinase 4*
2.356	4732493F09Rik	*RIKEN cDNA 4732493F09 gene*
2.355	Spg4	*spastic paraplegia 4 homolog (human)*
2.351	Rnf6	*ring finger protein (C3H2C3 type) 6*
2.35	E130113K08Rik	*RIKEN cDNA 6430570G24 gene*
2.34	Eya3	*eyes absent 3 homolog (Drosophila)*
2.339	4921513E08Rik	*RIKEN cDNA 4921513E08 gene*
2.339	A230106M15Rik	*RIKEN cDNA A230106M15 gene*
2.339	A930014D07Rik	*RIKEN cDNA A930014D07 gene*
2.338	Ccr4	*chemokine (C-C motif) receptor 4*
2.333	Gm179	*A012E07 GGTC Gene Trap Library GV03C04*
2.333	Spz1	*spermatogenic Zip 1*
2.332	Sap30	*sin3 associated polypeptide*
2.331	D930023J12Rik	*RIKEN cDNA D930023J12 gene*
2.33	Lats1	*large tumor supressor*
2.33	Rhced	*Rhesus blood group CE and D*
2.328	A930015D03Rik	*Mus musculus, clone IMAGE:5347090, mRNA.*

2.328	Hivep2	*Human immunodeficiency virus 1 enahancer binding protein 2*
2.317	Kcnmb4	*potassium large conductance calcium-activated channel, subfamily M, beta member 4*
2.314	Padi2	*peptidyl arginine deiminase, type II*
2.313	Stx1b2, Stx1b1	*syntaxin 1B1*
2.311	Klhl7	*kelch-like 7 (Drosophila)*
2.309	Actr2	*ARP2 actin-related protein 2 homolog (yeast)*
2.309	Tacstd1	*tumor-associated calcium signal transducer 1*
2.307	Il17rc	*interleukin 17 receptor C*
2.306	Ptger4	*cDNA, RIKEN D130004L12 :prostaglandin E receptor 4 (subtype EP4),.*
2.303	Dnajc7	*DnaJ (Hsp40) homolog, subfamily C, member 7*
2.301	Gle1l	*GLE1 RNA export mediator-like (yeast*
2.3	Grsf1	*G-rich RNA sequence binding factor 1*
2.3	Psap	*prosaposin*
2.294	Zdhhc16	*zinc finger, DHHC domain containing 16*
2.292	3830405G04Rik	*RIKEN cDNA 3830405G04 gene*
2.291	D11Bwg0280e	*DNA segment, Chr 11, Brigham & Women's Genetics 0280e expressed*
2.291	Rgs2	*regulator of G-protein signaling 2*
2.291	Usp33	*ubiquitin specific protease 33*
2.281	BC055757	*cDNA sequence BC055757*
2.274	Fgf18	*fibroblast growth factor 18*
2.271	Polr2b	*polymerase (RNA) II (DNA directed) polypeptide B*
2.269	Mllt3	*myeloid/lymphoid or mixed lineage-leukemia translocation to 3 homolog*
2.268	Baz2a	*bromodomain adjacent to zinc finger domain, 2A*
2.261	Gga3	*golgi associated, gamma adaptin ear containing, ARF binding protein 3*
2.242	Ibtk	*inhibitor of Bruton agammaglobulinemia tyrosine kinase*
2.242	Zfp319	*zinc finger protein 319*
2.233	Hsp25, Hspb1	*heat shock protein 1*
2.232	Psmd1	*RIKEN cDNA 4930438O05 gene*
2.225	Cdk7	*cyclin-dependent kinase 7 (homolog of Xenopus MO15 cdk-activating kinase)*
2.222	1300007B12Rik	*RIKEN cDNA 1300007B12 gene*
2.222	Ercc6	*excision repair cross-complementing rodent repair deficiency, complementation group 6*
2.221	Gale	*galactose-4-epimerase, UDP*
2.216	Arhgap11a	*Rho GTPase activating protein 11A*
2.215	AU040829	*expressed sequence AU040829*
2.214	Cai	*calcium binding protein, intestinal*
2.21	Og2x	*OG2 homeobox gene*
2.207	2310026L22Rik	*RIKEN cDNA 2310026L22 gene*
2.206	Sitpec	*signaling intermediate in Toll pathway-evolutionarily conserved*
2.199	A430008J24Rik	*RIKEN cDNA A430008J24*
2.183	4632412E09Rik	*RIKEN cDNA 4632412E09 gene*
2.183	Pank3	*pantothenate kinase 3*
2.181	Prom1	*prominin 1*
2.166	Prc1	*protein regulator of cytokinesis 1*
2.166	Sca7	*spinocerebellar ataxia 7 homolog (human)*
2.161	1700009P03Rik	*RIKEN cDNA 1700009P03 gene*
2.16	Ptprv	*protein tyrosine phosphatase, receptor type, V*
2.155	AW555464	*expressed sequence AW555464*
2.153	Rnf166	*ring finger protein 166*
2.149	Magoh	*mago-nashi homolog, proliferation-associated (Drosophila)*
2.145	Ncoa6	*nuclear receptor coactivator 6*
2.14	Gyk	*glycerol kinase*
2.14	Hnrpa2b1	*heterogeneous nuclear ribonucleoprotein A2/B1*
2.138	4732430I17 Rik	*RIKEN cDNA 4732430I17*

2.136	Ppm1a	*protein phosphatase 1A, magnesium dependent, alpha isoform*
2.132	Falz	*fetal Alzheimer antigen*
2.129	5730405K23Rik	*RIKEN cDNA 5730405K23 gene*
2.129	D730045A05Rik	*RIKEN cDNA D730045A05 gene*
2.129	Edaradd	*EDAR (ectodysplasin-A receptor)-associated death domain*
2.127	AU019823	*expressed sequence AU019823*
2.127	Klrd1	*killer cell lectin-like receptor, subfamily D, member 1*
2.126	Gpr125	*G protein-coupled receptor 125*
2.125	Pbef1	*pre-B-cell colony-enhancing factor 1*
2.122	Padi4	*peptidyl arginine deiminase, type IV*
2.12	Trub2	*TruB pseudouridine (psi) synthase homolog 2 (E. coli)*
2.118	2310003L22Rik	*RIKEN cDNA 2310003L22 gene*
2.117	Polr3a	*polymerase (RNA) III (DNA directed) polypeptide A*
2.115	1810073E21Rik	*RIKEN cDNA 1810073E21 gene*
2.115	F8	*coagulation factor VIII*
2.115	Rtkn	*rhotekin*
2.113	2610024G14Rik	*RIKEN cDNA 2610024G14 gene*
2.111	Mlycd	*malonyl-CoA decarboxylase*
2.108	6330503K22Rik	*RIKEN cDNA 6330503K22 gene*
2.108	Zfp1	*zinc finger protein 1*
2.107	Alms1	*Alstrom syndrome 1 homolog (human)*
2.107	Elk4,	*ELK4, member of ETS oncogene family*
2.106	Cpt2	*carnitine palmitoyltransferase 2*
2.102	E130016E03Rik	*W192F02 GGTC Gene Trap Library GV04C04*
2.098	Syncrip, Snx14	*sorting nexin 14*
2.097	Per3	*period homolog 3 (Drosophila)*
2.097	Tubb3	*tubulin, beta 3*
2.093	4930429E23Rik	*RIKEN cDNA 4930429E23 gene*
2.093	Bicd2	*bicaudal D homolog 2 (Drosophila)*
2.092	Spin	*spindlin*
2.09	Crlf3	*cytokine receptor-like factor 3*
2.087	Rtn4r	*reticulon 4 receptor*
2.085	Taf4a	*TAF4A RNA polymerase II, TATA box binding protein (TBP)-associated factor*
2.08	4932442K0Rik	*RIKEN cDNA 4932442K0 gene*
2.077	Sfrs4	*splicing factor, arginine/serine-rich 4 (SRp75)*
2.076	Cstf3	*cleavage stimulation factor, 3' pre-RNA, subunit 3*
2.073	Rnf40	*ring finger protein 40*
2.07	Jag1	*jagged 1*
2.069	Pnrc1	*proline-rich nuclear receptor coactivator 1*
2.066	,D230035M11Rik	*RIKEN cDNA 1700034P14 gene*
2.061	Igf2bp3	*insulin-like growth factor 2, binding protein 3*
2.06	Dhx30	*DEAH (Asp-Glu-Ala-His) box polypeptide 30*
2.059	C130036G08	*Mus musculus hypothetical protein C130036G08 (C130036G08), mRNA*
2.059	Dck	*deoxycytidine kinase*
2.059	9530060I07 Rik	*RIKEN cDNA 9530060I07*
2.057	Cdo1	*cysteine dioxygenase 1, cytosolic*
2.054	Eif2ak3	*eukaryotic translation initiation factor 2 alpha kinase 3*
2.054	Fhos2,	*Mus musculus formin-family protein FHOS2 (FHOS2), mRNA*
2.053	Inpp5b	*inositol polyphosphate-5-phosphatase B*
2.052	E2f6	*E2F transcription factor 6*
2.047	Arpc2	*actin related protein 2/3 complex, subunit 2*
2.045	5031400M07Rik	*RIKEN cDNA 5031400M07 gene*
2.044	Rbm10	*RNA binding motif protein 10*
2.041	6330505F04Rik	*RIKEN cDNA 6330505F04 gene*

2.039	Ldh2	*lactate dehydrogenase 2, B chain*
2.039	4930525M22 Rik	*RIKEN cDNA 4930525M22*
2.037	Prx	*periaxin*
2.036	Mbtd1	*mbt domain containing 1*
2.035	Fbxo17	*F-box protein 17*
2.035	A630051O22.Rik	*RIKEN cDNA A630051O22.*
2.033	LOC229751	*Mus musculus similar to Alpha-amylase, pancreatic precursor*
2.033	Prkcbp1	*protein kinase C binding protein 1*
2.033	Slc38a4	*solute carrier family 38, member 4*
2.031	Abcb9	*ATP-binding cassette, sub-family B (MDR/TAP), member 9*
2.031	Tjp3	*tight junction protein 3*
2.026	Ranbp2	*RAN binding protein 2*
2.022	Mllt10	*myeloid/lymphoid or mixed lineage-leukemia translocation to 10 homolog*
2.019	Rab10	*RAB10, member RAS oncogene family*
2.019	Thrap2	*thyroid hormone receptor associated protein 2*
2.018	AK129341	*Mus musculus 12 days embryo eyeball cDNA, RIKEN :D230007F04.*
2.018	Mertk	*c-mer proto-oncogene tyrosine kinase*
2.018	Morc	*microrchidia*
2.016	Frap1	*FK506 binding protein 12-rapamycin associated protein 1*
2.016	Nanos1	*nanos homolog 1 (Drosophila)*
2.015	B230113M03Rik	*RIKEN cDNA B230113M03 gene*
2.012	Ccnl2	*cyclin L2*
2.009	5033405K12Rik	*RIKEN cDNA 5033405K12 gene*
2.007	Ddr1	*discoidin domain receptor family, member 1*
2.007	Prcc	*papillary renal cell carcinoma (translocation-associated)*
2.006	Grcc9	*gene rich cluster, C9 gene*
1.998	Mllt2h	*homolog of human MLLT2 unidentified gene*
1.996	Frzb	*frizzled-related protein*
1.993	Rps27l	*ribosomal protein S27-like*
1.992	Dph2l2	*diptheria toxin resistance protein required for diphthamide biosynthesis-like 2*
1.991	Ube3a	*ubiquitin protein ligase E3A*
1.989	4632409L19Rik	*RIKEN cDNA 4632409L194gene*
1.989	Ltb	*lymphotoxin B*
1.987	1700041C02Rik	*RIKEN cDNA*
1.987	D430002O22Rik	*RIKEN cDNA D430002O22 gene*
1.987	Prdx4	*peroxiredoxin 4*
1.984	1300002F13Rik	*RIKEN cDNA 1300002F13 gene*
1.984	3200001K10Rik,	*RIKEN cDNA 3200001K10 gene*
1.981	Serpine2	*serine (or cysteine) proteinase inhibitor, clade E, member 2*
1.979	C80587	*expressed sequence C80587*
1.977	1500031M22Rik	*RIKEN cDNA 1500031M22 gene*
1.976	Ddx28	*DEAD (Asp-Glu-Ala-Asp) box polypeptide 28*
1.976	Eif4g1	*eukaryotic translation initiation factor 4, gamma 1*
1.97	Phactr4	*phosphatase and actin regulator 4*
1.968	Snx27	*sorting nexin family member 27*
1.964	BC054822	*cDNA sequence BC054822*
1.964	Lig1	*ligase I, DNA, ATP-dependent*
1.963	1700001K23Rik	*RIKEN cDNA 1700001K23*
1.962	8030493P09Rik	*RIKEN cDNA 8030493P09 gene*
1.961	Rbm10	*RNA binding motif protein 10*
1.961	Trp53inp1	*transformation related protein 53 inducible nuclear protein 1*
1.96	Cdk9	*cyclin-dependent kinase 9 (CDC2-related kinase)*
1.959	4732495E13Rik	*RIKEN cDNA 4732495E13 gene*
1.959	Dnclic1	*dynein, cytoplasmic, light intermediate chain 1*

1.958	1810045K06Rik	*RIKEN cDNA*
1.955	1700123A16Rik	*RIKEN cDNA 1700123A16 gene*
1.954	Utp14b, Acsl3	*acyl-CoA synthetase long-chain family member 3*
1.952	Ipo8	*importin 8*
1.949	Apc	*adenomatosis polyposis coli*
1.948	Ubp1	*upstream binding protein 1*
1.947	Cdc42se2	*CDC42 small effector 2*
1.947	Sod2	*superoxide dismutase 2*
1.946	Midn	*midnolin*
1.945	6720425G15Rik	*Mus musculus cDNA clone IMAGE:1264584, partial cds.*
1.943	Sfrs2	*splicing factor, arginine/serine-rich 2 (SC-35)*
1.943	Twistnb	*TWIST neighbor*
1.942	Arhgap17	*Rho GTPase activating protein 17*
1.942	Socs3	*suppressor of cytokine signaling 3*
1.941	1700003E16Rik	*RIKEN cDNA 1700003E16*
1.938	D5ertd585e	*DNA segment, Chr 5, ERATO Doi 585, expressed*
1.937	Mapk14	*mitogen activated protein kinase 14*
1.935	Col23a1	*procollagen, type XXIII, alpha 1*
1.931	Gnn	*Mus musculus cDNA sequence BC030307 (BC030307), mRNA*
1.927	Slc25a19	*solute carrier family 25 (mitochondrial deoxynucleotide carrier), member 19*
1.919	Socs2	*suppressor of cytokine signaling 2*
1.916	4930572J05Rik	*RIKEN cDNA 4930572J05 gene*
1.916	Rgs17	*regulator of G-protein signaling 17*
1.916	Spred2	*sprouty protein with EVH-1 domain 2, related sequence*
1.914	Vrk1	*vaccinia related kinase 1*
1.913	Slc1a3	*solute carrier family 1 (glial high affinity glutamate transporter), member 3*
1.911	Kcna5	*potassium voltage-gated channel, shaker-related subfamily, member 5*
1.91	B230339M05Rik,	*RIKEN cDNA B230339M05 gene*
1.908	Gng7	*guanine nucleotide binding protein (G protein), gamma 7 subunit*
1.905	D11Ertd461e	*DNA segment, Chr 11, ERATO Doi 461, expressed*
1.905	Hiat1	*hippocampus abundant gene transcript 1*
1.901	Tmem5	*transmembrane protein 5*
1.899	Gbp1	*guanylate nucleotide binding protein 1*
1.899	Zfp612	*zinc finger protein 612*
1.897	Ube2g1	*ubiquitin-conjugating enzyme E2G 1 (UBC7 homolog, C. elegans)*
1.896	Fut10	*fucosyltransferase 10*
1.895	B930088P06 Rik	*RIKEN cDNA B930088P06*
1.894	2700049P18Rik	*RIKEN cDNA 2700049P18 gene*
1.894	Fgf5	*fibroblast growth factor 5*
1.894	Gadd45g	*growth arrest and DNA-damage-inducible 45 gamma*
1.892	Tnnc2	*troponin C2, fast*
1.889	Celsr1	*cadherin EGF LAG seven-pass G-type receptor 1*
1.888	Hccs	*holocytochrome c synthetase*
1.884	Sp3	*trans-acting transcription factor 3*
1.883	Ccnb3	*cyclin B3*
1.882	Prkcb1	*protein kinase C, beta 1*
1.881	Mum1l1	*melanoma associated antigen (mutated) 1-like 1*
1.88	3010027A04Rik	*RIKEN cDNA 3010027A04 gene*
1.879	5430439M09Rik	*RIKEN cDNA 5430439M09 gene*
1.876	0610012D09Rik	*RIKEN cDNA 0610012D09 gene*
1.874	Cbll1	*Casitas B-lineage lymphoma-like 1*
1.873	Art5	*ADP-ribosyltransferase 5*
1.872	4930488P06Rik	*RIKEN cDNA 4930488P06 gene*
1.872	9430077D24Rik	*Mus musculus, clone IMAGE:4507201, mRNA.*

1.872	Rgs4	*regulator of G-protein signaling 4*
1.871	Cebpb	*CCAAT/enhancer binding protein (C/EBP), beta*
1.87	V2r14, Gm1844	*vomeronasal 2, receptor, 14*
1.867	Rab35	*RAB35, member RAS oncogene family*
1.866	Siah2	*seven in absentia 2*
1.865	Cstf2t	*cleavage stimulation factor, 3' pre-RNA subunit 2, tau*
1.865	Oit1	*oncoprotein induced transcript 1*
1.864	4933417K04Rik	*RIKEN cDNA 4933417K04 gene*
1.862	Flcn	*folliculin*
1.861	Tdrd3	*tudor domain containing 3*
1.858	Cdc6	*cell division cycle 6 homolog (S. cerevisiae)*
1.858	Cebpz	*CCAAT/enhancer binding protein zeta*
1.857	Ddx27	*DEAD (Asp-Glu-Ala-Asp) box polypeptide 27*
1.856	AI606181	*expressed sequence AI606181*
1.853	Ddx10	*W014H09 GGTC Gene Trap Library GV03C01*
1.852	LOC386163	*Mus musculus similar to RNP particle component (LOC386163), mRNA*
1.879	Kif23	*kinesin family member 2c*
1.851	Lamp2	*lysosomal membrane glycoprotein 2*
1.851	Numa1	*nuclear mitotic apparatus protein 1*
1.85	4933424A10Rik	*RIKEN cDNA 4933424A10 gene*
1.842	C330027C09Rik	*RIKEN cDNA C330027C09 gene*
1.842	Nmb	*neuromedin B*
1.842	Rnf34	*ring finger protein 34*
1.842	Zmynd19	*zinc finger, MYND domain containing 19*
1.841	Psme4,	*proteasome (prosome, macropain) activator subunit 4*
1.84	Card4	*caspase recruitment domain 4*
1.836	Sh3bp2	*SH3-domain binding protein 2*
1.834	Ppp1r7	*protein phosphatase 1, regulatory (inhibitor) subunit 7*
1.834	Tbc1d7	*TBC1 domain family, member 7*
1.831	BC005537	*cDNA sequence BC005537*
1.83	Gnpnat1	*Mus musculus glucosamine-phosphate N-acetyltransferase 1 (Gnpnat1), mRNA*
1.83	A630042D18 Rik	*RIKEN cDNA A630042D18*
1.829	Tcl1	*T-cell lymphoma breakpoint 1*
1.828	4930535B03Rik	*RIKEN cDNA. 4930535B03 gene*
1.827	Calmbp1	*calmodulin binding protein 1*
1.827	Gtf2h1	*general transcription factor II H, polypeptide 1*
1.827	Ly75	*lymphocyte antigen 75*
1.825	Top1	*topoisomerase (DNA) I*
1.824	A430078P17:Rik	*RIKEN cDNA A430078P17:*
1.823	2310004I24Rik	*RIKEN cDNA 2310004I24 gene*
1.821	Ndrg4	*N-myc downstream regulated gene 4*
1.815	Dnajc5	*DnaJ (Hsp40) homolog, subfamily C, member 5*
1.811	A830012D13 Rik	*RIKEN cDNA A830012D13*
1.81	Ddef1	*development and differentiation enhancing*
1.81	Tuba4	*tubulin, alpha 4*
1.808	Icsbp1	*interferon consensus sequence binding protein 1*
1.808	Pabpc4	*poly A binding protein, cytoplasmic 4*
1.807	Dirc2	*disrupted in renal carcinoma 2 (human)*
1.804	2610041P08Rik	*RIKEN cDNA 2610041P08 gene*
1.803	Anks1	*ankyrin repeat and SAM domain containing 1*
1.8	4930542G03Rik	*RIKEN cDNA 4930542G03 gene*
1.795	G630064G18Rik	*RIKEN cDNA G630064G18 gene*
1.792	D030062I09 Rik	*RIKEN cDNA D030062I09*
1.79	2610528A15Rik	*RIKEN cDNA 2610528A15 gene*

1.789	Pim3	*proviral integration site 3*
1.789	Plekhm2	*pleckstrin homology domain containing, family M (with RUN domain) member 2*
1.786	AI642036	*expressed sequence AI642036*
1.786	Mapk4	*mitogen-activated protein kinase 4*
1.784	Klf16	*Kruppel-like factor 16*
1.779	Pols	*polymerase (DNA directed) sigma*
1.779	Rara	*retinoic acid receptor, alpha*
1.778	Jak2	*Janus kinase 2*
1.773	Hrmt1l1	*heterogeneous nuclear ribonucleoprotein methyltransferase-like 1 (S. cerevisiae)*
1.773	Mak10	*MAK10 homolog, amino-acid N-acetyltransferase subunit, (S. cerevisiae)*
1.772	Kif1b	*kinesin family member 1B*
1.772	Socs1	*Suppressor of cytokine signalling 1*
1.77	Arid1b	*AT rich interactive domain 1B (Swi1 like)*
1.77	Prkar2a	*protein kinase, cAMP dependent regulatory, type II alpha*
1.768	Gorasp1	*golgi reassembly stacking protein 1*
1.768	6530401P13 Rik	*RIKEN cDNA 6530401P13*
1.766	Ostb	*Mus musculus organic solute transporter beta (Ostb), mRNA*
1.764	Evl	*Ena-vasodilator stimulated phosphoprotein*
1.763	Hnrph1	*heterogeneous nuclear ribonucleoprotein H1*
1.762	1700021I09Rik	*RIKEN cDNA 1700021I09 gene*
1.762	4930401O10Rik	*RIKEN cDNA 4930401O10 gene*
1.761	Tnfrsf13b	*tumor necrosis factor receptor superfamily, member 13b*
1.758	Chka	*choline kinase alpha*
1.757	2010110K18Rik	*RIKEN cDNA 2010110K18 gene*
1.757	Wsb2	*WD repeat and SOCS box-containing 2*
1.755	Zfp143	*zinc finger protein 143*
1.753	1110020M19Rik	*RIKEN cDNA 1110020M19 gene*
1.753	Bpy2ip1	*RIKEN cDNA Bpy2ip1*
1.753	Slc1a5	*solute carrier family 1 (neutral amino acid transporter), member 5*
1.752	Zfp346	*zinc finger protein 346*
1.751	Akt3	*thymoma viral proto-oncogene 3*
1.751	Hnrpf	*heterogeneous nuclear ribonucleoprotein F*
1.749	2410005K20Rik	*RIKEN cDNA 2410005K20 gene*
1.746	Gtf2h4	*general transcription factor II H, polypeptide 4*
1.739	Dnclc1	*dynein, cytoplasmic, light chain 1*
1.737	2610024N01Rik	*RIKEN cDNA 2610024N01 gene*
1.735	A730064F23 Rik	*RIKEN cDNA A730064F23*
1.733	Adnp	*activity-dependent neuroprotective protein*
1.731	Eda	*ectodysplasin-A*
1.731	Plk4	*polo-like kinase 4 (Drosophila)*
1.726	Abcc10	*ATP-binding cassette, sub-family C (CFTR/MRP), member 3*
1.725	Pprc1	*cDNA clone A039C05*
1.723	2810003C17Rik	*RIKEN cDNA 2810003C17 gene*
1.716	Rad21	*RAD21 homolog (S. pombe)*
1.715	Slc39a6	*solute carrier family 39 (metal ion transporter), member 6*
1.715	Wdr26	*WD repeat domain 26*
1.712	Cdkn2d	*cyclin-dependent kinase inhibitor 2D (p19, inhibits CDK4)*
1.712	C230051C19 Rik	*RIKEN cDNA C230051C19*
1.71	Prkcbp1	*protein kinase C binding protein 1*
1.706	Rpl17	*ribosomal protein L17*
1.705	Acly	*ATP citrate lyase*
1.704	Kif3c	*kinesin family member 3C*
1.701	7030408E01 Rik	*RIKEN cDNA 7030408E01*
1.7	1110025G12Rik	*RIKEN cDNA 1110025G12 gene*

1.7	Nags	*N-acetylglutamate synthase*
1.692	Phldb1	*pleckstrin homology-like domain, family B, member 1*
1.691	Dapk2	*death-associated kinase 2*
1.691	Nfatc3	*nuclear factor of activated T-cells, cytoplasmic, calcineurin-dependent 3*
1.691	Ppp4c	*protein phosphatase 4, catalytic subunit*
1.683	Glis1	*GLIS family zinc finger 1*
1.678	Spata5	*spermatogenesis associated 5*
1.674	Nfkbia	*nuclear factor of kappa light chain gene enhancer in B-cells inhibitor, alpha*
1.668	Myst2	*MYST histone acetyltransferase 2*
1.667	1300006C19Rik	*RIKEN cDNA. 1300006C19 gene*
1.667	Map4k2	*mitogen activated protein kinase kinase kinase kinase 2*
1.666	D1pas1	*DNA segment, Chr 1, Pasteur Institute 1*
1.664	1810003N24Rik	*RIKEN cDNA 1810003N24 gene*
1.663	Ercc4	*excision repair cross-complementing rodent repair deficiency, complementation group 4*
1.661	1110015K06Rik	*RIKEN cDNA 1110015K06 gene*
1.66	Rabep2	*rabaptin, RAB GTPase binding effector protein 2*
1.655	2010009L17Rik	*RIKEN cDNA 2010009L17 gene*
1.655	Mfi2	*antigen p97 (melanoma associated).*
1.651	8430417G17Rik	*RIKEN cDNA 8430417G17 gene*
1.651	Adprtl2	*ADP-ribosyltransferase (NAD+, poly(ADP-ribose) polymerase)-like 2*
1.639	Oxct1	*3-oxoacid CoA transferase 1*
1.627	Ndufa2	*NADH dehydrogenase (ubiquinone) 1 alpha subcomplex, 2*
1.626	Amd1	*S-adenosylmethionine decarboxylase 1*
1.62	A930010I02 Rik	*Mus musculus hypothetical protein A930010I02 (A930010I02), mRNA*
1.62	BC059842	*cDNA sequence BC059842*
1.62	Pkd1	*polycystic kidney disease 1 homolog*
1.618	2810405F18Rik	*RIKEN cDNA 2810405F18 gene*
1.615	Cpsf2	*cleavage and polyadenylation specific factor 2*
1.615	Lrdd	*leucine-rich and death domain containing*
1.614	Usf2	*Mus musculus upstream transcription factor 2 (Usf2), mRNA*
1.602	Slc7a1	*Mus musculus, clone IMAGE:3472087, mRNA.*
1.601	Cnn1	*calponin 1*
1.596	Casp2	*caspase 2*
1.596	Polr3d	*polymerase (RNA) III (DNA directed) polypeptide D*
1.587	Hist1h4j	*histone 1, H4j*
1.578	Ube2d2	*ubiquitin-conjugating enzyme E2D 2*
1.572	B130043D19 Rik	*RIKEN cDNA B130043D19*
1.566	Tubb4	*tubulin, beta 4*